University of Alberta

The inhibition of apoptosis and Bax activation by mitochondrial anti-apoptotic proteins encoded by vaccinia virus and ectromelia virus

by

John M. Taylor 

A thesis submitted to the Faculty of Graduate Studies and Research
in partial fulfillment of the requirements for the degree of

Doctor of Philosophy

Department of Medical Microbiology and Immunology

Edmonton, Alberta
Fall, 2007

Your file Votre référence
ISBN: 978-0-494-33076-0
Our file Notre référence
ISBN: 978-0-494-33076-0

Abstract

Vaccinia virus, the prototypic member of the orthopoxvirus genus, encodes the mitochondrial-localized protein F1L that protects cells from apoptosis and inhibits cytochrome c release. F1L is a 26kDa protein that interacts with the pro-apoptotic Bcl-2 family member Bak and inhibits activation of Bak during cell death. In addition to Bak, the pro-apoptotic protein Bax is also capable of initiating cytochrome c release, suggesting that vaccinia virus infection might also modulate Bax. Here we show that F1L inhibits the activity of Bax by inhibiting oligomerization and N-terminal activation of Bax. F1L expression also inhibited the subcellular redistribution of Bax to the mitochondria and Bax insertion into the outer mitochondrial membrane. The ability of F1L to inhibit Bax activation does not require Bak, as F1L expression inhibited cytochrome c release and Bax activation in Bak-deficient cells. No interaction between Bax and F1L was detected during infection, suggesting that F1L functions upstream of Bax activation. Notably, F1L was capable of interacting with the BH3-only protein BimL as shown by co-immunoprecipitation, and F1L expression inhibited BimL-induced apoptosis. Vaccinia virus-induced apoptosis was also partially inhibited in Bim-deficient cells, suggesting that Bim is an important mediator of vaccinia virus-induced apoptosis. We have also investigated the F1L orthologue from the related orthopoxvirus ectromelia virus, which is a natural pathogen of mice. This F1L orthologue, EVM025, is a 55 kDa protein that also inhibits apoptosis. EVM025 exhibits a large N-terminal extension consisting of an eight amino acid region repeated 30 times. While the function of this repeat region is unknown, EVM025 was expressed as a 55kDa protein, and deletion of

the gene encoding EVM025 from the ectromelia virus genome abrogated anti-apoptotic activity conferred by ectromelia virus infection. While the amino acid sequence of EVM025 exhibits a number of differences from F1L, a truncated version of EVM025 lacking the N-terminal repeat region still inhibited Bax activation and also constitutively interacted with Bak. These studies suggest that in addition to interacting with Bak, F1L and EVM025 can function to indirectly inhibit the activation of Bax, likely by interfering with the pro-apoptotic activity of BH3-only proteins such as BimL.

Acknowledgements

I would like to thank Michele for all of her support and guidance for the past several years. Without her patience and expertise, none of this would have been possible. I would also like to thank everyone I've had the opportunity to work with in the Barry lab during my tenure here . . . especially Shawn, who did so much for me as a friend and fellow 'trainee'. Big kudos to the old guard, Tara, Kim, Brianne, 007, and Robyn, and to the new guard and team TAP: Logan, Steph, Douggie, and our honorary member Josh "Finnigan" . . . to the new mayor of rageville, the van Buuren boys, and Craig . . . it's these types of friendships that make the tough days not so tough after all -- I'll miss you guys. Thank you to my in-laws for making me feel like a part of their family out here in 'the promised land' all these years. And of course, a very special thank you to my parents for their never-ending support and encouragement to pursue my dreams and aspirations. Nothing but strikes, dad.

And to Tracey, with all my love.

Table of Contents **Page**

List of Tables **Page**

List of Figures **Page**

Chapter 1. Introduction

Chapter 2. Materials and Methods

Chapter 3. The vaccinia virus protein F1L inhibits Bax activation

List of Abbreviations

µl – microlitre
µM – micromolar
AIF – apoptosis inducing factor
AraC – cytosine arabinoside
ATP – adenosine triphosphate
Bak – Bcl-2 antagonist of killing
Bax – Bcl-2 associated X gene
BCA – bichinconinic acid
Bcl – B-cell lymphoma
BGMK – baby green monkey kidney
BH – Bcl-2 homology
Bid – Bcl-2 interacting domain
Bim – Bcl-2 interacting mediator of cell death
BimEL – Bim extra long
BimL – Bim long
BimS – Bim short
BIR – baculovirus IAP repeat
BMK – baby mouse kidney
bp – base pair
CHAPS – 3-[(3-Cholamidopropyl)dimethylammonio]-1-propanesulfonate
Cpx - Cowpox
CrmA – cytokine response modifier A
CTL – cytotoxic T lymphocyte
DLC – dynein light chain
DMEM – Dulbecco's modified Eagle's media
DMF – dimethyl formamide
DMSO – dimethyl sulphoxide
DNA – deoxyribonucleic acid
dsRNA – double stranded ribonucleic acid
DTT – dithiothretitol
ECL – enhanced chemiluminescence
EDTA – ethylenediaminetetraacetic acid
EGFP – enhanced green fluorescent protein
EGTA – ethylene glycol tetraacetic acid
ERK – extracellular signal-regulated kinase
EVM – Ectromelia virus Moscow
FADD – Fas-associated death domain
FBS – fetal bovine serum
FITC – fluorescein isothiocyanate
HA – haemagglutinin
HEPES – 4-(2-hydroxyethyl)-1-piperazineethanesulfonic acid

HRP – horseradish peroxidase
IAP – inhibitor of apoptosis
IFN – interferon
Kb – kilobase
kDa – kilodalton
LB – Luria-Bertaini broth
LMP – Low melting point
M – molar
mA – milliamps
MCV – molluscum contagiosum virus
MEF – mouse embryonic fibroblast
MEK – mitogen activated protein kinase kinase
mg – milligram
ml – millilitre
MnSOD – manganese superoxide dismutase
MOI – multiplicity of infection
Mpx – Monkeypox
NF-κB – nuclear factor kappa-B
OD – optical density
ORF – open reading frame
PAGE – polyacrylamide gel electrophoresis
PARP – poly-ADP ribose polymerase
PBR – peripheral benzodiazepine receptor
PBS – phosphate buffered saline
PCR – polymerase chain reaction
Pfu – plaque forming unit
PKR – protein kinase R
PT – permeability transition
PVDF – polyvinylidene fluoride
RE – restriction endonuclease
RING – really interesting new gene
RIPA – radioimmunoprecipitation assay
RNA – ribonucleic acid
S.D. – standard deviation
SDS – sodium dodecyl sulfate
SMAC – Second mitochondrial activator of caspases
SPI – serine protease inhibitor
SSC – standard saline citrate
STS – staurosporine
TAE – tris acetate EDTA
TBST – tris buffered saline plus Tween 20
TK – thymidine kinase
TMRE – tetramethylrhodamine ethyl ester

TNF – tumour necrosis factor
TNFR – tumour necrosis factor receptor
TRADD – TNF receptor associated death domain
TUNEL – terminal deoxynucleotidyltransferase-mediated dUTP nick end labeling
TX-100 – triton-X-100
UTP – uridine triphosphate
UV – ultra-violet
vMIA – viral mitochondrial inhibitor of apoptosis
VarV – variola virus
VV – vaccinia virus
WT – wild type
X-gal – 5-bromo-4-chloro-3-indolyl-b-D-galactopyranoside
zVAD.fmk – Z-Val-Ala-Asp-fluoromethyl ketone

CHAPTER 1: Introduction

1.1. Poxviruses

The *Poxviridae* are a large and diverse family of viruses that contain double-stranded DNA genomes and replicate within the cytoplasm of the infected cell (237). This ancient family of viruses is divided into two subfamilies, the *Chordopoxvirinae*, which infect vertebrates, and the *Entomopoxvirinae*, which infect invertebrates (237) (Table 1.1). The *Chordopoxvirinae* contain poxviruses that infect vertebrates and mammals, and are subdivided into eight different genera (Table 1.1). The most notorious member of the poxviridae family was the *Orthopoxvirus* variola virus, the causative agent of smallpox. Various strains of smallpox caused human mortality rates greater than 30%, and the virus was endemic for centuries, dating back at least 2000 years (323). Aside from smallpox, multiple members of the *Chordopoxvirinae* can also cause infections in humans; the majority of these, however, are rare zoonoses and only cause localized skin lesions (109).

1.1.1. Smallpox and the origin of vaccination

In the late 1700's, the British physician Edward Jenner pioneered an approach that changed the world of microbiology. By inoculating patients with a related poxvirus from cows, known as cowpox virus, he effectively provided long-term immunity against smallpox (167). Dr. Jenner referred to the inoculation material as "vaccinia", from the Latin word "vacca" meaning "cow", and the concept of vaccination was officially born (167). Over the next two centuries, with the help of an intensive worldwide vaccination protocol led by the World Health Organization, smallpox was successfully eradicated in 1980 (323, 383). To date, variola virus remains the only viral pathogen that has been eliminated from the planet, and this effort remains the gold standard for vaccination protocols (383).

Table 1.1 *Poxviridae* Family

Subfamily	**Genus**	**Species Members**
Chordopovxirinae (vertebrate poxviruses)	*Orthopoxvirus*	Vaccinia, variola, ectromelia, monkeypox, cowpox, camelpox
	Avipoxvirus	Fowlpox, canarypox, quailpox
	Leporipoxvirus	Myxoma, rabbit fibroma, Shope fibroma
	Suipoxvirus	Swinepox
	Molluscipoxvirus	Molluscum contagiosum
	Parapoxvirus	Orf virus, bovine popular stomatitis
	Capripoxvirus	Goatpox, lumpy skin diseases
	Yatapoxvirus	Yaba monkey tumour
Entomopoxvirinae (insect poxviruses)	*Entomopoxvirus A*	*Melolontha melolontha entomopoxvirus*
	Entomopoxvirus B	*Amsacta moorei entomopoxvirus*
	Entomopoxvirus C	*Chironimus luridus entomopoxvirus*

1.1.2. Vaccinia virus

The virus used by the World Health Organization to vaccinate against smallpox was vaccinia virus, a related member of the *Orthopoxvirus* genus (383). Originally believed to have descended from either cowpox or horsepox, vaccinia virus has been cultivated primarily by human-to-human passage and in tissue culture for the last 200 years (47, 109). As such, vaccinia virus is considered genetically distinct from the other *orthopoxvirus* species (109), and has no known natural host. Although vaccinia virus does not normally cause disease in humans, it is antigenically similar enough to variola virus to provide long-term immunity (47). This, combined with the high stability of the vaccine, aided in the immense success of this vaccination program (323).

Vaccinia virus (VV) is considered the prototypic poxvirus, and is amenable to genetic manipulation through a multitude of available DNA recombination tools (50). VV has also been used extensively as a gene delivery mechanism, as its large DNA genome makes it relatively easy to insert foreign DNA sequences for protein expression in mammalian cells (50, 100). Despite the fact that the natural host for VV is unknown, VV remains an excellent model system in which to study virus:host interactions due to its complex genome and vast array of anti-immune mechanisms (169). In response to the selective pressures initiated by the host immune system, poxviruses such as vaccinia virus encode a vast array of proteins which modulate both innate and adaptive immune responses (Table 1.2) (21, 105)

1.1.3. Ectromelia virus

Ectromelia virus (EV), more commonly known as mousepox, is another member of the *Orthopoxviridae* that was first described in 1930 (220). A natural pathogen of mice, EV is characterized by the generalized swelling and eventual amputation of the infected foot, and is associated high rates of mortality in inbred stocks of mice (110, 220). The medical definition of ectromelia is a congenital imperfection or loss of limb, and since this particular disease was quite clearly not a congenital defect but rather the result

Table 1.2. Immune modulatory mechanisms encoded by vaccinia virus

Gene	Mode of action	Reference
A46R	Toll-like receptor inhibition	(38)
A52R	Toll-like receptor/NF-κB inhibition	(38)
B15R	Secreted interleukin-1β receptor	(327)
B8R	Interferon-γ receptor homologue	(7)
B19R	Interferon-α/β receptor homologue	(342)
B29R/C23L	Chemokine binding protein	(127, 322)
C11L	Viral growth factor	(31, 277)
CrmA/Spi-2	Intracellular serine protease inhibitor	(274)
CrmB, CrmC	TNF receptors	(159, 321)
E3L	dsRNA binding protein	(57, 58)
F1L	Mitochondrial inhibitor of apoptosis	(382)
K1L	NF-κB inhibitor	(315)
K2L	Serine protease inhibitor	(191, 406)
K3L/CrmD	eIF2α homologue, inhibits protein translation	(87)
M2L	NF-κB inhibitor	(121)
N1L	NF-κB inhibitor	(96)

of an infectious agent, the agent was termed *infectious ectromelia* (220). Mice are typically infected with EV through small abrasions in the skin from sources such as infected bedding, whereupon a primary lesion forms. Virus rapidly travels to the regional lymph nodes, proceeds to cause primary viremia and subsequently migrates to the liver and spleen (47, 110). Viral replication occurs in these internal organs, and if the mouse has not succumbed due to internal organ failure, secondary viremia occurs that leads to a generalized rash 7 days post-infection. The rash seen in EV-infected mice is similar to the rash produced by smallpox, hence the adoption of the name 'mousepox' (110). Interestingly, the pattern of EV replication in internal organs prior to secondary viremia appears to hold true for a number of viral infections that produce rashes (47, 110).

Various mouse genotypes demonstrate a wide range of susceptibilities to EV (102, 110). Ectromelia virus is also antigenically similar to VV, as vaccination of mice with vaccinia virus provides immunity against EV infection (110). The pattern of disease in mice can be readily manipulated by altering mouse genotype, virus strain, dose, and route of infection, making EV one of the best models for studying poxviral pathogenesis (110). EV strain Moscow (EVM) is one of the most thoroughly studied and virulent strains (110). The genome of EVM has been fully sequenced (62), and is roughly 175kb in size, shows 67% A+T content, and encodes 175 predicted open reading frames.

1.1.4. The poxviral genome, virus structure and life cycle

Poxvirus virions appear as brick-like particles approximately 250-350nm in size (Fig. 1.1*A*), making them visible by light microscopy. The virion consists of a phospholipid membrane surrounding a core structure, which contains the poxviral genome and required proteins for early viral replication (237). Orthopoxviral genomes are linear double-stranded DNA molecules approximately 200kb in size that have covalently closed terminal hairpin loops, and encode approximately 200 different open reading frames (Fig. 1.1*B*) (237). As virus replication occurs in the cytoplasm of infected cells, poxviruses encode many of the enzymes required for gene transcription and DNA

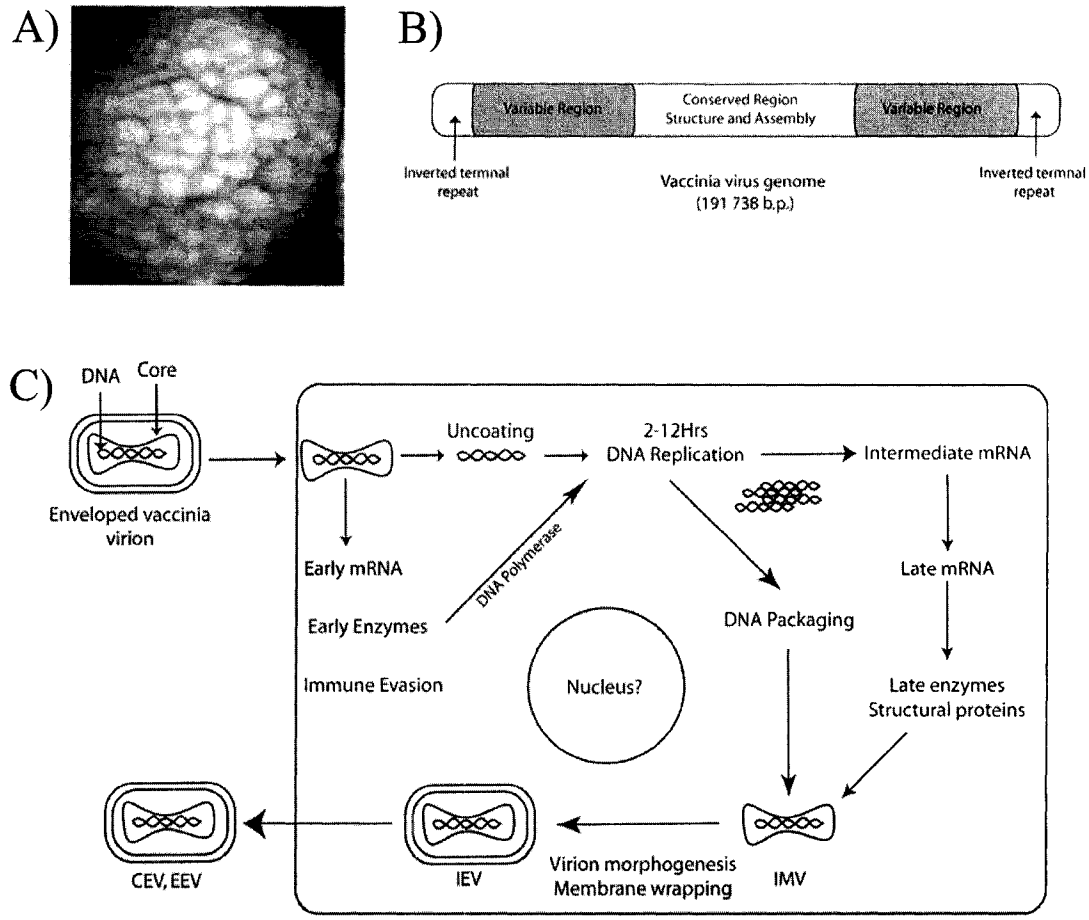

Figure 1.1. Vaccinia virus virion, genome, and replication
A, Atomic force micrograph of a vaccinia virus 'brick-shaped' virion (adapted from J. Virol. 2003. 77:6332). *B*, Structure of the vaccinia virus linear dsDNA genome. The central fragment encodes housekeeping genes for virus replication, while the variable regions encode host-specific genes. *C*, Depiction of the vaccinia virus life cycle. Following infection, early mRNA is synthesized immediately, producing enzymes (*ie.* DNA polymerase) that are essential for virus replication. Other early proteins are involved in host immune evasion. Following DNA replication, intermediate and late genes are transcribed, and newly synthesized viral DNA is packaged in new intracellular mature virions (IMV). These particles are then enveloped into intracellular enveloped virions (IEV), and either remain attached to the plasma membrane as cell-associated enveloped virus (CEV), or are released as extracellular enveloped virus (EEV) (Adapted from B.Moss. Poxviridae. *In*: Fields Virology, 3rd Edition. 1996. Raven Publishers.)

replication (Fig. 1.1*C*). These open reading frames are typically found within the central region of the genome and are highly conserved across poxviral species (Fig. 1.1*B*). The variable termini of the genome typically encode proteins involved in host-specific responses (Fig. 1.1*B*) (182, 237, 258).

Infectious enveloped virions attach to cells via an unknown receptor, and fuse with the host plasma membrane (Fig. 1.1*C*). The virus core is released into the cytoplasm, and viral transcription of early genes begins immediately (Fig. 1.1*C*). Early genes encode for various immune evasion proteins, DNA replication proteins, growth factors, and intermediate gene transcriptional regulators (237). DNA replication begins following synthesis of the viral DNA polymerase, and this is required for the subsequent synthesis of intermediate transcription factors and the transcription of late genes. Late gene products typically encode enzymes and structural proteins involved in new virion synthesis (Fig. 1.1*C*). Virus assembly occurs in cytoplasmic viral factories and produces intracellular mature virus (IMV), which are the most abundant virus particles present. These particles are fully infectious and are either retained until cell lysis, or are wrapped by membranes to form intracellular enveloped virus (IEV). IEV particles are able to travel to the cell surface via microtubules, and following further membrane wrapping, are released through plasma membrane fusion as cell-associated enveloped virus (CEV) (Fig. 1.1*C*) (237, 325). CEV particles can then either migrate towards neighbouring cells through the polymerization of actin tails in the cytoplasm, or are released as extracellular enveloped virus (EEV) for long range dissemination (237, 325). CEV and EEV are indistinguishable from each other, except for the fact that CEV are still associated with the plasma membrane (325).

1.1.5. Modulation of the immune system by poxviruses

In order to counteract a viral infection and protect itself from disease, the body uses a number of immune mechanisms to fend off viral infections. The primary response is the recruitment of "death-inducing" cells, such as natural killer (NK) cells or cytotoxic

T lymphocytes (CTLs), which recognize virally-infected cells and induce their destruction through apoptosis (18). Other immune tactics involve the production of cytokines/chemokines, interferons, complement, and antibodies, all of which not only aid in eliminating viruses and infected cells, but also help to establish anti-viral states in uninfected cells (112, 303, 305, 357). Due to the harsh environment presented by the human immune system, it is not surprising that viruses have adapted immune evasion strategies to survive *in vivo*.

A vast number of poxviral proteins have been identified that interfere with the immune response (169, 303), and these represent an incredibly diverse family of immune modulators. VV alone encodes for a number of proteins which interfere with cytokine signaling, the interferon response, toll-like receptor signaling, and nuclear-factor kappa-B (NF-κB) responses (Table 1.2)(169, 303). These proteins are also believed to be important in defining the host-range of poxviruses, as no single immune-evasion protein identified to date is expressed by all members of the *Chordopoxvirinae* (169, 303). Not surprisingly, poxviruses also express a number of proteins which interfere with programmed cell death, or apoptosis (349).

1.2 Apoptosis

1.2.1. Apoptosis

Apoptosis, or programmed cell death, was first described in 1972 (175), and the basic mechanisms are conserved from invertebrates to mammals. Indeed, much of our basic understanding of apoptosis was originally determined through studies in the worm *Caenorhabditis elegans* (205), and a number of proteins involved in executing apoptosis are conserved from *C. elegans* to mammals. Although the initial idea of a specialized cell suicide mechanism was viewed with skepticism, it is now clear that apoptosis plays a critical role in development, tissue homeostasis, and the elimination of unwanted cells by the immune system (151). Specialized immune effector cells, such as CTLs, play a key role in removing virus-infected cells through the induction of apoptosis (18, 273, 285). In

response, a large number of viruses have evolved mechanisms to block apoptosis, thereby ensuring successful replication and dissemination (24, 283).

Apoptotic cells display characteristic features such as DNA fragmentation, chromatin condensation, mitochondrial dysfunction, and plasma membrane blebbing (75, 151). These blebs, or apoptotic bodies, contain the cytoplasmic contents of the dying cell, and are engulfed by phagocytes to prevent an inflammatory response (75). Apoptosis is tightly regulated by the cleavage and activation of a family of cysteine proteases, known as caspases (311, 356). Caspase activation requires proteolytic processing at internal aspartate residues to convert the normally inactive zymogen to a fully active protease. Fourteen caspases have been identified in mammals. Certain caspases are necessary for cytokine maturation and inflammation, such as caspases 1, 4 and 5, while other caspases are directly involved in the initiation and execution of apoptosis (114). During apoptosis, initiator caspases, such as caspases 8, 9 and 10, can directly activate executioner caspases, such as caspases 3, 6 and 7, which are ultimately responsible for the proteolytic cleavage of a large number of cellular proteins leading to death of the cell (114). Consequently, tight regulation of caspase activity is vital within a healthy cell and is controlled by both cellular- and pathogen-encoded proteins (283, 328).

Apoptosis can be triggered by both extrinsic and intrinsic signals (Fig. 1.2). The extrinsic receptor-mediated pathway is activated through the binding of ligands to their appropriate death receptors. Ligands produced by cytotoxic cells, such as Fas ligand (FasL) or tumour necrosis factor (TNF), can interact with their receptors, Fas and TNF receptor 1 (TNFR1), on the cell surface (15, 16). This results in receptor trimerization and recruitment of caspase 8 to the intracellular domain of Fas and TNFR1 (15). Caspase 8 activation occurs via an interaction with the adaptor proteins Fas-associated death domain (FADD) and/or TNFR-associated death domain (TRADD) (Fig. 1.2)(15). In cells which recruit and cleave a high amount of caspase-8, caspase-3 can be directly cleaved and activated by active caspase-8 (292, 293, 400). In many cell types, however, only a small amount of caspase 8 is activated, and an amplification of the signal is required (212). This

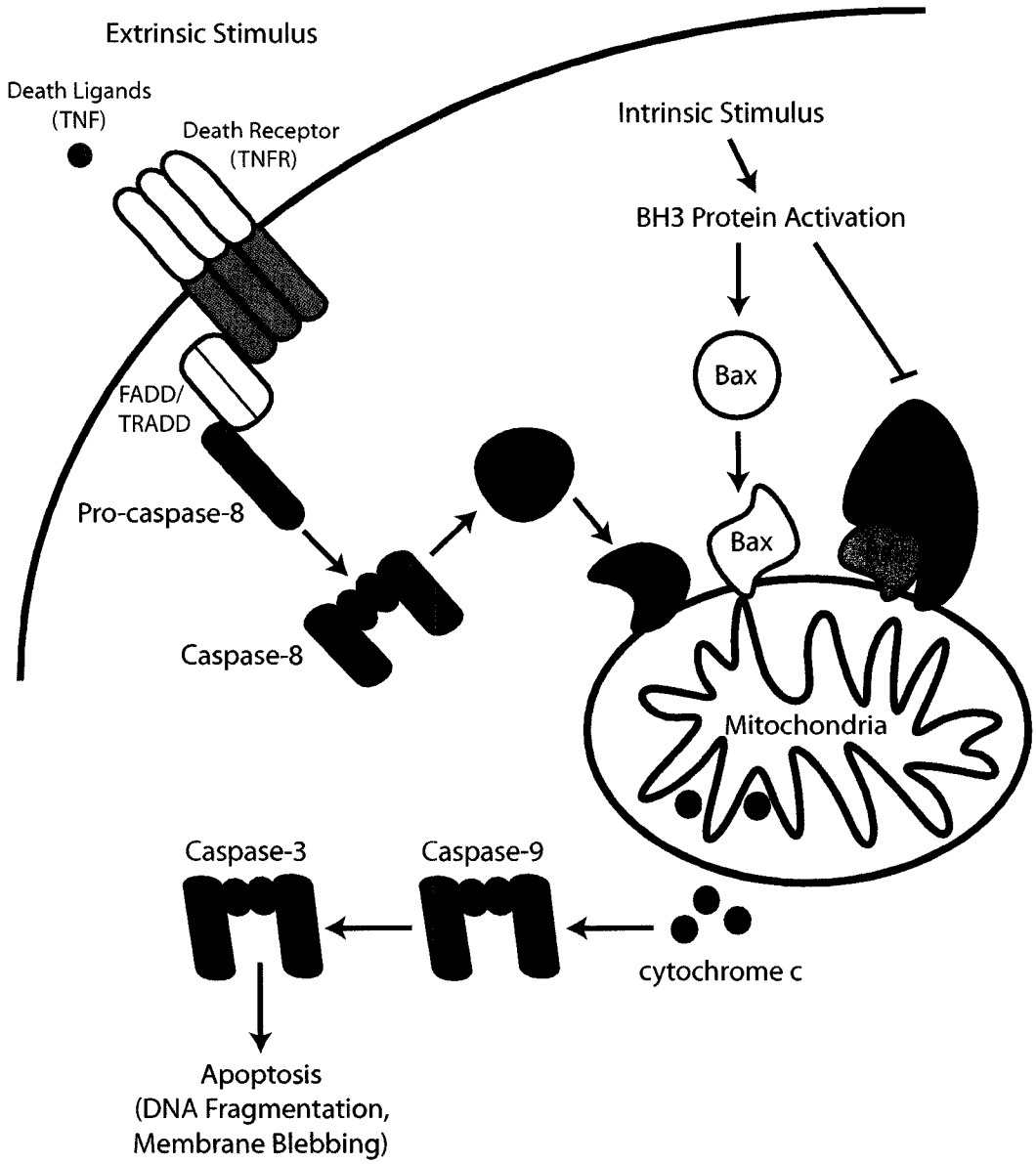

Figure 1.2 Extrinsic and intrinsic apoptotic stimuli.
Extrinsic apoptotic stimuli such as tumor necrosis factor (TNF) stimulate death receptor trimerization. Recruitment of Fas-associated death domain (FADD) or TNFR associated death domain (TRADD) leads to caspase 8 cleavage which cleaves and activates Bid. Activation of Bid results in its translocation to the mitochondria where it activates the pro-apoptotic proteins Bak and Bax. This results in mitochondrial membrane permeabilization and release of pro-apoptotic factors (cytochrome c), which activate downstream effector caspases (caspases 9 and 3) resulting in apoptosis. Intrinsic stimuli, in contrast, directly activate BH3-only proteins, which either directly activate Bak and Bax, or repress anti-apoptotic Bcl-2 proteins.

amplification requires the involvement of the intrinsic apoptotic pathway, where signals converge at the mitochondria to facilitate the downstream activation of executioner caspases (Fig. 1.2)(212, 292, 293). This intrinsic apoptotic pathway is also stimulated by a number of intracellular signals such as DNA damage, growth factor withdrawal, dsRNA, or virus infection itself, and absolutely requires the involvement of the mitochondria to execute death of the cell (Fig 1.2).

1.2.2. Mitochondria and apoptosis

Mitochondria were first characterized as small, membrane-wrapped organelles which generate ATP to provide biochemical energy for the cell. Believed to be bacterial in origin, mitochondria contain small circular genomes which encode a small number of proteins involved in electron transport, transcription, and translation (48, 217). Most mitochondrial proteins, however, are derived from nuclear genes, and are imported or localized to the mitochondria through specific localization signals or import mechanisms (229, 276).

The mitochondrion is an enveloped organelle consisting of an outer and inner membrane, an intermembrane space (IMS), and the matrix which is bound by the inner membrane (Fig. 1.3). The inner membrane is nearly impermeable to all molecules, including protons, as this membrane maintains the electro-chemical gradient generated by the electron transport chain (129, 233, 234). This gradient is essential for the bioenergetics of the cell as it facilitates ATP production, and is referred to as the inner mitochondrial membrane potential (233, 234). This membrane potential can be detected experimentally using cationic fluorochromes, such as tetramethylrhodamine ethyl ester (TMRE), which are specifically pumped across mitochondrial inner membranes with an intact membrane potential (228). Interestingly, long-lasting loss of the mitochondrial membrane potential, referred to as permeability transition (PT), is frequently associated with apoptosis (221). The inner membrane is comprised of a complex series of folds (cristae) that essentially form another compartment within the mitochondria, the

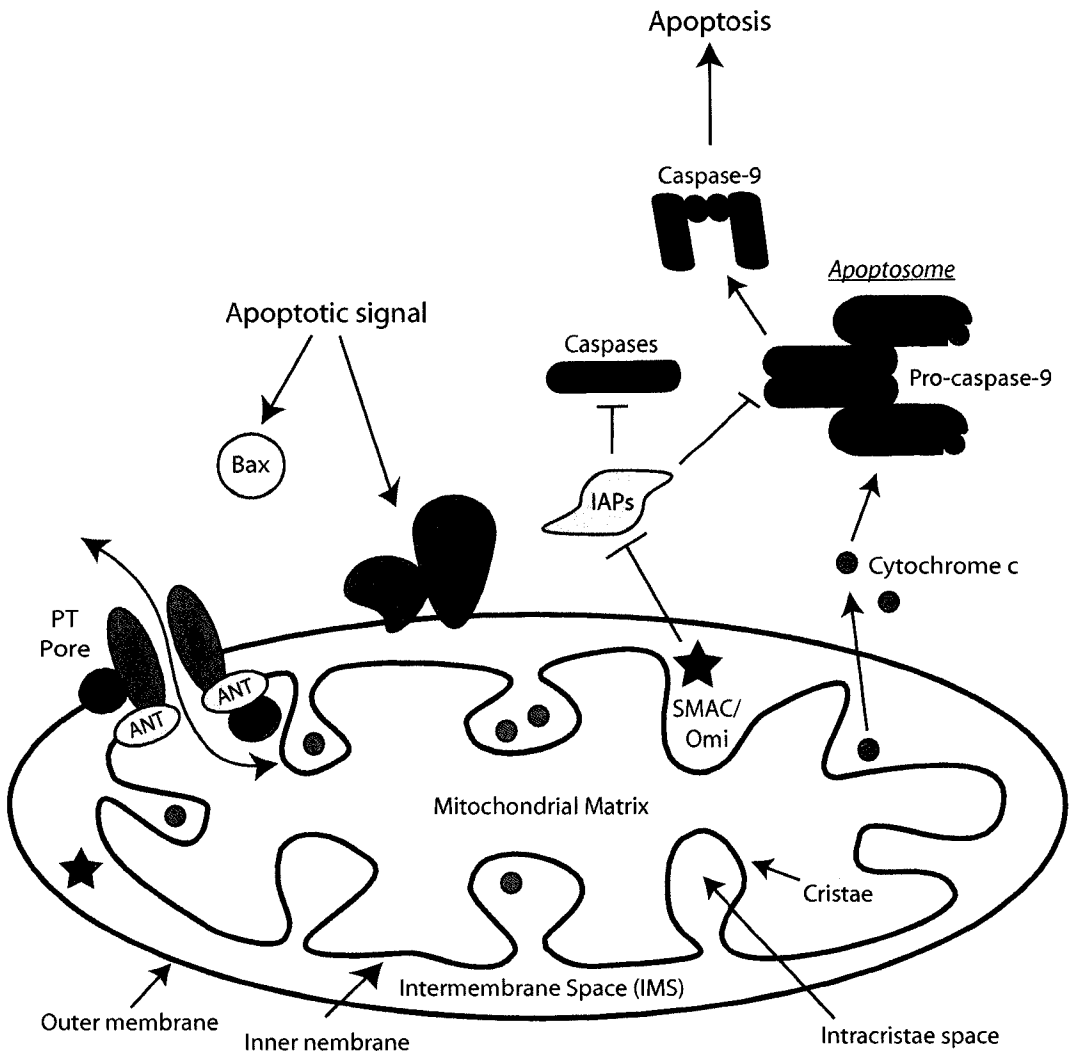

Figure 1.3. Mitochondria, cytochrome c, and the apoptosome.
Mitochondria are comprised of two membranes (inner and outer), an intermembrane space, and the internal matrix. The inner membrane folds to form distinct cristae and intracristae spaces, which contain >90% of the mitochondrial cytochrome c. Release of pro-apoptotic proteins, such as cytochrome c, SMAC, and Omi results in the activation of downstream caspases. Cytochrome c binds APAF-1 and pro-caspase-9 to form the apoptosome, cleaving and activating caspase-9, which leads to downstream caspase activation and apoptosis. SMAC and Omi inhibit inhibitors of apoptosis (IAPs), which are responsible for inhibiting executioner caspases. PT; permeability transition; IMS, intermembrane space; VDAC, voltage dependent anion channel; ANT, adenine nucleotide transporter; CypD, cyclophilin D; PBR, peripheral benzodiazepine receptor; SMAC, second mitochondrial activator of caspases.

intracristae space (ICS) (Fig. 1.3). This ICS compartment contains the majority of cytochrome c, which is critical for the induction of mitochondrial-mediated apoptosis (299).

The outer membrane, in contrast, is generally permeable to small molecules less than 5 kDa in size (185). This barrier is tightly regulated, nonetheless, by the presence of the abundant protein known as the voltage dependent anion channel (VDAC) (185). Through specific regulatory mechanisms that are still controversial, apoptosis induces the permeabilization of the outer mitochondrial membrane, resulting in the release of pro-apoptotic proteins into the cytosol (Fig. 1.3) (98, 130, 149, 207, 341). Indeed, outer mitochondrial membrane permeability is typically detected biochemically by assessing the subcellular localization of proteins normally sequestered in the intermembrane space of the mitochondria (98, 207, 287).

1.2.3. Cytochrome c and its involvement in apoptosis

Over a decade ago, mitochondria were shown to be intimately involved in the apoptotic cascade. A number of pro and anti-apoptotic proteins were shown to localize to the mitochondria, but why mitochondria were involved in regulating apoptosis remained a mystery. It was eventually discovered that the mitochondrial protein cytochrome c could induce caspase-activation and apoptosis (207). Cytochrome c is a 15kDa protein that is part of the electron transport chain, and is localized within the cristae of healthy mitochondria (Fig. 1.3)(25). During apoptosis, however, cytochrome c is dramatically released from the mitochondria into the cytosol and outer mitochondrial membrane permeabilization is required for this event (Fig. 1.3) (66, 130, 207). Cytosolic cytochrome c interacts with the adapter molecule apoptosis protease activating factor-1 (Apaf-1) and pro-caspase-9, forming the 'apoptosome' (Fig. 1.3) (201, 400). Procaspase-9 is then cleaved in an ATP-dependent manner into activated caspase-9, which can then cleave other 'effector' caspases such as caspase-3, leading to the systematic destruction of the cell. Cytochrome c release is required for apoptosome formation, as cells expressing a

membrane-tethered form of cytochrome c that is not released from mitochondria are protected from several apoptotic stimuli (146). Other mitochondrial factors have also been characterized that have pro-apoptotic effects when released. Proteins such as the second mitochondrial activator of caspases (SMAC/Diablo), high temperature requirement protein A2 (HtrA2)/Omi, apoptosis-inducing factor (AIF), and endonuclease G (EndoG) are also released during apoptosis (98, 106, 149, 200, 339, 341). EndoG and AIF act in the nucleus to induce DNA cleavage events (200, 339), while SMAC/Diablo and Omi/HtrA2 activate executioner caspases by inhibiting a group of anti-apoptotic proteins known as the inhibitors of apoptosis, or IAPs (Fig. 1.3)(55, 98, 149, 222, 341, 368). IAPs function downstream of the mitochondria by directly binding to caspase-9 to induce its degradation through ubiquitination, thereby maintaining a non-apoptotic state (367).

1.2.4.1. Mitochondrial control of apoptosis: The Bcl-2 family and BH domains

The mitochondrial events during apoptosis are tightly governed by a group of proteins known as the Bcl-2 family of proteins (Fig. 1.4)(77, 130, 134). The namesake of the family, Bcl-2, was originally identified as a proto-oncogene from a B-cell lymphoma (Bcl) (33, 73, 117, 154, 249, 358, 366). Bcl-2 localizes predominantly to the mitochondria and prolongs cell survival, even in the presence of a variety of strong pro-apoptotic stimuli, thereby accounting for the pro-oncogenic properties of this protein (33, 117, 154, 249, 366). Since the initial identification of Bcl-2, a number of other pro- and anti-apoptotic proteins have been discovered that show homology to Bcl-2 (Fig. 1.4). These proteins have been grouped into the "Bcl-2 family", and display amino acid homology within one of four so-called Bcl-2 homology (BH) domains (Fig. 1.5) (77, 134), even between pro- and anti-apoptotic members.

The Bcl-2 family is subdivided into anti-apoptotic (*i.e.* Bcl-2, Bcl-x_L, Mcl-1), multi-domain pro-apoptotic (*i.e.* Bak and Bax), and the BH3-only proteins (*i.e.* Bid, Bad, Bim, Bmf, Noxa, Puma, Nbk/Bik, Hrk) (Fig 1.4) (32, 183, 209). The anti-apoptotic

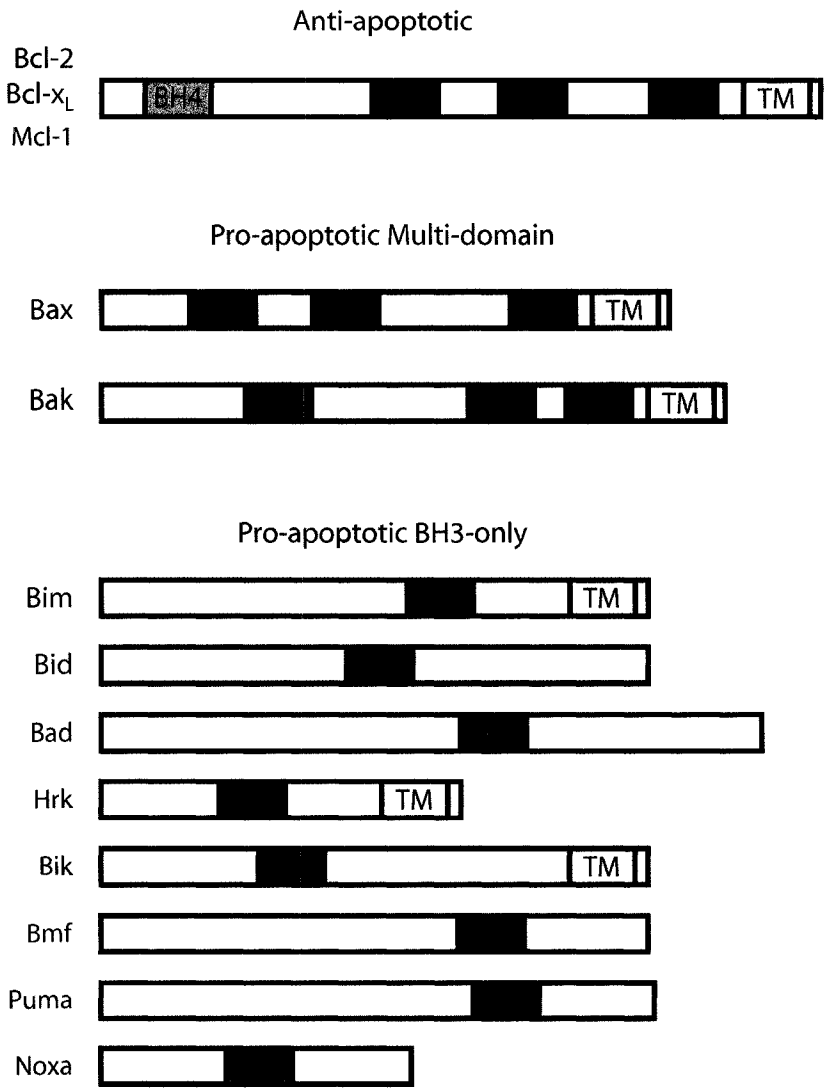

Figure 1.4 The Bcl-2 Family.
The Bcl-2 family of proteins can be separated into three classes: (1) the anti-apoptotic multi-domain proteins, which typically possess all four BH domains (BH1-4); (2) the pro-apoptotic multi-domain proteins (Bak and Bax), which contain BH1, 2, and 3 domains; (3) the BH3-only proteins, which possess only the BH3 domain, and certain members possess a transmembrane tail (TM) for mitochondrial localization.

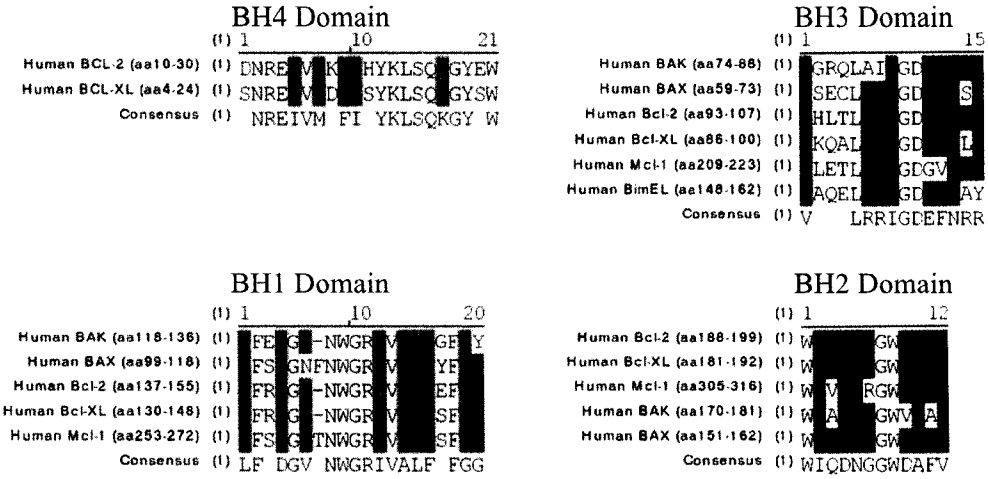

Figure 1.5. Alignment of BH domains from Bcl-2 family members.
The BH domains from Bak, Bax, Bcl-2, Bcl-x_L, Mcl-1, and BimEL were aligned using Align-X. Consensus sequences are listed below each alignment, with identical residues shaded in yellow, and similar residues in green.

members of the Bcl-2 family typically possess all 4 BH domains and prolong cell survival by inhibiting mitochondrial membrane permeabilization and cytochrome c release (179). The N-terminal BH4 domain is restricted to anti-apoptotic members, and caspase-mediated cleavage of the BH4 domain from Bcl-2 converts Bcl-2 into a pro-apoptotic protein (63), suggesting this region is required for inhibition of apoptosis. The BH1, 2 and 3 domains are found in both pro- and anti-apoptotic Bcl-2 family proteins, and the BH3-only proteins, as their name implies, only possess the BH3 domain (Fig. 1.4). Overall, BH domains have been implicated in mediating protein:protein interactions between family members (364). Indeed, mutation or deletion of BH domains greatly affects the function of Bcl-2 family members (1, 69, 399), and BH3 domain-containing peptides readily interact with anti-apoptotic family members (194, 392).

1.2.4.2. Structure of anti-apoptotic Bcl-2 family members

Bcl-x_L was the first Bcl-2 family protein to be structurally determined (239). Bcl-x_L consists of two central hydrophobic alpha helices surrounded by six other amphipathic alpha-helices (Fig. 1.6*A*). Interestingly, the structure of Bcl-x_L resembles the membrane spanning domain of bacterial pore-forming toxins such as diphtheria toxin and colicins, which can insert into membranes to facilitate the permeabilization of eukaryotic cell membranes (71, 232, 239). This led to the original hypothesis that Bcl-2 family members may form pores in the outer mitochondrial membrane, thereby controlling the release of pro-apoptotic proteins from mitochondria (294). In support of this, it has been demonstrated that Bcl-2 and Bcl-x_L can form ion channels in synthetic lipid bilayers (232, 294).

The structure of Bcl-x_L also revealed that the BH1, 2, and 3 regions in Bcl-x_L are clustered on the surface of the protein and form an expanded hydrophobic groove (Fig. 1.6*B*) (239). This groove is believed to be a 'binding pocket' which can interact with domains from pro-apoptotic proteins such as Bad and Bak (Fig. 1.6*B*). Accordingly, the

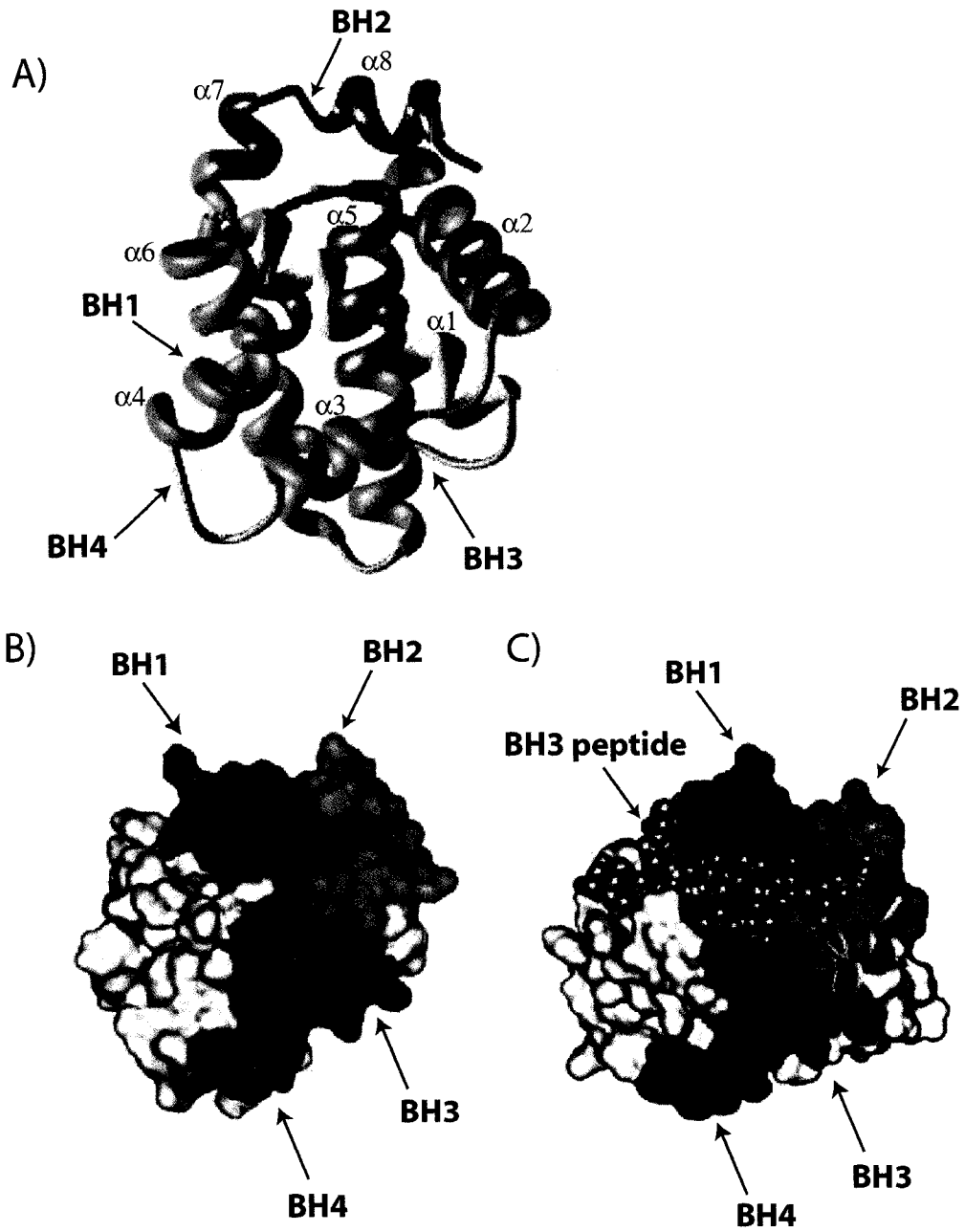

Figure 1.6. Structure of Bcl-x_L.
A, Ribbon diagram showing the anti-parallel alpha helices which comprise Bcl-x_L (adapted from Bioch. Bioph. Acta. 2004. 1644:83).
B, Globular representation of Bcl-x_L, with the BH1-4 domains indicated (Adapted from Nat. Rev. Cancer. 2002. 2:647).
C, Globular representation of Bcl-x_L bound to the BH3 peptide from Bak, which resides in the surface exposed hydrophobic pocket (Adapted from Nat. Rev. Cancer. 2002. 2:647).

BH3 peptide from the pro-apoptotic protein Bak interacts with this hydrophobic groove, supporting this hypothesis (Fig. 1.6*C*) (290).

Similar to Bcl-x_L, Bcl-2 is also comprised of a series of eight α-helices and displays a surface-exposed hydrophobic groove (259). The hydrophobic groove from Bcl-2 is elongated and much wider than that of Bcl-x_L, and alters the ability of Bcl-2 to interact with BH3 domains (239, 259). Indeed, BH3 peptides from Bak and Bad interact with the Bcl-2 groove at a 10-fold lower affinity than Bcl-x_L (65, 260). Because of this altered binding capacity, it remains to be seen what specific roles Bcl-2 and Bcl-x_L play in the inhibition of apoptosis. Despite these differences, both Bcl-2 and Bcl-x_L interact with BH3 domains as a mechanism to prevent Bak and Bax activation (65).

1.2.5. Multi-domain pro-apoptotic Bcl-2 family members: Bak and Bax

Two critical members of the Bcl-2 family are the pro-apoptotic multi-domain family members, known as Bak (Bcl-2 antagonist/killer) and Bax (Bcl-2 associated X protein). Cells deficient in both Bax and Bak are completely resistant to cytochrome c release, demonstrating the collective importance of these two pro-apoptotic proteins (91, 204, 385). As such, the activation of Bax and Bak must be tightly regulated to suppress death (91, 204, 385).

1.2.5.1. Bak

Bak localizes constitutively to the mitochondria via a C-terminal hydrophobic domain which inserts into the outer mitochondrial membrane (132). Following an apoptotic stimulus, Bak undergoes a conformational change revealing an N-terminal epitope and forms high-molecular weight oligomers (Fig. 1.7)(131, 132, 384, 404). The structure of Bak is similar to other Bcl-2 family members, in that Bak consists of a series of eight anti-parallel alpha-helices (235). Unlike anti-apoptotic Bcl-2 family members, Bak has a small, irregular surface hydrophobic groove which is not available for BH3-

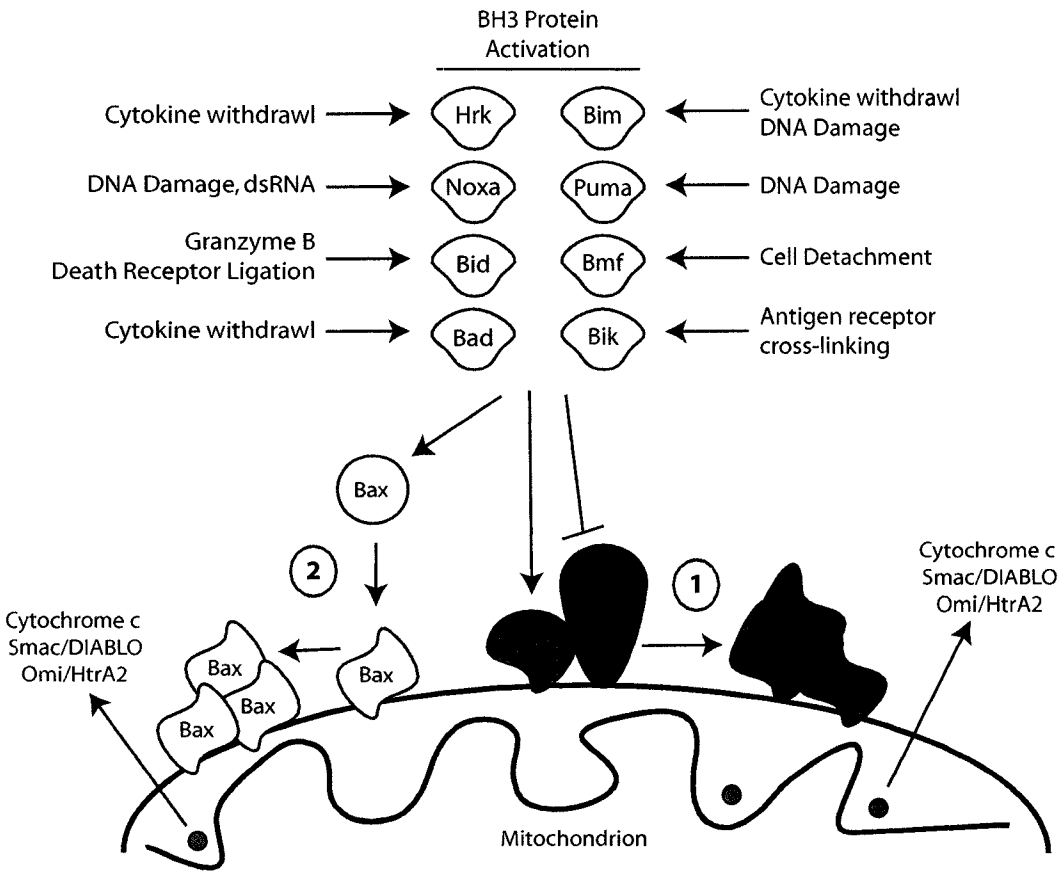

Figure 1.7. Activation of Bak and Bax.
The pro-apoptotic multi-domain Bcl-2 family members Bak and Bax are activated following an apoptotic stimulus. Following an apoptotic insult, BH3-only proteins induce a conformational change in the mitochondrial-localized protein Bak, and Bak homooligomerizes into a high molecular weight complex (1). Bax, on the other hand, is normally cytosolic. During apoptosis, Bax also undergoes a conformational change that allows it to target and insert into the mitochondrial outer membrane (2). Bax reveals an N-terminal epitope and homooligomerizes into a high molecular weight complex. Activation of Bak or Bax facilitates mitochondrial membrane permeabilization and the release of pro-apoptotic proteins (cytochrome c, SMAC/Diablo, Omi/HtrA2).

peptide binding (235). Additional structural modeling of Bak in comparison with Bcl-x_L suggests that the BH3 region of Bak is hidden within the interior of the folded protein and is therefore inaccessible (235). Following a conformational change, however, the BH3 domain is revealed and Bak oligomerization at the mitochondria facilitates the release of cytochrome c via an unknown mechanism (Fig. 1.7). Bak-mediated cytochrome c release can occur in the absence of Bax and vice versa, suggesting that Bak and Bax are somewhat redundant in function (91, 385).

Other proteins, such as VDAC2, Mcl-1, and Bcl-x_L have been shown to interact with and regulate Bak activation (64, 391). The anti-apoptotic Bcl-2 family member Mcl-1 forms a complex with Bak at the mitochondrial membrane, perhaps to keep Bak in an inactive state (81, 195, 391). During DNA-damage-induced apoptosis, Mcl-1 is degraded, thereby freeing Bak for activation (81, 248). A short 16 amino acid peptide corresponding to the BH3-region from Bak can interact with Bcl-x_L (290), and apoptosis induced by BH3-peptides from Bak are also inhibited by Bcl-x_L expression (290).

1.2.5.2. Bax

Bax is a 21 kDa monomeric protein that, contrary to Bak, resides in the cytoplasm or is found loosely attached to intracellular membranes (156, 253). Following an apoptotic stimulus, Bax inserts into the outer mitochondrial membrane (Fig. 1.7) (126, 156, 393), and forms high molecular weight oligomers as seen by gel filtration and co-immunoprecipitation (12). Bax oligomerization and insertion into the mitochondrial outer membrane is required for Bax-mediated cytochrome c release, and is also completely inhibited by the overexpression of Bcl-2 (10, 12).

1.2.5.3. Bax Structure

Bax is comprised of eight amphipathic alpha helices and one hydrophobic alpha helix (α5) (Fig. 1.8) (340), and these alpha helices fold to create a hydrophobic pocket on

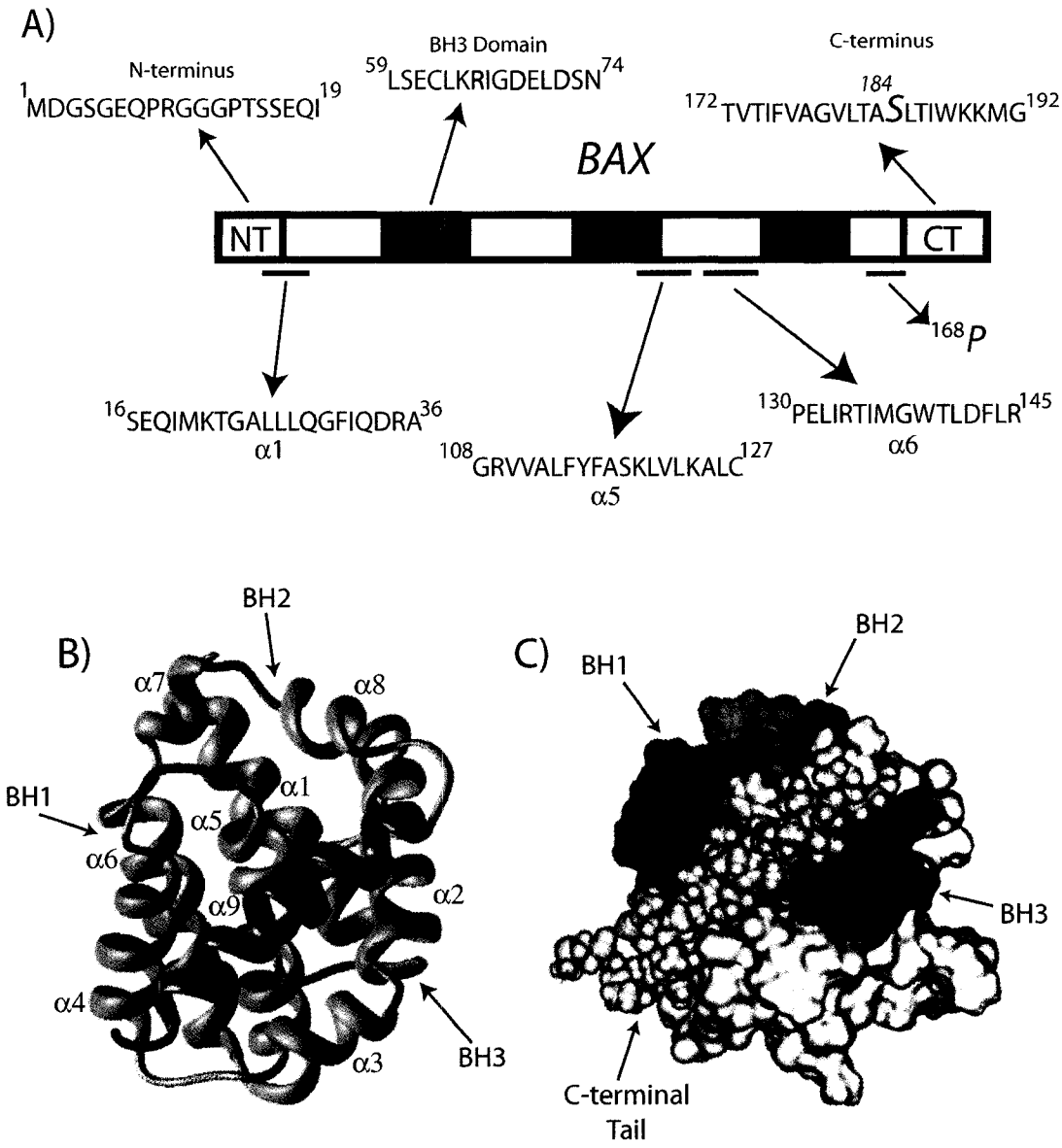

Figure 1.8. Structure of Bax.
A, Linear representation of the BH domains and alpha helices involved in Bax activation and targeting to the mitochondria. The C-terminal residues Pro168 and Ser184 which control Bax insertion into the mitochondrial memrbane, the N-terminal domain and the C-terminal hydrophobic tail are shown. The α5/α6 helices which comprise the 'pore-forming domain' of Bax are also shown. *B*, Ribbon diagram of the crystal structure of Bax, with the alpha helices labeled. The C-terminal α9 helix (in red) folds back onto the surface pocket of the protein, and helices 1, 5, an 6 are also not exposed (adapted from Bioch. Bioph. Acta. 2004. 1644:83).
C, Crystal structure of Bax, with the BH domains and the C-terminal tail coloured as in panel (A). The C-terminal tail (in yellow) is folded into the hydrophobic pocket. Also occluded are the BH3 domain and the α5/α6 helices, as seen in panel (B) (adapted from Nat. Rev. Cancer. 2002. 2:647).

the surface of the protein, similar to Bak and Bcl-x_L (Fig. 1.8). The hydrophobic pocket of Bax, however, is occluded by the C-terminal alpha helix (α9) which folds back and resides in the groove, rendering both the groove and the C-terminus inaccessible (Fig. 1.8*B* and *C*). This blockage of the hydrophobic pocket of Bax by the C-terminus also occludes the BH3 domain and additional alpha-helices, preventing Bax from dimerizing with other BH-containing proteins. Interestingly, the way in which the C-terminus folds into the hydrophobic pocket is structurally similar to how the BH3 peptide of Bak binds to the available hydrophobic pocket of Bcl-x_L (290).

1.2.5.4. Bax localization and insertion into the mitochondrial outer membrane

The C-terminus of Bax comprises a hydrophobic transmembrane domain which, in inactive Bax, is folded into the hydrophobic pocket (Fig. 1.8*C*)(340). Following an apoptotic stimulus, a conformational change frees the C-terminus, allowing Bax to insert into the mitochondrial outer membrane (12, 126). Although deletion of as few as five residues from the C-terminus of Bax eliminated mitochondrial targeting, gene fusions of green fluorescent protein (GFP) to the C-terminal 20 amino acids of Bax also did not target GFP to the mitochondria (244). However, when serine 184 (S184) was deleted from this fusion peptide, this construct localized to the mitochondrial outer membrane, implicating S184 in regulating the availability of the C-terminus (244). Bax mutants with a S184V substitution constitutively localize to the mitochondria, whereas other substitution mutants, such as S184K or S184D, do not translocate to the mitochondria, even during apoptosis (244). Interestingly, co-expression of Bcl-x_L does not inhibit mitochondrial insertion of Bax (S184V), but does inhibit cytochrome c release (245), suggesting that pro-survival Bcl-2 family members can inhibit Bax following translocation. Mutation of S184 of Bax is predicted to promote the dissociation of the hydrophobic tail from the hydrophobic pocket, thereby allowing Bax movement to the mitochondria and apoptosis (244, 245).

Intriguingly, Bax mutants lacking the C-terminal hydrophobic domain still appear to insert into the mitochondrial outer membrane and induce cytochrome c release during apoptosis (150). It has been suggested that the α5/α6 helices of Bax constitute a pore-forming domain which regulates cytochrome c release. Indeed, membrane topology studies revealed that the α5/α6 helices of Bax also insert into the outer mitochondrial membrane during apoptosis (9). As well, deletion of these helices and the C-terminal hydrophobic domain completely abolished mitochondrial insertion of Bax and cytochrome c release (150). Another residue, proline 168 (P168), has been implicated in regulating the targeting of Bax to the mitochondria, although P168 may regulate the availability of the pore forming α5/α6 helices (295).

Altogether, Bax may target to and insert into mitochondrial membranes via a two-step process. Upon release of the C-terminus of Bax, this hydrophobic domain initially inserts into the outer mitochondrial membrane, whereupon further conformational changes may allow insertion of the pore-forming α5/α6 helices. It has been proposed that Bax undergoes a significant conformational change when in contact with membranes (397). In support of the multiple helix insertion theory of Bax, Bcl-2 also appears to change its membrane topology during apoptosis (178). What specifically triggers Bax to adopt a membrane-spanning conformation remains unknown.

1.2.5.5. Bax conformation

The C-terminus is not the only domain of Bax which undergoes a conformational change during apoptosis. Early studies revealed that antibodies raised towards the N-terminus of Bax were only reactive against Bax from apoptotic thymocytes (157). One such antibody, anti-Bax(6A7) (158), was shown to recognize this activated form of Bax, indicating that the N-terminus of Bax undergoes a conformational change during apoptosis. The crystal structure of Bax later revealed that amino acids 13-19 are in fact hidden prior to an apoptotic stimulus (340). Various detergents can also alter the

availability of the N-terminus towards anti-Bax(6A7). Detergents such as Triton-X-100, Triton-X-114, or octyl-glucoside actually induce reactivity of Bax from healthy cells towards anti-Bax(6A7) (157). Dissolution of Bax in octyl-glucoside significantly altered the spectrum of crystallized Bax, supporting the idea of a detergent-induced conformational change in Bax (340). Other detergents such as CHAPS do not induce Bax reactivity towards anti-Bax(6A7), and are useful for examining the native conformation of Bax during apoptosis (157, 158). The N-terminal conformation appears to be controlled independently of the C-terminus as Bax (S184V) does not reveal the N-terminal epitope prior to apoptosis, but constitutively inserts into the mitochondria (244, 245).

In addition to the N- and C-termini, the BH3 domain of Bax is also hidden in healthy cells by the α9 helix which folds into the hydrophobic groove (340). Altogether, apoptotic stimuli induce a significant conformational change in Bax which reveals the BH3 domain, the hydrophobic groove, the C-terminus, and the N-terminal domain. These changes, in addition to binding to mitochondrial membranes, are believed to help reveal the pore-forming α5/α6 helices (9, 51). Recent observations describe Bax translocation to the mitochondrial membrane prior to undergoing a complete N-terminal conformational change (363), indicating that the events surrounding Bax activation are complex and remain to be elucidated.

1.2.5.6. Bax oligomerization and dimerization

Bax isolated from healthy cells is seen as a monomeric protein, while Bax isolated from apoptotic cells appears as a complex of approximately 260kDa in size as assessed by chemical cross-linking and gel filtration (12, 347). Stimuli such as tBid can induce Bax oligomerization and insertion into the outer mitochondrial membrane in a caspase-independent fashion (101, 282). Intriguingly, Bax does not oligomerize in the presence of purified tBid and liposomes. In fact, tBid only induced Bax oligomerization and insertion

when co-incubated with actual mitochondrial outer membrane vesicles (282). As well, mitochondria treated with proteinase K did not facilitate Bax oligomerization when incubated with tBid, implying that tBid-induced Bax oligomerization requires an additional mitochondrial protein, and not just a membrane surface (282). Bax oligomerization appears to be required for cytochrome c release, as recombinant oligomeric Bax, but not monomeric Bax, induces cytochrome c release in purified mitochondria (282). The exact mechanisms and interactions that induce and regulate Bax oligomerization are unknown.

It was observed using electron microscopy that Bax coalesces into massive clusters at specific sites at the mitochondrial outer membrane (245), and these clusters are required for apoptosis. A Bax mutant that constitutively localizes to the mitochondria, Bax (S184V), does not form clusters when co-expressed with the anti-apoptotic protein Bcl-x_L, suggesting that Bcl-x_L is able to inhibit Bax cluster formation and apoptosis (245). Bak was also seen to cluster at these sites, suggesting that Bak and Bax may function together to facilitate cytochrome c release. The significance of these sites remains unknown, although recent evidence suggests a connection between Bak and Bax and the ability of mitochondria to undergo membrane fission and fusion (171).

Whether Bax forms heterodimers with other proteins at the mitochondria is somewhat controversial. Several studies suggest that Bak and Bax can dimerize at the mitochondrial outer membrane during apoptosis (230, 337). As well, Bax heterodimerizes with Bcl-2 and Bcl-x_L in the presence of detergents such as Triton-X-100 and Triton-X-114 (158). Bax from apoptotic thymocytes, however, does not heterodimerize with either Bcl-x_L or Bcl-2, suggesting that Bax does not normally bind to these anti-apoptotic proteins either before or after an apoptotic stimulus (157). Bax targeting and activation are tightly regulated, so it is possible that Bax does not naturally dimerize with Bcl-2 during apoptosis, but can be induced to dimerize in the presence of strong detergents.

The temporal events regulating Bax translocation and oligomerization are still controversial. Bax can insert into mitochondria without oligomerization (9), although *in*

vitro studies show that Bax can also oligomerize in the absence of membranes (11, 133, 158), and Bax dimers and trimers could also be detected prior to Bax insertion into the mitochondrial outer membrane (101). Although Bax insertion and oligomerization are required for Bax-mediated cytochrome c release, the signals which induce these changes in Bax are still not well understood.

1.2.5.7. Proteins that regulate Bax activity

A number of non-Bcl-2-like proteins have been documented to regulate Bax activity. Humanin is a small, 3kDa peptide that can block Bax activation during apoptosis (403). 14-3-3 proteins also negatively regulate Bax, potentially keeping Bax in an inactive state until stimulated (359). Activation of the c-Jun N-terminal kinase pathway by cellular stress induces phosphorylation of 14-3-3 proteins, resulting in Bax dissociation and subsequent apoptosis (359). Ku70 interacts with and prevents Bax activation in the presence of an apoptotic stimulus (291). Previously shown to be required for repair of dsDNA breaks in the nucleus (37, 372), Ku70 also suppresses the mitochondrial translocation of Bax during apoptosis (291).

A number of other cellular proteins appear to induce the activation of Bax. Modulator of apoptosis-1 (Map-1) is a Bax-interacting protein that has a BH3-like domain and is enriched at mitochondria (344, 345). Knockdown of Map-1 levels using siRNA results in a decrease in apoptosis mediated by Bax but not Bak (344). Loss of the protein Bax-interacting factor 1 (Bif-1) also appeared to repress Bak and Bax activation (83, 343). Bif-1, a member of the endophilin B family that shows no homology to the Bcl-2 family, translocates to mitochondria during apoptosis and is required for maintenance of mitochondrial morphology (83, 164, 170). p53 has been shown to activate Bax at the mitochondrial membrane (67, 68). First identified as a nuclear transcriptional activator, p53 also localizes to the mitochondrial membrane and induces Bax activation (67, 68). One of the more intriguing Bax regulators identified to date is the oncoprotein Myc. Normally associated with gene transcription, Myc can induce apoptosis by

stimulating Bax activation (326). Interestingly, Myc is not required for Bax insertion during apoptosis, but both Bax oligomerization and cytochrome c release are suppressed in Myc-deficient cells (9, 326). Although the steps that regulate Bax activation are not well understood, it is apparent that a number of cellular proteins can regulate Bax activation and oligomerization to induce or inhibit apoptosis.

1.2.6. Mitochondrial membrane permeabilization

Mitochondrial membrane permeabilization is characterized by the release of mitochondrial proteins into the cytosol, a number of which are pro-apoptotic, such as cytochrome c, SMAC/Diablo, Omi/HtrA2, AIF, and EndoG (98, 149, 200, 339, 341). The activity of Bak or Bax is ultimately required for outer membrane permeabilization during apoptosis, as cells devoid of both Bak and Bax do not release cytochrome c (91, 385). Due to differences between *in vivo* and *in vitro* observations, mitochondrial membrane permeabilization is still controversial, so a number of theories have been proposed (Fig. 1.9) (130, 185, 300, 310).

It has been suggested that Bak and Bax can form pores in the outer mitochondrial membrane to directly permeabilize mitochondria (Fig. 1.9). Bax can directly permeabilize membranes following the integration and oligomerization of Bax into the outer mitochondrial membrane via helices 5, 6, and 9 (9). Indeed, Bax can insert into and form pores in synthetic liposomes which are large enough to allow the passage of proteins such as cytochrome c (11, 353).

Other studies suggest that Bax may cooperate with VDAC to facilitate mitochondrial membrane permeabilization (Fig. 1.9)(266, 313). VDAC is the most abundant outer mitochondrial membrane protein, and functions to permit the passage of small molecules across the outer membrane into the intermembrane space (76). VDAC activity also appears to be directly influenced by a number of Bcl-2 family members (312, 314, 335), although the overall role of VDAC in directly regulating cytochrome c release is controversial. VDAC2 has been shown to keep at least one pro-apoptotic

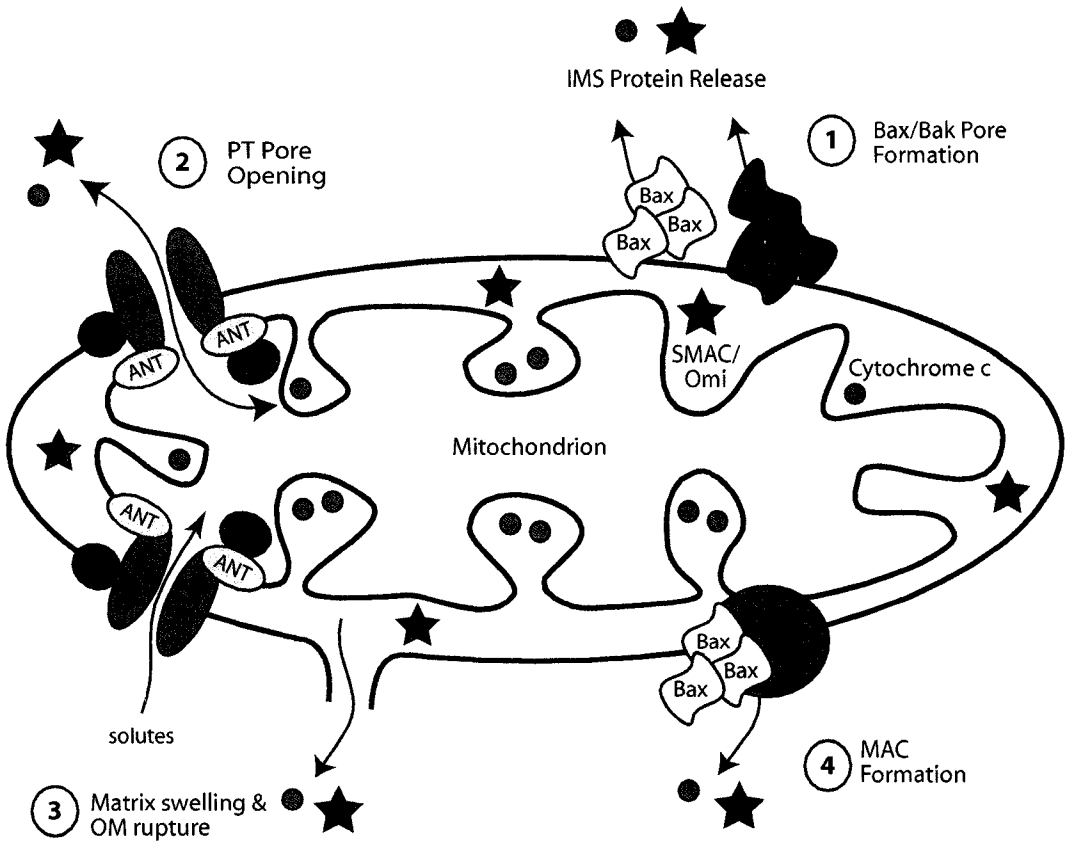

Figure 1.9. Mitochondrial membrane permeabilization.
The release of pro-apoptotic factors is believed to occur through one of four mechanisms, all of which require Bak and/or Bax: (1), oligomerized Bak and Bax forms pores in the outer mitochondrial membrane (OM); (2) Bak and Bax modulate existing pores such as the PT pore, which normally regulates the flow of small molecules in and out of mitochondria; (3) uncontrolled opening of pores results in matrix swelling, outer membrane rupture, and membrane permeabilization; (4) oligomerized Bax complexes with unknown proteins to form the mitochondrial apoptosis channel (MAC), which directly releases intermembrane space proteins (*i.e.* cytochrome c, SMAC, and Omi). PT; permeability transition; IMS, intermembrane space; VDAC, voltage dependent anion channel; ANT, adenine nucleotide transporter; CypD, cyclophilin D; PBR, peripheral benzodiazepine receptor; SMAC, second mitochondrial activator of caspases.

protein, Bak, inactive to prevent apoptosis (64), and VDAC2-deficient cells display enhanced apoptosis and Bak activation (64). It has also been reported that Bax does not modulate VDAC activity, arguing against the involvement of Bax with VDAC (281).

A third possible mechanism for cytochrome c release is that Bak and Bax may induce generalized mitochondrial dysfunction and matrix swelling, leading to rupture of the outer mitochondrial membrane (Fig. 1.9). VDAC, together with the adenine nucleotide transporter (ANT), peripheral benzodiazepine receptor (PBR) and cyclophilin D (CypD), comprise the permeability transition pore (PT pore) (139). The PT pore is a high conductance channel in the mitochondrial membrane that maintains the electrochemical gradient across the inner membrane by allowing small (<1.5kDa) solutes to pass into the matrix of mitochondria (78). Uncontrolled opening of the PT pore allows for the passage of ions into the matrix resulting in permeability transition, matrix swelling, and rupture and permeabilization of the outer mitochondrial membrane (130, 185). Mitochondrial permeability transition is seen in most, but not all, apoptotic cells (212). There is evidence against the involvement of the PT pore, however, as mitochondria deficient in the PT pore protein CypD are still able to undergo apoptotic cytochrome c release (17, 138, 242). Purified mitochondria from $CypD^{-/-}$ cells treated with recombinant Bax or Bak are also able to release cytochrome c, indicating that CypD and the PT pore is not solely responsible for mitochondrial membrane permeabilization during apoptosis (17, 242). The collapse of the mitochondrial membrane potential can also occur rapidly *after* permabilization of the outer membrane (125, 365, 400), and other approaches suggest that outer membrane permeabilization can occur in the absence of PT pore opening (34).

Another recent model has proposed that Bax cooperates as part of a mitochondrial apoptosis-induced channel (MAC) which facilitates cytochrome c release (Fig. 1.9) (256). MAC has been described as a high-conductance channel with a pore size of 4nm, which is large enough to allow for the passage of proteins such as cytochrome c (256). The exact components of MAC are not known, although oligomeric Bax is a likely constituent

as immunodepletion of Bax decreases MAC activity, and MAC activity is induced by Bax expression (92, 256). Bax is not believed to be the only component of MAC, as oligomeric recombinant Bax exhibits a pore conductance distinct from that of MAC *in vitro* (256). Indeed, MAC activity is still observed in cells lacking Bax, but not in cells doubly deficient in Bak and Bax, suggesting that Bak can also regulate MAC activity (92, 385). The core components of MAC are believed to be highly conserved across species, as the expression of human Bax in yeast mitochondria induced MAC activity (256). Aside from Bax, the proteins that comprise the MAC remain unknown.

1.2.7.1. BH3-only proteins

The third group of Bcl-2 family members contains the BH3-only proteins (Bid, Bim, Bad, Bik/Nbk, Noxa, Puma, Bmf and Hrk) (Fig. 1.4). These proteins are essential death sensors that respond to pro-apoptotic signals to activate Bak and Bax (Fig. 1.7) (330, 390). In the absence of Bak and Bax, BH3-only proteins are incapable of inducing apoptosis or cytochrome c release, highlighting the importance of Bak and Bax (91, 385).

Following an apoptotic stimulus, BH3-only proteins are specifically activated through various transcriptional or post-translational mechanisms. In response to death receptor induction, Bid is cleaved by caspase-8 into activated tBid (212, 376). Cytoskeletal changes induce the phosphorylation and activation of Bmf, resulting in Bmf release from myosin motor complexes (193, 271). In response to stimuli such as DNA damage, Noxa and Puma are transcriptionally up-regulated (243, 251). Bad activation is controlled by phosphorylation in response to changing cytokine levels (396, 402). Bik/Nbk and Hrk are transcriptionally regulated in response to cytokine withdrawl and antigen receptor cross-linking (41, 145, 165, 166).

Following activation, BH3-only proteins exert their pro-apoptotic effects by either directly activating Bak and Bax, or by binding and inhibiting the anti-apoptotic Bcl-2 family members (330, 390). BH3-only proteins have therefore been referred to as either 'direct activators' of Bax and Bak, or as 'death sensitizers'(61, 65, 187, 194, 236). tBid

and Bim can directly activate Bak and Bax, while the remaining BH3-only proteins may bind and repress the anti-apoptotic Bcl-2 family members, thereby "freeing" Bak and Bax for activation (61, 65, 187, 194, 236, 392). These hypotheses, however, are still controversial.

Binding between Bcl-2 and BH3-only proteins is believed to be mediated by the binding of the BH3-helix of the BH3-only protein with the Bcl-2 hydrophobic groove (206, 260, 394). This is supported by the crystal structure of the Bak BH3 domain in complex with Bcl-x_L which shows that the BH3 peptide binds to the hydrophobic pocket (290). Not all BH3-only proteins promiscuously interact with all of the pro-survival Bcl-2 family members. The BH3-only proteins Bim and Puma appear to interact with and suppress all of the anti-apoptotic family members, while other BH3-only proteins such as Bmf, Bid, and Noxa, selectively interact with and inhibit only certain pro-survival members (61, 187). Noxa, for instance, appears to bind only Mcl-1 (61), and Noxa can induce apoptosis by repressing Mcl-1, but not Bcl-x_L (187). By binding to anti-apoptotic Bcl-2 proteins, BH3-only proteins are believed to repress the survival advantage of these anti-apoptotic proteins, thereby sensitizing the cell to Bak and Bax activation and cytochrome c release.

1.2.7.2. Bid

Considered the classical BH3-only protein, Bid was first identified as a death-inducing protein that could interact with Bax and Bcl-2 (376). Similar to other Bcl-2 family proteins, Bid is composed of two central hydrophobic α-helices surrounded by six amphipathic helices, but lacks an obvious hydrophobic surface groove (72, 225). Bid also lacks an obvious hydrophobic tail, but instead contains two hydrophobic helices that can insert into the mitochondrial outer membrane (120). Bid is activated following death receptor activation and is proteolytically cleaved by caspase-8 into tBid (199, 212). tBid induces the activation and oligomerization of both Bak and Bax (93, 384), but cannot

induce cytochrome c release in the absence of both Bak and Bax (385). The BH3 domain of Bid is responsible for interacting with other Bcl-2 family proteins (376). Intriguingly, site-directed mutants of Bid within the BH3 domain that fail to interact with Bcl-2 but still interact with Bax are still capable of inducing apoptosis (376), supporting the hypothesis that tBid directly activates Bax.

1.2.7.3. Bim

Bim was originally identified as a novel BH3-only protein that promoted apoptosis (250). Bim is expressed as three different isoforms: EL, L, and S (extra-long, long and short, respectively), and all three of these isoforms have the capacity to induce apoptosis, with the shorter isoforms being more potent (250) (Fig. 1.10). Bim associates with Bcl-2 and Bcl-x_L *in vivo*, both of which inhibit the pro-apoptotic activity of Bim, while Bcl-2 mutants that lack survival function are correspondingly unable to bind to Bim (250). Cells deficient in Bim are resistant to apoptosis induced by stimuli such as cytokine withdrawl and microtubule alterations, and T-cells deficient in Bim no longer die when autoreactive (35, 36). In contrast, $Bim^{-/-}$ cells show no defect in apoptosis induced by FasL or the DNA damaging agent etoposide (35).

BH3-only proteins are under tight regulation, and are in an inactive state until needed. Apoptotic stimuli can upregulate mRNA transcription of all three Bim isoforms, leading to Bim-mediated apoptosis (94, 95, 268). As well, BimEL is believed to be sequestered by binding to microtubule complexes or Mcl-1 (140, 141, 269). Lastly, Bim has been shown to be phosphorylated at multiple sites, which can either activate or inactivate Bim (210, 267).

BimL and BimEL have been shown to interact with the cytoplasmic dynein light chain, LC8, of the microtubule complex and the binding region was localized to amino acids 51-57 of BimL, or amino acids 111-117 of BimEL (Fig. 1.10) (269). The exon which encodes these amino acids is alternatively spliced from BimS (Fig. 1.10), and BimS correspondingly does not bind to the dynein light chain. Sequestration of Bim to

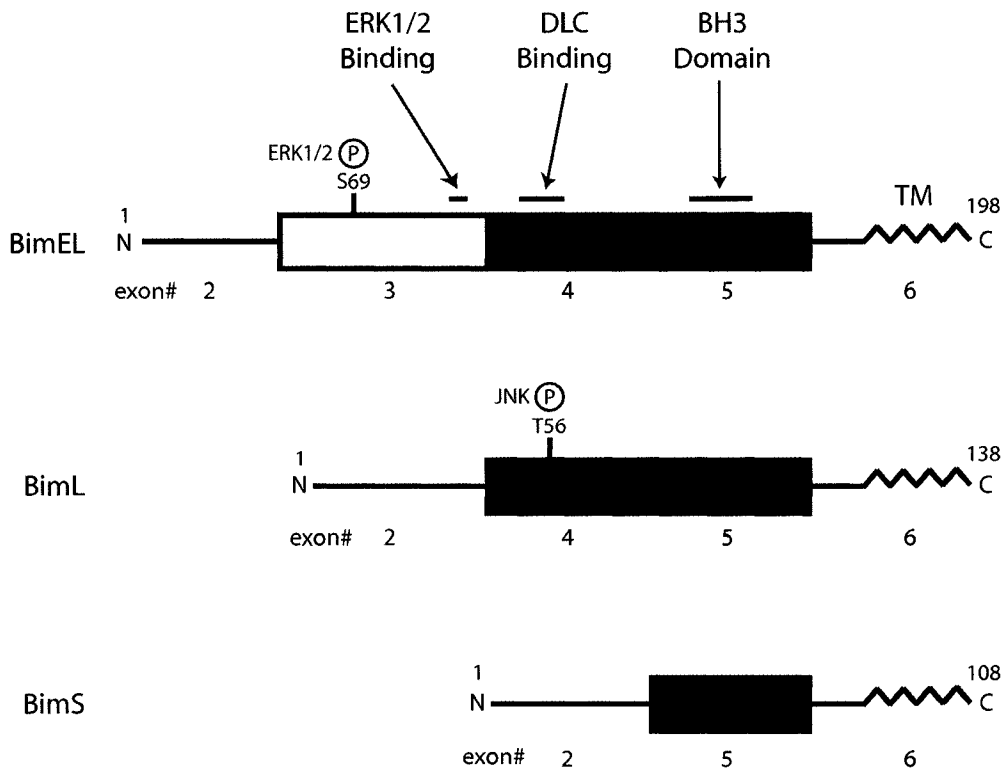

Figure 1.10 Schematic representation of Bim isoforms.
The BH3-only protein is synthesized as three alternatively spliced isoforms. Bim extra-long (EL) is comprised of exons 2, 3, 4, 5 and 6; Bim long (L) is encoded by exons 2, 4, 5 and 6; Bim short (S) is encoded by exons 2, 5, and 6. In addition to a BH3-domain that is responsible for pro-apoptotic activity, Bim possesses a transmembrane tail (TM) for mitochondrial localization, as well as two characterized docking domains. ERK1/2 kinases can dock at amino acids 97-99 in BimEL to faciliate Bim phosphorylation, is encoded on exon 3, and is spliced out of BimL and BimS. The dynein light chain (DLC) docking domain exists in both BimEL (amino acids 111-117) and BimL (amino acids 51-57), but it is alternatively spliced from the more potent BimS isoform. Two of the demonstrated phosphorylation sites are shown: ERK1/2 can phosphorylate serine 69 on BimEL, and JNK can phosphorlyate BimL on threonine 56.

the microtubule complex may regulate the proapoptotic activity of Bim. In support of this, mutants of BimL which lacked LC8-binding activity induce apoptosis as efficiently as BimS, which does not bind to LC8 (269). As well, proteins from healthy cells separated by sucrose gradients showed that both BimL and LC8 elute at a high molecular weight. In apoptotic cells, however, both BimL and LC8 exhibit a shift in size to a much lower molecular weight (269), suggesting that BimL is released from a complex during apoptosis.

Bim is also tightly regulated by phosphorylation. BimEL was shown to be a phosphoprotein and that the extracellular-signal related kinase (ERK1/2) pathway was involved (30). ERK1/2 phosphorylates BimEL at serine 69 *in vitro* (Fig. 1.10)(197, 210, 218), and mutation of this residue decreases ERK1/2 dependent phosphorylation of BimEL (197, 210, 218), but does not abolish BimEL phosphorylation. Other BimEL residues are phosphorylated, and these events may occur in a sequential fashion, with phosphorylation at one residue being required for modification at a second (197). The other residues phosphorylated by ERK1/2 are unknown, but serines 59 and 104 are candidates. ERK1/2 phosphorylation of BimEL requires the presence of a docking domain which resides within amino acids 97-99 in BimEL (Fig. 1.10) (197, 198). Interestingly, mutation of this docking domain eliminates BimEL phosphorylation at Ser69 by ERK1/2 *in vitro* and *in vivo*, but does not completely abolish BimEL phosphorylation. Phosphorylated BimEL appears to lose the ability to interact with Bax, thereby preventing BimEL-induced Bax activation (147). Significantly, phosphorylation of BimEL at serine 69 also induces the rapid polyubiquitination and degradation of BimEL by the 26S proteasome (197, 210), prolonging cell survival.

Other kinases have also been shown to phosphorylate Bim, although these observations are somewhat controversial (196). C-Jun N-terminal kinases (JNKs) phosphorylate BimL at threonine 56 following UV-treatment (Fig. 1.10)(193), and this results in the release of BimL from the dynein light chain. BimEL was also seen to be phosphorylated by JNK kinases on Serine 65 in apoptotic neurons (267), leading to Bax

activation and apoptosis (267). It is possible that different phosphorylation mechanisms may exist in different tissue types, depending on the specific stimulus.

The specific mechanisms used by Bim and other BH3-only proteins to induce cytochrome c release remain to be elucidated. For instance, the direct addition of tBid to purified mitochondria induces Bax-mediated pore-formation, leading to cytochrome c release (353). BimEL, on the other hand, does not induce Bax-mediated pore formation *in vitro* (353). Treatment of purified mitochondria with activated tBid also induces rapid cytochrome c release (199, 384), but whether Bim can also induce cytochrome c release in this manner is also controversial (187, 352).

Intriguingly, the structure of a fragment of a large helical region of BimL in complex with Bcl-x_L (206) indicates that Bim appears to fold somewhat differently than other Bcl-2 family members. The BH3 domains from the Bcl-2 family members Bak and Bax are hidden within the core of the protein. The BH3 region of Bim, in contrast, is extremely close to the C-terminal membrane anchor and is relatively exposed (206). This suggests that the BH3 domain of Bim is easily accessible thus necessitating the tight regulation of Bim.

1.3. Viral inhibitors of apoptosis

The induction of apoptosis is used extensively by the immune system to remove virus-infected cells (24, 283). In order to prolong survival within the host, viruses use multiple mechanisms to interfere with both intrinsic and extrinsic apoptotic cascades (24, 82, 283). Certain viruses encode IAPs to inhibit caspases, death receptor decoys, death receptor inhibitors, p53 inhibitors, and transcriptional regulators of Bcl-2 family genes (24, 283). As well, a large number of viral proteins localize to mitochondria to inhibit cytochrome c release (39, 82, 148). Poxviruses are quite remarkable in that numerous family members express several examples of the aforementioned anti-apoptotic proteins (Fig. 1.11) (349).

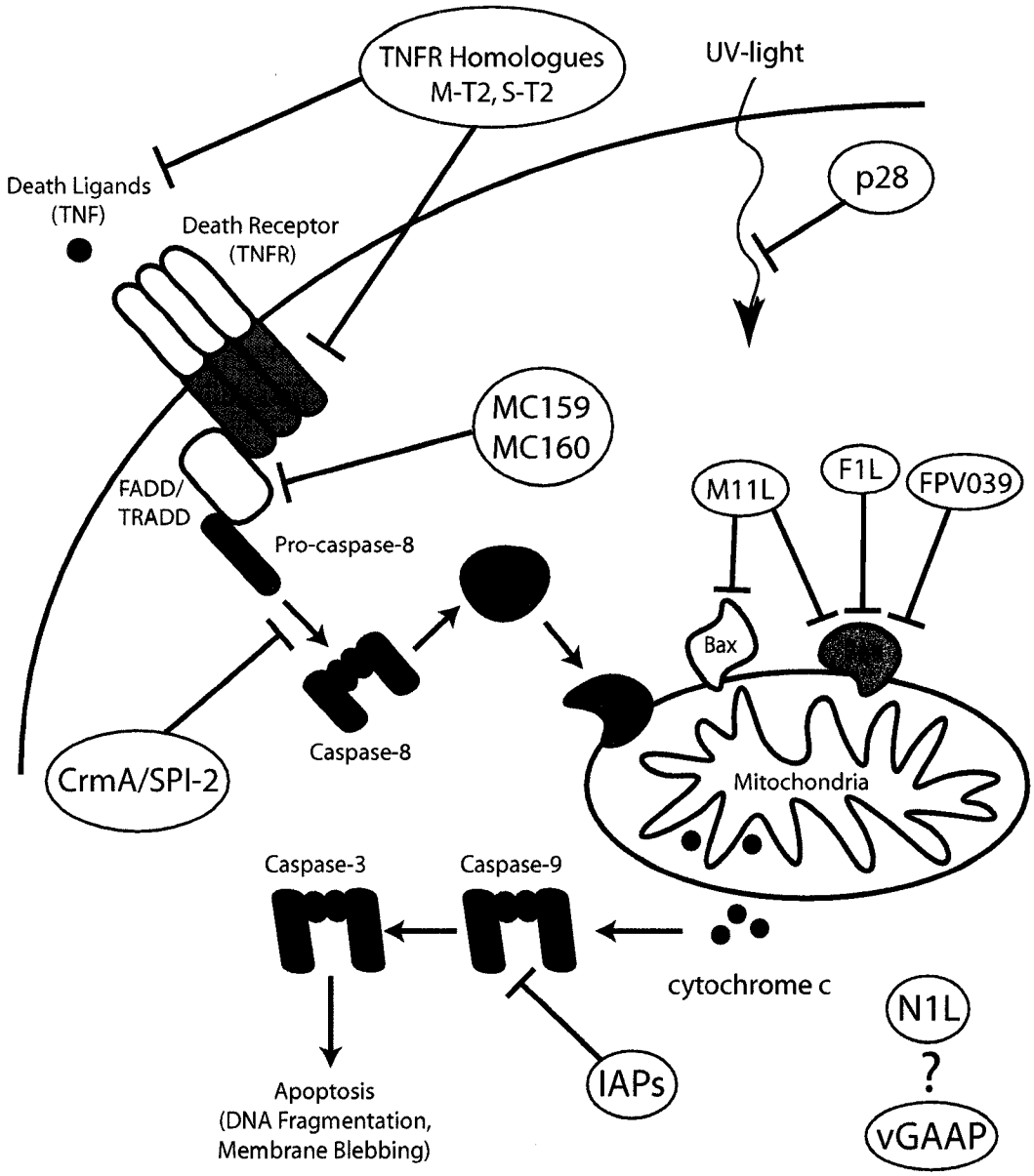

Figure 1.11. Poxviral inhibitors of apoptosis target multiple components of the apoptotic machinery. Poxviruses encode death recptor homologues which bind and inhibit TNF-mediated signaling (M-T2, S-T2), serine protease inhibtiors (CrmA/SPI-2) that inhibit caspase-8 activation, inhibitors of apoptosis (IAPs) which induce the degradation of executioner caspases, RING-finger containing proteins (p28) which inhibit UV-induced apoptosis, and mitochondrial-localized proteins which inhibit Bak and/or Bax and cytochrome c release (M11L, F1L, FPV039). MC159 and MC160 from molluscum contagiosum virus inhibit death domain-containing proteins. vGAAP is a golgi-localized protein which inhibits apoptosis by an unknown mechanism. N1L is structuraly related to Bcl-2 but has no known anti-apoptotic function.

1.3.1. Poxviral inhibitors of apoptosis

1.3.1.1. CrmA: A poxviral caspase inhibitor

The first identified poxviral inhibitor of apoptosis was a caspase inhibitor from cowpox virus, a member of the *Orthopoxviridae*. This protein, cytokine response modifier A (CrmA), inhibits caspase activity and is homologous to cellular members of the serine proteinase inhibitor (serpin/SPI) family (261, 318). Serpins function to inhibit proteases by forming stable inhibitory complexes as a suicide substrate (318), and the cowpox protein CrmA is unique in that it can inhibit both serine and cysteine proteases (180, 272, 407). CrmA is a potent inhibitor of caspase-1 which converts pro-interleukin-1β to its active form during inflammation (274). CrmA can also inhibit apoptosis induced by the death receptor ligands TNFα and FasL (354), and inhibits caspase-8 which is required to execute pro-apoptotic signals from death receptors (241, 407). Correspondingly, CrmA is unable to inhibit the intrinsic apoptotic cascade which does not require caspase-8 (85).

CrmA is not the only serpin encoded by poxviruses. Members of the *Orthopoxviridae* encode three distinct serpins, SPI-1, SPI-2 (CrmA), and SPI-3. Infection with a rabbitpox virus deficient in SPI-1 induced apoptosis in tissue culture, suggesting that SPI-1 expression inhibits apoptosis induced by virus infection through an unknown mechansism (45). Myxoma virus, a member of the *Leporipoxviridae*, encodes Serp-1 and Serp-2 (49), and a Serp-2-deficient myxoma virus is highly attenuated in Eurpoean rabbits, likely due in part to the observed increase in apoptosis in the draining lymph node (227). Serp-2 weakly inhibits human granzyme B and caspase-1 *in vitro* (361), and it has been recently suggested that Serp-2 is required for controlling inflammation and not apoptosis (216)

1.3.1.2. Poxvirus-encoded IAPs

The genomic sequencing of two insect poxviruses, *Amsacta moorei* entomopoxvirus (AmEPV) and *Melanoplus sanguinipes* entomopoxvirus (MsEPV), revealed that both of these poxviruses contained genes homologous to IAPs (4, 23). IAPs were first identified in baculoviruses, and cellular IAPs were later identified to control caspases (29, 74, 79, 99). IAPs function by inducing the polyubiquitination and degradation of effector caspases, thereby prolonging cell survival (Fig. 1.3)(288, 367). AmEPV-IAP was shown to function as a *bona fide* anti-apoptotic protein (202, 203), inhibits caspase-3 and caspase-9 activity *in vitro*, and protects cells from apoptosis induced by Drosophila pro-apoptotic proteins (202, 203). IAPs are also negatively regulated by the release of proteases such as SMAC/Diablo and Omi/HtrA2 from mitochondria (Fig. 1.3) (98, 341), and the suppression of IAPs allows the activation of effector caspases to facilitate execution of apoptosis.

1.3.1.3. The poxviral RING-protein p28

The RING-finger protein p28 is encoded by most members of the *Orthopoxviridae*, and homologues are found within several members of the *Chordopoxvirinae* (362). p28 contains a C-terminal RING-finger domain, localizes to virus factories, and has been shown to inhibit apoptosis induced by UV-light and virus infection, but not by death receptor ligation (43, 362). Although the precise mechanism of p28 apoptosis inhibition is unknown, RING-finger containing proteins have been shown to possess ubiquitin-ligase activity. Indeed, we and others have shown that p28 has ubiquitin ligase activity (161, 246), and that p28 expression recruits ubiquitin to viral factories (246). The synthesis of polyubiquitin chains via lysine 48 on ubiquitin targets proteins for degradation; proteins containing lysine 63 polyubiquitin side-chains, meanwhile, display altered function (152, 155, 386). p28 was shown to facilitate lysine 63 polyubiquitin chain synthesis *in vitro*, suggesting p28 may modify the function of cellular or viral proteins (161). Intriguingly, deletion of p28 from the genome of

ectromelia virus results in a highly attenuated disease in mice, indicating that p28 is a critical virulence factor of ectromelia virus (306, 307).

1.3.1.4. Inhibition of death receptors

Apoptosis of infected cells or tumour cells can be efficiently induced through the stimulation of death receptors belonging to the TNF receptor superfamily, such as Fas and TNF receptor-1 (TNFR1)(15). Most poxviruses, however, can inhibit the anti-viral activity of TNF through the expression of secreted viral proteins that display significant homology to the cellular TNF receptor (84). This mimicry is abundant in poxviral biology, as poxviruses also encode homologues of cellular receptors that bind interferon α, interferon α/β, interleukin 1β, interleukin 18 and assorted other chemokines (Table 1.2)(304, 324). The first identified viral TNF receptor decoys, M-T2 and S-T2, were discovered in the genomes of myxoma virus and Shope fibroma virus respectively, and sequester extracellular TNF to inhibit TNF-mediated signaling (296, 297, 319, 320, 362). Other TNF receptor homologues have since been discovered in other poxviruses, including vaccinia virus, ectromelia virus and variola virus (84). In addition to binding extracellular TNF, these viral TNF inhibitors also inhibit and associate with the intracellular domain of TNFR (301). The poxvirus Molluscum contagiosum virus also expresses two unique proteins, MC159 and MC160, which possess homology to death effector domains found in adaptor molecules such as FADD and TRADD, as well as pro-caspases. MC159 and MC160 can interact with effector domains from FADD and caspase-8, and can inhibit Fas-mediated apoptosis (26, 160, 316, 355).

1.3.1.5 Other poxviral inhibitors of apoptosis

Four other poxviral proteins have been identified to possess potential anti-apoptotic functions. One protein, known as vGAAP (Golgi anti-apoptotic protein), localizes to the golgi-apparatus and is homologous to a family of cellular GAAP proteins (135). Both cellular and viral GAAP exhibit anti-apoptotic activity, and the deletion of

vGAAP from the vaccinia virus genome results in an attenuated virus *in vivo* in a murine infection model (135). A second protein, N1L, has been crystallized and has a structure reminiscent of Bcl-2 family proteins (13). Previously characterized to play a role in the inhibition of NF-kB (96), N1L interacts with the BH3 domains of Bid, Bim and Bak (13). The role of N1L in the regulation of apoptosis, if any, remains to be determined. As well, deletion of the copper-zinc superoxide dismutase from myxoma virus renders infected cells susceptible to apoptosis induced by anti-Fas (351), and a selenoprotein from molluscum contagiosum that shows homology to cellular glutathione peroxidase protects cells from UV and peroxidase-induced cell death (317).

1.3.2. Viruses and mitochondrial apoptosis

Considering the importance of the mitochondria in regulating apoptosis, it is not surprising that viruses possess a variety of mechanisms to regulate apoptosis at the mitochondria (39, 82). Indeed two classes of viral mitochondrial-localized anti-apoptotic proteins have been identified: those that show obvious sequence homology to cellular Bcl-2, and those that lack obvious sequence homology to known cellular proteins (82, 148, 262).

1.3.2.1. Viral Bcl-2 homologues

Viral-encoded Bcl-2 homologues have been found in African swine fever virus and all members of the gammaherpesvirus family, including Kaposi's Sarcoma-associated herpes virus (KSHV), Epstein-Barr Virus (EBV), murine γ-herpesvirus-68 (γHV68), herpesvirus saimiri, and bovine herpesvirus 4 (82, 148). The Bcl-2 homologue from KSHV contains 7 alpha helices which fold similar to cellular Bcl-2, and also encodes four predicted BH domains (162). The EBV Bcl-2 homologue, BamHI-H right reading frame-1 (BHRF1), is also structurally similar to Bcl-2 (163), and both BHRF1 and KSHV-Bcl-2 inhibit a wide range of pro-apoptotic stimuli (174, 348). BHRF1 has a reduced capacity to interact with BH3 peptides compared to Bcl-2, suggesting that while

BHRF1 has sequence and structural homology to Bcl-2, it may function in a different manner (163). These viral Bcl-2 homologues also appear to be non-essential in tissue culture, as strains of EBV and KSHV lacking their respective Bcl-2 homologues replicate normally *in vitro*. Deletion of vBcl-2 from murine γHV68, however, results in a dramatic decrease in viral pathogenicity (208). Specific mutation of the hydrophobic residues lining the hydrophobic surface groove also severely attenuates murine γ-HV68 *in vivo* but has no effect on virus growth *in vitro* (116, 208, 369), suggesting that the hydrophobic groove of this vBcl-2 is required for pathogenicity.

African swine fever virus, a DNA virus distantly related to the poxviruses, encodes an obvious Bcl-2 homologue that inhibits apoptosis at the mitochondria (3, 46, 395). This homologue also shows amino acid similarity in all four predicted BH domains, and mutations in the BH1 domain abolish anti-apoptotic activity, similar to cellular Bcl-2 (278).

1.3.2.2. Adenovirus E1B 19K

The first viral mitochondrial inhibitor of apoptosis identified was a protein from adenovirus, E1B 19K, which functions to inhibit the cytopathic effects of adenovirus infection (388). Indeed, expression of the adenovirus protein E1A induces apoptosis, and this is inhibited by E1B 19K (90). E1B 19K is predicted to encode the four BH domains, and localizes to the mitochondrial membrane following an apoptotic stimulus (257, 388). Expression of E1B 19K inhibits apoptosis and cytochrome c release induced by a number of stimuli, and E1B 19K interacts with both Bak and Bax as a mechanism of action (60, 70, 143, 144, 177, 388). Interestingly, E1B 19K binds to activated Bax at the mitochondria, but does not interact with Bax in the absence of an apoptotic stimulus (143, 257, 338).

Unlike Bcl-2, E1B 19K does not inhibit the initial tBid-induced conformational change in Bax, which is detectable using N-terminal conformation specific antibodies

(257). Only following this conformational change does E1B 19K then interact with Bax, inhibit Bax oligomerization and prevent cytochrome c release (257, 338). As such, it is believed that E1B 19K interacts with the BH3 domain of Bax which is exposed following a conformational change in Bax (82). Indeed, replacement of the BH3 domain of Bax with the BH3 domain from Bcl-2 eliminates the E1B 19K-Bax interaction while simultaneously inducing apoptosis (144). In addition to Bak and Bax, E1B 19K interacts with the BH3-only protein Bik/Nbk, but not with the BH3-only proteins BimL or Bad (60, 145, 250).

1.3.2.3. Human cytomegalovirus vMIA

Human cytomegalovirus encodes a small inhibitor of apoptosis, vMIA (viral mitochondrial inhibitor of apoptosis), that shows no homology to Bcl-2 (124). vMIA consists of an N-terminal sequence required for mitochondrial localization, and a C-terminal region which is required for the inhibition of apoptosis. The C-terminal functional domain binds to and recruits Bax to the mitochondrial membrane (14, 263), and vMIA-associated Bax inserts into the outer mitochondrial membrane as a high molecular weight complex (14, 263). Whether these Bax oligomers are identical to those seen in apoptotic cells is unknown. The Bax-binding domain of vMIA somewhat resembles a BH3-like domain, which may allow it to interact with Bax (40). Interestingly, a small fusion that contains only the small N-terminal targeting domain and the small C-terminal Bax-binding domain of vMIA still binds Bax and inhibits cell death, suggesting that the ability to interact with Bax at the mitochondria is the primary mechanism used by vMIA (14, 263). This Bax-inhibitory mechanism used by vMIA is quite unique, as all other cellular and viral Bcl-2 homologues characterized to date inhibit Bax oligomerization during apoptosis (77, 82).

1.4 Poxviral mitochondrial-localized inhibitors of apoptosis

Only two members of the *Poxviridae* family sequenced to date, fowlpox and canarypox, encode obvious Bcl-2 homologues (5, 360). These proteins are predicted to possess multiple BH domains, as well as a putative C-terminal mitochondrial targeting sequence (5, 360). Research in our lab has shown that the fowlpox Bcl-2 homologue, FPV039, is a functional inhibitor of apoptosis that localizes to the mitochondria, and interacts with the Bcl-2 family protein Bak (L. Banadyga and M. Barry. Unpublished results).

Aside from canarypox and fowlpox, no other poxviruses encode obvious Bcl-2 homologues. Research has shown, however, that mammalian poxviruses such as myxoma virus and vaccinia virus express unique proteins which function to inhibit apoptosis at the mitochondria (103, 382). These proteins, while lacking sequence similarity to Bcl-2, appear to possess functional similarity to cellular anti-apoptotic Bcl-2 family members.

1.4.1 Myxoma virus M11L

Myxoma virus, a member of the *Leporipoxviridae*, causes a highly lethal disease in European rabbits and encodes a unique anti-apoptotic protein, M11L (103, 104, 373). M11L localizes to the mitochondria where it inhibits cytochrome c release and the loss of the mitochondrial membrane potential (103, 104). M11L is 166 amino acids in size and inserts into the outer mitochondrial membrane via a short C-terminal hydrophobic tail flanked by positively charged residues (103). Myxoma virus deficient in M11L is highly attenuated *in vivo* and infected European rabbits completely recover (128, 254). M11L interacts with the mitochondrial peripheral benzodiazepine receptor (PBR), a component of the PT pore complex present in the mitochondrial outer membrane (104). M11L, but not Bcl-2, inhibits apoptosis induced by the addition of PBR-specific ligands, suggesting that M11L can function in a manner different than cellular Bcl-2 (104). An additional mechanism of action is likely involved, however, as M11L also protects against apoptosis in cells lacking PBR (104).

M11L has also been shown to interact with and inhibits activation of the pro-apoptotic multi-domain Bcl-2 family member Bak, and this interaction can be seen independent of other Bcl-2 family members *in vitro* (373). M11L displays no obvious amino acid similarity to Bcl-2 family members, but may contain a putative BH3 domain near the N-terminus of M11L (373). More recently, M11L has been shown to interact with and inhibit the activation of Bax (332). M11L expression inhibits Bax activation, but appears to recruit Bax to the mitochondria where M11L can interact with Bax (332). It is currently unknown whether the interactions between M11L and either PBR, Bak, or Bax are absolutely required for the inhibition of apoptosis by M11L.

1.4.2.1 Vaccinia virus F1L

Although M11L orthologues are present in members of the *Leporipoxviridae*, *Suipoxviridae*, *Capripoxviridae* and *Yatapoxviridae*, no members of the *Orthopoxviridae* encode M11L homologues. The genome of the *Orthopoxvirus* vaccinia virus, for instance, contains no obvious homologues to either Bcl-2 or M11L (123). Work in our lab a number of years ago showed that cells infected with VV strain Copenhagen (VV(Cop)), which is naturally devoid of the caspase-8-inhibitor CrmA, were still protected from mitochondrial cytochrome c release following intrinsic or extrinsic apoptotic triggers (381). In contrast, infection with a deletion virus which lacks 55 open reading frames, VV811 (258), did not inhibit apoptosis, suggesting that VV encoded a novel anti-apoptotic protein (382). The sequencing of the genome of VV(Cop) allowed us to identify putative mitochondrial-localized proteins by examining genes which encoded predicted hydrophobic domains (123). Our lab identified one open reading frame, F1L, that restores anti-apoptotic activity during infection with VV811 (382). F1L predominantly localizes to the mitochondria and inhibited the loss of the inner mitochondrial membrane potential and the mitochondrial release of cytochrome c induced by a wide variety of stimuli, including staurosporine, TNF and anti-Fas (329, 379, 382). We recently generated a strain of vaccinia virus specifically devoid of F1L,

VV(Cop)ΔF1L, which does not inhibit apoptosis (379). Instead, infection with VV(Cop)ΔF1L actually triggers apoptosis indicating that the expression of F1L is crucial for inhibiting vaccinia virus-induced apoptosis (379, 382).

Obvious orthologues of F1L are only found within members of the *Orthopoxviridae* (Fig. 1.12), and all of these orthologues contain a predicted C-terminal transmembrane domain flanked by positively charged amino acids, similar to the transmembrane domain found in M11L and Bcl-2 (247, 329). Indeed, work in our lab demonstrated that the transmembrane domain of F1L is necessary and sufficient for localization to the mitochondria, and permits F1L to insert into the outer mitochondrial membrane post-translationally with the N-terminus exposed to the cytoplasm (329). Mutation of the positively charged residues C-terminal to the hydrophobic domain results in altered localization of F1L from the mitochondria to the endoplasmic reticulum (329). Neither F1L targeted to the endoplasmic reticulum nor cytoplasmic F1L lacking the hydrophobic tail are able to inhibit apoptosis induced by TNFα or αFas, indicating that localization of F1L to the mitochondria is necessary for anti-apoptotic activity (329).

Sequence alignment of F1L with orthologues from the *Orthopoxviridae* indicates that the C-terminal 210 amino acids amongst orthologues share greater than 90% amino acid identity (Fig. 1.12). Multiple orthologues, however, exhibit predicted extensions at the N-terminus of the protein (Fig. 1.12). The orthologue from ectromelia virus strain Moscow (EVM), EVM025, is perhaps the most dramatic. EVM025 is predicted to express a long N-terminal extension consisting of an eight amino acid motif repeated 30 times (62). This motif, 'DNGIVQDI' (Asp-Asn-Gly-Ile-Val-Gln-Asp-Ile) shares no homology with any known motifs or domains, and has no significant predicted secondary structure. The orthologue from variola virus strain South Africa 102 is also predicted to encode an N-terminal repeat comprised of 31 copies of 'DDI' (Asp-Asp-Ile) (Fig. 1.12), and a similar 'DDI' N-terminal repeat is found in the campelpox orthologue (6). The orthologue from cowpox strain Brighton red also encodes an N-terminal extension of

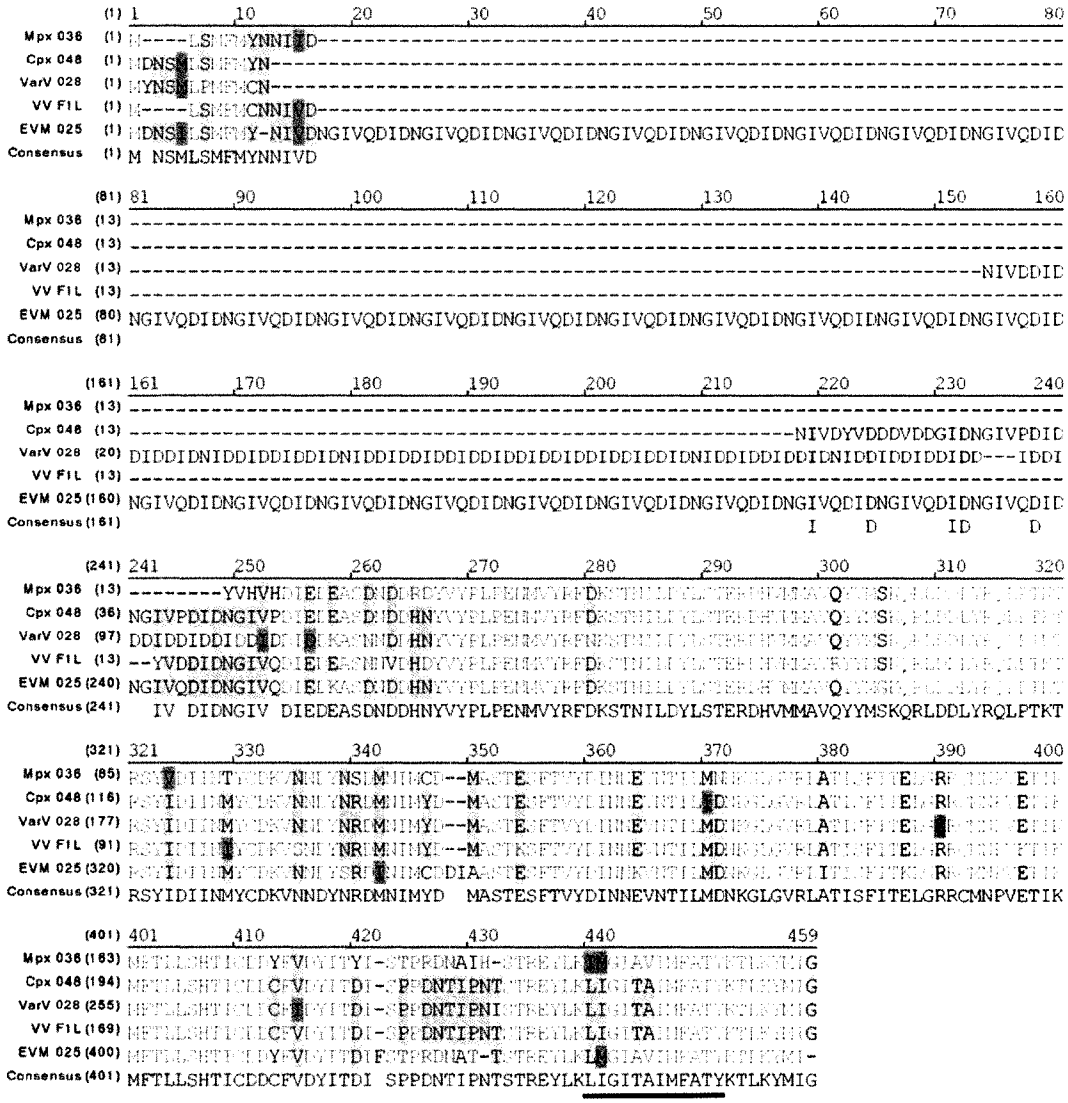

Figure 1.12 Alignment of Orthopoxviral F1L Orthologues.
Amino acid alignment of F1L orthologues from monkeypox strain Congo (Mpx036), cowpox strain Brighton red (Cpx048), variola virus strain South Africa 1965 (102) (VarV028), vaccinia virus strain Copenhagen (VV F1L), and Ectromelia virus strain Moscow (EVM025). Consensus sequence is listed at bottom. The putative C-terminal transmembrane domain is underlined . Note the long variable N-terminal extensions present in EVM025, VarV102 and Cpx048. Within the C-terminal 209 amino acids, these orthologues share >90% amino acid identity.

approximately 30 amino acids with no particular repeat region (Fig. 1.12). Whether these N-terminal extensions have any effect on the predicted anti-apoptotic function of these orthologues is currently unknown.

1.4.2.2 F1L and Bak

F1L localizes to the mitochondrial outer membrane and inhibits cytochrome c release. Using co-immunoprecipitations and affinity purifications, we and others demonstrated that in the absence of an apoptotic trigger, F1L associates with the pro-apoptotic Bcl-2 family member Bak (265, 379). During apoptosis, Bak undergoes a conformational change revealing an N-terminal epitope and oligomerizes into a high molecular weight complex (131, 245, 404). Interestingly, VV-infected cells were resistant to Bak oligomerization and the N-terminal conformational change of Bak during apoptosis, whereas cells infected with VV(Cop)ΔF1L readily underwent Bak activation and apoptosis (265, 379). Since Bax and Bak are essential for the release of cytochrome c (91, 385), the most straight-forward explanation for this observation is that F1L directly interacts with Bak to inhibit Bak activation. A somewhat similar mechanism has been suggested for E1B 19K, which can interact with both Bak and Bax (80, 337), and vMIA, which interacts with Bax (14, 263). These viral proteins, however, interact with conformationally activated forms of Bak or Bax (14, 257, 263), whereas F1L appears to interact with conformationally inactive Bak (379). F1L expression also inhibited apoptosis regulated by Bak, as Bax-deficient cells infected with VV(Cop) were protected from cytochrome c release induced by the BH3-only protein tBid (379). Whether the interaction with Bak is necessary for the anti-apoptotic activity of F1L remains to be determined. Bak or Bax are absolutely required for induction of the mitochondrial apoptotic pathway, although there is no evidence to date as to whether F1L, in addition to inhibiting Bak activation, can also inhibit the activation of Bax.

1.4.2.3 Infection with VV(Cop)ΔF1L induces apoptosis

Previous work in our lab using a deletion virus, VV811, demonstrated that this virus was unable to inhibit apoptosis (382). Interestingly, not only did this virus lack anti-apoptotic activity, but infection with VV811 actually induced cell death in tissue culture (380). F1L expression, however, protected VV811-infected cells from apoptosis suggesting that vaccinia virus triggers an innate cellular apoptotic pathway which is inhibited by F1L (380). Infection with a virus specifically devoid of F1L, VV(Cop)ΔF1L, also induces apoptosis in tissue culture (379). What is becoming increasingly apparent is that infected cells have an innate ability to detect virus infection and induce apoptosis in the absence of an immune response. Indeed, a number of poxviruses lacking various anti-apoptotic proteins induce apoptosis by infection alone (20, 213, 214, 238, 275). Virus-induced apoptosis either triggers the direct activation of caspases or stimulates the activation of BH3-only proteins and subsequent mitochondrial mediated apoptosis, both of which can be effectively blocked by virus-encoded anti-apoptotic proteins (39, 349). These virus-encoded anti-apoptotic proteins may thus provide a dual apoptotic inhibitory function against both the immune response, and the innate cellular response to virus infection (105, 283). How poxviruses such as vaccinia virus trigger apoptosis during infection, however, is currently unknown.

Thesis Objectives

The vaccinia virus protein F1L is a mitochondrial-localized inhibitor of apoptosis which interacts with the pro-apoptotic protein Bak. Bak and Bax are the so-called 'gatekeepers' of apoptosis at the mitochondria, as cells deficient in both of these proteins do not release cytochrome c during apoptosis (91, 385). Since infection with vaccinia virus protects cells from apoptosis induced by a variety of stimuli, we hypothesized that vaccinia virus would also inhibit the activation of the pro-apoptotic protein Bax. This hypothesis led us to investigate the role of F1L in the inhibition of Bax, and the involvement of BH3-only proteins in the induction of Bax activation and apoptosis. Lastly, we investigated the role of the F1L orthologue in the natural murine pathogen ectromelia virus, as ectromelia is an excellent model system for studying host:pathogen interactions.

Objectives

1) To examine the ability of vaccinia virus and/or F1L to interfere with Bax activation

2) To investigate the ability of vaccinia virus to interfere with the BH3-only protein Bim

3) To characterize the potential anti-apoptotic activity of the F1L orthologue from ectromelia virus, EVM025

CHAPTER 2: Materials and Methods

2.1 Cell lines and viruses

2.1.1 Cell lines

All cell lines used in this study are listed in Table 2.1. HeLa, HEK293T, CV-1 and $Bak^{-/-}$, $Bim^{-/-}$, and $Bak^{-/-}/Bax^{-/-}$ baby mouse kidney (BMK) cells (kindly provided by E. White, Rutgers University, Pistcataway NJ) were grown in Dulbecco's modified Eagle's medium (DMEM) (Invitrogen) supplemented with 10% fetal bovine serum (FBS) (Invitrogen), 2 mM L-glutamine (Invitrogen), 50 units/ml penicillin (Invitrogen), and 50 μg/ml streptomycin (Invitrogen). HeLa cells stably expressing Bcl-2 were generated as described and cultured as above (19). $Bak^{-/-}$ and $Bak^{-/-}/Bax^{-/-}$ mouse embryonic fibroblasts (MEF) were a generous gift from S. Korsmeyer (Harvard Medical School, Boston, Massachusetts), and were cultured in DMEM, 10% FBS, 2 mM L-glutamine, 50 units/ml penicillin, 50 μg/ml streptomycin, plus 100 μM MEM non-essential amino acids (Invitrogen)(385). BGMK cells were maintained in DMEM, 10% newborn calf serum (NCS) (Invitrogen), 50 units/ml penicillin, and 50 μg/ml streptomycin. TK-H143 cells were cultured in DMEM, 20% FBS, 2 mM L-glutamine, 50 units/ml penicillin, 50 μg/ml streptomycin, and 25μg/ml 5-bromodeoxyuridine (Sigma-Aldrich). Jurkat cells were maintained in Roswell Park Memorial Institute 1640 medium (RPMI) supplemented with 10% FBS (Invitrogen), 50units/ml penicillin, 50μg/ml streptomycin, and 100μM β-mercaptoethanol (Sigma-Aldrich). Jurkat cells stably expressing Bcl-2 were generated as previously described (19). Jurkat cells deficient in Bak and Bax were kindly provided by H. Rabinowich (University of Pittsburgh) (374). All cell lines were maintained at 37°C in the presence of 5% CO_2.

2.1.2 Viruses

All viruses used and generated in this study are listed in Table 2.2. Vaccinia virus (VV) strain Copenhagen, VV(Cop), and recombinant vaccinia virus strain Copenhagen expressing enhanced green fluorescent protein (EGFP), VV(Cop)EGFP, were kindly

Table 2.1. Cell lines used in this study

Cell Line	Tissue Type	Characteristics/Uses	Source
HeLa	Fibroblast		ATCC
HeLa Bcl-2	Fibroblast	Stably expressing Bcl-2	(19)
Jurkat-HP21	T-cell		R.C. Bleackley
Jurkat Bcl-2	T-cell	Stably expressing Bcl-2	(19)
Jurkat $Bak^{-/-}/Bax^{-/-}$	T-cell	Devoid of Bak and Bax	(374)
HEK293T	Kidney	Used for transient transfections	ATCC
CV-1	African green monkey kidney fibroblast	Used for virus propagation/titrations	ATCC
TK-H143	Fibroblast	Recombinant virus selection Thymidine $kinase^{-/-}$	ATCC
BGMK	Baby green monkey kidney	Used for virus propagation	S. Dales
WT MEF	Mouse embryonic fibroblast	Wild type	(385)
$Bak^{-/-}$ MEF	Mouse embryonic fibroblast	Bak-deficient	(385)
$Bax^{-/-}$ MEF	Mouse embryonic fibroblast	Bax-deficient	(385)
$Bak^{-/-}/Bax^{-/-}$ MEF	Mouse embryonic fibroblast	Bak and Bax-deficient, resistant to apoptosis	(385)
$Bak^{-/-}$ BMK	Baby mouse kidney	Bak-deficient	(91)
$Bim^{-/-}$ BMK	Baby mouse kidney	Bim-deficient	(346)
$Bak^{-/-}/Bax^{-/-}$ BMK	Baby mouse kidney	Bak and Bax-deficient, expresses BimL	(91)

Table 2.2. Viruses used in this study

Virus	Background	Characteristics	Source
VV(Cop)	VV(Cop)	ΔCrmA	G. McFadden(153)
VV(Cop)EGFP	VV(Cop)	Expresses EGFP from synthetic promoter; ΔTK	G. McFadden
VV(Cop)ΔF1L	VV(Cop)	ΔCrmA; ΔF1L	(379)
EVM	EV Moscow	Wild type	M. Buller
EVMΔcrmA	EV Moscow	ΔCrmA	M. Buller
EVMΔcrmAΔ025	EV Moscow ΔcrmA	ΔCrmA, ΔEVM025	This Study
VV:FLAG-F1L	VV Western Reserve	Expresses FLAG-F1L from synthetic promoter; ΔTK	(329)
VV(Cop)ΔF1L:FLAG-EVM025(E255)	VV(Cop)ΔF1L	Expresses FLAG-EVM025(E255) from synthetic promoter; ΔF1L, ΔTK	This Study

provided by G. McFadden (Robarts Research Institute, London, Ontario). VV(Cop)ΔF1L was generated by insertion of EGFP into the F1L open reading frame as previously described (379). A recombinant vaccinia virus strain Western Reserve expressing FLAG-F1L, VV:FLAG-F1L, was generated as described (329). Ectromelia virus strain Moscow (EVM) and EVMΔcrmA were generously provided by M. Buller (St. Louis University). EVMΔcrmAΔ025 was generated as described in section 2.6. Recombinant VV(Cop)ΔF1L expressing FLAG-EVM025(E255) was generated as described in section 2.5.7. All viruses were stored at -80°C and were thawed and sonicated for 20 seconds (0.5 second pulsing on/off cycles) (Misonix Inc.) prior to usage.

2.2. DNA methodology

2.2.1 Plasmids

All plasmids used in this study are listed in Table 2.3. pGEM-T (Promega) was used for all TA cloning reactions, and pEGFPC3 (Clontech) was used to generate all EGFP fusions. pEGFP-F1L and pEGFP-F1L(206-226) were generated as described previously (329, 382). pEGFP-Bcl-2 was a generous gift from G. McFadden (Robarts Research Institute, London, Ontario) (103). pcDNA3-FLAG-BimL and pcDNA3-T7-Bmf were generous gifts from R. Davis (University of Massachussets) (193). pSC66, which contains a poxviral promoter for expression during poxviral infection, was kindly provided by D. Burshtyn (University of Alberta) (56). pSC66-FLAG-F1L was generated as described previously (382). pET15-Bid was kindly provided by Dr. X. Wang (University of Texas) (212). All other vectors were constructed as described in section 2.3.

2.2.2 Plasmid isolation

High-purity DNA for transfections was isolated using a Maxi-Prep kit (Qiagen). Approximately 200 ml of bacterial culture was pelleted, and DNA was isolated as per

Table 2.3. Vectors used in this study

Plasmid	Gene/Description	Backbone	Reference
pJMT16	EVM025(D237) in pGEM-T	pGEM-T	This Study
pJMT17	EGFP-EVM025(D237) fusion in pEGFP-C3	pEGFP-C3	This Study
pJMT28	EVM025 knockout vector containing 5' and 3' EVM025 fragments separated by a BglII site	pGEM-T	This Study
pJMT29	EVM025 knockout vector; 5' and 3' EVM025 fragments flanking EGFP behind a poxviral promoter	pGEM-T	This Study
pJMT30	EGFP behind a strong poxviral promoter from pSC66	pGEM-T	This Study
pJMT39	*lacZ* under poxviral promoter	pCMV5	This Study
pJMT40	FLAG-tagged N-terminal 153bp of EVM025	pGEM-T	This Study
pJMT43	FLAG-EVM025(D231) in pGEM-T	pGEM-T	This Study
pJMT44	FLAG-EVM025(D231) behind a poxviral promoter in pSC66	pSC66	This Study
pJMT45	FLAG-EVM025(E255) in pGEM-T	pGEM-T	This Study
pJMT46	EVM026 in pGEM-T	pGEM-T	This Study
pJMT48	FLAG-EVM025 (E255) behind a poxviral promoter in pSC66	pSC66	This Study
pJF1	EVM025(E255) in pGEM-T	pGEM-T	This Study
pJF2	EGFP-EVM025(E255) fusion	pEGFP-C3	This Study
pGEM-T	TA-Cloning vector	n/a	Promega
pCMV5	Eukaryotic expression vector; CMV promoter	n/a	Qbiogene
pEGFP-C3	EGFP expression vector; CMV promoter	n/a	Clontech
pEGFP-F1L	EGFP-F1L fusion	pEGFP-C3	(382)
pEGFP-F1L (206-226)	EGFP-F1L(206-226) fusion	pEGFP-C3	(329)
pEGFP-Bcl-2	EGFP-Bcl-2 fusion	pEGFP	(103)
pcDNA3-T7-Bmf	T7-tagged Bmf eukaryotic expression vector	pcDNA3	(193)
pcDNA3-FLAG-BimL	FLAG-BimL eukaryotic expression vector	pcDNA3	(193)
pCMV5-Bid	His-Bid eukaryotic expression vector	pCMV5	This Study
pET15-Bid	His-Bid in bacterial expression vector	pET15b	(212)
pSC66-EGFP	EGFP behind the poxviral early/late promoter	pSC66	(382)
pSC66-FLAG-F1L	FLAG-tagged F1L behind poxviral promoter	pSC66	(382)
pSC66	Poxviral expression vector also used for recombinant virus generation; thymidine kinase gene fragments flank *lacZ*	n/a	(56)

manufacturer's instructions. For low copy plasmids, such as those derived from pSC66 (56), 170μg/ml chloramphenicol (Sigma-Aldrich) was added approximately 16 hours prior to harvesting to increase the plasmid copy number per cell. Sequencing grade DNA was prepared using a DNA mini-prep kit (Qiagen) as per manufacturer's instructions. Five ml of an overnight bacterial culture was used and DNA was eluted with 50μl of dH_2O.

For cloning purposes, all other plasmids were prepared by the alkaline lysis method (289). Briefly, 1.5ml of an overnight culture of *E. coli* DH5α was resuspended in 100 μl of resuspension buffer, containing 50mM glucose, 25mM Tris (pH 8.0), and 10mM EDTA. Bacteria were lysed in 200μl of lysis buffer containing 1% SDS and 0.1M NaOH. Proteins and membranes were precipitated with the addition of 150 μl of neutralization buffer containing 3M potassium acetate and 11.5% glacial acetic acid, followed by incubation on ice for 5 minutes. Suspensions were then centrifuged at 18000 ×*g* for 10 minutes, and the supernatant fractions were extracted with one volume of phenol:chloroform (1:1). Aqueous layers were subsequently extracted with one volume of chloroform, and DNA was precipitated with 2.5 volumes of ice cold 95% ethanol. DNA was then centrifuged, and pellets were resuspended in dH_2O.

DNA yields were determined by determining the optical density at 280nm using a spectrophotometer (Eppendorf), and DNA quality was assessed by agarose gel electrophoresis (section 2.2.4)

2.2.3 Polymerase chain reaction

Polymerase chain reactions (PCR) were performed in 50μl volumes that, in general, contained 10mM Tris-HCl (pH 8.85), 25mM KCl, 5mM $(NH_4)_2SO_4$, 2mM $MgSO_4$, 100μM dNTPs (Roche Diagnostics), 200pmol of each primer, and 2.5 units of Pwo (Roche) or Taq (Invitrogen) DNA polymerase. Reactions were carried out in a thermocycler (Techne) for 30 cycles consisting of a 95°C melting step for 30 seconds, a

52° annealing step for 30 seconds, followed by a 72°C extension step for 1 minute/kilobase. All primers used in this study are listed in Table 2.4, and were obtained from the indicated company. To remove contaminating DNA and primers, all PCR products were gel extracted as described in section 2.2.4 prior to cloning, and modified using an A-Addition Kit (Qiagen) as described in 2.2.5.

2.2.4 Agarose gel electrophoresis and gel extractions

Agarose gel electrophoresis was used to separate all DNA fragments. Agarose gels, 0.8%(w/v), were prepared in 1X TAE buffer containing 40mM Tris-acetate and 1mM EDTA. Samples were loaded in the presence of sample loading dye containing 5% glycerol, 0.04%(w/v) bromophenol blue, 0.04%(w/v) xylene cyanol, 10mM EDTA (pH 7.5), and gels were electrophoresed at 100V. Gels were stained with 10μg/mL ethidium bromide and bands were visualized using Scion imaging software (Scion Corporation).

DNA fragments were excised from agarose gels using a gel extraction kit (Qiagen) as per the manufacturers instructions. Briefly, bands were excised and resuspended in 3 volumes (g/mL) of gel solubilization buffer and incubated at 50°C for 10 minutes. Solubilized gel slabs were then passed over a DNA column and eluted with 40μl 10mM Tris (pH 8.0). Gel extraction yields were assessed by agarose gel electrophoresis.

2.2.5 Restriction digests and DNA end-modification

All restriction enzymes and buffers were purchased from Invitrogen or New England Biolabs. Restriction digests were typically performed in 10μl reaction volumes for 1 hour at the appropriate incubation temperature. PCR products amplified with Pwo polymerase possess blunt ends and were modified using an A-Addition Kit (Qiagen) to facilitate TA-cloning into pGEM-T (Promega).

Table 2.4. Oligonucleotides used in this study

Oligonucleotide	Sequence[a]	RE Site[b]	Company
EVF1LGFPSense	TGAATTCTTATGGACAATAGTATTTT GTCG	EcoRI	Qiagen
EVF1LGFPAnti	TGGATCCTTATCATATCATGTATTTG AG	BamHI	Qiagen
EVF1LSenseTrunc	TGAATTCATGGATATAGATAATGGT ATAGTA	EcoRI	Qiagen
EVM025koF1	AGAATAGCTCAGCTAATCTAT	None	Qiagen
EVM025koR1	AATGCAGATCTGGATCTACGATATT ATACATAAACATCGA	BglII	Qiagen
EVM025koF2	GATCCAGATCTGCATTTCGCATACTA TATGCGATGAT	BglII	Qiagen
EVM025koR2	TGGATCCTTATCATATCATGTATTTG AG	BamHI	Qiagen
EVM025Tr(E255) Sense	TGAATTCTTATGGAGGATAAGGCTA GCGAT	EcoRI	IDT
EVM025 NheI Antisense	TTGGTACCTTAGCTAGCCTTATCCTC TATATC	KpnI	IDT
Flag EVM025 Sense	TTTGTCGACATGGACTACAAAGACG ATGACGACAAGGACAATAGTATTTT GTCGATG	SalI	IDT
FlagEVM025 (E255)	TTGTCGACATGGACTACAAAGACGA TGACGACAAGGAGGATAAGGCTAGC GATAAT	SalI	IDT
E/LSynFor	AGATCTAAAAATTGAAATTTTATTTT TTTT	BglII	Qiagen
EGFPR(BglII)	AGATCTTTACTTGTACAGCTCGTCCA TGCC	BglII	Qiagen

[a]Restriction endonuclease sites are underlined
[b]Identity of restriction endonuclease (RE) site underlined in sequence column

2.2.6 DNA ligations

All TA cloning ligations into pGEM-T (Promega) were performed as per manufacturer's instructions. Briefly, 50ng of pGEM-T, 150ng of PCR product, 5 units of T4 DNA ligase and 5µl of 2x ligation buffer containing 60mM Tris-HCl (pH 7.8), 20mM $MgCl_2$, 20mM DTT, 2mM ATP, 10% (v/v) polyethylene glycol, were mixed and incubated at room temperature for 1 hour. Ligations were then transformed into *E. coli* DH5α, and plated onto Luria-Bertani (LB) agar plates containing 100µg/ml ampicillin (Sigma-Aldrich) or 30µg/ml kanamycin (Sigma-Aldrich) where required. All other ligations were performed using T4 DNA ligase (New England Biolabs) as per manufacturer's instructions. Briefly, vector to insert ratios of 1:3 were ligated using 5 units of T4 DNA ligase in a reaction volume of 20µl at room temperature for 15 minutes prior to transformation into *E. coli* DH5α (section 2.2.8).

2.2.7 DNA sequencing and computer analyses

DNA sequencing was performed at the Molecular Biology Unit in the Department of Biosciences at the University of Alberta. DNA sequence analyses were performed using Vector NTI Suite 7 (Invitrogen). BLAST searches were performed using programs available through the National Centre for Biotechnology Information. Sequence alignments were performed using AlignX (Invitrogen).

2.2.8 Bacterial transformation and competent cells

Chemically competent *E. coli* DH5α were prepared as described (289). Cells were transformed by incubating DNA with competent cells on ice for one hour. Cells were then incubated at 42°C for 45 seconds, on ice for 2 minutes, and 700µl of LB broth was added. Cells were allowed to recover at 37°C for one hour prior to plating on LB agar plates containing the appropriate antibiotic. Kanamycin (30µg/ml), and ampicillin (100µg/ml) were included where required.

2.3 Cloning methods

2.3.1 Generation of EVM025 truncation mutants

2.3.1.1 EGFP-EVM025(D237) (pJMT17)

We generated a version of the ectromelia virus orthologue of F1L, EVM025, which contained two copies of the N-terminal "DNGIVQDI" repeat beginning at aspartic acid 237 (D237). This truncation, EVM025(D237), was PCR amplified from EVM chromosomal DNA using primers EVF1LSenseTrunc and EVF1LGFPAnti (Fig. 2.1). The primer EVF1LSenseTrunc corresponds to the nucleotide sequence of the N-terminal repeat region of EVM025. A PCR product of 669bp was isolated, modified using an A-Addition Kit (Qiagen) (section 2.2.5), and ligated into pGEM-T to generate pJMT16. DNA sequencing revealed that two copies of the "DNGIVQDI" repeat had been incorporated into the PCR product. The resulting EVM025(D237) fragment was subcloned into pEGFPC3 as an EcoRI/BamHI fragment to generate pJMT17, which consisted of an N-terminal EGFP-fusion of EVM025(D237) (Fig. 2.1*B*).

2.3.1.2 EGFP-EVM025(E255) (pJF2)

In order to generate a version of EVM025 lacking the entire N-terminal "DNGIVQDI" repeat region beginning at glutamate 255 (E255), EVM025(E255) was PCR amplified from ectromelia virus chromosomal DNA using primers EVM025Tr(E255)Sense and EVF1LGFPAnti (Fig. 2.1). The resulting 609 base pair PCR product was treated with an A-Addition reaction (Qiagen) and TA-cloned into pGEM-T (Promega), generating pJF1. EVM025(E255) was subcloned into pEGFPC3 as an EcoRI/BamHI fragment, generating an EGFP-EVM025(E255) fusion (Fig. 2.1*C*).

2.3.1.3 FLAG-EVM025(D231) (pJMT44)

We generated a FLAG-tagged truncated version of EVM025 containing three copies of the N-terminal repeat sequence, 'DNGIVQDI', for expression during virus

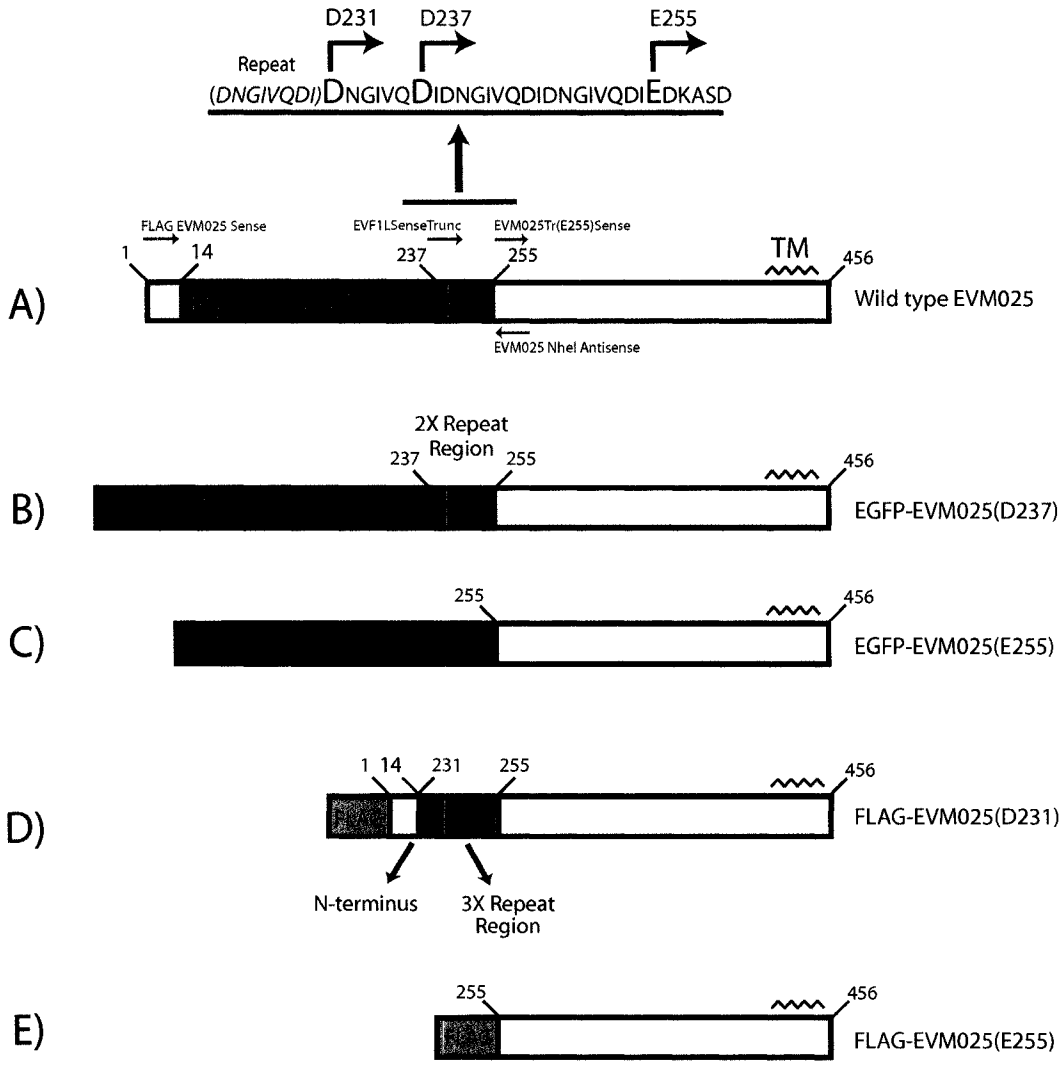

Figure 2.1 Generation of EVM025 truncation mutants.
To generate two truncation mutants of EVM025, two fragments were amplified from wild type EVM025 (A) with two primers, EVF1LSenseTrunc, which is complementary for the repeat region, an EVM025Tr(E255)Sense, which anneals immediately downstream of the repeat. The resulting gene fragments begin at D237 and E255, and are designated EVM025(D237) (B) and EVM025(E255) (C). These were used to generate two constructs which possessed N-terminal EGFP tags (in green). *D*, To generate FLAG-EVM025(E255), a primer beginning at E255 and containing an N-terminal FLAG-tag was used to amplify FLAG-EVM025(E255). *E*, To generate FLAG-EVM025(D231), the small N-terminal 5' fragment upstream of the repeat region (14 amino acids long, in yellow) linked to three copies of the repeat region (231-255) was generated with a FLAG tag, and was ligated to EVM025(E255) in frame. The only difference between FLAG-EVM025(D231) and wild type EVM025 is the absence of 27 copies of the repeat. Numbers indicate amino acids of EVM025. TM, Transmembrane domain.

infection. First, a small N-terminal fragment of EVM025 containing three copies of the N-terminal 'DNGIVQDI' repeat was cloned. Using primers Flag EVM025 Sense and EVM025 NheI Antisense, the N-terminal 780 base pairs of EVM025 was PCR amplified from ectromelia virus chromosomal DNA. This fragment was treated with an A-Addition Kit (Qiagen), and cloned into pGEM-T, resulting in pJMT40. Sequencing of positive clones revealed that the 5' and 3' ends of the fragment were correct and in frame, but precisely 648 nucleotides encoding 27 copies of the 'DNGIVQDI' repeat had been spontaneously deleted. The resulting DNA insert was 153 bp in size and the vector was designated pJMT40. This N-terminal fragment of EVM025 from pJMT40 was subcloned using an internal NheI restriction site which lies immediately downstream of the repeat, and NcoI which lies upstream of the FLAG-tagged N-terminus in pJMT40. This small 130bp fragment was cloned as an NcoI/NheI fragment into pJF1, which contains EVM025(E255). The resulting vector, pJMT43, contains a FLAG-tagged fusion of the N-terminus of EVM025 containing three copies of 'DNGIVQDI' appended to the C-terminal half of EVM025 from pJF1 (Fig. 2.1*D*). The resulting FLAG-tagged EVM025(D231) was subcloned from pJMT43 into pSC66 as a SalI/NotI fragment to place FLAG-EVM025(D231) under the control of the poxviral promoter of pSC66 (Fig. 2.1), generating pJMT44.

2.3.1.4 FLAG-EVM025(E255) (pJMT48)

To generate a FLAG-tagged version of EVM025(E255) containing no copies of the N-terminal repeat region for expression during virus infection (Fig. 2.1c), EVM025(E255) was amplified from pJF1 using primers FlagEVM025(E255) and EVF1LGFPAnti. The resulting PCR product was subjected to an A-Addition reaction (Qiagen), and was TA-cloned into pGEM-T to generate pJMT46. FLAG-EVM025(E255) was subcloned from pJMT46 into pSC66 as a SalI/NotI fragment to generate pJMT48.

2.3.2 Generation of a Bid expression vector, pCMV5-Bid

A mammalian expression vector expressing His-tagged Bid was generated by subcloning His-Bid from pET15-Bid (a generous gift from Dr. X. Wang, Texas)(212) into pCMV5 (QBiogene) as a XbaI/BamHI fragment, generating pCMV5-Bid.

2.4 Transfections

2.4.1 General transfection protocol

HeLa cells and HEK293T cells were transfected with Lipofectamine 2000 (Invitrogen) according to the manufacturer's specifications. DNA (1-4μg) and 2 μl of Lipofectamine 2000 were separately resuspended in 50μl of OptiMEM (Invitrogen) for 5 minutes, and then were gently mixed together and incubated at room temperature for 15 minutes. Cells were washed with 1ml of OptiMEM, and the 100μl lipid-DNA mixture was then added in combination with 900μl of OptiMEM to the cell monolayer. Cells were transfected for 90 minutes prior to the addition of 1ml DMEM containing 20% FBS, and were incubated overnight for 16 hours at 37°C. For cells co-transfected with the BH3-only proteins Bid, BimL, or Bmf, the broad-spectrum caspase inhibitor zVAD.fmk (100μM) (Kamiya Biomedical Company) was included to preserve cellular integrity (119).

2.4.2 Infection/transfections for expression of proteins during virus infection

To express FLAG-F1L, FLAG-EVM025(E255) or FLAG-EVM025(D231) during virus infection for confocal microscopy or western blot analysis, HeLa cells were infected with EVM at a multiplicity of infection (MOI) of 1 for 1 hour. Cells were then washed to remove excess virus and media, and transfected with 2μg of each FLAG-tagged construct in pSC66 under the synthetic early/late poxviral promoter, pSC66-FLAG-F1L, pJMT48 consisting of pSC66-FLAG-EVM025(E255), or pJMT44 consisting of pSC66-FLAG-EVM025(D231) (56). At 10 hours post-infection, cells were fixed and stained with anti-

cytochrome c and anti-mouse Alexa546 (section 2.7.6). Cells were washed extensively and were co-stained with anti-FLAG-FITC. Alternatively, cells were allowed to transfect for 16 hours, and samples were harvested in SDS-PAGE sample buffer and analyzed by western blotting with anti-FLAG(M2) (Sigma-Aldrich).

2.5 Virus manipulation and generation

2.5.1 Virus infection protocol

To infect 1×10^6 HeLa, CV-1, BMK, or MEF cell monolayers, virus at the indicated MOI was added to 0.5ml of cell media. Plates were incubated at 37°C for 1 hour with rocking every ten minutes, 2ml of fresh media was added, and infected cells were incubated at 37°C for the appropriate times. For infections in 10cm plates, 4 ml of media was used for the initial 1 hour infection, after which cells were replenished with an additional 4 ml of media.

To infect suspension Jurkat cells, cells were counted and resuspended at 5×10^6 cells/ml. The appropriate amount of each virus was added to 200µl of cells, and cells were incubated at 37°C for one hour on a rotator. Cells were then transferred to a tissue culture 6 well plate containing 2 ml of media, and incubated at 37°C in 5% CO_2.

2.5.2 Virus isolation

To isolate virus, infected BGMKs were harvested with SSC containing 0.15M NaCl and 0.015M tri-sodium citrate, and cell pellets were resuspended in 20ml swelling buffer containing 10mM Tris (pH 8.0), and 2mM $MgCl_2$ (331). Cells were subjected to three freeze/thaw cycles between -80°C/+37°C. Cells were then dounce homogenized using a B pestle (Bellco Biotechnology) 60 times on ice. Dounce homogenates were centrifuged at 300 ×*g* for 5 min, and supernatants transferred to a new tube. Cell pellets were resuspended in 10ml swelling buffer and dounce homogenized again with 30 strokes and re-centrifuged, 300 ×*g* for 5 min. Total supernatants were then pooled and

centrifuged at 10,000 ×*g* for one hour at 4°C, and the virus-containing pellet was resuspended in 1ml DMEM.

2.5.3 Inhibition of late gene synthesis

To inhibit late gene synthesis in infected cells, the nucleoside analogue cytosine arabinoside (AraC) (Sigma-Aldrich) was included in infections at 80μg/ml. Inhibition of late gene synthesis was confirmed by western blotting for viral protein I5L, which has been previously shown to be a late gene product. VV was UV-inactivated by treating virus stocks with 200mJ/cm^2 UV-light in a Stratalinker (Stratagene).

2.5.4 Virus chromosomal DNA preparations

To isolate viral chromosomal DNA, 1×10^6 CV-1 cells were infected at an MOI of 10 for 16 hours, and harvested with SSC. Cells were then centrifuged at 2000 × *g* for 5 minutes, and resuspended in DNA isolation buffer containing 2.25% (v/v) NP-40, 2.25% (v/v) Tween20, 5mM Tris (pH 8.0), and Proteinase K (250ng/ml) (Sigma-Aldrich). Lysis was performed at 55°C for 4 hours with periodic mixing, followed by boiling for 10 minutes. DNA was then phenol:chloroform extracted with 1 volume of phenol:chloroform, followed by a second extraction with 1 volume of chloroform. DNA was precipitated using 2.5 volumes of 95% ice-cold ethanol for 30 minutes on ice. DNA was then centrifuged for 10 minutes at 18000 ×*g*, and resuspended in water.

2.5.5 Growth curves

Single step growth curves were performed by infecting WT, Bak$^{-/-}$, Bax$^{-/-}$, or Bak$^{-/-}$/Bax$^{-/-}$ mouse embryonic fibroblasts at an MOI of 1 for 1 hour. Infected cells were washed with phosphate buffered saline (PBS) containing 4.3mM Na_2HPO_4, 1.4mM KH_2PO_4,137mM NaCl, 2.7mM KCl, pH 7.4. Cells were then replenished with fresh media and harvested at 0, 4, 8, 12, and 24 hours post infection. Harvested viruses were resuspended in swelling buffer, subjected to three freeze/thaw cycles between

-80°C/+37°C, and 200 µl of 2×DMEM added. Purified viruses were titred on CV-1 cells, and at 48 hours post-infection, cells were fixed for 5 minutes in neutral buffered formalin containing 11% formaldehyde (pH 7.4), 145mM NaCl, 55mM Na_2HPO_4, and 30mM NaH_2PO_4, and plaques were visualized by staining with crystal violet (0.1%(w/v) in 20% ethanol).

2.5.6 Plaque purifications and agarose overlays

To purify recombinant viruses, cells were overlaid with a low melting point (LMP) agarose overlay consisting of 1ml 2×DMEM (2.7% (w/v) DMEM, 88mM $NaHCO_3$), 1mL 2% (w/v) LMP agarose (Sigma-Aldrich), 400µl FBS. To visualize plaques that express *lacZ*, 100µl X-gal (5-bromo-4-chloro-3-indolyl-β-D-galatopyranoside; Rose Scientific) at 100mg/ml in dimethylformamide (Sigma-Aldrich) was added to the overlay. Overlays were allowed to cool prior to incubation at 37°C. Blue plaques expressing *lacZ* were selected and picked with a Pasteur pipette into 150µl of swelling buffer. Plaques were subjected to three freeze/thaw (-80°C, 37°C) cycles to lyse cells and release virus, and an equal volume of 2×DMEM was added. Prior to usage, viruses were sonicated for 20 seconds (0.5 second pulsing on/off cycles) (Misonix).

2.5.7 Generation of a recombinant virus expressing FLAG-EVM025(E255)

To generate a recombinant vaccinia virus expressing FLAG-tagged EVM025(E255) (100, 215), CV-1 cells were infected with VV(Cop)ΔF1L at a MOI of 0.1 for one hour. A total of 5µg of pJMT48, which consists of pSC66-FLAG-EVM025(E255) under the control of a synthetic poxviral promoter flanked by regions of the viral thymidine kinase (TK) gene, was linearized with PstI for one hour at 37°C. Double cross-over events between the TK fragments of pJMT48 and the endogenous viral TK gene will result in a virus that is TK^- (Fig. 2.2) (215), and as pJMT48 also encodes *lacZ* behind a poxviral promoter, recombinant viruses will also be $lacZ^+$.

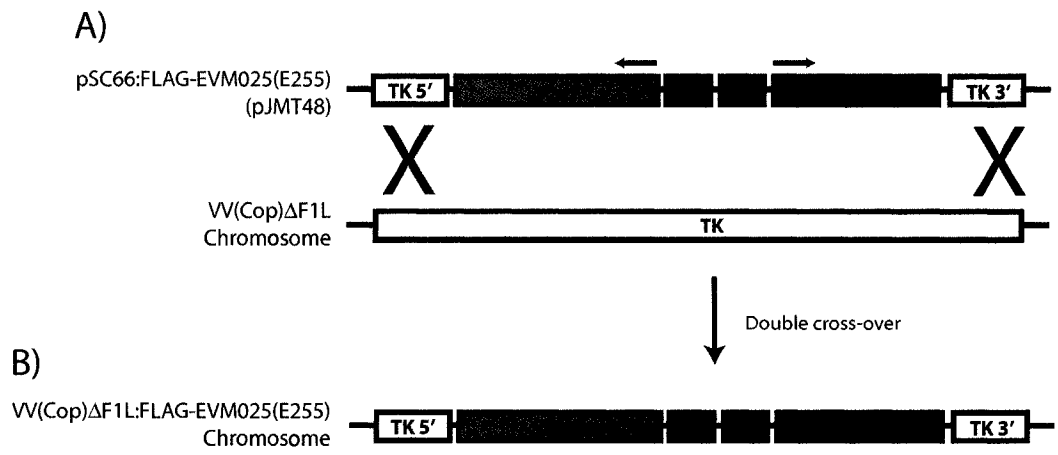

Figure 2.2 Generation of recombinant vaccinia virus expressing FLAG-EVM025(E255).
A, To generate recombinant viruses expressing FLAG-EVM025(E255), linearized vector (pJMT48) was transfected into cells infected with VV(Cop)ΔF1L. This vector contains flanking regions of the viral thymidine kinase (TK) gene, a copy of *lacZ* under control of a poxviral p7.5 promoter, and FLAG-EVM025(E255) under control of the strong synthetic early/late (E/L) poxviral promoter. Double-cross over events into the vaccinia virus TK gene will effectively disrupt the TK gene, and this was selected for in the presence of 5'-bromodeoxyuridine, which inhibits the growth of viruses expressing wild type TK. Viruses were also selected by overlaying infected monolayers with x-gal, which will reveal blue plaques expressing *lacZ*.
B, The resulting insertional double cross-over event results in a virus which expresses FLAG-EVM025(E255) from a strong synthetic poxviral promoter (E/L).

Following linearization of plasmid, the enzyme was heat inactivated at 80°C for 20 minutes. Cells were washed with OptiMEM (Invitrogen), and transfected with 5μg of linearized vector using Lipofectin (Invitrogen). For each transfection, 10μl of Lipofectin and 5μg of linearized pJMT48 were each incubated in 100μl of OptiMEM for 45 min. The two solutions were then mixed and incubated for another 15 min at room temperature, and the mixture was added to the cell monolayer with 800μl of fresh OptiMEM. At 48 hours post-transfection, cells were harvested with SSC and resuspended in 200μl of swelling buffer. Viruses were then titrated on a cell line lacking a functional TK gene, TK-H143, in the presence of 25μg/ml 5-bromodeoxyuridine (Sigma-Aldrich) which prevents the growth of cells and viruses expressing a functional TK gene. Viruses were plaque purified four times using X-gal to visualize recombinant plaques expressing β-galactosidase (*lacZ*). Viruses were amplified on CV-1 cells and the presence of FLAG-EVM025(E255) was confirmed by western blotting with anti-FLAG(M2) (Sigma-Aldrich).

2.6 Generation of EVMΔ025

2.6.1 Cloning of EGFP for the generation of recombinant knockout viruses

To generate an EGFP-cassette to use to insertionally inactivate EVM025, we cloned EGFP under control of a synthetic poxviral early/late promoter (pE/L) with flanking BglII restriction sites. EGFP including the poxviral early/late promoter (pE/L) was amplified from pSC66-EGFP using primers E/LSynFor and EGFPR(BglII). This PCR product was TA-cloned into pGEM-T, resulting in pJMT30.

2.6.2 Construction of a vector for inactivation of EVM025 (pJMT29)

To generate a strain of EVM deficient in EVM025, the ectromelia virus orthologue of F1L, we generated a knockout cassette to insertionally inactivate EVM025. To create this 025 knockout cassette, a region of EVM025 containing 158 base pairs

upstream of EVM025 and the first 45 base pairs of the 5' end of EVM025 was amplified using primersEVM025koF1 and EVM025koR1 (Fig. 2.3*A*). A downstream region comprising the last 159 base pairs of EVM025 was amplified using primers EVM025koF2 and EVM025koR2. The primers EVM025koR1 and EVM025koF2 both contain an overhanging linker region that encodes a BglII restriction site (Fig 2.3*A*). These PCR products were included in an overlapping PCR mixture with the primers EVM025koF1 and EVM025koR2 to obtain a continuous fragment encompassing both the upstream and downstream fragments of EVM025 separated by the BglII restriction site (Fig 2.3*A*). This 350bp fragment was subjected to an A-Addition reaction and cloned into pGEM-T to generate pJMT28. An EGFP cassette from pJMT30, under the control of a synthetic early/late poxviral promoter (section 2.6.1), was inserted as a BglII fragment in between the upstream and downstream EVM025 fragments, generating pJMT29. This effectively encodes a disrupted version of EVM025 that lacks approximately 80% of the EVM025 open reading frame (Fig. 2.3*B*)

2.6.3 Generation of EVMΔcrmAΔ025

To generate a strain of EVM deficient in CrmA and 025, pJMT29 was generated as described in section 2.6.2. pJMT29 (5μg) was linearized with NotI for one hour at 37°C, and the enzyme was heat inactivated at 65°C for 20 minutes. CV-1 cells were infected at an MOI of 0.1 for one hour with EVMΔcrmA, which lacks the caspase inhibitor CrmA. Cells were washed with warm OptiMEM, and 5μg of linear pJMT29 was transfected with 10μl of Lipofectin. Two days post-infection, cells were harvested into 200μl of swelling buffer, and CV-1 cells re-infected. Following LMP agarose overlays (section 2.5.6), recombinant foci were purified by selecting and picking GFP-fluorescent foci using an inverted fluorescent microscope (Leica Microsystems). Successful recombinants will express EGFP, and the EVM025 open reading frame will have been effectively insertionally inactivated (Fig. 2.3*C*). Recombinant EVMΔcrmAΔ025 was plaque purified 6 times, amplified in CV-1 cells, and purified virus was assessed by PCR

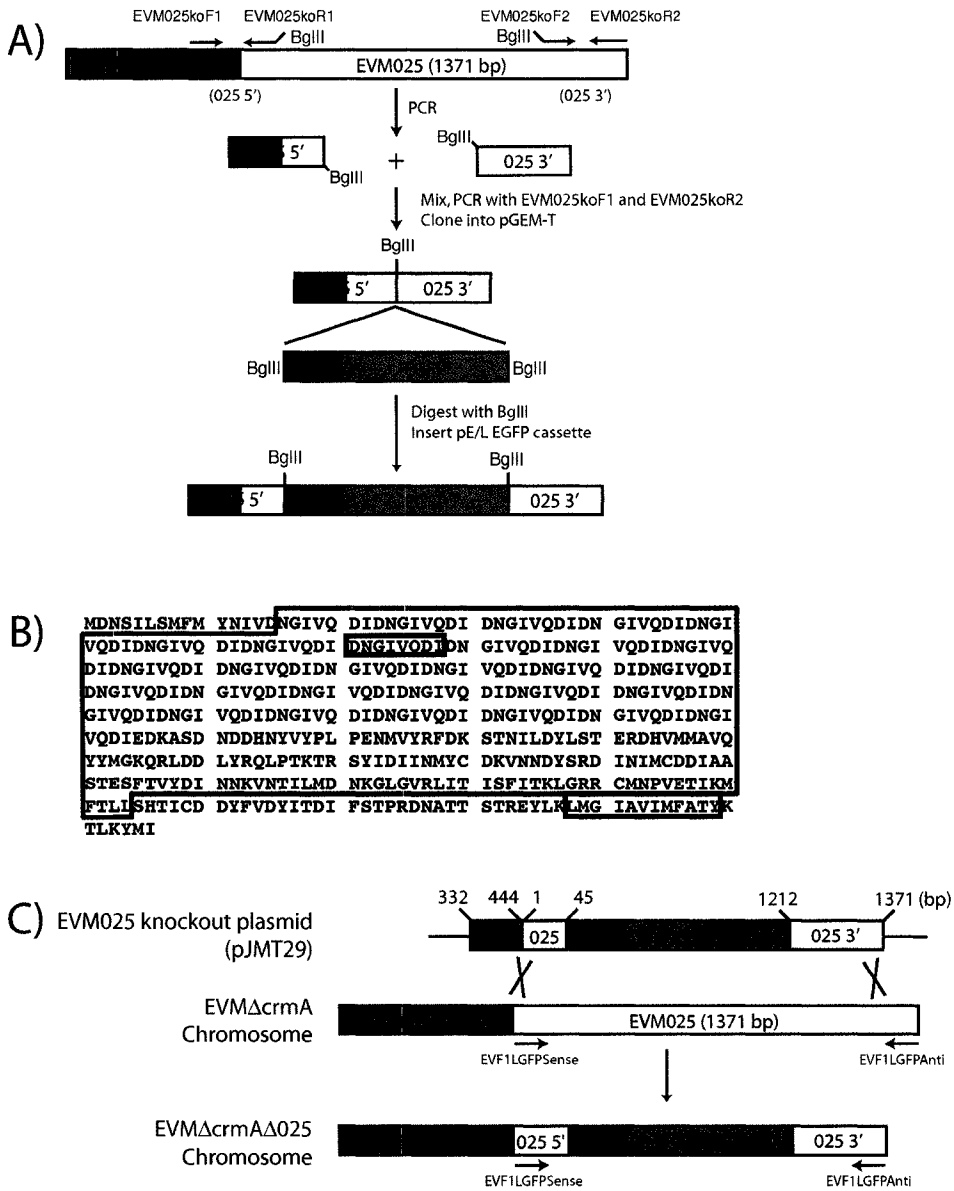

Figure 2.3 Generation of EVMΔcrmAΔ025.
A, To generate a strain of ectromelia virus deficient in EVM025, two small regions flanking EVM025 were amplified with an overlapping linker region containing a BglII restriction site. These fragments were used as template in an overlapping PCR reaction to generate one contiguous fragment with a BglII site separating the fragments. An EGFP cassette behind a poxviral promoter (pE/L) was then inserted into the BglII site to create the knockout plasmid pJMT29. *B*, amino acid sequence of EVM025, with the red boxed region indicating amino acids deleted from the EVM025 knockout cassette, the green box indicating the 8 amino adic repeat, and the blue underlined region indicating the transmembrane tail. *C*, a double-cross over event between the homologous regions of EVM chromosome and the EVM025 knockout vector, pJMT29, described in (A). The double cross-over will replace the majority of EVM025 with the EGFP-cassette, and recombinant viruses can be selected for by EGFP-expression.

using the primers EVF1LGFPSense and EVF1LGFPAnti (Table 2.4), and by western blotting with anti-F1L antibody.

2.7 Protein methodology

2.7.1 Protein quantification using a bichinconinic acid kit

Protein preparations were quantified using a bichinconinic acid (BCA) Protein Assay Kit (Pierce Biotechnology) according to manufacturer's instructions. Bovine serum albumin (Roche) was used to create a standard curve, and both standard and protein samples were added to 200µl of BCA reagent. After 30 minutes at 37°C, samples were read at 570nm using a 96-well plate reader (Softmax Inc.), and protein concentrations determined by plotting optical densities against the standard curve.

2.7.2 SDS polyacrylamide gel electrophoresis

SDS polyacrylamide gel electrophoresis (SDS-PAGE) was performed essentially as described (190) using the Mini-PROTEAN3 Cell (BioRad). Protein samples were suspended in SDS-PAGE sample buffer containing 62.5mM Tris (pH 8.0), 10% (v/v) glycerol, 2% (w/v) SDS, 50mM β-mercaptoethanol, and 0.1% (w/v) bromophenol blue (190), and were boiled at 95°C for 10 minutes. Pre-stained low range molecular weight markers (BioRad) were used as molecular markers for all western blots. Gels were run in Tris-glycine running buffer containing 25mM Tris, 190mM glycine, and 3.5mM SDS at 150V until resolved.

2.7.3 Western transfer

Proteins were transferred from SDS-PAGE gels to either nitrocellulose (GE Water and Process Technologies) or polyvinylidene difluoride (PVDF) membranes (GE Healthcare) for 2 hours at 420mA using a semi-dry transfer apparatus (Tyler Research) in semi-dry transfer buffer containing 192mM glycine, 25mM Tris, and 20% methanol.

Membranes were then blocked overnight at 4°C or at room temperature for one hour in 5% (w/v) skim milk in Tris-buffered saline plus Tween20 (TBST) consisting of 20mM Tris, 15mM NaCl, pH 7.5, plus 0.1% (v/v) Tween20 (Fisher Scientific).

2.7.4 Antibodies and immunoblotting

All antibodies are listed in Table 2.5, and were diluted to the indicated concentration in TBST and allowed to incubate on membranes for 2 hours at room temperature. Cleavage of poly ADP-ribose polymerase (PARP) was detected with anti-PARP (clone C2-10)(BD Biosciences) at a dilution of 1:2000. Bak was detected with anti-Bak(NT)(Upstate) at 1:2000, and FLAG was probed with anti-FLAG-horseradish peroxidase (HRP) (M2; Sigma-Aldrich) at 1:2000. Bax was detected using anti-Bax(N20) at a dilution of 1:500 (BD Biosciences) and cytochrome c was detected using anti-cytochrome c (clone 7H8.2C12) (BD Biosciences) at 1:1000. Manganese superoxide dismutase (MnSOD) was detected using anti-MnSOD (clone 110) (Stressgen Bioreagents) at a dilution of 1:5000. Bid was detected using anti-Bid at 1:5000 (381), and T7-Bmf was detected with anti-T7 (Novagen) at 1:5000. BimEL and BimL were detected with anti-Bim (Calbiochem) at 1:2000. EGFP was detected with anti-EGFP (Cedarlane) at 1:30,000. Anti-caspase-3 was generated as described previously, and was used at 1:5000 (381). Anti-F1L was generated in rabbits against the N-terminal 120 amino acids of F1L as previously described (329), and was used at 1:5000. Anti-I5L was generated in rabbits against a C-terminal peptide from the I5L viral protein, 'TYVKSLLMKS' (Sigma-Aldrich), and was used at 1:5000. Following primary antiobody incubations, membranes were washed four times for ten minutes with TBST, and incubated with either anti-rabbit-HRP (1:10000) (Jackson Laboratories), anti-mouse-HRP (1:10000) (Jackson Laboratories), anti-rabbit-HRP (1:10000) (BioRad) or anti-mouse-HRP (1:3000) (BioRad) in TBST for 1 hour at room temperature. Proteins were visualized with enhanced chemiluminescence (ECL) (GE Healthcare) and XAR radiography film (Kodak).

Table 2.5. Antibodies used in this study

Antibody (Western blot)	Species	Dilution	Source
Anti-Bax (N20)	Rabbit	1:500	BD Pharmingen
Anti-Bak (NT)	Rabbit	1:2000	Upstate
Anti-FLAG-HRP (M2)	Mouse	1:2000	Sigma
Anti-Bim	Rabbit	1:1000	Calbiochem
Anti-EGFP	Rabbit	1:30000	L. Berthiaume
Anti-PARP (C2-10)	Mouse	1:2000	BD Pharmingen
Anti-cytochrome c (7H8.2C12)	Mouse	1:200	BD Pharmingen
Anti-MnSOD (110)	Rabbit	1:5000	Stressgen Bioreagents
Anti-Bid	Rabbit	1:5000	(381)
Anti-caspase-3	Rabbit	1:5000	(381)
Anti-T7	Rabbit	1:10000	Novagen
Anti-I5L	Rabbit	1:5000	This study (Sigma)
Anti-F1L	Rabbit	1:5000	(329)
Anti-mouse-HRP	Goat	1:3000	BioRad
Anti-rabbit-HRP	Goat	1:10000	BioRad
Anti-mouse-HRP	Goat	1:10000	Jackson Laboratories
Anti-rabbit-HRP	Goat	1:10000	Jackson Laboratories

Antibody (Immunofluorescence)	Species	Dilution	Source
Anti-FLAG-FITC (M2)	Mouse	1:200	Sigma
Anti-cytochrome c (6H2.B4)	Mouse	1:150	BD Pharmingen
Anti-Bax (6A7)	Mouse	1:500	BD Pharmingen
Anti-Bax (rabbit polyclonal)	Rabbit	1:500	BD Pharmingen
Anti-Bim	Rabbit	1:500	Calbiochem
Anti-Bid	Rabbit	1:500	(381)
Anti-mouse-Alexa546	Goat	1:300	Invitrogen
Anti-rabbit-Alexa546	Goat	1:300	Invitrogen
Anti-mouse-Alexa633	Goat	1:150	Invitrogen

Antibody (Immunoprecipitation)	Species	Amount	Source
Anti-Bax (6A7)	Mouse	0.5 µg	BD Pharmingen
Anti-FLAG (M2)	Mouse	1µg	Sigma
Anti-EGFP	Goat	1µl	L. Berthiaume
Anti-Bim	Rabbit	1µg	Calbiochem

2.7.5 Immunoprecipitations

Immunoprecipitations were performed in either 2% CHAPS lysis buffer containing 2% CHAPS (w/v), 137mM NaCl, 20mM Tris pH 7.4, and Complete protease inhibitor (Roche Diagnostics), or 1% Triton-X-100 lysis buffer containing 1% Triton-X-100 (v/v), 137mM NaCl, 20mM Tris pH 7.4, and Complete protease inhibitor (Roche Diagnostics). Cells were lysed at 4°C for one hour, and the insoluble material was pelleted at 18000 × *g* for 10 minutes. Ten percent of the supernatant was kept as the lysate input and was resuspended in one volume of SDS-PAGE sample buffer (section 2.7.2). The remaining supernatant fraction was transferred to a new tube and used for the immunoprecipitation. Proteins were immunoprecipitated with either anti-FLAG(M2), anti-Bax(6A7), anti-EGFP, or anti-Bim, as indicated in Table 2.5.

2.7.5 a) Immunoprecipitation of activated Bax

To immunoprecipitate activated Bax, cells were lysed in 2% CHAPS lysis buffer, and soluble protein fractions were incubated with 1μg of anti-Bax (6A7) (Pharmingen) overnight at 4°C (157). Immune complexes were bound to protein A sepharose (GE Healthcare) for 2 h at 4°C, washed three times with 2% CHAPS lysis buffer and resuspended in SDS-PAGE sample buffer.

2.7.5 b) Anti-FLAG immunoprecipitations

For transient transfections, HEK293T cells were transfected with 1μg of pcDNA3-FLAG-BimL in conjunction with 4μg of either pEGFP-C3, pEGFP-F1L, pEGFP-F1L(206-226), or pEGFP-Bcl-2. Cells were transfected for 16 hours prior to lysis. For FLAG-F1L or FLAG-EVM025(E255) immunoprecipitations, HeLa cells were infected with VV:FLAG-F1L or VV(Cop)ΔF1L:FLAG-EVM025(E255) at an MOI of 5 for 12 hours. To immunoprecipitate FLAG-tagged proteins, cells were lysed in either 2% CHAPS lysis buffer or 1% Triton-X-100 lysis buffer, and soluble fractions were

incubated with 1μg of anti-FLAG(M2) (Sigma Aldrich) overnight at 4°C. Immune complexes were then precipitated with protein A sepharose (GE Healthcare) for 2 hours at 4°C. Samples were then washed three times with the appropriate lysis buffer, and proteins were eluted with SDS-PAGE sample buffer.

2.7.5 c) Immunoprecipitation of endogenous Bim

To immunoprecipitate endogenous Bim, $Bak^{-/-}/Bax^{-/-}$ (also designated $Bim^{+/+}$) or $Bim^{-/-}$ BMK cells were infected with VV:FLAG-F1L for 12 hours, and lysed in 2% CHAPS lysis buffer. Soluble fractions were incubated with 0.5μg of anti-Bim (Calbiochem) overnight at 4°C. Immune complexes were isolated with protein A sepharose (GE Healthcare) for 2 hours at 4°C, washed three times with 2% CHAPS lysis buffer, and resuspended in SDS-PAGE sample buffer to elute bound proteins.

2.7.5 d) Anti-EGFP immunoprecipitations

To express EGFP-tagged proteins and BimL in HEK293T cells, cells were transfected with 1μg of pcDNA3-FLAG-BimL in conjunction with 4μg of either pEGFP-C3, pEGFP-F1L, pEGFP-F1L(206-226), or pEGFP-Bcl-2. Cells were transfected for 16 hours prior to lysis. Transfected cells were lysed in 2% CHAPS lysis buffer, and lysates were immunoprecipitated with 1μl of goat anti-EGFP (L. Berthiaume, University of Alberta, Edmonton, Alberta) for 2 hours at 4°C (379). Immune complexes were then purified with 35μl of protein G sepharose (GE Healthcare) for 2 hours at 4°C, and after 3 washes with 2% CHAPS lysis buffer, protein complexes were released with SDS-PAGE sample buffer.

2.7.6 Confocal microscopy

For examination of activated Bax in HeLa cells, approximately 2×10^5 HeLa cells were seeded on glass coverslips, and were transfected with 2μg of each EGFP construct (EGFP-C3, EGFP-F1L, EGFP-F1L(206-226), EGFP-EVM025(E255), EGFP-

EVM025(D237)) in the presence or absence of 1μg of pcDNA3-FLAG-BimL or pCMV5-Bid. To preserve cellular integrity, 100μM zVAD.fmk (Kamiya Biomedical Company) was included in all transfections(119). Alternatively, cells were infected with either VV(Cop)EGFP, VV(Cop), or VV(Cop)ΔF1L for 8 hours, and were treated with or without UV-light and allowed to recover for 5 hours prior to fixation.

For localization of EVM025 constructs, HeLa cells were transfected with 2μg of either pEGFPC3, pEGFP-F1L, pJF2 (EGFP-EVM025(E255)), or pJMT17 (EGFP-EVM025(D237)) for 16 hours, and fixed and stained as described below. Alternatively, HeLa cells were infected with EV at an MOI of 1 for 1 hour, and transfected with either pSC66-FLAG-F1L, pJMT44, or pJMT48, which express FLAG-F1L, FLAG-EVM025(D231), or FLAG-EVM025(E255) respectively.

For transient transfections of $Bak^{-/-}$ MEFs, approximately 2×10^5 cells were co-transfected with either 1μg of pCMV5-Bid or pcDNA3-FLAG-BimL plus 4μg of either pEGFP-F1L of pEGFP-F1L(206-226) in the presence of 100μM zVAD.fmk (Kamiya Biomedical Company) for 16 hours (119).

All cells were fixed with 4% (w/v) paraformaldehyde (Sigma-Aldrich) in PBS for 10 minutes at room temperature, permeabilized with 0.04% saponin (Sigma-Aldrich) in PBS for 10 minutes at room temperature, and blocked with 30% normal goat serum (Invitrogen) for 30 minutes at room temperature. All primary antibodies were incubated for 2 hours at room temperature in PBS containing 1% (v/v) FBS, and are listed in Table 2.5. EGFP-tagged proteins were visualized through their natural fluorescence using a 488nm laser. Bax activation was detected by staining with anti-Bax(6A7) (BD Biosciences) at 1:500 (156, 158) and Bax subcellular redistribution was detected by staining with rabbit polyclonal anti-Bax (BD Biosciences) at 1:500 (184). Cytochrome c was stained with anti-cytochrome c (clone 6H2.B4) (BD Pharmingen). Bim localization was detected using anti-Bim (Calbiochem) at 1:500. Bid was stained with rabbit anti-Bid at 1:200 and co-stained with mouse anti-cytochrome c (clone 6H2.B4; BD Biosciences)

at 1:200. Primary antibodies were detected using anti-rabbit Alexa546 or anti-mouse Alexa546 (Invitrogen) at 1:300, or anti-mouse Alexa633 (Invitrogen) at a 1:150 dilution. Cells were washed three time with PBS containing 1% (v/v) FBS for 10 minutes at room temperature. Coverslips were mounted with 4mg/ml N-propyl-galate (Sigma-Aldrich) in 50% glycerol and analyzed using laser scanning microscopy and LSM 510 imaging software (Zeiss) at the Cross Cancer Institute Imaging Facility. Laser wavelengths were 488nm for EGFP fluorescence and FITC fluorescence, 543nm for Alexa546 staining, and 633nm for Alexa633. Data was quantified by counting 200 cells per experiment. The means and standard deviation from three replicate experiments are shown.

2.7.7 Assessment of BimEL phosphorylation

To assess BimEL phosphorylation, mock and VV-infected HeLa cells were lysed in SDS-PAGE sample buffer, and samples were separated by SDS-PAGE and immunoblotted with anti-Bim (Calbiochem). To inhibit BimEL phosphorylation, the mitogen-activated protein/extracellular signal-regulated kinase (MEK) inhibitor U0126 (Sigma-Aldrich) or the phosphatidylinositol 3-kinase (PI-3-kinase) inhibitor Wortmannin (Calbiochem) were included at 30μM and 200nM respectively for 30 minutes prior to infection or treatment with TNFα.

2.8. Apoptosis assays

2.8.1 Induction of apoptosis

To induce apoptosis with UV-light, cells were subjected to 200 mJ/cm^2 of UV-C in PBS without a lid using a Stratalinker UV Crosslinker (Stratagene), supplemented with fresh media and allowed to recover for the indicated times. Apoptosis was also induced with 10ng/ml TNF-α (Roche Diagnositics) plus 5μg/ml cycloheximide (Sigma-Aldrich), 250ng αFas (Clone CH11) (Upstate Biotechnology) plus 5μg/ml cycloheximide, or 1μM

staurosporine (Sigma-Aldrich). Alternatively, apoptosis was induced by infection alone with VV(Cop)ΔF1L or EVMΔcrmAΔ025 at a MOI of 10 for the indicated times.

2.8.2 Measurement of mitochondrial membrane potential

To examine TNFα and αFas-mediated apoptosis in HeLa cells by flow cytometry, cells were transfected with 4μg of pEGFP, pEGFP-F1L, pEGFP-F1L(206-226), or pJF2 (EGFP-EVM025(E255)), or pJMT17 (EGFP-EVM025(D237)) for 16 hours. Cells were then treated with TNFα or αFas in the presence of cycloheximide for 6 hours.

To examine BH3-only protein-induced apoptosis in HeLa cells by flow cytometry, cells were transfected with either 1μg pcDNA3-T7-Bmf, pcDNA3-FLAG-BimL, or pCMV5-Bid in combination with 4μg of pEGFP-C3, pEGFP-F1L, pEGFP-F1L(206-226), or pEGFP-Bcl-2 for 16 hours. To preserve cellular integrity, 100μM zVAD.fmk (Kamiya Biomedical Company) was included in all transfections (119).

Alterations in the mitochondrial membrane potential were detected by staining cells with tetramethylrhodamine ethyl ester (TMRE) (Invitrogen)(228). Following transfection and treatment with an apoptotic stimulus, cells were stained with 0.2 μM TMRE for 30 minutes at 37°C, washed with PBS containing 1% (v/v) FBS, and fluorescence was detected with a Becton Dickinson FACScan through the FL-2 channel. Loss of the mitochondrial membrane potential in EGFP-positive cells was measured as a decrease in TMRE fluorescence by two-color flow cytometry as described (329). Data were acquired on 20000 cells per sample, and analyzed with CellQuest software. Loss of the inner mitochondrial membrane potential was calculated as (number of $EGFP^+TMRE^-$ cells/total number of $EGFP^+$ cells) x 100, and data are represented as the mean (±S.D.) from three replicate experiments.

2.8.3 Detection of PARP cleavage

Protein samples were resuspended in SDS-PAGE sample buffer (section 2.7.2) containing 8M urea, and were resolved by 8% SDS-PAGE prior to western transfer to nitrocellulose membrane. Membranes were then probed with anti-PARP antibody (1:2000; Pharmingen).

2.8.4 Detection of Bax N-terminal conformational change

2.8.4 a) Detection of Bax N-terminal conformational change by confocal microscopy

HeLa cells were seeded on glass coverslips and were infected with VV(Cop) or VV(Cop)ΔF1L at an MOI of 10. At 8 hours post-infection, cells were treated with UV-light, allowed to recover for 5 hours, and were fixed with 4% paraformaldehyde. Cells were permeabilized with 0.04% saponin (Sigma-Aldrich) for 10 minutes at room temperature, and were blocked with 30% normal goat serum (Invitrogen) for 30 minutes at room temperature. Cells were stained with anti-Bax(6A7) (157) at 1:500 for 2 hours at room temperature, and were co-stained with anti-mouse-Alexa546 (1:300) for 1 hour. Cells were mounted onto glass slides with N-propyl-galate, and were visualized with confocal microscopy (section 2.7.6).

2.8.4 b) Detection of Bax conformational change by immunoprecipitation

Anti-Bax immunoprecipitations were performed as described in section 2.7.4. Approximately 6×10^6 HeLa, $Bak^{-/-}$ BMK, or $Bak^{-/-}$ MEF cells were seeded in 10cm dishes and were infected with either VV(Cop), VV(Cop)ΔF1L, EVMΔcrmA, or EVMΔcrmAΔ025 at an MOI of 10. Cells were induced with either virus infection alone, UV-light, TNFα, or staurosporine, harvested with SSC and washed with 10ml of PBS. Cell pellets were then lysed in either 2% CHAPS or 1% Triton-X-100 lysis buffer for one hour at 4°C (section 2.7.5), and were passed through a 22 gauge needle 20 times to facilitate lysis. Cell debris was pelleted at 18000×*g* for 10 minutes, and supernatant

fractions were immunoprecipitated with 0.5μg of anti-Bax(6A7) overnight at 4°C. Antibody complexes were precipitated with the addition of protein A beads (GE Healthcare) for 2 hours at 4°C. Beads were washed three times with lysis buffer and immunocomplexes were released in SDS-PAGE sample buffer. Samples were western blotted with anti-Bax(N20).

2.8.5 Gel filtration chromatography

Gel filtration chromatography was used to separate Bax oligomers from monomers, and was performed as described (12, 379, 404). Briefly, HeLa cells ($1x10^7$), or Hela cells overexpressing Bcl-2, were infected with either VV(Cop)EGFP or VV(Cop)ΔF1L at an MOI of 10 for 8 h, exposed to UV light and allowed to recover for 5 h. Cells were lysed in CHAPS lysis buffer containing 2% (w/v) CHAPS, 137mM NaCl, 0.2mM DTT, 20mM Tris (pH 7.4), and disrupted by passage through a 22 gauge needle 60 times followed by incubation at 4°C for one hour. Lysates were centrifuged for 15 min at 18000 x*g*, and protein concentrations were normalized using a BCA protein quantification kit (section 2.7.1). Supernatants were loaded at a flow rate of 0.1 ml/min on a Superose6 HR (10/30) column (GE Healthcare) equilibrated in 1% (w/v) CHAPS, 137mM NaCl, 0.2mM DTT, 20mM Tris (pH 7.4). The column was calibrated using thyroglobulin (669 kDa), ferritin (440kDa), catalase (232 kDa), aldolase (158 kDa), albumin (67 kDa), and ovalbumin (43 kDa). Fractions of 150μl were collected, and aliquots were analyzed by western blotting with anti-Bax(N20) (BD Biosciences).

2.8.6 Mitochondrial isolation

Mitochondria were isolated as described (379, 408). HeLa cells ($1x10^7$) or $Bak^{-/-}$ MEFs ($1x10^7$) were infected at an MOI of 10 with either VV(Cop)EGFP or VV(Cop)ΔF1L for 8 h. Cells were washed and resuspended in 1ml hypotonic lysis buffer containing 250mM sucrose, 20mM HEPES (pH 7.5), 10mM KCl, 1.5mM $MgCl_2$, 1mM

EDTA, 1mM EGTA, and incubated on ice for 30 min (408). Cells were passed through a 22 gauge needle 60 times, and crude membranes and nuclei were pelleted at 750 ×*g* for 10 min. The pellet was resuspended in 1 ml hypotonic lysis buffer and again passed through a 22 gauge needle 60 times. Membranes and nuclei were pelleted at 750 ×*g*, and the supernatant containing the mitochondria was centrifuged at 10000 ×*g* for 15 min at 4°C to isolate mitochondria. Protein concentrations were determined using a BCA assay (see 2.7.1).

2.8.6 a) Assessment of Bax insertion from purified mitochondria

To remove loosely associated proteins from mitochondria, mitochondrial pellets were washed with either 0.1M Na_2CO_3 (pH 12) for 20 min on ice (12), or with hypotonic lysis buffer as a negative control, and mitochondria were centrifuged at 100,000 ×*g* for 35 min at 4°C using an ultracentrifuge (Beckman), and Ti.50 rotor (Beckman). Mitochondrial membrane pellets were resuspended in hypotonic lysis buffer containing 2% (w/v) CHAPS and protein concentrations were determined using a standard BCA test (Pierce Biotechnology). Equilibrated protein samples were then western blotted for Bak or Bax.

2.8.6 b) Cytochrome c release from purified mitochondria

To induce cytochrome c release in purified mitochondria, increasing amounts of recombinant tBid (R&D Biosystems) were added to 50μg of mitochondria, and incubated for 45 min at 30°C. Mitochondria were harvested by centrifugation at 10000 x*g* for 15 min at 4°C, and supernatant and pellet fractions were analyzed by western blotting.

2.8.6 c) tBid-induced Bax activation in isolated mitochondria

To detect tBid-induced activated Bax, purified mitochondria (100μg) were incubated with 300ng of recombinant tBid for 40 minutes at 30°C. Purified mitochondria were pelleted and resuspended in 2% CHAPS lysis buffer containing 2% (w/v) CHAPS,

137mM NaCl, 20mM Tris pH 7.4, and Complete mini proteasome inhibitor (Roche Diagnostics). Activated Bax was immunoprecipitated with anti-Bax(6A7) as described in section 2.8.4b.

2.8.7 Cytochrome c release assays

2.8.7 a) Cytochrome c release by fractionation of Jurkat cells

Cytochrome c release was monitored by western blotting as previously described (381). Jurkat cells ($1x10^6$) were infected at an MOI of 10, and at 6 hours post-infection, were induced with either staurosporine (1μM) (Sigma-Aldrich) or UV-light ($200mJ/cm^2$). Cells were then permeabilized in freshly prepared lysis buffer containing 75 mM NaCl, 1 mM NaH_2PO_4, 8 mM Na_2HPO_4, 250 mM sucrose and 190 μg of digitonin (Sigma-Aldrich) for 10 minutes on ice. Mitochondria-containing supernatants and pellets were separated by centrifugation at 10,000 ×*g* for 5 minutes, and pellets were lysed in 0.1% (w/v) Triton-X-100 containing 25mM Tris (pH 8.0). Both supernatant and pellet fractions were resuspended in SDS-PAGE sample buffer, and cytochrome c release was monitored by western blotting supernatant and pellet fractions.

2.8.7 b) Cytochrome c release by confocal microscopy

To assess cytochrome c release by confocal microscopy, $Bak^{-/-}$ MEFs were transfected with 1μg of either pcDNA3-FLAG-BimL or pCMV5-Bid, in conjunction with 4μg of either pEGFP-F1L or pEGFP-F1L-(206-226) for 16 hours, and cells were fixed in 4% (w/v) paraformaldehyde for 10 minutes at room temperature. Cells were permeabilized in 0.04% (w/v) saponin for 10 minutes at room temperature, and were stained with anti-Bim, anti-Bid, or anti-cytochrome c. Cells were then stained with secondary anti-rabbit-Alexa546 or anti-mouse-Alexa633, and then washed and mounted on N-propyl galate (section 2.7.6).

2.8.7 c) Cytochrome c release from tBid-treated mitochondria

To detect cytochrome c release in purified mitochondria, increasing amounts of recombinant tBid (R&D Biosystems), from 0 to 150ng, were added to 50μg of mitochondria and incubated for 45 min at 30°C. Mitochondria were then pelleted at 10000 ×*g* for 15 minutes at 4°C, and the supernatant and pellet fractions were western blotted for cytochrome c.

2.8.8 Detection of DNA fragmentation by TUNEL

DNA fragmentation was assessed by using the terminal deoxynucleotidyltransferase-mediated dUTP nick end labeling method (TUNEL) (Roche Diagnostics) (381). Jurkat cells were infected at an MOI of 10 for 5 hours. Cells were subjected to UV-light, and zVAD.fmk was included as a control at 100μM. Cells were fixed with 2% (w/v) paraformaldehyde in PBS for 10 minutes at room temperature, and permeabilized with 0.1% (v/v) Triton-X-100, 0.1% (w/v) sodium citrate for 10 minutes on ice. Cells were then stained for 1 hour at 37°C with 25 mM Tris (pH 6.6), 200 mM cacodylate, 1 mM $CoCl_2$, 0.6 nM fluorescein-12-dUTP, and 25 U of terminal deoxynucleotidyltransferase according to manufacturer's instructions. Cells were washed with PBS containing 1% (v/v) FBS, analysis was performed on a Becton Dickinson FACScan and data were acquired on a minimum of 10,000 cells per sample. TUNEL positive cells were measured through the FL-1 channel equipped with a 488nm filter (42nm band pass), and data were analyzed with CellQuest software.

2.8.9 Detection of apoptosis in baby mouse kidney cells

Wild type and $Bim^{-/-}$ BMK cells were infected with VV(Cop) or VV(Cop)ΔF1L at a MOI of 10 in the absence and presence of 100 μM zVAD.fmk. Apoptosis was determined by counting the number of adherent cells remaining, and the percentage of adherent cells (% cell survival) was determine by normalizing values against the number

of adherent cells following infection with VV(Cop). Standard deviations were calculated from three independent experiments. To detect PARP cleavage, floating and adherent cells were harvested, lysed in SDS-PAGE sample buffer containing 8M urea, and analyzed by western blotting with anti-PARP (1:1000; Pharmingen). PARP cleavage products were quantified using ImageQuant™

CHAPTER 3: The Vaccinia Virus Protein F1L Inhibits Bax Activation

A portion of this chapter has been published:

Taylor J.M., D. Quilty, L. Banadyga, and M. Barry. The vaccinia virus protein F1L interacts with Bim and inhibits activation of the pro-apoptotic protein Bax. 2006. Journal of Biological Chemistry. 281:39728-39.

All of the experiments included within this chapter were performed by J. Taylor. The original manuscript was written by J. Taylor, and a major editorial contribution was made by M. Barry.

3.1 Introduction

Apoptosis, or programmed cell death, is used extensively by the immune system to eliminate unwanted or infected cells (18, 75, 330). Apoptotic death intimately involves the mitochondria of the cell, and ultimately results in mitochondrial dysfunction and the release of pro-apoptotic factors such as cytochrome c from the mitochondria (186, 377). Events at the mitochondria are coordinated by a family of proteins, known as the Bcl-2 family, that localize to the mitochondria and regulate cytochrome c release (77, 130). The Bcl-2 family is subdivided into anti-apoptotic members (*ie.* Bcl-2), pro-apoptotic multi-domain family members (*ie.* Bak and Bax), and the BH3-only proteins (*ie.* Bid, Bim) that activate Bak and Bax (1, 130). The pro-apoptotic multi-domain Bcl-2 family members Bak and Bax regulate cytochrome c release at the mitochondria, and expression of either Bak or Bax is absolutely required to facilitate apoptosis at the mitochondria (91, 204, 385).

Work in our lab has previously shown that the vaccinia virus protein F1L is a potent anti-apoptotic protein (329, 379, 382). F1L localizes to and inserts into the outer mitochondrial membrane via a C-terminal hydrophobic anchor (329, 382). While anchored at the mitochondria, F1L serves to inhibit cytochrome c release and the loss of the mitochondrial membrane potential induced by a variety of pro-apoptotic stimuli (329, 382). It was shown recently that F1L can interact with the pro-apoptotic protein Bak (265, 379). F1L expression also inhibited the initial N-terminal conformational change in Bak, and the oligomerization of Bak following an apoptotic stimulus (265, 379). Bax, however, can mediate cytochrome c release independently of Bak, and only the inhibition of both Bak and Bax results in the complete blockage of cytochrome c release (91, 204, 385). Indeed, certain viruses inhibit the activation of both Bak and Bax to inhibit apoptosis during infection (39, 82). Unlike Bak, which is constitutively localized to the outer mitochondrial membrane, Bax is normally found in the cytosol of healthy cells (156). Following an apoptotic stimulus, Bax undergoes a conformational change which

reveals N-terminal and C-terminal epitopes, and Bax inserts into the mitochondrial outer membrane and oligomerizes into a high molecular weight complex (12, 126, 156, 157).

Although it has been established that F1L inhibits Bak activation and interacts with Bak (265, 379), it is not known whether vaccinia virus can inhibit Bax activation during apoptosis. Vaccinia viruses devoid of F1L induce apoptosis and Bak activation in tissue culture (113, 379), so we examined whether infection with VV(Cop)ΔF1L also induced Bax activation. We investigated the ability of vaccinia virus and F1L to inhibit Bax activation during apoptosis, both in the presence and absence of Bak. As F1L interacts with Bak to inhibit Bak activation (265, 379), we also examined whether F1L interacts with Bax. Here we show that F1L can inhibit the activation of the pro-apoptotic protein Bax, although no direct interaction between F1L and Bax was observed. These results suggest that F1L expression potently inhibits Bax activation and apoptosis mediated by Bax, but that F1L likely accomplishes this indirectly.

3.2 Results

3.2.1 F1L expression inhibits UV-induced apoptosis

We have previously shown that vaccinia virus can inhibit apoptosis induced by a number of stimuli, including TNFα, staurosporine, and anti-Fas (329, 381, 382), and that the mitochondrial-localized vaccinia virus protein F1L is essential for this anti-apoptotic activity (265, 329, 379, 382). UV-light potently induces the intrinsic apoptotic cascade and readily induces Bax activation (12, 172). To determine if F1L can inhibit UV-light induced apoptosis, Jurkat cells were infected with wild-type VV(Cop), stimulated with UV-light, and apoptosis was quantified using terminal deoxynucleotidyl transferase biotin-dUTP nick end labeling (TUNEL) to measure DNA fragmentation (Fig. 3.1*A*). All untreated healthy cells showed similar levels of fluorescence indicative of intact nuclear DNA (Fig. 3.1*A* panels a, d, f, h). Treatment of Jurkat cells with UV-light, however, resulted in a significant increase in DNA fragmentation (Fig. 3.1*A*, panel b), and this

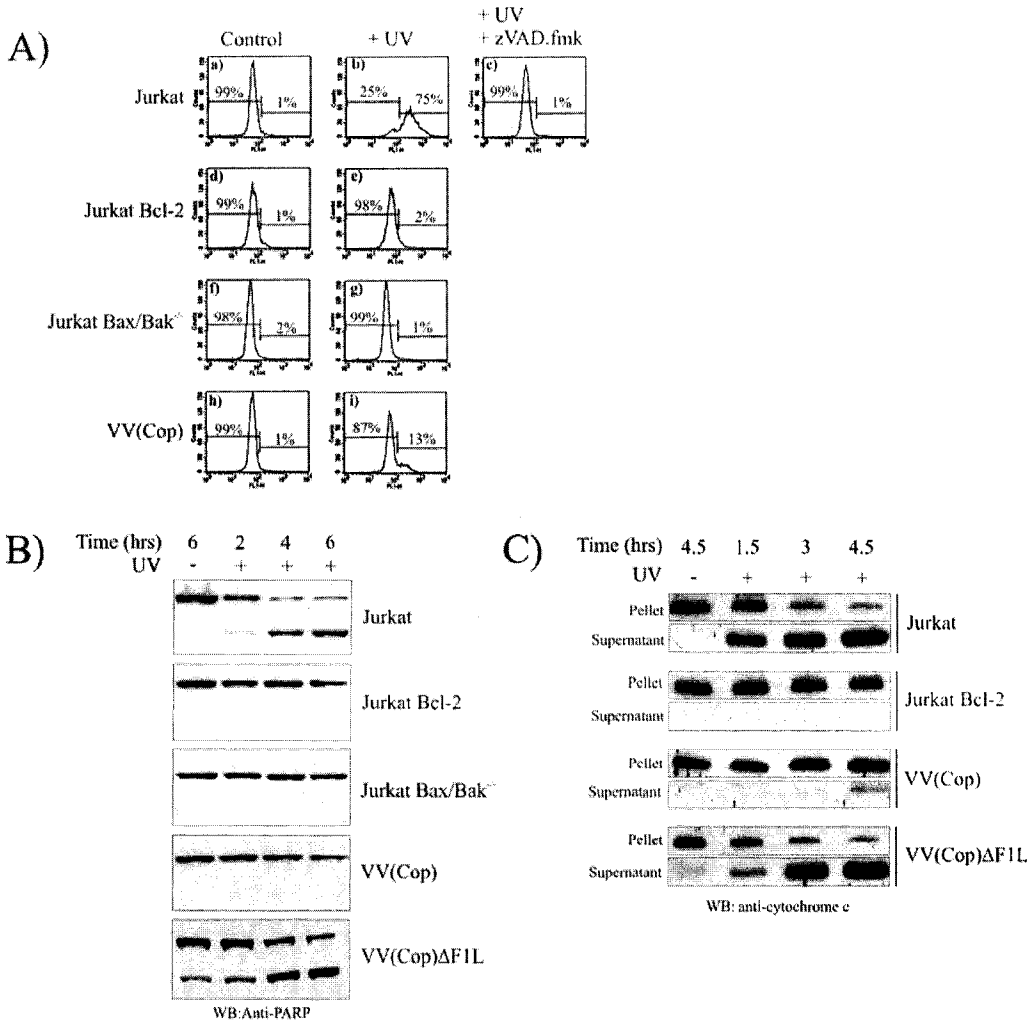

Figure 3.1. Vaccinia virus F1L inhibits apoptosis induced by UV-light.
A, Jurkat cells, Jurkat cells overexpressing Bcl-2, Jurkat cells deficient in Bax and Bak (Bax/Bak$^{-/-}$), or Jurkat cells infected with VV(Cop) at an MOI of 10 for 6 hours were treated with UV-light. Four hours post-treatment, DNA fragmentation was assessed by TUNEL and flow cytometry. The broad-spectrum caspase inhibitor, zVAD.fmk, was used to inhibit apoptosis. *B*, Jurkat cells, Jurkat cells overexpressing Bcl-2, or Jurkat cells deficient in Bak and Bax (Bax/Bak$^{-/-}$) were mock infected or infected with VV(Cop) or VV(Cop)ΔF1L at an MOI of 10 for 6 hours, treated with UV-light and apoptosis assessed at the indicated times post-treatment by western blotting for PARP cleavage. *C*, Jurkat cells or Jurkat cells overexpresssing Bcl-2 were mock infected or infected as in (B) and treated with UV-light. At the indicated times post-treatment, cells were fractionated into mitochondria (pellet) and soluble (supernatant) fractions, and cytochrome c release assessed by western blotting.

DNA fragmentation could be inhibited with the broad-spectrum caspase inhibitor zVAD.fmk (Fig. 3.1*A* panel c). Jurkat cells overexpressing Bcl-2 or Jurkat cells lacking both Bak and Bax showed no detectable increase in DNA fragmentation following UV-treatment (Fig. 3.1*A*, panels e, g), indicating that UV-light induced death required the intrinsic mitochondrial apoptotic pathway (19, 374). Notably, cells infected with VV(Cop) were also resistant to UV-induced DNA fragmentation, suggesting the presence of a strong viral inhibitor of apoptosis (Fig. 3.1*A* panel i).

We have previously generated a strain of VV(Cop) that is devoid of F1L, VV(Cop)ΔF1L (379). This virus expresses high amounts of EGFP, which interferes with detection of the fluorescent label used in TUNEL staining. To examine whether VV(Cop)ΔF1L could inhibit UV-induced apoptosis, we instead assessed cleavage of the nuclear apoptotic substrate poly-ADP-ribose polymerase (PARP) (173). Jurkat cells were infected for 6 hours with wild-type VV(Cop) or VV(Cop)ΔF1L (379). Cells were treated with UV-light, lysates were harvested at 2, 4, and 6 hours post-treatment, and cleavage of PARP was assessed by western blotting. As expected, mock-infected Jurkat cells gradually exhibited cleavage of PARP at all times post-UV treatment (Fig. 3.1*B*), whereas cells overexpressing Bcl-2 or cells devoid of both Bak and Bax were resistant to UV-induced PARP cleavage (Fig. 3.1*B*). Infection of cells with wild-type VV(Cop), but not infection with VV(Cop)ΔF1L, inhibited UV-induced PARP cleavage (Fig. 3.1*B*), demonstrating that F1L expression was necessary to inhibit UV-induced apoptosis. In fact, we routinely observed PARP cleavage in cells infected for 12 hours with VV(Cop)ΔF1L in the absence of UV-light (Fig. 3.1*B*). Indeed, infection of Jurkat cells with VV(Cop)ΔF1L has been shown to induce cytochrome c release and apoptosis at 12 hours post infection (379, 382).

Cytochrome c release from the mitochondria is a critical event in the intrinsic pro-apoptotic cascade (146, 207), and F1L localizes to the mitochondria to inhibit cytochrome c release induced by a variety of apoptotic stimuli (379, 382). In order to

assess the ability of F1L to also inhibit UV-induced cytochrome c release, we monitored the release of mitochondrial-sequestered cytochrome c by cell fractionation and western blotting (382). Jurkat cells were infected with VV(Cop) or VV(Cop)ΔF1L for 6 hours, treated with UV-light, and fractionated into mitochondrial and cytosolic fractions at 1.5, 3, and 4.5 hours post-treatment. The release of cytochrome c into the cytosolic fraction was detected by western blotting with anti-cytochrome c (Fig 3.1*C*). Mock-infected Jurkat cells treated with UV-light demonstrated translocation of cytochrome c from the mitochondrial to the cytosolic fraction as early as 1.5 hours post treatment (Fig. 3.1*C*). Cells overexpressing Bcl-2, however, were protected from cytochrome c release at all times post-treatment (Fig. 3.1*C*). Cells infected with VV(Cop) were also protected from cytochrome c release following treatment with UV-light (Fig. 3.1*C*). VV(Cop)ΔF1L-infected cells, on the other hand, readily released cytochrome c following UV-light treatment (Fig. 3.1*C*), similar to our previous observations examining PARP cleavage (Fig. 3.1*B*). These results demonstrate that, in addition to inhibiting apoptosis induced by TNFα, αFas or staurosporine, F1L is an important inhibitor of the mitochondrial checkpoint during UV-induced apoptosis.

3.2.2 Vaccinia Virus Infection Induces Bax Activation

Induction of apoptosis at the mitochondria is achieved through the activation of Bax and Bak, two pro-apoptotic members of the Bcl-2 family (91, 204, 385), and viral anti-apoptotic proteins such as M11L and E1B 19K inhibit both Bak and Bax to block the intrinsic mitochondrial apoptotic pathway (39, 82, 148). Given that infection with a recombinant vaccinia virus deficient for F1L, VV(Cop)ΔF1L, induces apoptosis and Bak activation (379), we assessed whether infection with VV(Cop)ΔF1L also stimulated Bax activation. HeLa cells were infected with a recombinant wild type vaccinia virus expressing EGFP, VV(Cop)EGFP, or VV(Cop)ΔF1L, which induces apoptosis due to the lack of F1L expression (379). Bax undergoes a conformational change during apoptosis

exposing an N-terminal epitope, so we used the N-terminal conformation specific Bax antibody, anti-Bax(6A7), to detect Bax activation by confocal microscopy (51, 126, 157, 158, 244). Anti-Bax (6A7) specifically interacts with the N-terminus of Bax that is accessible only following Bax activation, and only stains cells containing active Bax (157, 158). Cells infected with VV(Cop) for 24 hours resulted in very few cells exhibiting anti-Bax(6A7) reactivity (Fig. 3.2*A*, panels a-c). Infection with VV(Cop)ΔF1L, on the other hand, resulted in Bax activation in approximately 50% of infected cells (Fig. 3.2*A*, panels d-f), and results were quantified by counting EGFP-expressing cells positive for anti-Bax(6A7) (Fig. 3.2*B*). We also assessed Bax activation by immunoprecipitation using the anti-Bax(6A7) antibody (157, 158), followed by western blotting with anti-Bax(N20). As anti-Bax(6A7) interacts with the activated N-terminus of Bax, only active Bax will be immunoprecipitated (157, 158). HeLa cells were infected with either VV(Cop)EGFP or VV(Cop)ΔF1L for 12, 18, or 24 hours. Cells were lysed in 2% CHAPS, a detergent that maintains the native conformation of Bax, and active Bax was immunoprecipitated with anti-Bax(6A7) (157). Mock-infected HeLa cells displayed no active Bax, as expected (Fig. 3.2*C*). HeLa cells infected with VV(Cop)EGFP showed no Bax activation at 12 hours post-infection, and only minimal amounts of Bax activation at 18 or 24 hours post infection (Fig. 3.2*C*). Cells infected with VV(Cop)ΔF1L, meanwhile, demonstrated Bax activation at 12 hours post-infection which increased substantially at 18 and 24 hours post-infection (Fig. 3.2*C*). The total amount of Bax in each sample was equivalent as western blotting lysates with anti-Bax showed similar amounts of Bax (Fig. 3.2*C*). These results indicate that in the absence of F1L, VV infection stimulated Bax activation (Fig. 3.2*C*).

3.2.3 F1L Inhibits Bax Activation

Infection with VV(Cop)ΔF1L, but not with VV(Cop), induced significant Bax activation, suggesting that F1L can inhibit VV-induced Bax activation. Therefore, we

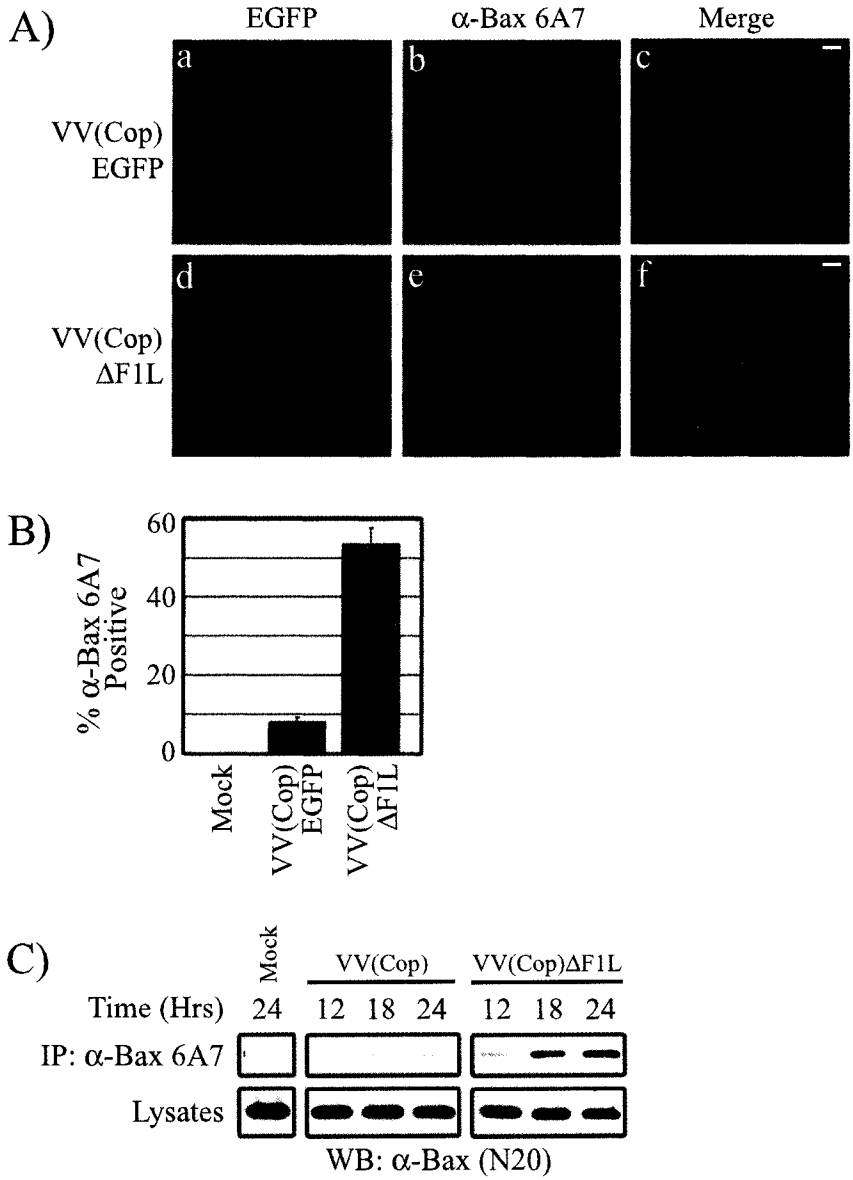

Figure 3.2. Infection with a vaccinia virus devoid of F1L induces Bax activation.
A, HeLa cells were infected at a MOI of 10 with either VV(Cop)EGFP, or VV(Cop)ΔF1L for 24 h. Cells were fixed, permeabilized and stained with anti-Bax(6A7) to visualize activated Bax (scale bar = 10μm). *B*, Results were quantified as a percentage of EGFP-positive cells exhibiting anti-Bax 6A7 reactivity (mean ± S.D.). *C*, HeLa cells were infected for the indicated times with either VV(Cop)EGFP or VV(Cop)ΔF1L, and immunoprecipitated using anti-Bax(6A7). Immunoprecipitates and whole cell lysates were western blotted with anti-Bax(N20).

also examined the ability of F1L to inhibit Bax activation induced by an intrinsic apoptotic stimulus such as UV-light (12, 172). HeLa cells or HeLa cells overexpressing Bcl-2 were treated with UV-light to induce apoptosis, stained with the conformation-specific anti-Bax(6A7) antibody, and visualized by confocal microscopy. Mock treated HeLa cells demonstrated no anti-Bax(6A7) reactivity (Fig. 3.3*A*, panel a), whereas HeLa cells treated with UV-light showed extensive anti-Bax(6A7) reactivity (Fig. 3.3*A*, panel b). In contrast, HeLa cells stably expressing Bcl-2 were completely resistant to UV-induced anti-Bax(6A7) reactivity (Fig. 3.3*A*, panels c and d). To determine if F1L expression inhibited anti-Bax(6A7) reactivity, HeLa cells were infected with either wild-type VV(Cop)EGFP or VV(Cop)ΔF1L, treated with UV-light, and stained with anti-Bax(6A7). Infection with VV(Cop)ΔF1L did not protect cells from Bax activation induced by UV-light (Fig. 3.3*B* panel e). Infection with VV(Cop)EGFP, however, significantly protected cells from UV-induced anti-Bax(6A7) positivity (Fig. 3.3*B* panel b). These results were quantified by determining the percentage of EGFP-positive cells that were anti-Bax(6A7)-positive (Fig. 3.3*D*). We also examined the ability of VV(Cop) to inhibit Bax activation by immunoprecipitating active Bax following treatment with UV-light or TNFα. HeLa cells were infected with VV(Cop)EGFP or VV(Cop)ΔF1L for 8 hours and treated with either UV-light or TNFα. Cells were then lysed in 2% CHAPS and immunoprecipitated with anti-Bax(6A7). No active Bax was immunoprecipitated from mock-treated cells, as expected (Fig. 3.3*C*, lane 1). Similarly, no active Bax was immunoprecipitated from cells infected with VV(Cop) in the absence of an apoptotic stimulus (Fig. 3.3*C*, lane 4), while infection with VV(Cop)ΔF1L alone induced a small amount of Bax activation (Fig. 3.3*C*, lane 7). Treatment of mock-infected or VV(Cop)ΔF1L-infected cells with either TNF-α or UV-light resulted in significant Bax activation as assessed by immunoprecipitation (Fig 3.3*C*, lanes 2-3, 8-9). Notably, cells infected with VV(Cop)EGFP were completely resistant to TNF-α or UV-induced Bax N-

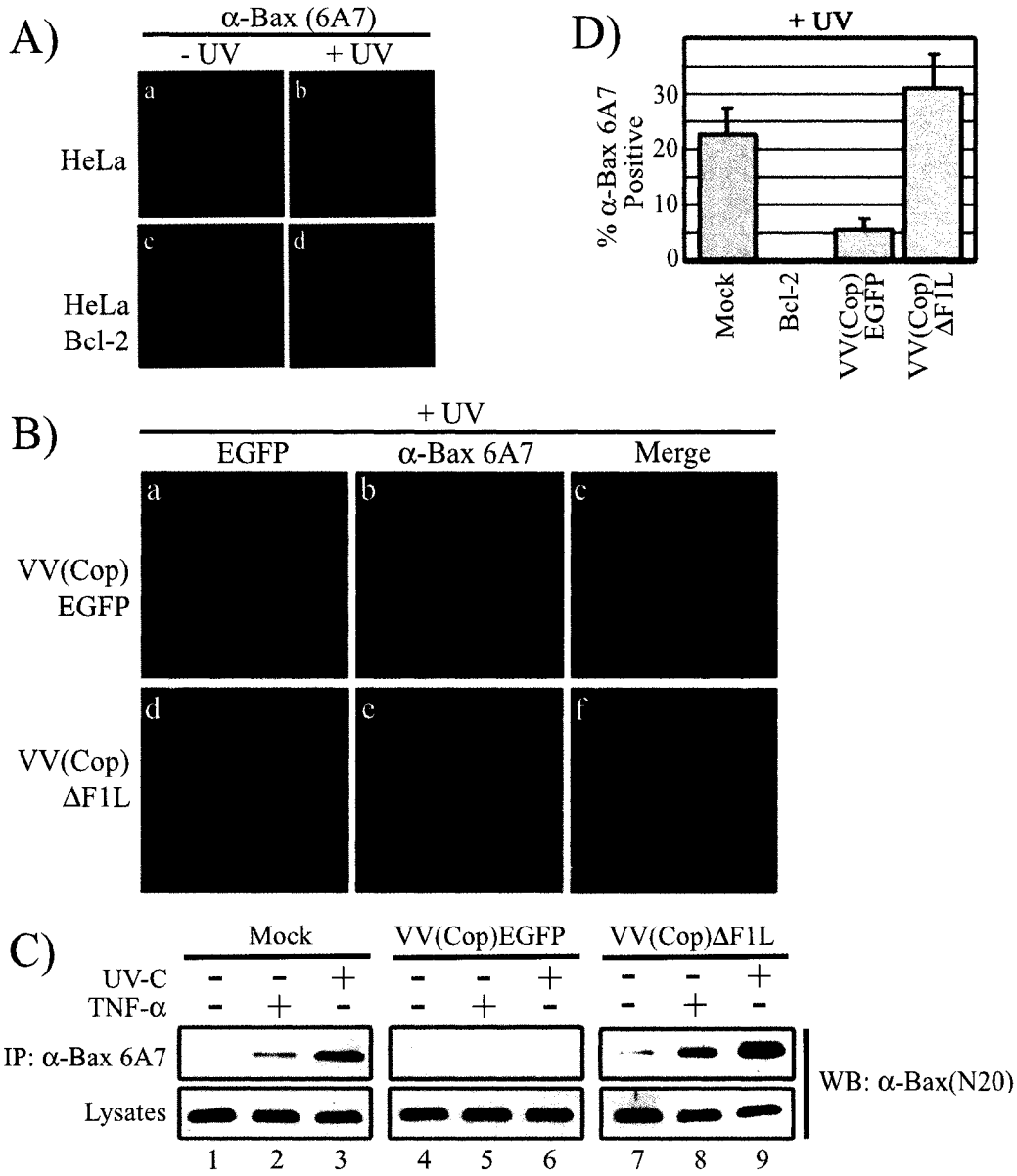

Figure 3.3. F1L inhibits Bax activation induced by an apoptotic stimulus. *A*, HeLa cells or HeLa cells that overexpress Bcl-2 were treated with UV-light to induce apoptosis and Bax activation was monitored by staining with anti-Bax (6A7) to detect the conformationally active form of Bax. *B*, HeLa cells were infected with either VV(Cop)EGFP or VV(Cop)ΔF1L at a MOI of 10 for 8 h. Cells were treated with UV-light to induce apoptosis, and 5 h post-treatment, cells were fixed and stained with anti-Bax(6A7). *C*, HeLa cells were infected with VV(Cop)EGFP or VV(Cop)ΔF1L at an MOI of 10 for 8 h, and Bax activation was induced with UV-light or TNFα. Active Bax was immunoprecipitated with anti-Bax(6A7), and immunoprecipitates and whole cell lysates were analyzed by western blotting with anti-Bax(N20). *D*, Infected cells from (B) were visualized by EGFP fluorescence, and the mean percentage of cells demonstrating anti-Bax 6A7 positivity (± S.D.) was quantified.

terminal activation as assessed by immunoprecipitation with anti-Bax(6A7) (Fig. 3.3*C*, lanes 5-6). Again, no significant change was seen in Bax amounts present in lysates from each sample (Fig. 3.3*C*).

Our lab has shown that F1L can function in the absence of virus infection to inhibit TNFα or αFas-induced apoptosis (329, 382), indicating that no other viral proteins are required for inhibition. To determine whether F1L could inhibit Bax activation independent of other viral proteins, cells were transiently transfected with either an EGFP-tagged version of full-length F1L, or EGFP-F1L(206-226) which consists of EGFP appended to the C-terminal mitochondrial-targeting domain of F1L (amino acids 206-226) and localizes to the mitochondria but fails to inhibit apoptosis (329, 382). Apoptosis was induced with UV-light and cells were stained with anti-Bax(6A7). Transient expression of F1L in the absence of virus infection inhibited Bax activation, as HeLa cells expressing EGFP- F1L inhibited UV-induced anti-Bax(6A7) reactivity (Fig. 3.4*A* panels a, b and c, dashed arrows) compared with untransfected cells (Fig. 3.4*A*, panels a, b, c, solid arrows). In contrast, HeLa cells expressing EGFP-F1L(206-226), the hydrophobic tail construct of F1L that fails to inhibit apoptosis (329, 382), displayed significant UV-induced anti-Bax(6A7) reactivity (Fig. 3.4*A* panels d, e and f). Results were quantified as shown in figure 3.4*B* as a percentage of EGFP-positive cells also displaying Bax activation. Furthermore, EGFP-F1L(206-226), which localizes to the mitochondria (329, 382), co-localized with active Bax indicating that activated Bax localizes to mitochondria (Fig. 3.4*A* panels d, e and f). These results indicate that F1L expression inhibits the conformational change in Bax initiated by either virus infection or extrinsic stimuli.

3.2.4 F1L Inhibits Bax Oligomerization

Following an apoptotic trigger, Bax oligomerizes into high-molecular weight complexes to facilitate cytochrome c release (12, 101), so we investigated the ability of

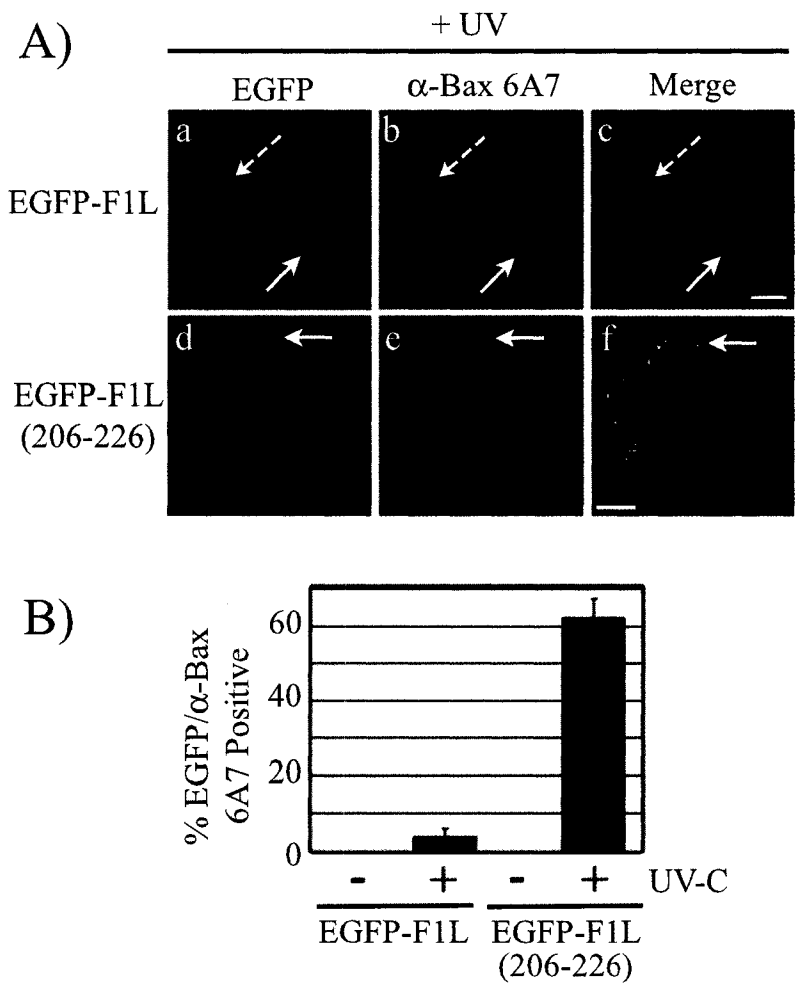

Figure 3.4. Transient expression of F1L inhibits UV-induced Bax N-terminal exposure. *A*, HeLa cells were transfected with either pEGFP-F1L or pEGFP-F1L(206-226) for16h, treated with UV-light, and fixed cells were stained with anti-Bax (6A7) and anti-mouse Alexa546 to detect activated Bax (scale bar = 10μm). Dashed arrows indicate transfected cells displaying no anti-Bax6A7) staining, and solid arrows indicate transfected or untransfected cells displaying anti-Bax(6A7) reactivity. *B*, Results were quantified as a mean percentage (± S.D.) of EGFP-positive cells that also were anti-Bax(6A7) positive.

F1L to also inhibit Bax oligomerization. HeLa cells were either mock infected or infected with wild type VV(Cop) or VV(Cop)ΔF1L. Following treatment with UV-light, cells were lysed in 2% CHAPS which maintains the native conformation and oligomerization state of Bax (157, 158), and protein complexes were separated based on size by gel filtration chromatography. In the absence of UV-light, Bax was detected in mock-infected cells as a monomer which eluted in fractions below 43kDa in size (Fig. 3.5*A*). In contrast, cells treated with UV-light exhibited a loss of monomeric Bax and the majority of Bax eluted in high molecular weight fractions in excess of 149kDa, indicative of Bax oligomerization (Fig. 3.5*A*). In samples from HeLa cells overexpressing Bcl-2 and HeLa cells infected with VV(Cop), Bax predominantly eluted in low molecular weight fractions below 43kDa, even following treatment with UV-light, indicating that both Bcl-2 overexpression and VV infection inhibited Bax oligomerization (Fig. 3.5*A*). In cells infected with VV(Cop)ΔF1L, however, Bax eluted as a high molecular weight oligomer following UV-treatment (Fig. 3.5*A*), and virtually no Bax was retained in the low molecular weight fractions. We also observed a small amount of oligomerized Bax in cells infected with VV(Cop)ΔF1L alone (Fig. 3.5*A*), indicative of the ability of VV(Cop)ΔF1L to induce apoptosis (379). This indicates that F1L expression can strongly inhibit Bax oligomerization following an apoptotic stimulus. Bax oligomerization was not influenced by changes in Bax expression, as infection with either VV(Cop) or VV(Cop)ΔF1L had no effect on Bax protein expression over time (Fig. 3.5*B*).

3.2.5 F1L Inhibits Bax Recruitment to the Mitochondria and Insertion into the Outer Mitochondrial Membrane

F1L expression clearly inhibited the conformational alteration and the oligomerization of Bax, so we investigated whether F1L could also prevent Bax localization and insertion into the mitochondrial membrane following an apoptotic stimulus (51, 126, 156, 244). To determine the effect of F1L on Bax integration into the

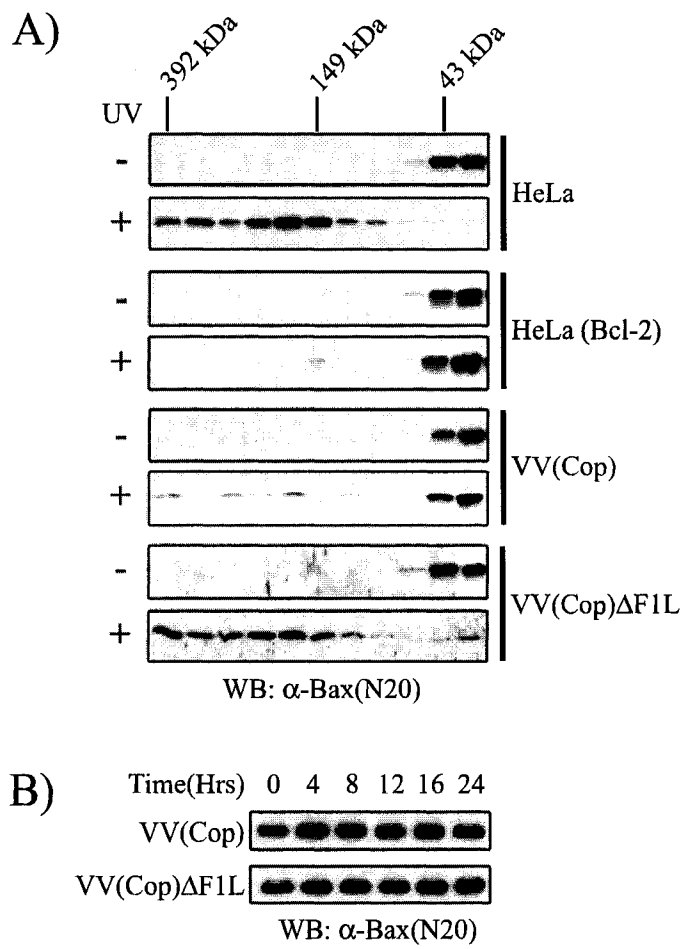

Figure 3.5. F1L inhibits Bax oligomerization.
A, HeLa cells were infected with either VV(Cop) or VV(Cop)ΔF1L at a MOI of 10 for 8 h. HeLa cells were treated with UV-light and gel filtration lysates were prepared in 2% CHAPS as described in materials and methods.Bax oligomerization was assessed by gel filtration chromatography and western blotting with anti-Bax(N20). *B*, Bax expression in cells infected with VV(Cop) or VV(Cop)ΔF1L was analyzed by western blotting with anti-Bax(N20).

outer mitochondrial membrane, mitochondria were isolated and treated with a sodium carbonate alkali wash to remove loosely associated proteins (115). Mitochondria from mock-infected HeLa cells displayed loosely associated Bax that was removed following the alkali wash (Fig. 3.6*A*, lanes 1 and 2). Following treatment with UV-light, however, Bax remained membrane associated following the alkali wash, indicative of Bax integration into the outer mitochondrial membrane (Fig. 3.6*A*, lanes 3 and 4) (12). Bak, on the other hand, is constitutively integrated into the outer mitochondrial membrane, and was not removed following the alkali wash (Fig. 3.6*A*, lanes 2 and 4) (12, 132). HeLa cells overexpressing Bcl-2, as well as cells infected with VV(Cop), displayed no insertion of Bax into the mitochondrial membrane following treatment with UV-light (Fig. 3.6*B* and *C*, lane 4), indicating that F1L, similar to Bcl-2, can inhibit Bax insertion into mitochondrial membranes. Cells infected with VV(Cop)ΔF1L, however, displayed UV-induced Bax insertion, as Bax was still associated with the membrane fraction following the alkali wash (Fig. 3.6*D*, lanes 3 and 4). Significantly, we also detected some Bax integrated in the mitochondrial membrane from cells infected with VV(Cop)ΔF1L alone, again indicating the ability of this virus to initiate apoptosis and induce Bax activation (Fig. 3.6*D*, lane 2). These results demonstrated that F1L expression inhibited the insertion of Bax into the mitochondrial outer membrane during apoptosis.

While the events surrounding Bax activation are complex and controversial, a recent report suggests that release of the N-terminus of Bax is only observed after Bax translocation to the mitochondria (363). To investigate the possibility that F1L may inhibit Bax oligomerization and insertion, but not translocation, we assessed Bax subcellular distribution in the presence or absence of F1L. HeLa cells were infected with either VV(Cop) or VV(Cop)ΔF1L for 24 hours and stained with a polyclonal anti-Bax antibody which, unlike anti-Bax(6A7), detects Bax in the cytosol and at the mitochondria in apoptotic and non-apoptotic cells (184). Mock infected HeLa cells stained with polyclonal anti-Bax demonstrated a diffuse cytoplasmic staining pattern for Bax when

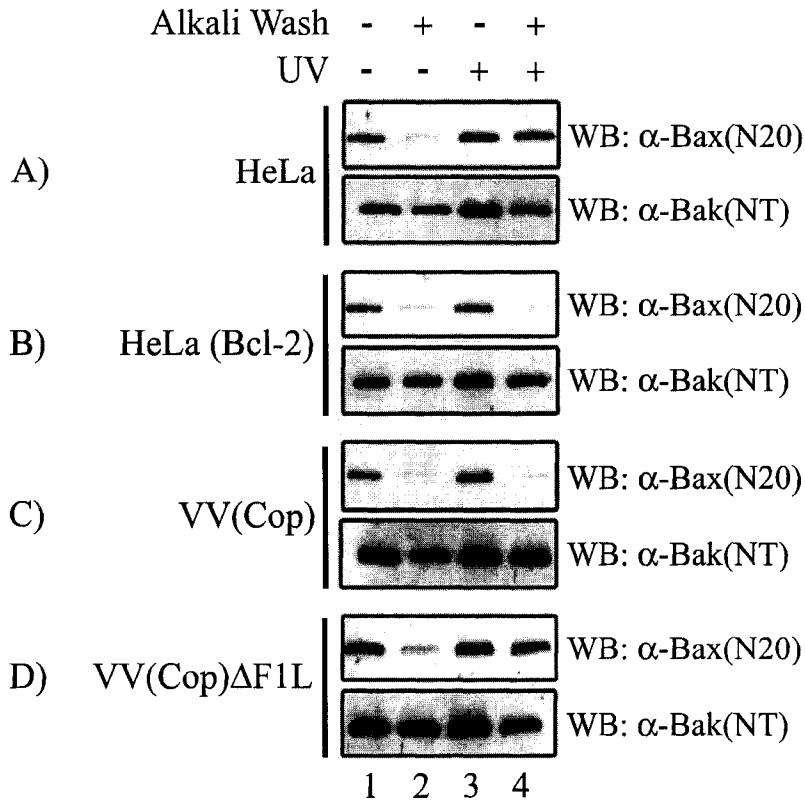

Figure 3.6. Bax insertion into the outer mitochondrial membrane is inhibited by F1L. HeLa cells (A), HeLa cells overexpressing Bcl-2 (B), or HeLa cells infected with either VV(Cop) (C) or VV(Cop)ΔF1L (D) for 8 h at a MOI of 10 were treated with UV-light (lanes 3 and 4) and mitochondria were isolated as described in materials and methods. Isolated mitochondria were either washed in the absence (lanes 1 and 3) or presence of a 0.1M Na_2CO_3 (pH 12) alkali solution (lanes 2 and 4) and Bax insertion assessed by western blotting with anti-Bax(N20). Bak expression was detected using anti-Bak(NT).

visualized by confocal microscopy (Fig. 3.7*A*, panels a, b, c). This diffuse cytoplasmic staining of Bax was also detected in cells infected for 24 hours with VV(Cop)EGFP (Fig. 3.7*A*, panels d, e, f). Cells infected for 24 hours with VV(Cop)ΔF1L, however, frequently demonstrated a punctate staining pattern indicative of Bax recruitment to the mitochondria, reflecting the ability of this virus to activate Bax and induce apoptosis (Fig. 3.7*A*, panels g, h, i). Results were quantified by counting EGFP-positive cells demonstrating punctate Bax staining (Fig. 3.7*B*). We also assessed Bax recruitment following treatment with an intrinsic apoptotic stimulus, UV-light. Following treatment with UV-light, mock-infected HeLa cells displayed the recruitment of Bax to the mitochondria (Fig. 3.8*A*, panels a, b, c). Significantly, in cells infected with VV(Cop) and treated with UV-light, Bax remained cytosolic and diffuse (Fig. 3.8*A*, panels d, e, f,) whereas cells infected with VV(Cop)ΔF1L and treated with UV-light showed Bax recruitment to the mitochondria (Fig. 3.8*A*, panels g, h, i). This punctate Bax staining pattern was confirmed to be mitochondrial, as cells transfected with EGFP-F1L(206-226), which targets EGFP to the mitochondria but does not inhibit apoptosis, demonstrated a distinct co-localization between EGFP and Bax following UV-stimulation (Fig. 3.8*A*, panels j, k, l). Results were quantified by counting EGFP-positive cells demonstrating punctate Bax staining (Fig. 3.8*B*). These results together indicate that F1L inhibited the insertion of Bax into the outer mitochondrial membrane as well as the subcellular redistribution of Bax to the mitochondria, suggesting that F1L functions upstream of both Bax activation and the recruitment of Bax to the mitochondria.

3.2.6 F1L Inhibits Cytochrome c Release and Bax Activation in the Absence of Bak

The presence of either Bak or Bax is absolutely required for cytochrome c release (91, 204, 385), and viral mitochondrial inhibitors of apoptosis such as M11L and E1B 19K function by inhibiting the effects of both Bak and Bax (39, 82). F1L associates with and inhibits the activation of Bak (265, 379), so we asked if the interaction between F1L

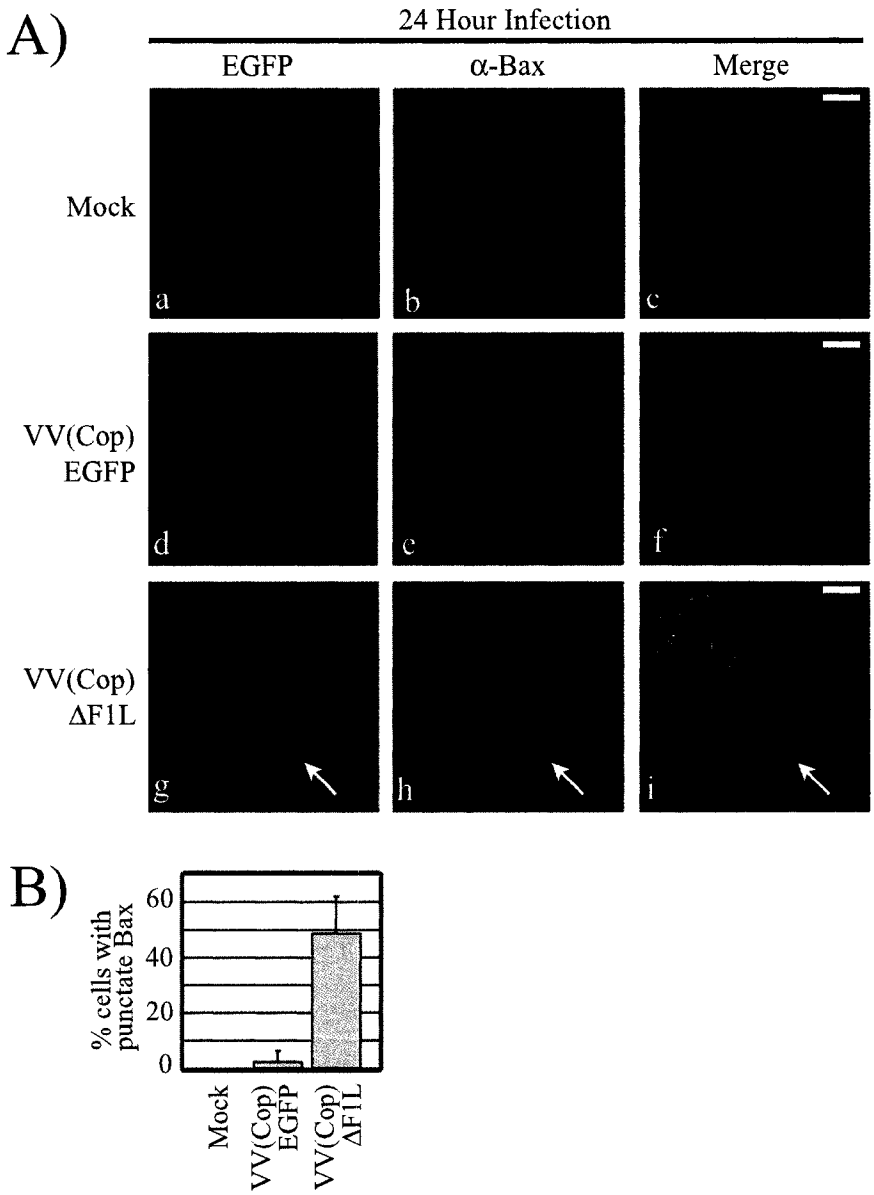

Figure 3.7. Infection with VV(Cop)ΔF1L induces Bax recruitment to mitochondria.
A, HeLa cells were infected at an MOI of 10 with either VV(Cop)EGFP or VV(Cop)ΔF1L for 24h. Cells were fixed and stained with polyclonal anti-Bax annd anti-rabbit Alexa546 to assess Bax localization and recruitment to the mitochondria. Arrows indicate cells displaying punctate Bax (scale bar =10 μm). *B*, Results were quantified as a percentage of EGFP-positive cells also demonstrating punctate Bax staining (mean ± S.D.).

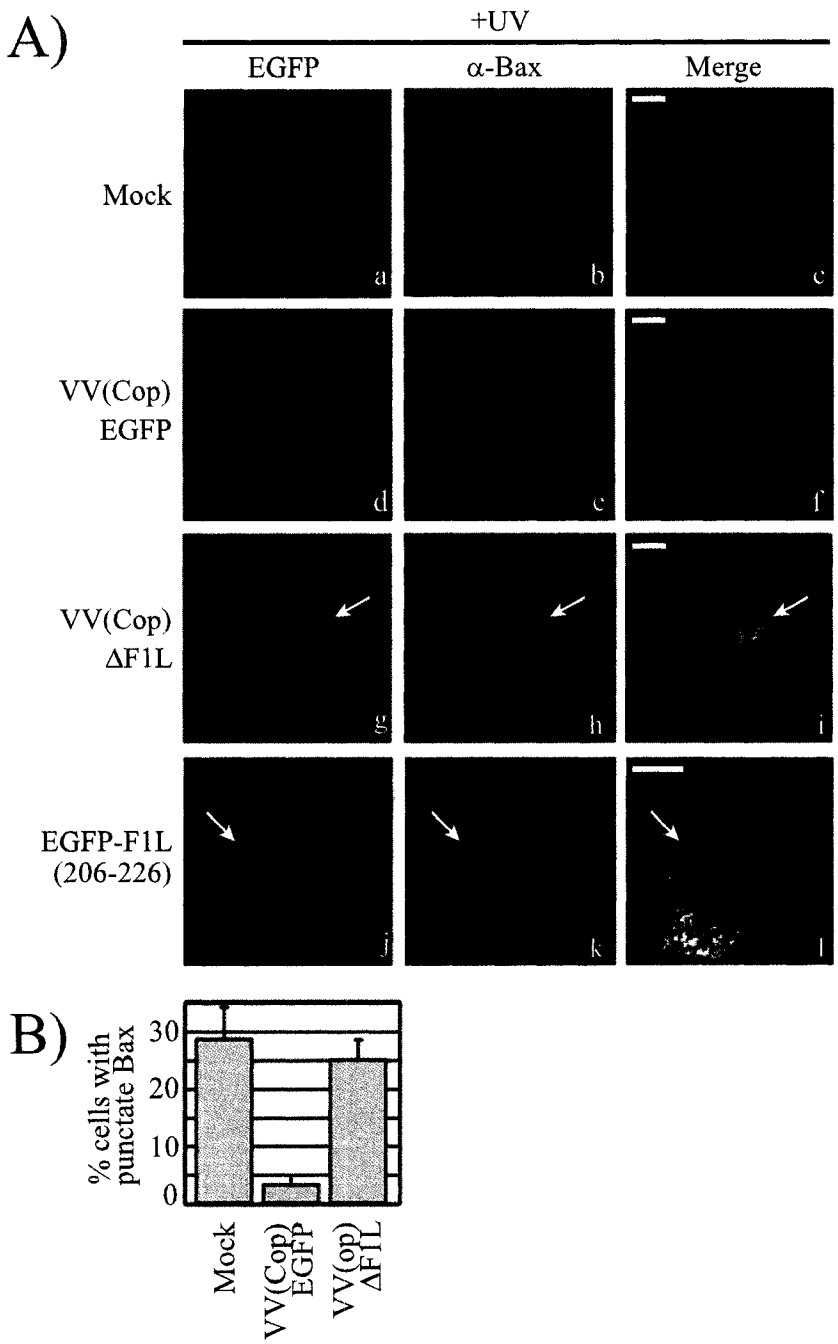

Figure 3.8. F1L inhibits UV-induced mitochondrial recruitment of Bax.
A, To detect Bax recruitment to the mitochondria following an apoptotic stimulus, cells were infected for 8 hours with VV(Cop) or VV(Cop)ΔF1L, or transfected with EGFP-F1L(206-226), treated with UV-light, and fixed and stained with polyclonal anti-Bax and anti-rabbit Alexa546 to assess Bax localization. Arrows indicate cells displaying punctate Bax staining (scale bar = 10μm). *B*, Results were quantified as a percentage of EGFP-positive cells also demonstrating punctate Bax staining (mean ± S.D.).

and Bak was absolutely required for the inhibition of cytochrome c release by F1L. To address this question, we utilized Bak-deficient mouse embryonic fibroblasts ($Bak^{-/-}$ MEFs) in an *in vitro* cytochrome c release assay (385). $Bak^{-/-}$ MEFs were infected with VV(Cop)EGFP or VV(Cop)ΔF1L and purified mitochondria were treated with increasing amounts of the active recombinant BH3-only protein Bid (tBid) to induce cytochrome c release (101, 199, 384). Supernatant and pellet fractions were then blotted for cytochrome c, and pellet fractions were also blotted for Bax and the mitochondrial protein manganese superoxide dismutase (MnSOD) as controls. Treatment of mock-infected Bak-deficient mitochondria with increasing amounts of tBid resulted in the loss of cytochrome c from the pellet fraction and accumulation of cytochrome c in the supernatant fraction (Fig. 3.9*A*). Mitochondria from $Bak^{-/-}$ MEFs infected with VV(Cop)EGFP, meanwhile, showed clear retention of cytochrome c in the pellet fraction following treatment with tBid (Fig. 3.9*A*). In contrast, mitochondria isolated from VV(Cop)ΔF1L-infected $Bak^{-/-}$ MEFs were unable to inhibit tBid-induced cytochrome c release (Fig. 3.9*A*). This indicates that F1L is able to inhibit cytochrome c release in the absence of Bak. Mitochondria purified from MEFs lacking both Bak and Bax ($Bak^{-/-}/Bax^{-/-}$MEF) did not display cytochrome c translocation into the supernatant as expected (Fig. 3.9*A*), as at least one of Bak or Bax are required to facilitate cytochrome c release (91, 385).

Addition of tBid to purified mitochondria *in vitro* induces the activation of the pro-apoptotic proteins Bak and Bax (93, 384). As F1L expression inhibited tBid-induced cytochrome c release (Fig. 3.9*A*), we assessed whether F1L also inhibited Bax activation following tBid-treatment. Bak-deficient MEFs were again infected with VV(Cop) or VV(Cop)ΔF1L, and purified mitochondria were treated with tBid to induce Bax activation. Mitochondria were then lysed in 2% CHAPS and immunoprecipitated with anti-Bax (6A7). As seen in Fig 3.9*B*, Bax was activated in Bak-deficient mitochondria following treatment with tBid, since cytochrome c release in these cells must occur through Bax (91, 204, 385). Infection with VV(Cop) dramatically inhibited tBid-induced

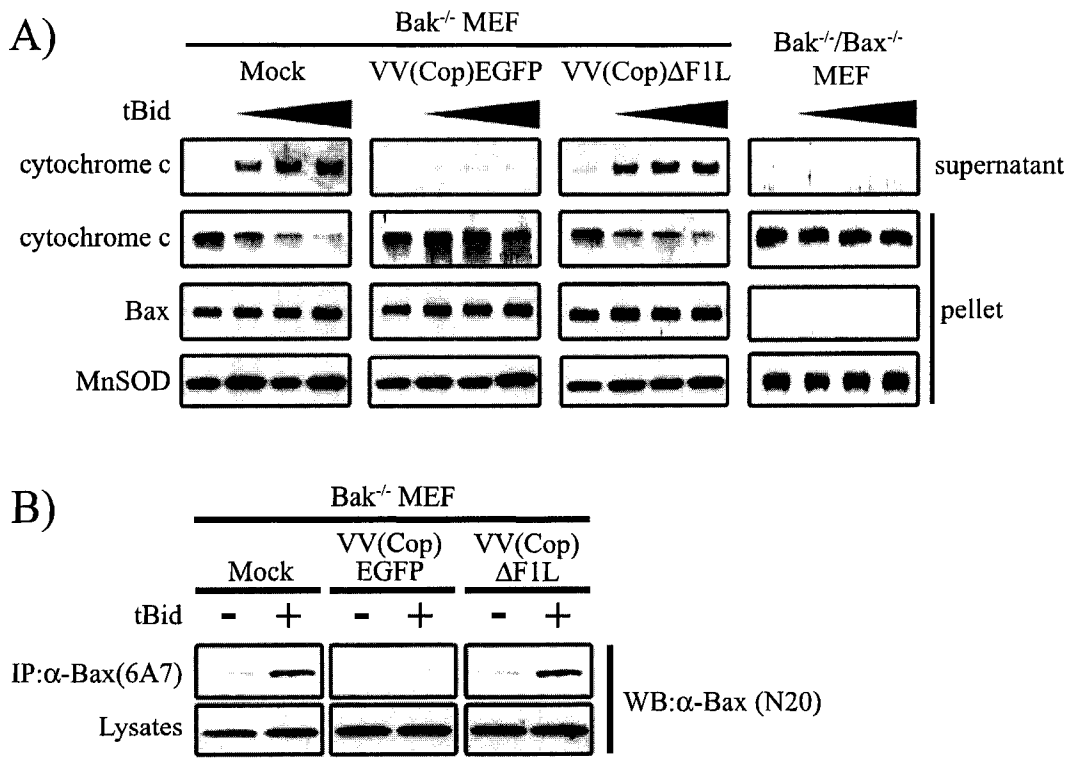

Figure 3.9. F1L inhibits apoptosis in the absence of Bak *in vitro*.
A, Bak$^{-/-}$ MEFs were infected with either VV(Cop)EGFP or VV(Cop)ΔF1L at an MOI of 10 for 8 h, isolated mitochondria were incubated with either 0, 50, 100, or 150ng of tBid for 45 min, and supernatant and mitochondrial pellet fractions were analyzed by western blotting for cytochrome c. Mitochondria from Bak$^{-/-}$/Bax$^{-/-}$ MEFs were also isolated and treated with tBid as a negative control. Mitochondria-containing pellet fractions were also immunoblotted for the presence of MnSOD and Bax as controls. *B*, Mitochondria from Bak$^{-/-}$ MEFs were purified, and mitochondria were incubated with 0 or 300ng of recombinant tBid. Mitochondria were lysed in 2% CHAPS lysis buffer and immunoprecipitated with anti-Bax(6A7). Lysates and immunoprecipitates were analyzed by western blotting with anti-Bax(N20).

Bax activation (Fig. 3.9*B*), while infection with VV(Cop)ΔF1L had no effect on the levels of Bax activation induced by tBid (Fig. 3.9*B*). These results indicate that, in addition to inhibiting cytochrome c release in Bak-deficient cells, F1L also inhibits Bax activation in cells that lack Bak.

The addition of tBid to purified mitochondria is a simplified *in vitro* assay to examine cytochrome c release and Bax activation. To determine whether F1L could inhibit Bax activation in intact cells, we examined whether F1L could inhibit virus-induced Bax activation using $Bak^{-/-}$ MEFs and Bak-deficient baby mouse kidney cells ($Bak^{-/-}$ BMKs) (91). $Bak^{-/-}$ MEFs or $Bak^{-/-}$ BMKs were infected with VV(Cop) or VV(Cop)ΔF1L for 18 hours, lysed in 2% CHAPS, and immunoprecipitated with anti-Bax(6A7). Mock-infected $Bak^{-/-}$ MEFs and $Bak^{-/-}$ BMK cells showed no Bax activation, as assessed by immunoprecipitation with anti-Bax(6A7) (Fig. 3.10*A*). Infection with VV(Cop) also showed minimal or no active Bax from either $Bak^{-/-}$ MEFs or $Bak^{-/-}$ BMKs (Fig. 3.10*A*). Infection with VV(Cop)ΔF1L, however, dramatically induced Bax activation in both Bak-deficient cell lines, as a significant amount of Bax was immunoprecipitated using anti-Bax(6A7) (Fig. 3.10*A*). We also assessed the ability of F1L to inhibit Bax activation in Bak-deficient cells induced by an intrinsic apoptotic stimulus. $Bak^{-/-}$ BMKs were infected with either VV(Cop) or VV(Cop)ΔF1L, and cells were treated with the broad-specificity kinase inhibitor staurosporine which induces apoptosis at the mitochondria (27). Cells were then lysed in 2% CHAPS and immunoprecipitated with anti-Bax(6A7). Treatment of $Bak^{-/-}$ BMKs with staurosporine induced Bax activation as assessed by anti-Bax(6A7) immunoprecipitation (Fig. 3.10*B*). Infection with VV(Cop) strongly inhibited staurosporine-induced Bax-activation in $Bak^{-/-}$ BMKs (Fig. 3.10*B*). Infection with VV(Cop)ΔF1L, on the other hand, was unable to inhibit staurosporine-induced Bax activation in $Bak^{-/-}$ BMKs (Fig. 3.10*B*). These observations indicate that F1L can inhibit Bax activation induced by virus infection or staurosporine and, importantly, that Bak is not required for this inhibition.

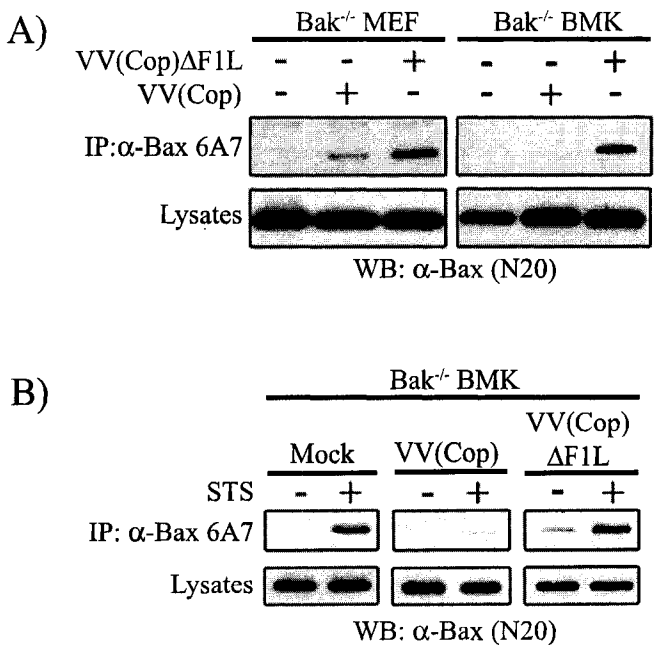

Figure 3.10. F1L expression inhibits Bax activation in the absence of Bak.
A, Bak$^{-/-}$ BMKs or Bak$^{-/-}$ MEFs were mock infected or infected with VV(Cop) or VV(Cop)ΔF1L for 24 h, and cell lysates were immunoprecipitated with anti-Bax(6A7). Immunoprecipitates and lysates were probed with anti-Bax(N20). *B*, Bak$^{-/-}$ BMKs were infected with VV(Cop) or VV(Cop)ΔF1L for 8 h, treated with 1μM staurosporine(STS) for 3 h, and activated Bax was immunoprecipitated using anti-Bax(6A7). Lysates and immunoprecipitates were probed with anti-Bax(N20).

3.2.7 VV(Cop)ΔF1L Replicates Normally in Various Cell Lines

Vaccinia viruses devoid of F1L induce apoptosis during infection (Fig. 3.2) (265, 379, 382). Since F1L is an important regulator of apoptosis, we hypothesized that vaccinia viruses devoid of F1L might display a decrease in progeny virus production compared to wild type VV(Cop) *in vitro*. To test this prediction, we performed single step growth curves in four mouse embryonic fibroblast cell lines: WT, $Bak^{-/-}$, $Bax^{-/-}$, and $Bak^{-/-}$ /$Bax^{-/-}$ MEFs (385). Cells were infected at a MOI of 1 for 4, 8, 12, and 24 hours, and viral titres were determined by plaque assays on CV-1 cells (Fig. 3.11). Interestingly, both VV(Cop) and VV(Cop)ΔF1L replicated equally well in each of the cell lines tested (Fig. 3.11), suggesting that any apoptosis induced by VV(Cop)ΔF1L has little effect on growth *in vitro*. While there appears to be a slight decrease in the final virus titre at 24 hours post infection in the $Bax^{-/-}$ MEFs (Fig. 3.11*C*), this trend is seen with both VV(Cop) and VV(Cop)ΔF1L, suggesting that there may be a non-specific effect on vaccinia replication in these cells. Previous observations in CV-1 cells also showed no difference in growth between VV(Cop) and VV(Cop)ΔF1L (379).

3.2.8 F1L Fails to Interact with Bax During Infection

F1L can inhibit the activation and oligomerization of Bak and also interacts with Bak as a mechanism for this activity (265, 379). We therefore assessed whether F1L inhibited Bax activation by directly interacting with Bax. Although F1L is a mitochondria-localized protein, and we fail to see recruitment and integration of Bax into the mitochondrial membrane in the presence of F1L (Fig. 3.6-3.8), there remained a possibility that F1L could still interact directly with Bax. M11L, a mitochondrial-localized anti-apoptotic protein from myxoma virus, has recently been shown to interact with Bax (332). To investigate a possible interaction between Bax and F1L, HeLa cells were infected with a recombinant VV expressing a FLAG-tagged version of F1L,

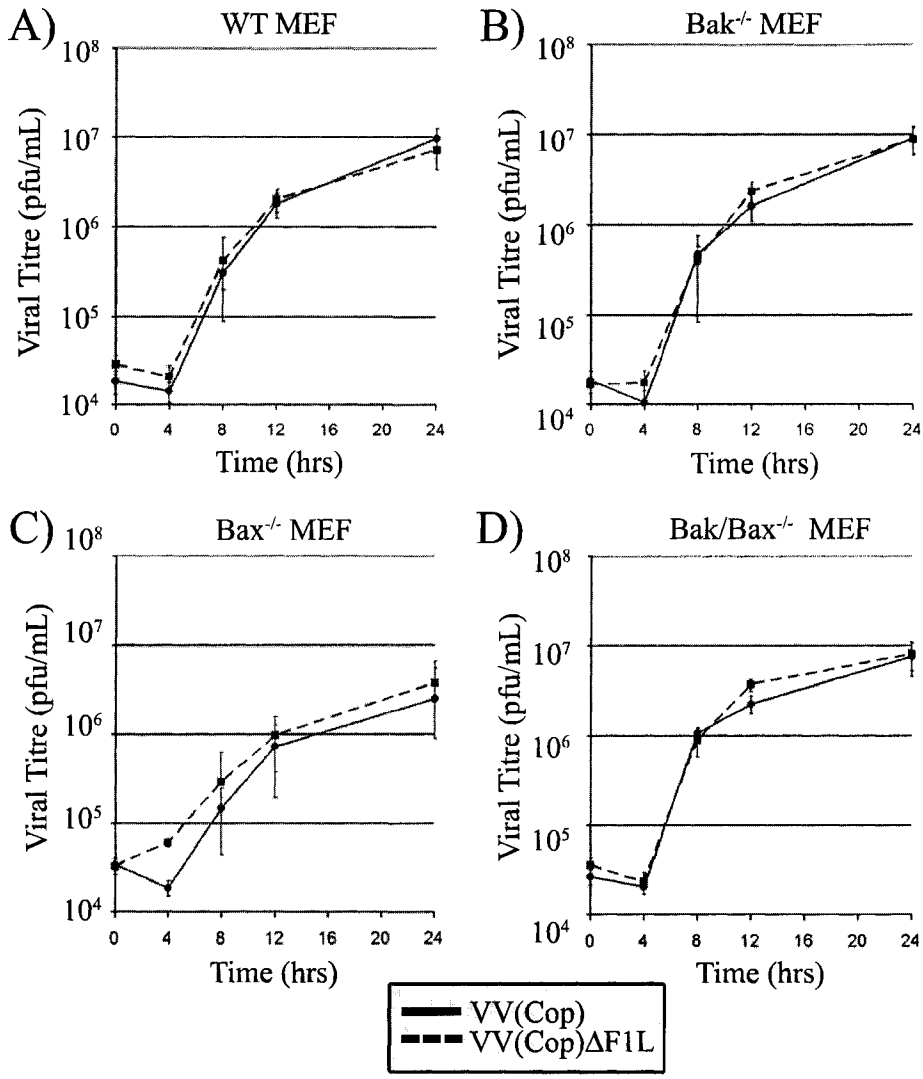

Figure 3.11. Growth rates of VV(Cop) and VV(Cop)ΔF1L in MEFs. Wild type (A), Bak$^{-/-}$(B), Bax$^{-/-}$(C), or Bak$^{-/-}$/Bax$^{-/-}$(D) MEFs were infected with VV(Cop) (solid line) or VV(Cop)ΔF1L (dashed line) in triplicate at a MOI of 1 and were harvested at 0, 4, 8, 16, or 24 hours post-infection. Titrations were performed for each time point on CV-1 cells in duplicate, and viral titres are shown as plaque forming units per ml (pfu/ml) (± S.D.).

VV:FLAG-F1L, and treated with either UV-light or TNF-α. Cells were lysed in 2% CHAPS buffer and immunoprecipitated with anti-FLAG (157, 158). In all cases, FLAG-F1L co-immunoprecipitated with endogenous Bak (Fig 3.12), demonstrating that the interaction between Bak and F1L was maintained following treatment with an apoptotic stimulus (379). Interestingly, no observable interaction was seen between endogenous Bax and F1L either before or after induction with an apoptotic stimulus (Fig. 3.12).

Expression of F1L inhibits the conformational change in Bax induced during apoptosis (Fig. 3.2-3.4). It was recently reported, however, that a soluble version of F1L interacts with a peptide encompassing the BH3 domain of Bax (113). Since the BH3 domain is believed to be hidden within a hydrophobic pocket along with the N-terminal domain prior to Bax activation (340), it is unlikely that the BH3 domain of Bax is exposed during VV infection. Nevertheless, if F1L has an intrinsic ability to interact with BH3-domains, F1L may be capable of interacting with active Bax. To confirm this prediction, we performed co-immunoprecipitations under conditions that artificially activate Bax. The detergent CHAPS maintains Bax in its natural conformation, whereas Triton-X-100 causes Bax to unfold into an 'active' state (156-158), resulting in N-terminal activation and oligomerization. HeLa cells were infected with VV:FLAG-F1L and lysed in Triton-X-100 to induce a conformational change in Bax (Fig. 3.13*A*). Immunoprecipitation with anti-FLAG co-precipitated a significant amount of Bax when cells were lysed in Triton-X-100, but not in CHAPS (Fig. 3.13*A*), suggesting that F1L has the capacity to interact with Bax following a conformational change in Bax.

To determine whether F1L could interact with Bax in the absence of Bak, we repeated our anti-FLAG immunoprecipitations in $Bak^{-/-}$ BMKs. Bak-deficient BMKs were infected with VV:FLAG-F1L, immunoprecipitated with anti-FLAG, and blotted for Bax (Fig.. 3.13*B*). Similar to our results from HeLa cells, no interaction between F1L and Bax was detected in $Bak^{-/-}$ BMKs lysed in CHAPS, even upon addition of staurosporine to induce apoptosis (Fig. 3.13*B*). Following lysis in Triton-X-100, however, F1L and Bax

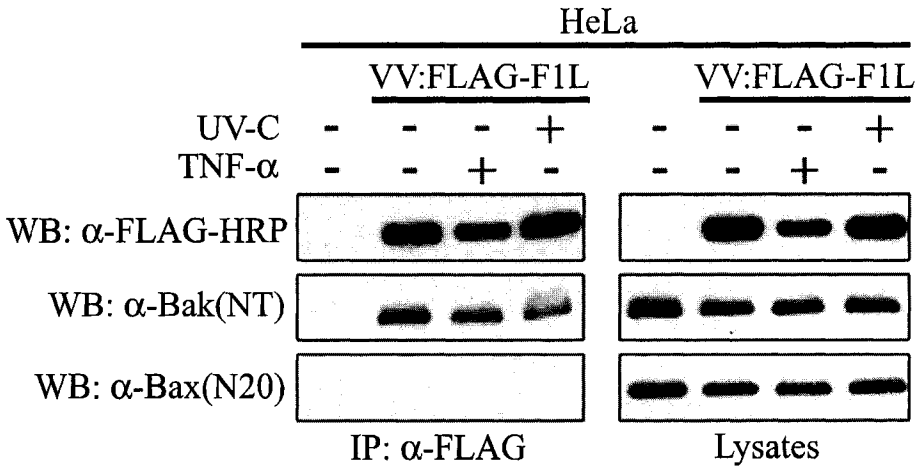

Figure 3.12. F1L interacts with Bak, but not with Bax, following an apoptotic stimulus. HeLa cells were infected with VV:FLAG-F1L for 8 h, and treated with either UV-light or TNFα for 3 or 6 h, respectively. Following apoptotic induction, cells were lysed in 2% CHAPS lysis buffer, and immunoprecipitated with anti-FLAG (M2). Immunoprecipitates and lysates were analyzed by western blotting with either anti-FLAG-HRP to detect F1L, anti-Bak(NT), or anti-Bax(N20).

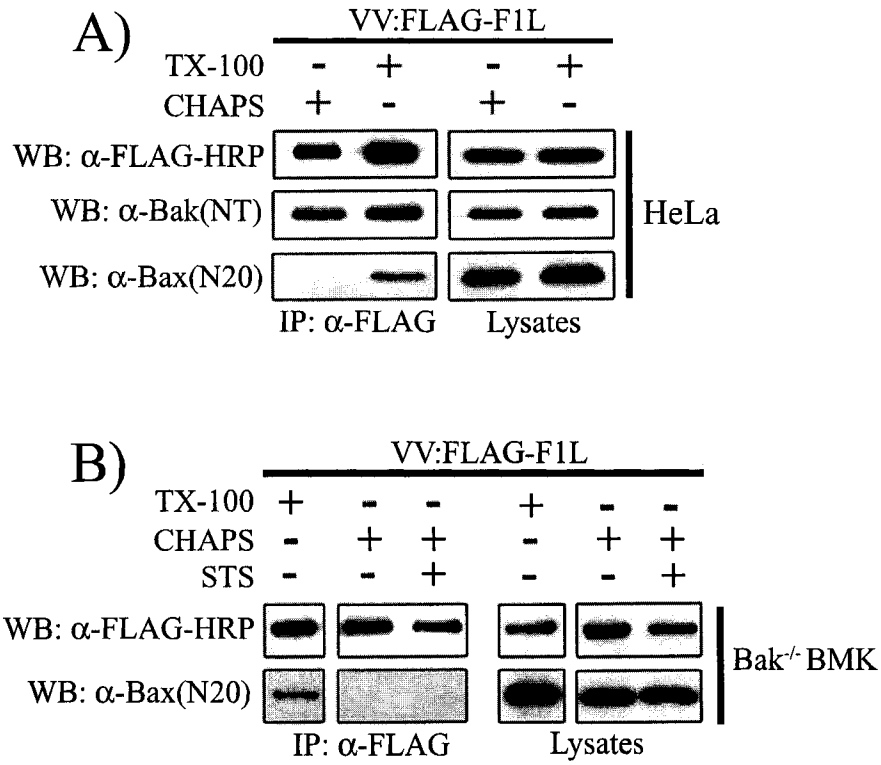

Figure 3.13. F1L interacts with Bax in Triton-X-100.
A, HeLa cells were infected with VV:FLAG-F1L, lysed in either 2% CHAPS lysis buffer or 1% Triton-X-100 (TX-100) buffer. FLAG-tagged F1L was immunoprecipitated with anti-FLAG, and western blotted with α-FLAG-HRP to detect F1L, or anti-Bak(NT) or anti-Bax(N20) to detect Bak and Bax respectively. *B*, $Bak^{-/-}$ BMKs were infected with VV:FLAG-F1L in the absence or presence of 1μM staurosporine (STS). Cells were lysed in either 2% CHAPS or 1% Triton-X-100 (TX-100), and any interaction between F1L and Bax was detected by co-immunoprecipitation with anti-FLAG and western blotting with anti-Bax(N20).

co-precipitated (Fig. 3.13*B*). These results demonstrate that, even following an apoptotic stimulus, F1L does not interact with Bax. Intriguingly, however, F1L does have the ability to interact with conformationally active Bax following lysis in Triton-X-100, and the expression of Bak is not required for this interaction.

3.3 Discussion

The activity of Bak or Bax is critical for the release of cytochrome c from the mitochondria and subsequent death of the cell (77, 204, 385). As such, viruses have evolved strategies to inhibit the pro-apoptotic activity of Bax and Bak, thereby ensuring successful virus propagation (40, 82, 262). The anti-apoptotic protein F1L, encoded by vaccinia virus, localizes to the outer mitochondrial membrane via a C-terminal mitochondrial targeting sequence where it inhibits mitochondrial membrane permeabilization and cytochrome c release (329, 382). F1L expression inhibits the activation and oligomerization of Bax following an apoptotic stimulus (265, 379). We hypothesized that F1L, in addition to inhibiting Bak, would also encode a mechanism to inhibit the activity of Bax.

Following an apoptotic stimulus, Bax undergoes a conformational change that results in the availability of an N-terminal epitope, the release of a C-terminal transmembrane tail for insertion into the mitochondrial membrane, and oligomerization into high molecular weight complexes (12, 101, 156, 158). We demonstrated that F1L expression could potently inhibit the N-terminal activation, mitochondrial insertion, and oligomerization of Bax following an apoptotic stimulus (Fig. 3.1-3.8). These results clearly indicated that F1L could inhibit Bax activation following an apoptotic insult.

As a mechanism for inhibiting Bak activation, our lab previously showed that F1L constitutively interacts with Bak (265, 379). Indeed, members of the Bcl-2 family interact with each other to induce or repress apoptotic responses (364). F1L expression potently inhibited Bax activation (Fig. 3.2-3.6), so we investigated whether F1L and Bax could

directly interact. Both in the absence and the presence of pro-apoptotic stimuli, we failed to see an interaction between F1L and Bax (Fig. 3.12, 3.13). Considering that F1L is a mitochondrial-anchored protein and Bax is normally found in the cytoplasm, this suggests that F1L does not naturally interact with Bax to inhibit Bax activation.

As F1L does not interact with Bax, yet F1L inhibits Bax activation during apoptosis, F1L likely has an indirect effect upstream of Bax activation. Indeed, a number of proteins regulate Bax activation, including several proteins from the Bcl-2 family (330, 390). Bak has been shown to coalesce with Bax at discrete sites at the mitochondria (245), and Bak/Bax may even form heterodimers during apoptosis (337). Using Bak-deficient cells, however, we clearly demonstrated that F1L is still capable of inhibiting apoptosis and Bax activation (Fig. 3.9, 3.10), indicating that Bak is not required for F1L-mediated inhibition of apoptosis.

Another sub-group of the Bcl-2 family which regulates Bax activation are the BH3-only proteins. These small pro-apoptotic proteins (*ie.* tBid, Bim) are activated following an apoptotic stimulus and either directly bind and activate Bak and Bax, or bind and repress the anti-apoptotic Bcl-2 family members (61, 65, 187, 194, 236). A number of non-Bcl-2 family proteins also activate or repress Bax. Map-1, Bif-1, and p53, for instance, have all been shown to induce Bax activation (67, 343, 344), while proteins such as Ku70, 14-3-3, and Humanin can inhibit Bax activation (137, 291, 359). Whether F1L modulates the activity of any of these proteins to indirectly regulate Bax remains to be determined.

The anti-apoptotic effect of F1L does not appear to be required for *in vitro* virus replication. Growth curves demonstrated that VV(Cop)ΔF1L replicated as well as wild type VV(Cop) *in vitro* in various MEF cell lines, suggesting that despite inducing apoptosis in tissue culture, viruses lacking F1L show no growth deficiency *in vitro* (Fig. 3.11). Future work using ectromelia virus, a closely related orthopoxvirus which is a natural pathogen of mice and encodes a predicted orthologue of F1L, will allow us to

investigate the potential role of F1L *in vivo*. Indeed, deletion of anti-apoptotic genes from other viral genomes, such as M11L from myxoma virus and the viral Bcl-2 homologue from murine γ-herpesvirus 68, has little effect *in vitro*, but profoundly affects virus virulence (128, 208, 254).

Although F1L expression strongly inhibits Bax activation, co-immunoprecipitations in CHAPS failed to detect any interaction between F1L and Bax (Fig. 3.12), and this has also been observed by others (265). Interestingly, lysis of healthy cells in Triton-X-100, but not CHAPS, did induce an interaction between Bax and F1L (Fig. 3.13). The detergent CHAPS maintains Bax in a native conformation, while Triton-X-100 induces the activation/oligomerization of Bax (157, 158). This suggests that F1L has the ability to interact with conformationally active Bax (Fig. 3.13) (157, 158). The BH3-domain of Bax is normally hidden prior to activation, and detergents such as Triton-X-100 make the BH3-domain available (157, 340). A recent report also suggests that F1L can interact with the BH3 peptides from Bak and Bax *in vitro* (113), so we speculate that F1L can interact with the BH3 domain of Bax. This binding ability is similar to Bcl-2, which also binds to Bax in Triron-X-100, but not in CHAPS (158). E1B 19K from adenovirus interacts with Bax only after an apoptotic stimulus induces a conformational change in Bax (257), indicating that E1B 19K does not inhibit the initial activation of Bax. In contrast, F1L inhibits Bax activation (Fig. 3.2-3.4), and correspondingly does not interact with Bax even after an apoptotic stimulus (Fig. 3.12). Although F1L may interact with small amounts of active Bax during apoptosis, our results indicate that F1L primarily inhibits Bax activation upstream. The exact mechanism used by F1L to inhibit Bax activation, however, remains to be determined. Based on our results, it is likely that F1L inhibits Bax activation indirectly by functioning upstream of Bax activation. As well, considering the preliminary evidence that F1L can interact with BH3 peptides and activated Bax, it is possible that F1L may inhibit Bax activation by interfering with other

BH3-domain containing proteins. Nevertheless, it is apparent that F1L can potently inhibit Bak and Bax, and that F1L accomplishes this by two discrete mechanisms.

CHAPTER 4: Vaccinia Virus F1L Interacts With and Modulates the BH3-only Protein BimL

A portion of this chapter has been published:

Taylor J.M., D. Quilty, L. Banadyga, and M. Barry. The vaccinia virus protein F1L interacts with Bim and inhibits activation of the pro-apoptotic protein Bax. 2006. Journal of Biological Chemistry. 281:39728-39.

All of the experiments included within this chapter were performed by J. Taylor, with the exception of Figure 4.7, which was performed by D. Quilty. The original manuscript was written by J. Taylor, and a major editorial contribution was made by M. Barry.

4.1 Introduction

Apoptosis at the mitochondria is controlled by the pro-apoptotic proteins Bak and Bax, and at least one of Bak or Bax is required to induce mitochondrial membrane permeablization during apoptosis (91, 204, 385). In order to effectively inhibit cell death during infection, certain viruses are able to inhibit both Bak and Bax activation thereby protecting the integrity of the mitochondrial membrane (107, 144, 332, 337, 338, 373). The expression of the vaccinia virus protein F1L inhibits the activation of both Bak and Bax (265, 379), but appears to do so by two different mechanisms. F1L inhibits the N-terminal activation and oligomerization of Bak, and interacts with Bak as a mechanism to inhibit Bak activation (265, 329, 379). F1L also inhibits the activation, translocation, and insertion of Bax into the mitochondrial outer membrane during apoptosis (Chapter 3) (350). Intriguingly, F1L does not interact with Bax, even following an apoptotic stimulus, suggesting that F1L indirectly inhibits Bax by modulating events upstream of Bax activation (350). Interestingly, F1L can be induced to interact with Bax in the presence of the detergent Triton-X-100 which unfolds Bax and reveals the BH3 domain (350). It is possible that F1L may be able to bind to the BH3 domain of Bax and other Bcl-2 family proteins, as a recent report has shown that a soluble version of F1L can bind to BH3 peptides from Bak, Bax, and Bim (113).

The BH3-only proteins are members of the Bcl-2 family that induce Bax and Bak activation in response to pro-apoptotic stimuli (187, 330). BH3-only proteins are believed to activate Bak and Bax either by directly interacting with Bak and Bax, or by binding and repressing the pro-survival Bcl-2 family proteins (52, 61, 187, 236, 392). The BH3-only protein Bim is a potent activator of apoptosis that directly activates Bak and Bax (187, 194, 219, 250). Cells deficient in Bim are resistant to apoptosis induced by cytokine withdrawl and microtubule alterations (35, 268). Bim is produced as three different isoforms: BimS (short), BimL (long), and BimEL (extra-long) (Fig. 1.10), with the shorter isoforms being more potent inducers of apoptosis.

At least three different mechanisms regulate the pro-apoptotic activity of Bim. Bim can be transcriptionally up-regulated following an apoptotic insult (35, 268, 270, 389), and BimL and BimS are not detected in most healthy cell populations, but are up-regulated during apoptosis (147, 268). BimEL is a less potent pro-apoptotic protein, and is naturally found in most cell types (250). BimEL or BimL are sequestered by the microtubule dynein light chain or by Mcl-1 (141, 142, 193, 269). Alternatively, Bim isoforms are also regulated post-translationally via phosphorylation (196).

BimEL has been shown to be phosphorylated through activation of the extracellular signal-regulated kinase (ERK1/2) pathway (30, 197, 210, 218, 387). The primary site for BimEL phosphorylation by ERK1/2 kinases is serine 69 (Ser69) (Fig. 1.10), and this promotes the ubiquitination and subsequent degradation of BimEL by the 26S proteasome (197, 210, 218). BimEL is phosphorylated by other mechanisms, however, as BimEL lacking either Ser69 or the ERK1/2 binding domain is still able to be phosphorylated (197, 210, 218). Indeed, BimEL and BimL can be phosphorylated for activation, as JNK kinases phosphorylate BimL following UV-treatment and JNK kinases phosphorylate BimEL in neurons resulting in Bim activation (193, 267). The exact signals that induce and control Bim phosphorylation are not understood, although numerous phosphorylation events can modify Bim, with either pro- or anti-apoptotic effects.

Considering the fact that F1L is able to inhibit Bax activation in the absence of a direct interaction, we hypothesized that F1L may modulate upstream signaling proteins. The BH3-only protein family can directly and indirectly induce Bax activation. F1L constitutively interacts with Bak, F1L interacts with BH3 peptides from Bim, Bak and Bax (113), and F1L also interacts with Bax in the presence of Triton-X-100 (265, 349, 379)., altogether suggesting that F1L may interact with BH3 domains. As F1L also inhibits Bax activation without interacting with Bax, we hypothesized that F1L may be a BH3-only binding protein, The BH3-only protein Bim is a direct activator of Bak and

Bax (147, 187, 194), and F1L was previously reported to interact with a soluble BH3 domain from Bim. We investigated whether F1L interacts with and inhibits apoptosis induced by the BH3-only protein Bim. Here we show that F1L interacted with and inhibited apoptosis mediated by Bim.

4.2 Results

4.2.1 F1L expression inhibits apoptosis induced by the BH3-only proteins Bid, Bmf and BimL

Cells infected with VV(Cop)ΔF1L undergo apoptosis and Bax activation (379), and our data suggests that F1L can inhibit Bax activation independent of a direct interaction with Bax (Chapter 3). Given that BH3-only proteins are the initial pro-apoptotic effector molecules that function upstream of Bax (330), we examined the ability of F1L to inhibit apoptosis induced by the overexpression of three BH3-only proteins, Bmf, full-length Bid, and BimL, all of which induce mitochondrial dysfunction and apoptosis in tissue culture (250, 271, 376). Although full-length Bid is usually cleaved by caspase-8 to give rise to active tBid, overexpression of full-length Bid also induces mitochondrial dysfunction in transfected cells, and this is inhibited by Bcl-2 (376). In order to examine the ability of F1L to inhibit apoptosis induced by Bmf, Bid, or BimL, we co-transfected cells with either pEGFP-C3, pEGFP-F1L, pEGFP-Bcl-2, or pEGFP-F1L(206-226) which contains only the C-terminal hydrophobic domain of F1L and targets EGFP to the mitochondrial membrane but does not inhibit apoptosis (329). At 16 hours post-transfection, cells were stained with the fluorescent mitochondrial dye TMRE to assess the mitochondrial membrane potential. Cells co-transfected with EGFP and either Bmf, Bid, or BimL exhibited significant mitochondrial membrane depolarization (Fig. 4.1*A, B,* and *C*). Similarly, cells co-transfected with EGFP-F1L(206-226) and either Bmf, Bid or BimL also exhibited loss of the mitochondrial membrane potential (Fig. 4.1*A, B,* and *C*). Cells co-transfected with EGFP-Bcl-2 were significantly

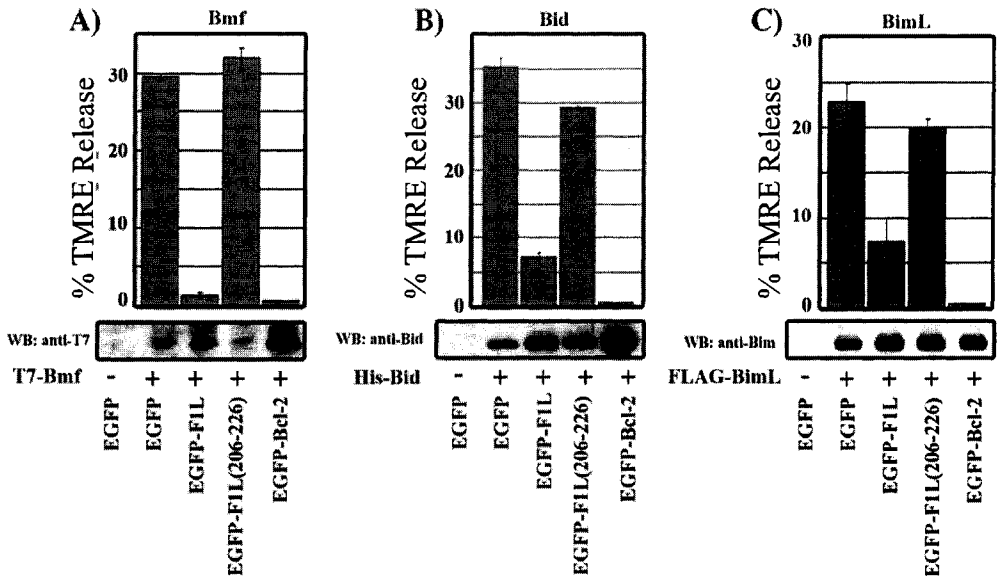

Figure 4.1. F1L inhibits BH3-only protein induced apoptosis.
HeLa cells were co-transfected with either pEGFP, pEGFP-F1L, pEGFP-F1L(206-226), or pEGFP-Bcl-2, along with either pcDNA3-T7-Bmf (A), pCMV5-Bid (B), or pcDNA3-FLAG-BimL (C) for 16 hours. Cells were stained with TMRE to label healthy mitochondria and analyzed using two-colour flow cytometry. TMRE release was calculated as a percentage of EGFP-positive cells showing a loss of mitochondrial membrane potential when co-transfected with each BH3-only protein. Following flow cytometry analysis, protein samples were analyzed by western blotting with either anti-T7 (A), anti-Bid (B), or anti-Bim (C) to detect Bmf, Bid, and BimL respectively.

protected from Bmf, Bid or BimL-induced loss of the mitochondrial membrane potential as expected (Fig. 4.1*A, B,* and *C*). Co-transfection of EGFP-F1L also strongly inhibited the loss of the mitochondrial membrane potential induced by either Bmf, Bid, or BimL overexpression (Fig. 4.1*A, B,* and *C*). F1L or Bcl-2-mediated inhibition of apoptosis in this experiment was not due to lower expression levels of Bmf, Bid, and BimL. Western blotting lysates from all samples showed equivalent or elevated levels of Bmf, Bid, or BimL expression in EGFP-F1L or EGFP-Bcl-2 transfected samples when compared to cells co-expressing EGFP or EGFP-F1L(206-226) (Fig. 4.1*A, B* and *C*). The increased expression of each BH3-only protein in F1L or Bcl-2 expressing cells was perhaps due to the protective effects of F1L or Bcl-2 on cell viability, thus enhancing protein expression (Fig. 4.1*A-C*). Altogether, F1L has the ability to inhibit apoptosis induced by the direct overexpression of the BH3-only proteins Bmf, Bid, and BimL.

F1L interacts with Bak as a mechanism to inhibit cytochrome c release and mitochondrial dysfunction (265, 379). We investigated whether Bak was required for the F1L-mediated inhibition of BH3-only proteins. We expressed either full-length Bid or BimL in $Bak^{-/-}$ MEFs, and co-expressed either EGFP-F1L or EGFP-F1L(206-226). Cells were fixed and stained with anti-cytochrome c to detect cytochrome c localization. In healthy cells, cytochrome c appears as a punctate mitochondrial staining pattern when visualized using confocal microscopy. Apoptotic cells instead display a diffuse cytochrome c staining pattern indicative of cytochrome c release from the mitochondria into the cytosol. To detect Bid and Bim expression in transfected cells, cells were also co-stained with either anti-Bid or anti-Bim. As seen in Figure 4.2*A*, cells co-expressing EGFP-F1L(206-226) and Bid displayed a diffuse cytochrome c staining pattern (Fig. 4.2*A*, panels a-c), indicating cytochrome c release into the cytoplasm. Neighbouring healthy cells not expressing Bid, however, showed a punctate cytochrome c staining pattern, indicative of mitochondrial-localized cytochrome c (Fig. 4.2*A*, panels a-c). In contrast, cells co-expressing EGFP-F1L and Bid still displayed a punctate cytochrome c

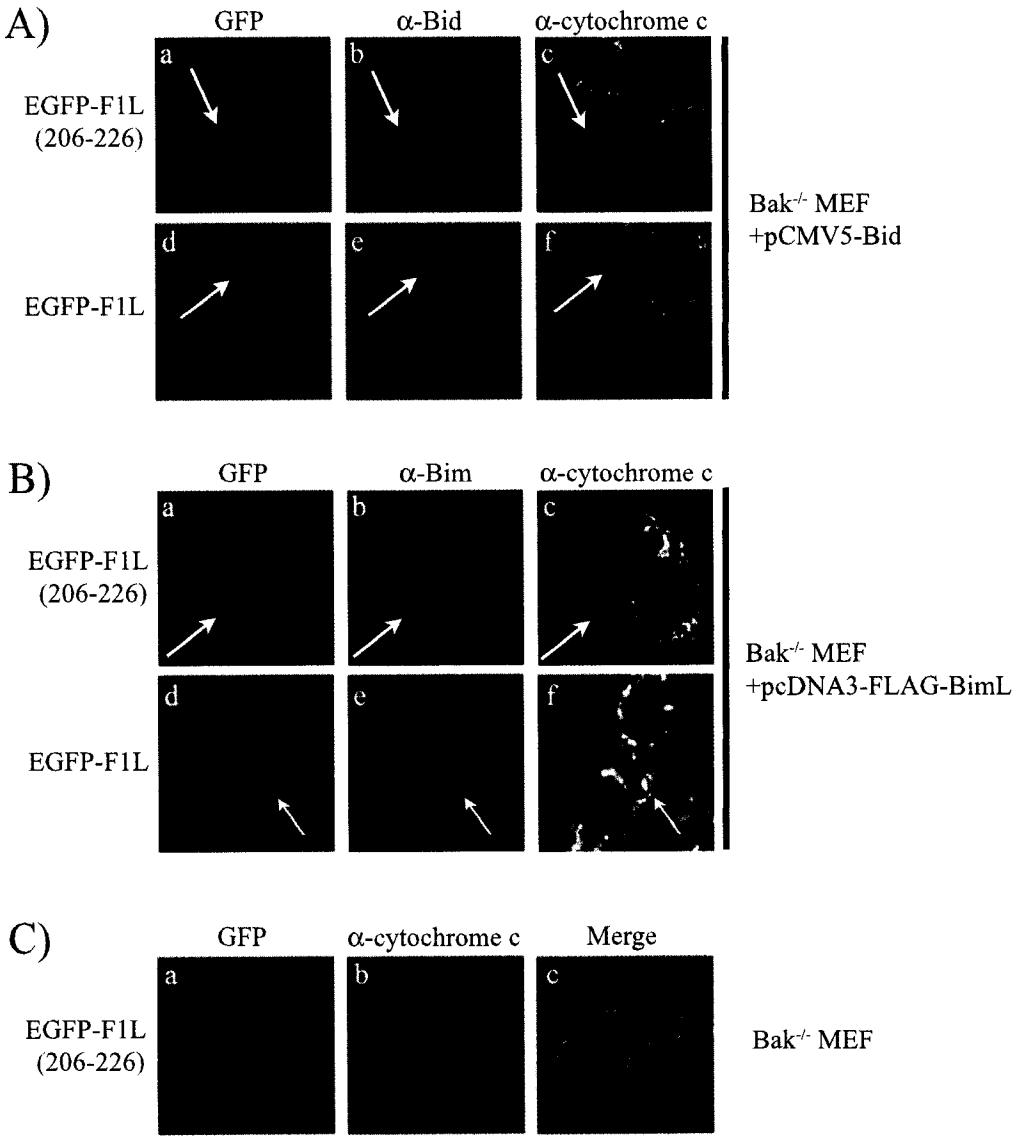

Figure 4.2. F1L expression inhibits BH3-only induced cytochrome c release in Bak-deficient cells. Bak-deficient MEFs were co-transfected with 1μg of either pCMV5-Bid (A) or pcDNA3-FLAG-BimL (B), along with 4μg of either EGFP-F1L or EGFP-F1L (206-226) for 16 hours. Cells were then fixed and stained with anti-cytochrome c (clone 6H2.B4) and either anti-Bim or anti-Bid. Cells were stained with anti-mouse-Alexa633 and anti-rabbit-Alexa546 secondary antibodies, and visualized using confocal microscopy. Arrows indicate cells expressing of either Bid or BimL. *C*, cells were singly transfected with EGFP-F1L(206-226), stained with anti-cytochrome c and visualized as above.

staining pattern (Fig. 4.2*A*, panels d-f), indicating that F1L expression in $Bak^{-/-}$ cells inhibited Bid-induced release of cytochrome c from mitochondria. The expression of EGFP-F1L(206-226) alone did not induce cytochrome c release from mitochondria (Fig. 4.2*C*, panels a-c), as cells singly transfected with EGFP-F1L(206-226) displayed punctate cytochrome c, as expected (329).

We also investigated the ability of F1L to inhibit BimL-induced cytochrome c in Bak-deficient cells. Similar to our results with Bid, co-expression of the BH3-only protein BimL dramatically induced cytochrome c release from cells expressing EGFP-F1L(206-226) (Fig. 4.2*B*, panels a-c). $Bak^{-/-}$ MEFs co-expressing EGFP-F1L, however, displayed a healthy punctate staining pattern for cytochrome c despite the expression of BimL (Fig. 4.2*B*, panels d-f). These results demonstrate that F1L can inhibit cytochrome c release induced by overexpression of the BH3-only proteins Bid and BimL, even in cells that lack Bak.

4.2.2 Vaccinia virus infection induces BimEL phosphorylation

A recent report indicated that a soluble version of F1L was able to interact with purified BH3 peptides from Bak, Bax and Bim (113). F1L can inhibit apoptosis induced by BimL, so we investigated the role of Bim in vaccinia-induced apoptosis. We first addressed whether vaccinia virus infection had any effect on Bim protein expression, as Bim is regulated transcriptionally, and post-translationally by phosphorylation (196, 270, 330). Western blotting of whole cell lysates demonstrated that HeLa cells express natural levels of BimEL, but no BimL or BimS, while Bim-deficient baby mouse kidney cells do not express any of the Bim isoforms as expected (Fig. 4.3*A*) (346). Infection with VV induces apoptosis, and BH3-only proteins such as Bim are transcriptionally and post-translationally regulated during apoptosis (196, 270), so we examined whether vaccinia infection altered the expression of BimEL. HeLa cells were infected with VV(Cop) for 2, 4, 6, or 8 hours, and lysates were western blotted with anti-Bim. While infection with

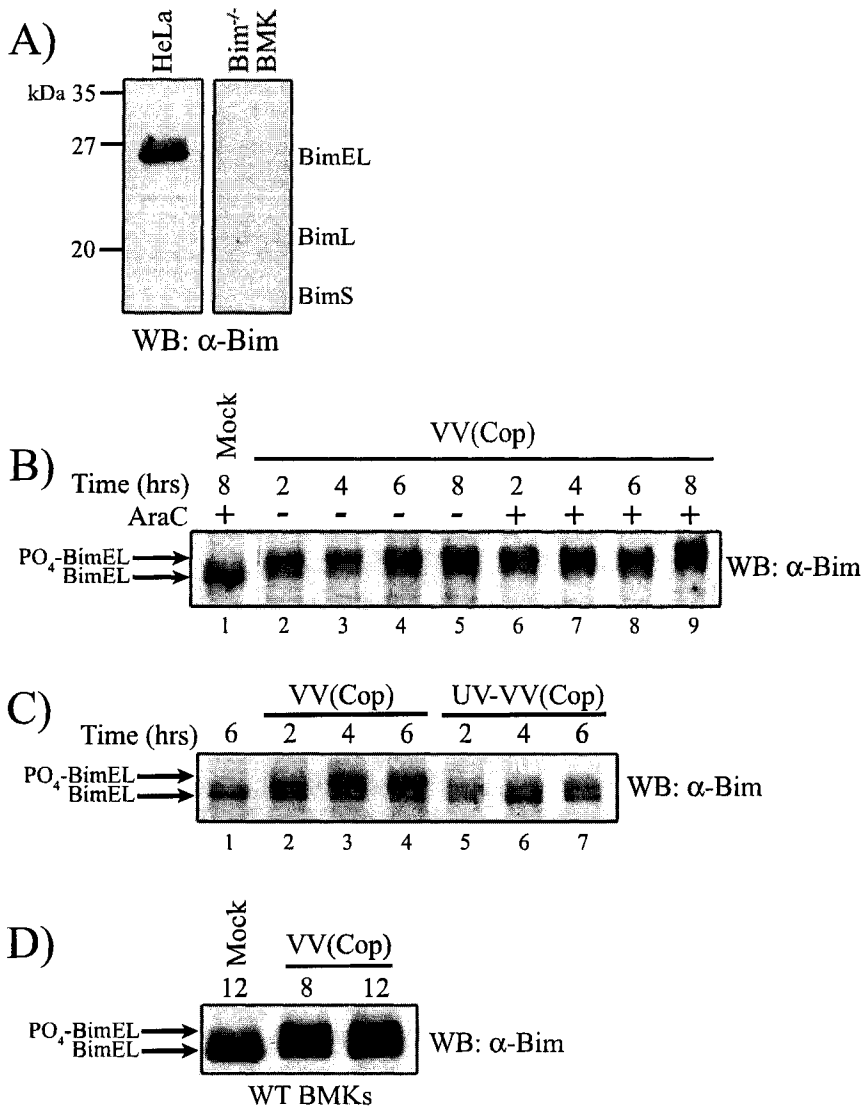

Figure 4.3. Vaccinia virus infection induces BimEL phosphorylation.
A, HeLa or $Bim^{-/-}$ BMK cell lysates were probed with anti-Bim, and the predicted migration of each Bim isoform is indicated. *B*, HeLa cells were infected with VV(Cop) at a MOI of 10 for the indicated times in the presence or absence of AraC (80μg/ml). Cells were lysed in SDS-PAGE sample buffer and western blotted with anti-Bim. Slower migrating BimEL bands are indicative of phosphorylated BimEL (PO_4-BimEL). *C*, HeLa cells were infected with VV(Cop) or UV-inactivated VV(Cop) (UV-VV(Cop)) at an MOI of 10 for 2, 4, or 6 hours. Lysatses were western blotted with anti-Bim. *D*, Wild type BMKs were infected with VV(Cop) at an MOI of 10 for 8 or 12 hours, and lysates were western blotted with anti-Bim.

VV(Cop) resulted in no significant change in the amounts of BimEL when compared to uninfected cells (Fig. 4.3*B*, lanes 1-5), BimEL from VV(Cop)-infected cells migrated slower by SDS-PAGE (Fig. 4.3*B* lanes 2-5) than BimEL from mock-infected lysates (Fig. 4.3*B* lane 1), and this change in BimEL migration has been shown to be the result of phosphorylation (147, 196, 197, 210). This effect was seen as early as 2 hours post-infection, and was maintained at 4, 6, and 8 hours post infection (Fig. 4.3*B* lanes 2-5).

To assess whether a late viral protein was required for VV-induced phosphorylation of BimEL, we treated cells with the nucleoside analogue cytosine arabinoside (AraC). AraC interferes with viral DNA replication and, as a result, inhibits viral late gene transcription which is dependent on viral DNA replication (252, 370). Cells were infected with VV(Cop) for 2, 4, 6, or 8 hours in the presence of AraC, and lysates were blotted with anti-Bim. Inclusion of AraC in VV(Cop)-infected cells had no effect on the appearance of the slower-migrating phosphorylated form of BimEL (Fig. 4.3*B*, lanes 5-8). This result suggests that viral late gene synthesis is not required for this virus-induced change in BimEL. Combined with the fact that this slow migrating form of BimEL was seen at only 2 hours post-infection (Fig. 4.3*B*, lane 2), this effect is induced very early during infection and is independent of late viral protein synthesis. To determine if the active process of VV infection is required to induce BimEL phosphorylation, cells were infected with UV-inactivated VV to ensure that the induced change in BimEL was not due to contaminating cellular membranes or proteins in virus preparations. Cells were infected with VV(Cop) or UV-inactivated VV(Cop) at an MOI of 10, lysates harvested at 2, 4 and 6 hours post-infection, and samples were western blotted with anti-Bim. Infection with VV(Cop) again displayed a dramatic shift in the migration of BimEL at all time points post infection (Fig. 4.3C, lanes 2-4), when compared to uninfected cell lysates (Fig. 4.3C, lane 1). Infection with UV-inactivated VV(Cop), however, did not induce the phosphorylation of BimEL (Fig. 4.3C, lanes 5-7). To determine whether this VV-induced phosphorylation of BimEL was specific for HeLa

cells, we also assessed the ability of VV to induce this change in BimEL migration in wild type BMKs. BMKs were infected with VV(Cop) for 8 or 12 hours, and lysates were western blotted with anti-Bim. Protein samples from VV(Cop)-infected BMKs also demonstrated a change in BimEL migration by SDS-PAGE (Fig. 4.3*D*, lanes 2-3) when compared to uninfected BMKs (Fig. 4.3*D*, lane 1). Although this effect does not appear to be as dramatic and complete as the effect seen in HeLa cells, this suggests that the VV-induced change in BimEL is not limited to HeLa cells.

The pro-apoptotic activity of Bim is controlled by both transcriptional and post-translational mechanisms. For instance, BimEL and BimL are phosphorylated by different kinases resulting in either activation or inhibition of Bim (193, 196, 197, 210, 267). ERK1/2 kinases can phosphorylate BimEL on serine69, and this induces the ubiquitination and subsequent degradation of BimEL by the 26S proteasome (30, 387). We therefore assessed whether the activation of ERK1/2 kinases is responsible for the VV-induced phosphorylation of BimEL. The kinase inhibitor U0126 inhibits MEK kinases which are responsible for the direct activation of ERK1/2 kinases and as a result inhibits ERK1/2-dependent BimEL phosphorylation (30, 108). Cells were infected with VV(Cop) in the presence or absence of U0126 and samples harvested at 2, 4, and 6 hours post-infection were western blotted with anti-Bim. HeLa cells infected with VV(Cop) again demonstrated a shift in BimEL migration (Fig. 4.4*A*, lanes 3-5) when compared to BimEL from uninfected cells (Fig. 4.4*A*, lane 1). Treatment of uninfected cells with U0126 had a minor effect on BimEL migration (Fig. 4.4*A*, lane 2), as BimEL appeared as a more compact band compared to the slightly diffuse band from untreated cells (Fig 4.4*A* lane 1). Lysates from cells infected with VV(Cop) in the presence of U0126, however, showed a dramatic decrease in the VV-induced slow-migrating form of BimEL (Fig. 4.4*A*, lanes 6-8). Although this altered form of BimEL was reduced in the presence of U0126, the profile of BimEL was not identical to the single tight band seen in uninfected cells (Fig. 4.4*A*, lane 2), suggesting that there may be other VV-induced effects on

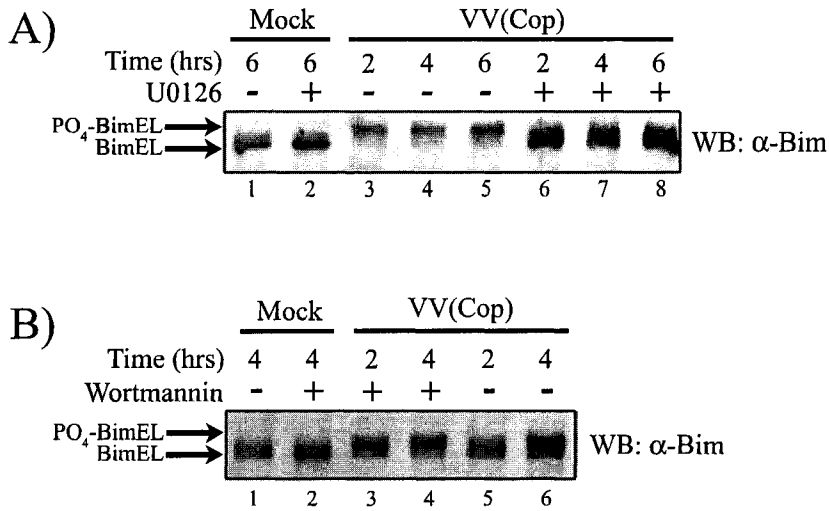

Figure 4.4. Inhibition of ERK kinases inhibits BimEL phosphorylation.
A, HeLa cells were pre-treated with the MEK-inhibitor U0126 (30μM) for 30 minutes, and infected with VV(Cop) at an MOI of 10. Samples were harvested at 2, 4, and 6 hours post-infection and were western blotted with anti-Bim. *B*, Hela cells were pre-treated with the PI-3 kinase inhibitor wortmannin (200nM) for 30 minutes, infected with VV(Cop) at an MOI of 10, and samples harvested at 2 and 4 hours post-infection were western blotted with anti-Bim.

BimEL. To examine whether other kinases are required for BimEL phosphorylation, we inhibited phosphatidylinositol-3-kinase (PI-3-kinase), which has not been reported to be required for BimEL phosphorylation (147, 210). Cells were infected with VV(Cop) in the presence or absence of the PI-3-kinase inhibitor, wortmannin (Fig. 4.4*B*). Cells infected with VV(Cop) again demonstrated a shift in BimEL migration (Fig. 4.4*B*, lanes 5-6), compared to BimEL from uninfected cells (Fig. 4.4*B*, lane 1). Treatment of mock-infected cells with wortmannin had no effect on BimEL expression or migration (Fig. 4.4*B*, lane 2). VV(Cop)-infected cells treated with wortmannin, however, still displayed a shift in BimEL migration by SDS-PAGE (Fig 4.4*B*, lanes 3-4). These results suggest that infection with vaccinia virus induces a rapid post-translational change in BimEL that is likely due in part to ERK1/2-dependent phosphorylation.

Reports indicate that BimEL phosphorylated on Ser69 is rapidly ubiquitinated and degraded by the 26S proteasome within 3-6 hours (210). In VV(Cop)-infected lysates, this phosphorylated form of BimEL is maintained at 8 hours post-infection. As other phosphorylated forms of BimEL or BimL can act as pro-apoptotic molecules (193, 267), we hypothesized that this phosphorylated form of BimEL may be pro-apoptotic. To address the effect of VV-induced BimEL phosphorylation on virus-induced apoptosis, cells were infected with VV(Cop)ΔF1L in the presence and absence of U0126. Cells were then lysed and probed with anti-Bim to detect BimEL, or with anti-PARP to examine VV-induced PARP cleavage and apoptosis (173). Infection with VV(Cop)ΔF1L, similar to infection with VV(Cop), induced the appearance of slower-migrating BimEL, and this was dramatically maintained at 12, 18, and 24 hours post infection (Fig. 4.5*A*, lanes 3-5). Treatment of cells with TNFα, on the other hand, did not induce the appearance of the slow-migrating form of BimEL (Fig. 4.5*A*, lane 1). Inclusion of U0126 also had no significant effect on the migration of BimEL from TNFα-treated cells (Fig. 4.5*A*, lane 2). Inclusion of U0126 in cells infected with VV(Cop)ΔF1L, however, inhibited BimEL phosphorylation (Fig. 4.5*A*, lanes 6-8), even at 24 hours post-infection. To determine

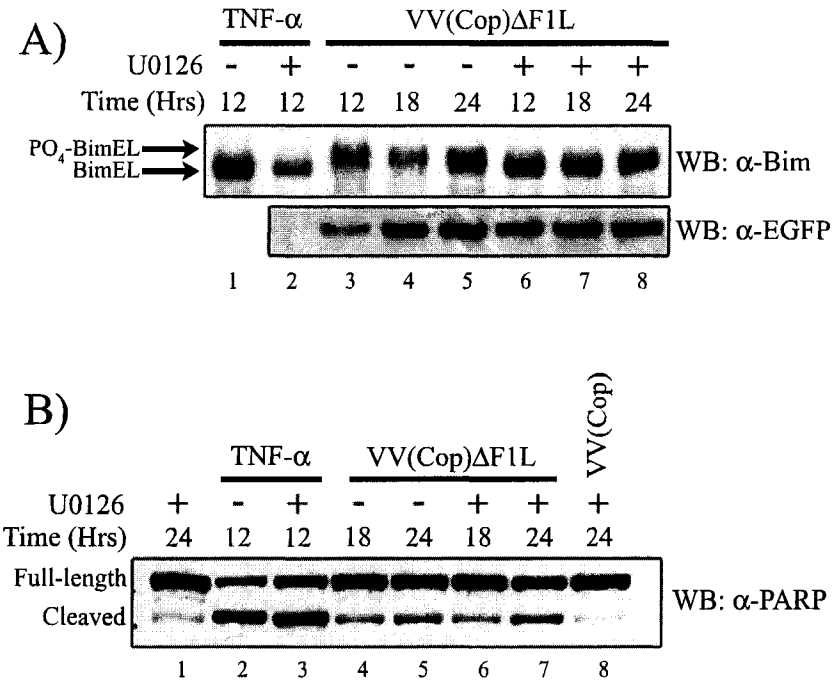

Figure 4.5. Inhibition of BimEL phosphorylation does not inhibit VV(Cop)ΔF1L-induced apoptosis. HeLa cells were pre-treated for 30 minutes where indicated with U0126 (30μM). Cells were either infected with VV(Cop) or VV(Cop)ΔF1L at a MOI of 10 for the indicated times, or treated with 10ng/ml TNF-α plus 5μg/ml cycloheximide for 12 hours. Cells were harvested in SDS-PAGE sample buffer containing 8M urea and western blotted with anti-Bim and anti-GFP (A), or anti-PARP (B).

whether inclusion of U0126 had any significant effect on viral protein expression, samples were also blotted for EGFP expression, as VV(Cop)ΔF1L expresses EGFP from a poxviral promoter (379). Inclusion of U0126 had no significant effect on EGFP expression (Fig. 4.5*A*), although ERK activity has been reported to be required for optimal virus replication (8, 89). To examine the effect of U0126 on VV(Cop)ΔF1L-induced apoptosis, samples from Figure 4.5*A* were also probed with anti-PARP to detect PARP cleavage. As expected, treatment of cells for 12 hours with TNFα induced dramatic PARP cleavage as compared to untreated cells (Fig. 4.5*B*, lanes 1 and 2), and treatment with U0126 had no effect on TNFα-induced PARP cleavage (Fig. 4.5*B*, lane 3).(199, 212). As expected, infection with VV(Cop)ΔF1L induced PARP cleavage at 18 and 24 hours post-infection (Fig. 4.5*B*, lanes 4-5), while infection with wild type VV(Cop) only induced minor amounts of PARP cleavage at 24 hours post-infection (Fig. 4.5*B*, lane 8). Intriguingly, inclusion of U0126 to inhibit VV(Cop)ΔF1L-induced BimEL phosphorylation had no significant effect on VV(Cop)ΔF1L-induced PARP cleavage (Fig. 4.5*B*, lanes 6-7). This suggests that virus-induced phosphorylation of BimEL is not absolutely required for VV-induced apoptosis, and that virus-induced death likely stimulates the activation of Bim or other BH3-only proteins by different mechanisms.

4.2.3 F1L expression inhibits Bax activation induced by BimL

The BH3-only protein Bim is reported to function as a direct activator of Bax (54, 147, 187, 194, 219), and previous observations indicate that a peptide encompassing the BH3 domain of Bim strongly interacts with F1L, suggesting that F1L may exert its anti-apoptotic activity by binding with full-length Bim (113). Since F1L indirectly inhibits Bax activation (350), we examined whether F1L could inhibit Bax activation induced by BimL. HeLa cells were transiently transfected to express BimL along with either EGFP-F1L or EGFP-F1L(206-226) (329). Bax activation was then assessed by staining with the conformation-specific anti-Bax(6A7) and visualized using confocal microscopy. Mock

transfected cells showed no Bax activation (Fig. 4.6*A*, panel a), while cells transfected with BimL alone demonstrated significant reactivity with anti-Bax(6A7), indicative of Bax activation (Fig. 4.6*A*, panel b). HeLa cells singly-transfected with EGFP-F1L(206-226) were healthy and showed no Bax activation (Fig. 4.6*B*, panels a-c). Cells co-transfected with BimL and EGFP-F1L(206-226), however, resulted in significant levels of Bax activation in transfected cells (Fig. 4.6*B*, panels d-f), as EGFP-F1L(206-226) does not inhibit apoptosis (329). In contrast, expression of EGFP-F1L dramatically inhibited Bax activation induced by BimL overexpression (Fig. 4.6*B*, panels g-i). EGFP-F1L-mediated inhibition of Bax activation was not due to the lack of BimL expression, as EGFP-F1L expressing cells (Fig. 4.6*C*, panels a-c) and EGFP-F1L(206-226)-expressing cells (Fig. 4.6*C*, panels d-f) both expressed BimL. Results were quantified by determining the percentage of EGFP-positive cells demonstrating anti-Bax(6A7) reactivity (Fig. 4.6*D*). Altogether, these results suggest that F1L can inhibit BimL-induced Bax activation.

4.2.4 F1L Interacts with BimL

F1L does not interact with Bax, yet F1L inhibits Bax activation induced by a number of stimuli, including BimL expression. Considering that soluble F1L interacts with the BH3 domains from Bak, Bax, and Bim, we hypothesized that F1L may inhibit Bax by interacting with BH3-only proteins (330, 390). To examine whether F1L interacts with BimL, HEK293T cells were co-transfected to express FLAG-BimL and either EGFP, EGFP-F1L, EGFP-Bcl-2 or EGFP-F1L(206-226). Co-transfected cells were lysed in 2% CHAPS and immunoprecipitated with anti-EGFP. Western blotting of lysates with anti-Bim showed that all samples contained equivalent amounts of FLAG-BimL (Fig. 4.7*A*), while western blotting of immunoprecipitations with anti-EGFP showed that each EGFP-tagged protein was precipitated, as expected (Fig. 4.7*A*). Intriguingly, western blotting of immunoprecipitates with anti-Bim revealed that both EGFP-F1L and EGFP-

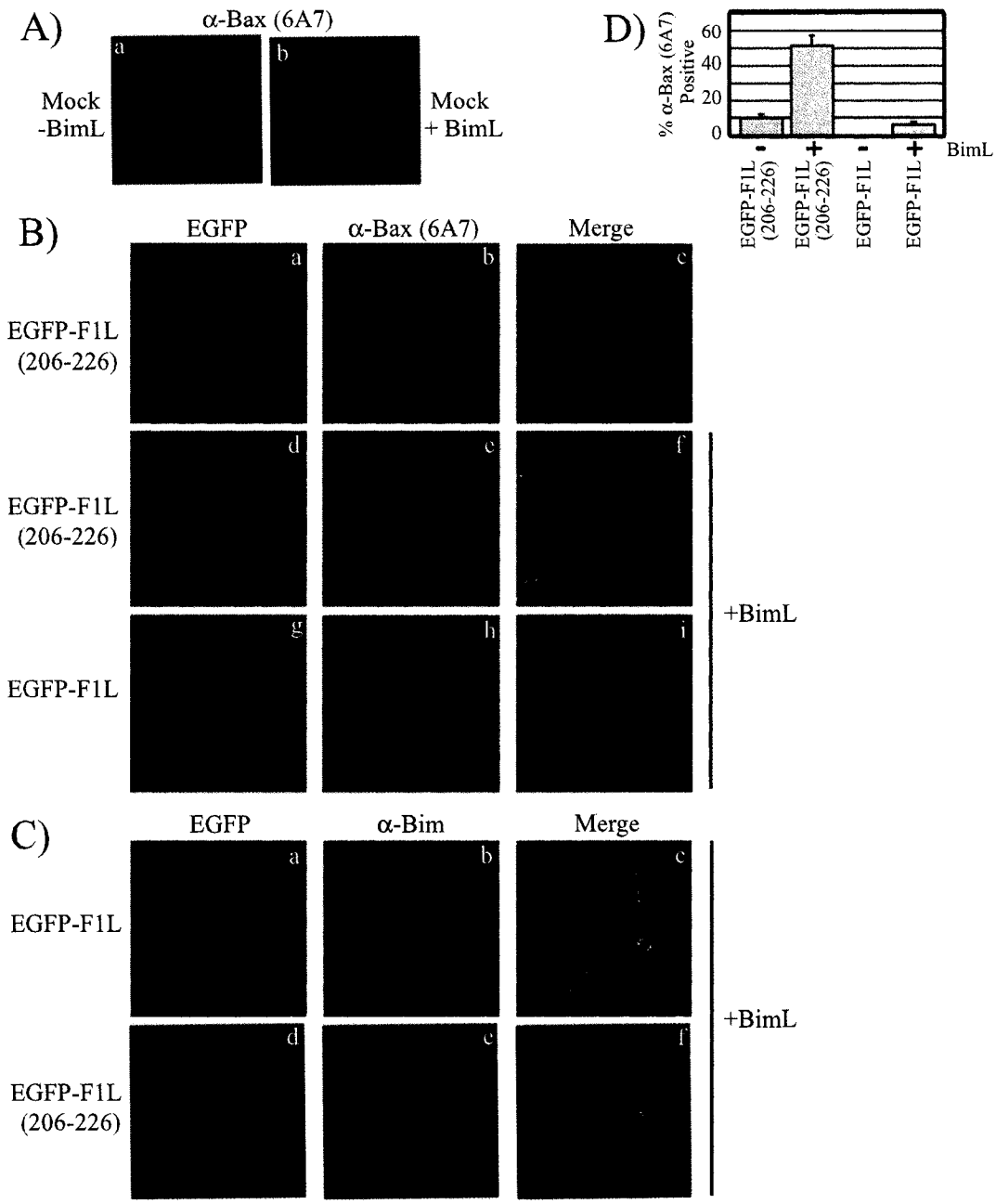

Figure 4.6. F1L inhibits BimL-induced Bax activation. *A*, HeLa cells were mock transfected or transfected with pcDNA3-FLAG-BimL for 16hrs, fixed and stained with anti-Bax(6A7) and anti-mouse Alexa546 to detect activated Bax. Cells were visualized with confocal microscopy. *B*, HeLa cells were co-transfected with pcDNA3-FLAG-BimL and either EGFP-F1L or EGFP-F1L(206-226) for 16 hours. Cells were fixed and stained with anti-Bax(6A7) and anti-mouse-Alexa546 to visualize activated Bax by confocal microscopy. *C*, HeLa cells were transfected with EGFP-F1L, or EGFP-F1L(206-226) and pcDNA3-FLAG-BimL, and stained with anti-Bim and anti-rabbit Alexa546 to detect BimL. *D*, EGFP positive cells reactive with anti-Bax(6A7) from (B) were quantified, with 200 cells counted in triplicate (±S.D.)

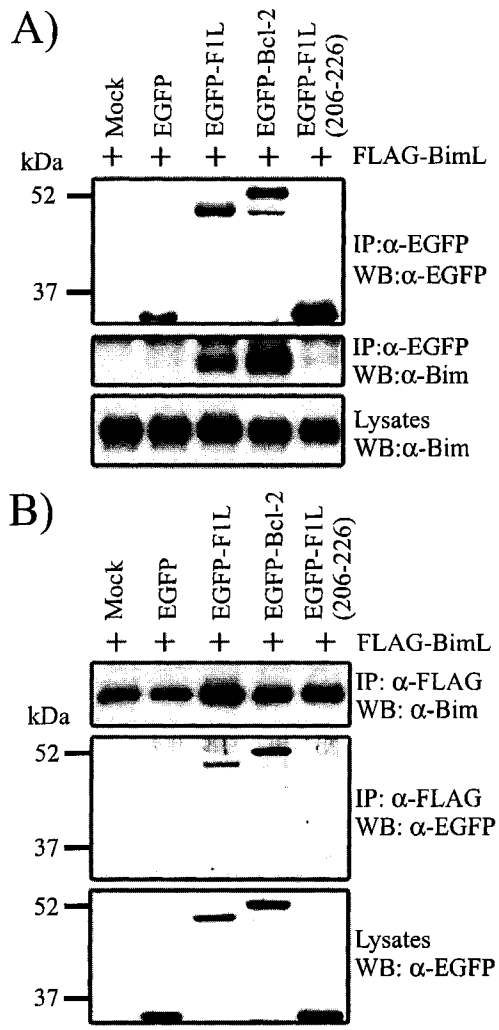

Figure 4.7. F1L interacts with the BH3-only protein BimL.
A, HEK293T cells were co-transfected with 4μg of pEGFP, pEGFP-F1L, pEGFP-Bcl-2, or pEGFP-F1L(206-226), along with 1μg of pcDNA3-FLAG-BimL for 16 hours, lysed in 2% CHAPS lysis buffer, and immunoprecipitated with goat anti-EGFP. IPs were probed with rabbit anti-EGFP or anti-Bim to detect precipitated proteins, and lysates were probed with anti-Bim. *B*, HEK293T cells were transfected and lysed as in (A), and immunoprecipitated with anti-FLAG(M2). IPs were immunoblotted with either rabbit anti-EGFP or anti-Bim to detect co-precipitated proteins, and lysates were blotted with rabbit anti-EGFP.

Bcl-2 co-precipitated significant amounts of BimL, whereas no interaction was observed between BimL and either EGFP or EGFP-F1L(206-226) (Fig. 4.7*A*). Reciprocal co-immunoprecipitations were performed by immunoprecipitating with anti-FLAG to precipitate FLAG-BimL. Lysates from each sample displayed similar levels of each EGFP-tagged protein as assessed by anti-EGFP western blots (Fig. 4.7*B*), and an equivalent amount of FLAG-BimL was immunoprecipitated in each sample as shown by western blotting with anti-Bim (Fig. 4.7*B*). Western blotting of immunoprecipitations with anti-EGFP revealed that FLAG-BimL did not co-immunoprecipitate with either EGFP or EGFP-F1L(206-226) (Fig. 4.7*B*). In contrast, immunoprecipitation of FLAG-BimL resulted in co-precipitation of both EGFP-Bcl-2 and EGFP-F1L (Fig. 4.7*B*), indicating that F1L interacts with ectopically expressed BimL.

Given that F1L localizes to the mitochondria and interacts with FLAG-BimL, we examined the distribution of ectopically expressed BimL. HeLa cells were transfected with BimL along with either pEGFP, pEGFP-F1L, or pEGFP-F1L(206-226). Cells were fixed and stained with anti-Bim, and visualized using confocal microscopy. As expected, EGFP alone gave a diffuse cytoplasmic staining pattern (Fig. 4.8*A*, panel a), while both EGFP-F1L and EGFP-F1L(206-226) exhibited a punctate distribution pattern (Fig. 4.8*A*, panels d, g), which is mitochondrial in nature (329, 382). Ectopic BimL was also punctate and mitochondrial in each sample (Fig. 4.8*A*, panels b, e, h) and colocalized with EGFP-F1L but not EGFP alone (Fig. 4.8*A*, panels c, f), indicating that F1L and BimL co-localize at the mitochondria. As well, expression of EGFP-F1L(206-226) also co-localized with BimL (Fig. 4.8*A*, panel i), despite failing to co-immunoprecipitate BimL (Fig. 4.7). This indicates that the interaction between EGFP-F1L and FLAG-BimL is dependent on more than the final 20 amino acids of F1L.

We also assessed the ability of F1L to interact with endogenous BimL by using $Bak^{-/-}/Bax^{-/-}$ BMKs which naturally express detectable levels of BimL (designated as $Bim^{+/+}$ BMKs)(346). $Bim^{+/+}$ and $Bim^{-/-}$ BMKs were infected with VV:FLAG-F1L to

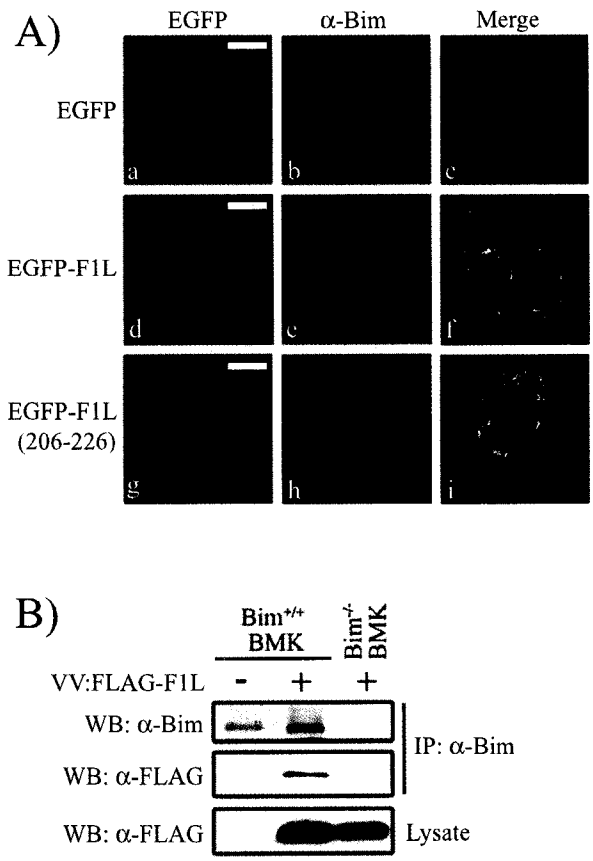

Figure 4.8. F1L co-localizes with exogenous BimL and interacts with endogenous BimL. *A*, HeLa cells were co-transfected with pcDNA3FLAG-BimL and either pEGFPC3, pEGFP-F1L or pEGFP-F1L(206-226). Cells were stained with anti-Bim, co-stained with secondary anti-rabbit-Alexa546 and visualized using confocal microscopy (bar = 10μm). *B*, F1L interacts with endogenous BimL. $Bak^{-/-}$ $Bax^{-/-}$ BMKs (designated $Bim^{+/+}$) or $Bim^{-/-}$ BMKs were infected with VV:FLAG-F1L for 16 h, lysed in 2% CHAPS lysis buffer, and immunoprecipitated with anti-Bim. Immunoprecipitations were immunoblotted with anti-Bim to detect precipitated BimL, or anti-FLAG (M2) to detect any co-precipitated FLAG-F1L. Lysates were probed with anti-FLAG to detect FLAG-F1L.

express FLAG-tagged F1L (346). Cells were lysed in 2% CHAPS and immunoprecipitated with a Bim specific antibody. Immunoprecipitates were western blotted with anti-Bim to detect immunoprecipitated BimL or with anti-FLAG to detect FLAG-F1L. As expected, BimL was immunoprecipitated from both infected and uninfected $Bim^{+/+}$ BMKs (Fig. 4.8*B*). Although western blotting of lysates with anti-FLAG revealed a significant amount of FLAG-F1L in infected $Bim^{-/-}$ cells, no FLAG-F1L was co-immunoprecipitated from $Bim^{-/-}$ cells with anti-Bim (Fig. 4.8*B*), indicating that the anti-Bim antibody does not interact with FLAG-F1L. In contrast, anti-Bim immunoprecipitations from VV:FLAG-F1L-infected $Bim^{+/+}$ BMKs did co-precipitate FLAG-F1L, indicating that F1L interacts with endogenous BimL, and reinforces the observation that F1L has the capacity to interact with the BH3-only protein BimL.

4.2.5 Bim is involved in vaccinia virus-induced apoptosis

F1L interacts with BimL, suggesting that Bim may be a natural target for F1L during infection and that Bim may mediate VV-induced apoptosis. We assessed whether Bim was required for VV-induced apoptosis by infecting Bim-deficient cells with VV(Cop)ΔF1L and measuring apoptosis. Wild type (WT) or $Bim^{-/-}$ BMKs were infected with VV(Cop) or VV(Cop)ΔF1L at an MOI of 10, and apoptosis was assessed at 10 or 15 hours post-infection by counting surviving adherent cells. WT BMKs infected with VV(Cop) displayed limited amounts of cell death with the majority of infected cells still adherent (Fig. 4.9*A*). VV(Cop)ΔF1L-infected WT BMKs demonstrated a significant reduction in cell survival at 10 and 15 hours post infection, as assessed by a loss of adherent cells. Pretreatment of WT BMKs with the broad-spectrum caspase inhibitor zVAD.fmk inhibited VV(Cop)ΔF1L-induced cellular loss, indicating that cell death was the result of caspase-dependent apoptosis (Fig. 4.8*A*). Similar to wild type cells, $Bim^{-/-}$ cells infected with VV(Cop) showed no significant loss of adherent cells. Interestingly, infection of $Bim^{-/-}$ BMKs with VV(Cop)ΔF1L induced the apoptotic loss of adherent

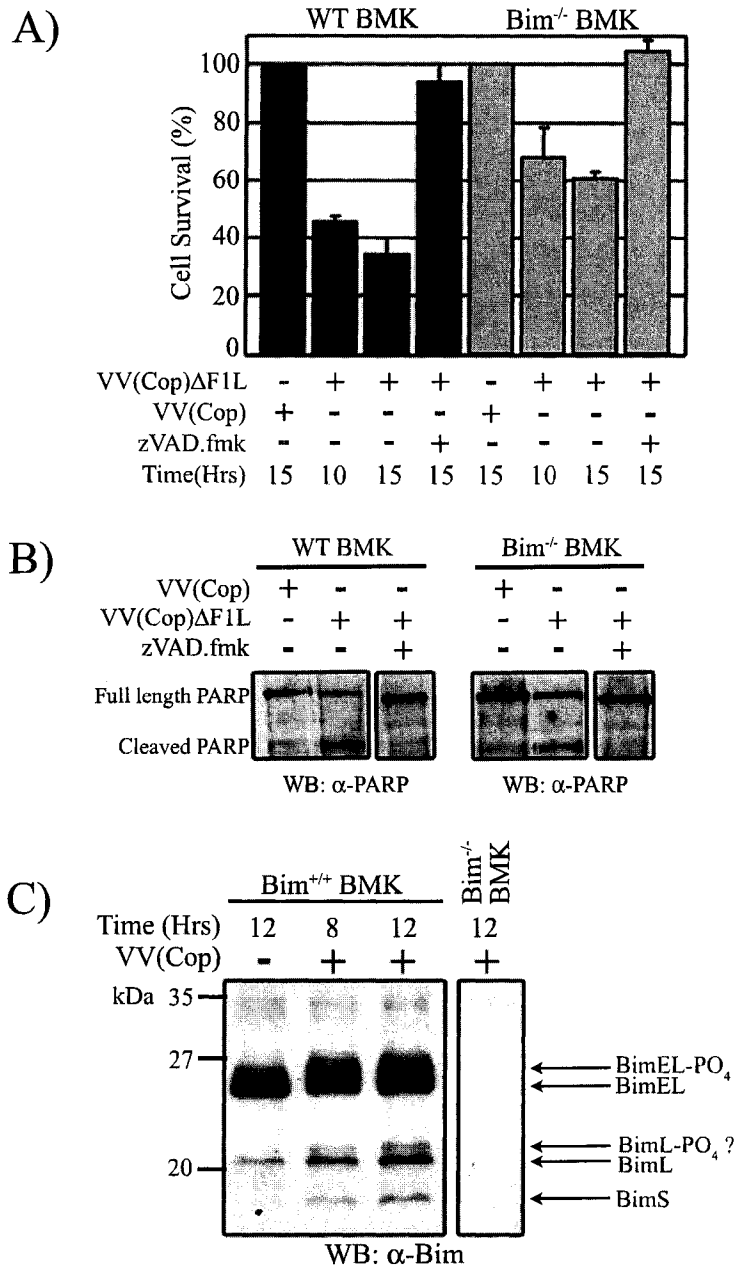

Figure 4.9. Bim is required for vaccinia virus-induced apoptosis.
A, Apoptosis in WT or Bim$^{-/-}$ BMKs was assessed by determining the number of healthy adherent cells. WT or Bim$^{-/-}$ BMKs were infected with with VV(Cop) or VV(Cop)ΔF1L for 10 or 15 hrs, in the absence or presence of 100μM zVAD.fmk to inhibit caspase activation, and healthy adherent cells were quantified as described in the materials and methods. Standard deviations were calculated from three independent experiments. *B*, WT or Bim$^{-/-}$ BMKs were infected with either VV(Cop) or VV(Cop)ΔF1L in the absence or presence of 100μM zVAD.fmk for 8 hrs. Samples were harvested and analyzed by western blotting with anti-PARP. *C*, Bim$^{+/+}$ or Bim$^{-/-}$ BMKs were infected with VV(Cop) for 8 or 12 hours, and lysates were western blotted with anti-Bim to detect BimEL, BimL, or BimS isoforms.

cells, but at a reduced rate when compared to WT BMKs (Fig. 4.9*A*). VV(Cop)ΔF1L-induced apoptosis was also inhibited with the addition of zVAD.fmk (Fig. 4.9*A*), indicating that cell death was dependent on caspases. These results suggest that Bim is partially required for VV(Cop)ΔF1L-induced death. Notably, however, VV-induced apoptosis was not completely abolished in Bim-deficient BMKs, indicating that other pro-apoptotic effector molecules are likely activated following VV infection.

To confirm these observations, we also examined VV(Cop)ΔF1L-induced PARP cleavage in WT or $Bim^{-/-}$ BMKs. BMKs were infected with VV(Cop) or VV(Cop)ΔF1L for 8 hours, and lysates were western blotted with anti-PARP (173). Infection of either $Bim^{-/-}$ or WT BMKs with wild type VV(Cop) did not result in significant PARP cleavage (Fig. 4.9*B*), indicating that F1L inhibited VV-induced apoptosis in both cell lines. Infection with VV(Cop)ΔF1L, however, induced the cleavage of PARP in WT BMKs, but to a lesser extent in $Bim^{-/-}$ BMKs (Fig. 4.9*B*). Pre-treatment of both cell lines with the caspase inhibitor zVAD.fmk inhibited VV(Cop)ΔF1L-induced PARP cleavage, indicating that PARP cleavage was the result of caspase-dependent apoptosis (114, 173). Densitometric analysis of PARP revealed that in VV(Cop)ΔF1L-infected WT BMKs, nearly 80% of PARP existed as a cleaved form, whereas only 40% of PARP was cleaved in $Bim^{-/-}$ BMKs infected with VV(Cop)ΔF1L. These observations suggest that the pro-apoptotic activity of Bim is required for efficient VV-induced apoptosis and F1L expression inhibits this activity. As VV(Cop) was protected from VV-induced apoptosis in wild type BMKs, these results suggest that F1L can also inhibit apoptosis mediated by BimL during virus infection.

We observed that BimEL was phosphorylated during VV-infection, but that this is not required for VV-induced apoptosis (Fig. 4.3-4.5). Bim, however, appears to be required for VV-induced apoptosis in BMKs (Fig.. 4.9*A, B*), suggesting that Bim is somehow activated during VV-infection. To investigate whether Bim is transcriptionally or post-translationally modified following virus infection, $Bim^{+/+}$ BMKs ($Bak^{-/-}$/$Bax^{-/-}$

BMKs) or $Bim^{-/-}$ BMKs were infected with VV(Cop) for 8 or 12 hours, and lysates were harvested and immunoblotted with anti-Bim. As expected, a significant amount of BimEL and a much lesser amount of BimL was seen in $Bim^{+/+}$ BMKs , but not $Bim^{-/-}$ BMKs (Fig. 4.9*C*) (346). Dramatically, infection with VV(Cop) induced the apparent up-regulation of BimS and BimL as well as an apparent change in the migration of BimL (Fig. 4.9*C*), which may also be the result of phosphorylation (193). Although the specific effect that VV-infection has on Bim expression remains to be determined, these observations suggest that Bim is an important regulator of apoptosis during VV-infection, and that F1L can specifically inhibit apoptosis mediated by Bim.

4.3. Discussion

The vaccinia virus protein F1L inhibits the activation of the pro-apoptotic multi-domain proteins Bak and Bax (265, 350, 379)(Chapter 3). F1L, which constitutively interacts with Bak (265, 379), does not interact with Bax before or after an apoptotic stimulus (Chapter 3)(265, 350). As such, we hypothesized that F1L might function upstream through the inhibition of one or more Bax regulatory proteins. One set of proteins which regulate Bak and Bax are the BH3-only proteins, and the BH3-only protein Bim has been documented to be a direct activator of Bak and Bax (147, 187, 194). Intriguingly, a soluble version of F1L interacts with BH3-peptides from Bim, Bak and Bax (113), suggesting that F1L may interact with BH3 domains as a mechanism of action. In support of this, our data indicate that F1L can interact with Bax in the presence of Triton-X-100, which induces a conformational change in Bax and reveals the BH3 domain (Chapter 3) (157, 158, 350). As such, we investigated the ability of F1L to modulate the pro-apoptotic effects of the BH3-only protein Bim.

Several studies have shown that Bim is a direct activator of Bak and Bax (187, 194, 250), and phosphorylation by ERK1/2 kinases also target Bim for ubiquitination and degradation by the 26S proteasome (30, 147, 197, 210, 218). Intriguingly, infection with

either VV(Cop) or VV(Cop)ΔF1L induces the appearance of a slower migrating form of BimEL, which is characteristic of phosphorylated BimEL (Fig. 4.3-4.5). Inclusion of the kinase inhibitor U0126, which inhibits ERK1/2 activation, predominantly inhibited VV-induced BimEL phosphorylation (Fig, 4.4*A*), suggesting that ERK1/2 is likely responsible for the dramatic shift in BimEL migration, although other kinases may be activated during VV-infection. The ERK1/2 kinase pathway is activated during VV infection, and ERK1/2 activation is not dependent on viral DNA replication (8, 89). Indeed, we also observed BimEL phosphorylation in the presence of the DNA replication inhibitor AraC (Fig. 4.3*B*). VV-induced ERK1/2 activation has been shown to require *de novo* protein synthesis during infection (8), suggesting that a viral protein is responsible for triggering this pathway, and consequently BimEL phosphorylation. The identification of specific viral proteins which regulate and trigger the ERK kinase pathway remains to be determined.

Reports demonstrating BimEL phosphorylation by ERK1/2 indicate that BimEL is subsequently ubiquitinated and degraded by 6 hours post-phosphorylation (147, 197, 210). Interestingly, infection with VV induced the long-lasting phosphorylation of BimEL up to 24 hours post-infection (Fig. 4.3-4.5), suggesting that this form of BimEL is not ubiquitinated and degraded. VV-induced phosphorylation of BimEL may therefore not occur on the same residues which typically lead to BimEL ubiquitination. Alternatively, it is possible that the ubiquitin-mediated degradation pathway is negatively affected during VV-infection. BimEL phosphorylated during VV-infection did not appear to be pro-apoptotic, as inclusion of U0126 to inhibit BimEL phosphorylation had no effect on VV(Cop)ΔF1L-induced apoptosis (Fig. 4.5). We did, however, observe a decrease in VV(Cop)ΔF1L-induced apoptosis in Bim-deficient cells, indicating that Bim is at least partly required for VV-mediated apoptosis (Fig. 4.9*A* and *B*). In support of this, both BimL and BimS appear to be up-regulated in $Bim^{+/+}$ cells infected with VV(Cop), and the migration of BimL also appears to be altered following VV infection (Fig. 4.9*C*).

This altered form of BimL may also be the result of phosphorylation and activation (193). The inclusion of U0126 in VV-infected HeLa cells did not completely abolish the shift in BimEL migration (Fig. 4.4*A*), suggesting that other events may modify BimEL during virus infection. Indeed, other kinases, such as JNK kinases, have been documented to phosphorylate BimEL and BimL (193, 267). How infection with VV induces Bim phosphorylation and up-regulation remains to be determined, and further work is needed to characterize the expression and modification of Bim isoforms during VV-infection.

Wild type BMKs infected with VV(Cop) were protected from virus-induced apoptosis (Fig. 4.9*A* and *B*), indicating that F1L can inhibit apoptosis mediated by Bim. In support of this, F1L expression inhibited the loss of the mitochondrial membrane potential induced by the overexpression of BimL (Fig. 4.1). F1L expression also inhibited cytochrome c release induced by overexpression of Bim in Bak-deficient MEFs (Fig 4.2), demonstrating that the interaction between F1L and Bak is not required to inhibit Bim-induced apoptosis. BimL is a direct activator of Bak and Bax (147, 187, 194), so we assessed the ability of F1L to inhibit Bax activation induced by BimL. The activation of Bax by BimL was inhibited by F1L (Fig 4.6), but not by F1L(206-226) which lacks anti-apoptotic activity (329), demonstrating that F1L can inhibit apoptosis and Bax activation induced by BimL.

Pro-survival Bcl-2 proteins interact with and inhibit the activity of BH3-only proteins (61, 187, 194, 392). Considering that F1L inhibits apoptosis induced by BimL (Fig. 4.1-4.2), and a soluble version of F1L interacts with the BH3-peptide from BimL (113), we investigated whether full-length F1L could interact with BimL. Co-immunoprecipitations revealed that full-length F1L was capable of interacting with overexpressed BimL by co-immunoprecipitation (Fig. 4.7*A* and *B*). Significantly, FLAG-F1L was able to interact with endogenous BimL during virus infection, as immunoprecipitation of BimL co-precipitated FLAG-F1L (Fig. 4.8*B*). The mitochondrial-targeted construct EGFP-F1L(206-226), however, failed to co-immunoprecipitate BimL

(Fig. 4.6*A* and *B*), despite displaying dramatic co-localization to the mitochondria with BimL (Fig. 4.7*A*). Taken together, this data supports a scenario by which F1L inhibits Bax activation by binding and sequestering BH3-only proteins, such as BimL. The crystal structure of a fragment of Bim indicates that the BH3 domain of Bim is relatively unobstructed, and may make this domain more available for protein:protein interactions (206). Indeed, Bim and Puma are the only two BH3-only proteins which can interact with all of the cellular pro-survival Bcl-2 family members (61, 65, 187). VV(Cop)-infected $Bim^{-/-}$ BMKs were still protected from VV-induced apoptosis (Fig. 4.9*A*, and *B*), suggesting that F1L can function in the absence of Bim. As well, F1L expression inhibits the loss of the mitochondrial membrane potential induced by the overexpression of Bid or Bmf (Fig. 4.1), and F1L can inhibit cytochrome c release and Bax activation induced by Bid (Fig. 4.2) (350). These results suggest that F1L inhibits apoptosis mediated by multiple BH3-only proteins, although it remains to be determined whether F1L can directly interact with these or other BH3-only proteins. No members of the pro-survival Bcl-2 family appear to interact with all of the BH3-only proteins. Mcl-1, for instance, only interacts with Bim, Puma and Noxa, while Bcl-2 interacts with Bim, Puma, Bmf and Bad (61, 65). Bcl-x_L is the most promiscuous and appears to interact with all of the BH3-only proteins with the exception of Noxa (61, 187). Considering this, it is entirely possible that F1L may selectively interact with certain BH3-only proteins to inhibit apoptosis and Bax activation. The identification of BH3-only proteins which F1L can interact with will aid in our understanding of the mechanism F1L uses to inhibit apoptosis, as well as how VV induces apoptosis through BH3-only protein activation.

CHAPTER 5: Ectromelia Virus EVM025 is a Functional Anti-Apoptotic Protein

The results contained within this chapter consist of unpublished material. The initial cloning of EVM025(E255), and the results presented in Fig. 5.3*B* were generated by J. Fanaiean, a summer student mentored by J. Taylor. The results presented in Fig. 5.3*C* were generated by T. Stewart. All of the other experiments contained herein were performed by J. Taylor. The original manuscript was written by J. Taylor, and a major editorial contribution was made by M. Barry.

5.1 Introduction

Ectromelia virus, also known as mousepox, is a member of the *Orthopoxviridae* which causes a lethal disease in several strains of mice (102, 110). Illness is typically associated with spontaneous amputation of infected limbs and the appearance of pox-like lesions, and generalized organ failure ultimately results in death (102, 110). Ectromelia virus strain Moscow (EVM) is one of the most virulent strains, and possesses a genome of approximately 175 kb in size which encodes 175 open reading frames (62). Considering the genetic tools available for studying both poxviruses and mice, EVM is an excellent model system in which to study host:pathogen interactions. Indeed, EVM encodes a number of proteins which inhibit various aspects of the host immune system, and the inhibition of apoptosis is no exception (62). Ectromelia virus encodes cytokine response modifier A (CrmA) which was originally identified as an inhibitor of the inteleukin-1β-converting enzyme (ICE/Caspase-1) (180, 274), and also inhibits caspase-8 activation to interfere with death receptor-mediated apoptosis (241, 354). EVM also encodes the RING-finger protein p28, which is a ubiquitin ligase that was shown to have protective effects against UV-induced apoptosis, but not TNF-induced apoptosis (43, 161, 246).

The closely related *Orthopoxvirus* vaccinia virus encodes the potent anti-apoptotic protein F1L (382) (329, 379). In contrast to CrmA which specifically inhibits the extrinsic death receptor pathway (241, 354), F1L is a mitochondrial-localized protein which inhibits both extrinsic and intrinsic apoptotic stimuli (329, 382). F1L localizes to the mitochondrial outer membrane via a C-terminal hydrophobic domain where it inhibits cytochrome c release (329, 379, 382). Following an apoptotic stimulus, the pro-apoptotic proteins Bak and Bax homo-oligomerize into high molecular weight species at the mitochondria to facilitate cytochrome c release (11, 12, 384, 404). As a mechanism of action, F1L interacts constitutively with the pro-apoptotic protein Bak and inhibits the activation and oligomerization of Bak following an apoptotic stimulus (265, 379).

Recently, we showed that F1L is also able to inhibit activation of the pro-apoptotic protein Bax, although no interaction between F1L has been detected before or after an apoptotic stimulus (265, 350). F1L instead interacts with the BH3-only protein BimL (350), and the inhibition of BH3-only proteins by F1L is the current model by which F1L can inhibit Bax activation.

Alignment of the genomes of vaccinia virus and ectromelia virus reveals an ectromelia virus open reading frame, EVM025, which is homologous to F1L (www.poxvirus.org) (Fig. 5.1) (62). EVM025 encodes a putative hydrophobic transmembrane domain at the C-terminus similar to F1L (329), which targets F1L to the mitochondrial outer membrane (Fig. 5.1). While the C-terminal 210 amino acids of both proteins share greater than 90 percent amino acid identity, EVM025 encodes a large N-terminal extension comprised of 30 copies of an eight amino acid motif, "Asp-Asn-Gly-Ile-Val-Gln-Asp-Ile" (DNGIVQDI) (Fig. 5.1). This eight amino acid motif is also present 25 times in the orthologue from EV strain Naval, but is not found more than once in any other poxviral orthologue (www.poxvirus.org). The 'DNGIVQDI' repeat has no homology with any known proteins, does not display any obvious predicted secondary structure, and has no known predicted function. Although F1L and EVM025 share homology at the C-termini, there are a number of notable amino acid differences within this conserved region (Fig. 5.1). For example, within the amino acid sequence of EVM025, there is an "Asp-Ile" insertion at amino acid 346, there are five Lys to Glu substitutions, two Ser to Asn substitutions, two Cys to Tyr substitutions, and a Phe insertion at amino acid 421 followed by a stretch of 10 amino acids which show very low homology (Fig. 5.1). Single amino acid substitutions have been shown to dramatically alter the pro- or anti-apoptotic activities of proteins at the mitochondria (208, 375, 399). As well, mutation of Met 67 from F1L abrogates the interaction with Bak and eliminates the anti-apoptotic activity of F1L (265). Considering the obvious amino acid differences

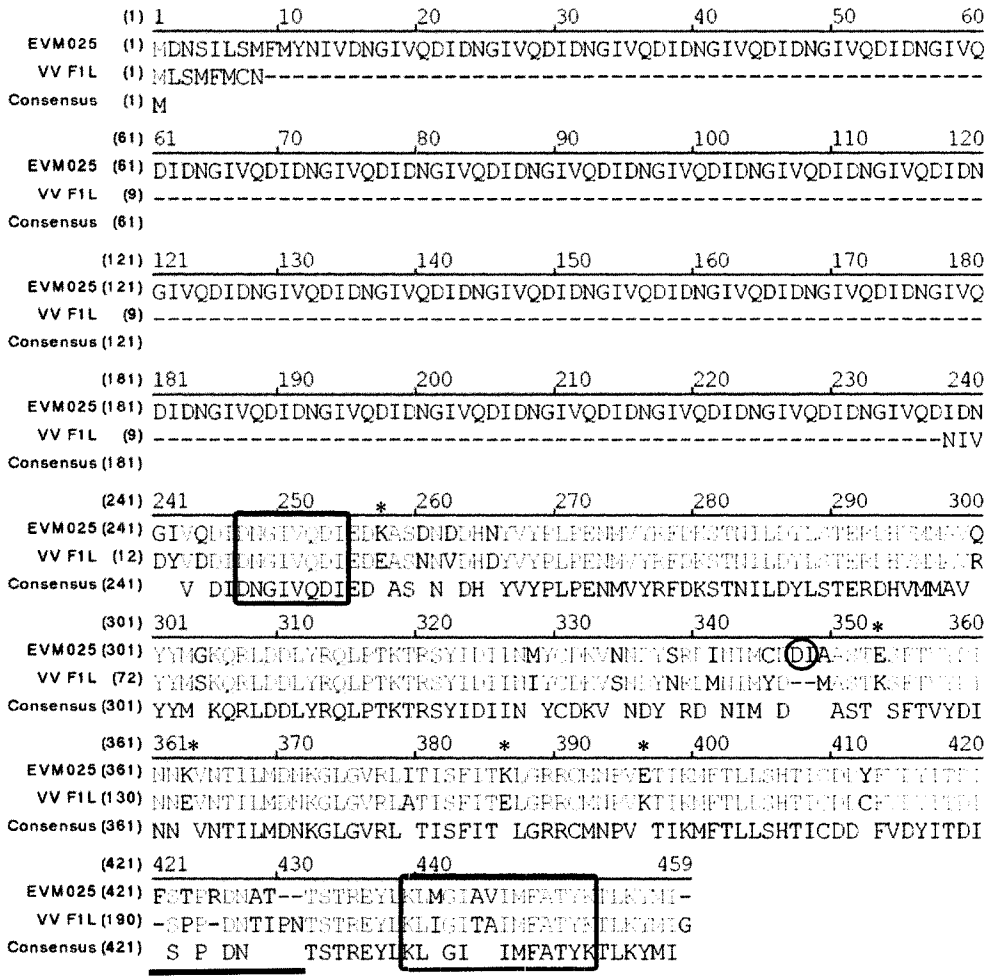

Figure 5.1 Alignment of EVM025 and VVF1L. Amino acid alignment of EVM025 and F1L from vaccinia virus, with the consensus sequence indicated below. The red box indicates the mitochondrial targeting domain. The blue box indicates the eight amino acid repeat motif present 30 times in EVM025, and present in VVF1L only once. The green circle indicates the insertion of Asp-Ile (DI) in the middle of the C-terminal region of EVM025. Note the series of single amino acid substitutions, including five lysine-glutamate changes (denoted with asterixes). As well, the region between aminos acids 421 and 430 of EVM025 is highly variable compared to F1L (underlined). AlignX (Invitrogen) was used to generate the alignment.

between F1L and EVM025, it is unknown whether EVM025 functions in a manner similar to F1L.

The ability to inhibit apoptosis is an important virulence mechanism for a number of pathogenic viruses (39, 82). Here we investigated whether EVM025 encodes a functional anti-apoptotic protein. We generated a strain of EVM deficient in EVM025 and also generated truncation mutants of EVM025 in order to investigate the ability of EVM025 to interact with Bak and Bax.

5.2. Results

5.2.1 Ectromelia virus infection inhibits apoptosis.

Ectromelia virus strain Moscow (EVM) encodes two anti-apoptotic proteins, p28 and CrmA (43, 44, 62). The protein p28 has been shown to inhibit UV-induced, but not Fas- or TNFα -induced apoptosis (43), and CrmA inhibits caspase-8 activation following treatment with TNFα or FasL, but does not inhibit the intrinsic apoptotic cascade involving the mitochondria (241, 354). To examine whether ectromelia virus encoded a functional mitochondrial inhibitor of apoptosis, we induced death through the intrinsic pathway at the mitochondria by treating cells with the kinase inhibitor staurosporine (27). Jurkat cells were infected with either VV(Cop), EVM, or EVM lacking the caspase inhibitor CrmA (EVMΔcrmA), and treated with staurosporine to induce apoptosis. At 2 hours post-treatment, cells were fixed and stained for DNA fragmentation using TUNEL, and analyzed by flow cytometry. Uninfected Jurkat cells or cells infected with either VV(Cop), EVM, or EVMΔcrmA all displayed similar levels of DNA fragmentation when left untreated (Fig. 5.2*A*, panels a, c, e, g), indicative of healthy cell populations. Jurkat cells treated with staurosporine exhibited a dramatic increase in fluorescence, which is characteristic of DNA fragmentation and apoptosis (Fig. 5.2*A*, panel b). Infection with VV(Cop) inhibited staurosporine-induced DNA fragmentation, as expected (Fig. 5.2*A*, panel d) (381). Similarly, infection with either EVM or EVMΔcrmA also inhibited

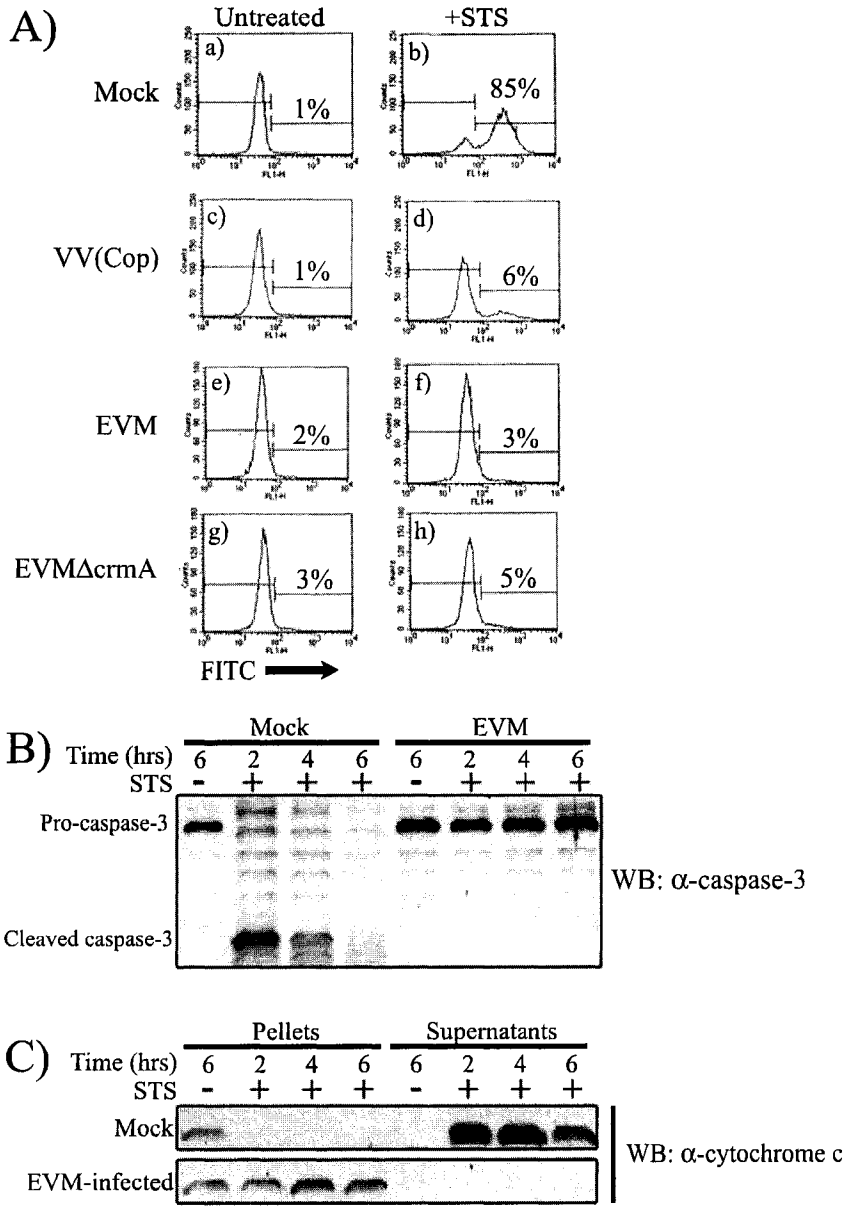

Figure 5.2. Infection with ectromelia virus strain Moscow inhibits apoptosis. *A*, Jurkat cells were infected with VV(Cop), EVM, or EVMΔcrmA at a MOI of 10 for 6 hours. Cells were treated with staurosporine (STS) to induce apoptosis, and two hours post-treatment, DNA fragmentation was assessed by TUNEL and flow cytometry. *B*, Jurkat cells were mock infected or infected with EVM, treated with STS, and samples analyzed by western blotting for cleavage of procaspase-3 at the indicated times post-treatment. *C*, Jurkat cells were infected as in (A), treated with STS, and cells were fractionated into mitochondria-containing pellet and soluble (cytoplasmic) fractions. Cytochrome c release was assessed by western blotting with anti-cytochrome c.

staurosporine-induced DNA fragmentation (Fig. 5.2*A*, panels f, h). These results suggest that infection with EVM can inhibit apoptosis induced by intrinsic stimuli such as staurosporine, and that this is independent of the caspase inhibitor CrmA.

Staurosporine induces apoptosis specifically through the mitochondria (27), so we assessed the ability of ectromelia virus to inhibit events upstream of DNA fragmentation, specifically the cleavage of caspase-3 and the release of cytochrome c from mitochondria. Jurkat cells were infected with EVM for 6 hours and treated with staurosporine. Cells were fractionated into a cytosolic supernatant fraction and a mitochondrial-containing fraction at various time points post-treatment, and fractions were analyzed by western blotting with anti-caspase-3 or anti-cytochrome c. As expected, treatment of uninfected Jurkat cells with staurosporine resulted in the rapid cleavage of procaspase-3 (Fig. 5.2*B*) (111). Cleaved caspase-3 fragments appeared as early as 2 hours post-treatment, and corresponded with the loss of the immature 32kDa form of procaspase-3 (Fig. 5.2*B*) (381). Infection with EVM, however, dramatically inhibited caspase-3 cleavage, even at 6 hours post-staurosporine treatment (Fig. 5.2*B*). We also assessed the translocation of cytochrome c from the mitochondria into the cytosol by western blotting the mitochondrial pellet and cytosolic supernatant fractions with anti-cytochrome c. Uninfected Jurkat cells treated with staurosporine exhibited a rapid and complete translocation of cytochrome c from the mitochondrial pellet fraction to the cytosolic supernatant fraction as early as 2 hours post treatment (Fig 5.2*C*). Infection with EVM, however, completely inhibited staurosporine-induced cytochrome c release (Fig. 5.2*C*), even at 6 hours post-treatment. These observations suggest that ectromelia virus can inhibit staurosporine-induced apoptosis at the mitochondria, similar to vaccinia virus (381).

5.2.2. EVM025 is a 55kDa protein expressed throughout infection

Infection with EVM potently inhibits apoptosis and cytochrome c release induced by staurosporine, suggesting that EVM may encode a mitochondrial anti-apoptotic protein. As EVM025 is a predicted orthologue of F1L, we first examined the expression of EVM025 during infection using an antibody specific for F1L (329). This anti-F1L antibody was raised against the first 120 amino acids of F1L, which shares greater than 90% amino acid identity with EVM025 (329). CV-1 cells were infected with VV(Cop), EVM, or VV:FLAG-F1L which expresses FLAG-F1L from a strong synthetic viral promoter, and lysates were western blotted with anti-F1L (329). VV:FLAG-F1L expresses high amounts of FLAG-F1L at early and late time points as FLAG-F1L is behind a strong synthetic poxviral promoter (56). Western blotting lysates from cells infected with VV:FLAG-F1L with anti-F1L detected a band at the expected size of approximately 32 kDa (Fig. 5.3*A*). Blotting of EVM-infected lysates also demonstrated EVM025 expression at 55kDa at all times post-infection (Fig. 5.3*A*). Interestingly, blotting of VV(Cop)-infected lysates with anti-F1L failed to detect any endogenous F1L at either 4, 8, or 24 hours post-infection. This observation may be due to the ubiquitination and degradation of F1L by the 26S proteasome, as inclusion of proteasome inhibitors dramatically increases F1L expression (265), and F1L appears to be ubiquitinated itself (Appendix B.2). Western blotting with an antibody specific for the viral late protein I5L demonstrated that cells were infected with either VV(Cop) or EVM. These results suggest that EVM025 is produced throughout infection as its predicted size of 55kDa.

To determine whether EVM025 was expressed early during virus infection, cells were infected in the presence of AraC, an inhibitor of viral DNA synthesis and late gene expression (252). Infection of cells with EVM demonstrated the production of EVM025 at all times post-infection (Fig. 5.3*B*), and EVM025 was observed in cells infected in the presence of AraC, indicating that EVM025 is expressed early during infection (Fig.

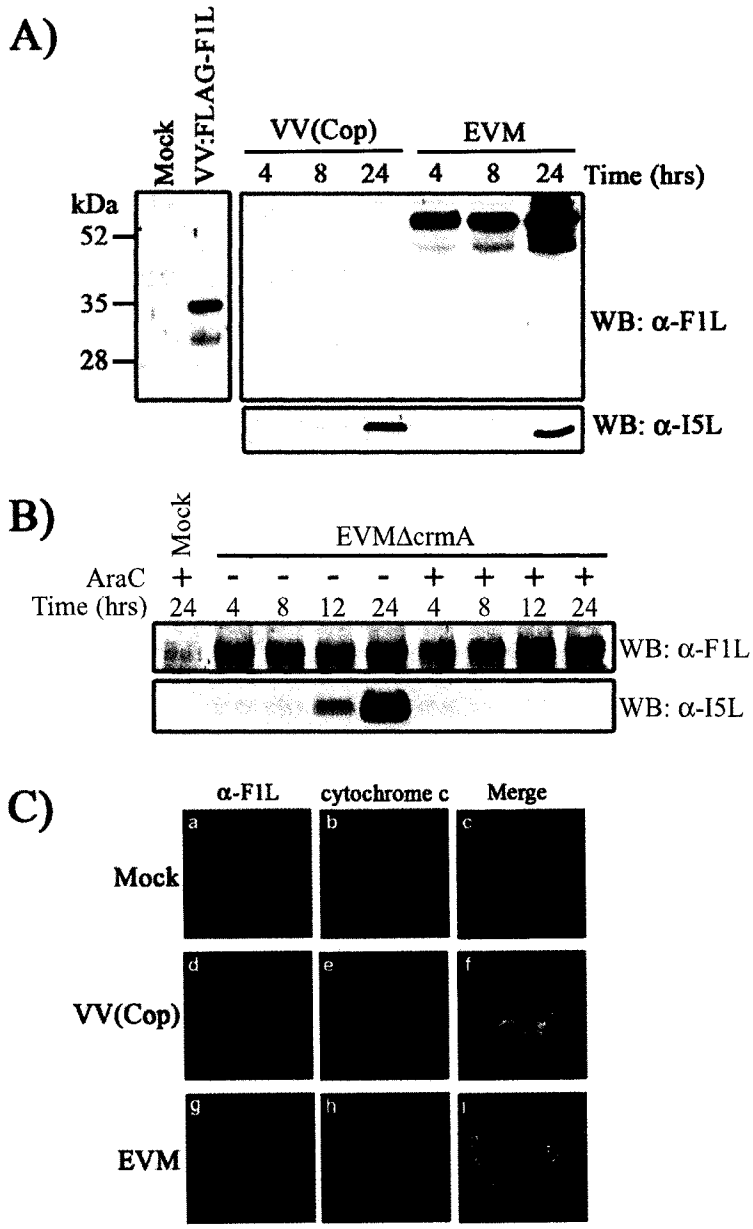

Figure 5.3. EVM025 is expressed as a 55kDa protein. *A*, CV-1 cells were infected with VV(Cop) or EVMΔcrmA at an MOI of 10, and lysates were western blotted with either anti-F1L or anti-I5L. Cells were also infected with VV:FLAG-F1L for 8 hours as a control for anti-F1L staining. *B*, EVM025 is an early protein expressed throughout infection. HeLa cells were infected with EVMΔcrmA for the indicated times at an MOI of 5, and lysates were western blotted with anti-F1L or anti-I5L. Cytosine arabinoside (AraC) was included at 80μg/ml to inhibit late gene transcription. *C*, HeLa cells were infected with either VV(Cop) or EVM at an MOI of 5 for 8 hours, fixed, and stained with anti-F1L and anti-cytochrome c, and visualized by confocal microscopy.

5.3*B*). In contrast, the late viral protein I5L was produced in EVM-infected cells, but was not produced in EVM-infected cells treated with AraC (Fig. 5.3*B*). These results indicated that EVM025 is produced early during infection as a 55kDa protein. F1L is a mitochondrial-localized protein (329, 382), so we investigated whether the anti-F1L reactive 55kDa EVM025 was also localized to the mitochondria during infection. HeLa cells were infected with either VV(Cop) or EVM at an MOI of 3 for 8 hours, and cells were stained with anti-F1L and anti-cytochrome c to label mitochondria. Uninfected cells demonstrated a punctate mitochondrial cytochrome c staining pattern (Fig. 5.3*C*, panels a-c). Cells infected with either VV(Cop) or EVM displayed a punctate anti-F1L staining pattern which co-localized with cytochrome c (Fig. 5.3*C*, panels d-i), indicating that both VV(Cop) and EVM synthesize mitochondrial-localized proteins that can be detected using an anti-F1L antibody.

5.2.3. Generation of an EVMΔcrmAΔ025 virus.

To assess whether EVM025 is required for the EVM-mediated inhibition of apoptosis, we generated an EVM025 knockout virus. A vector was generated encoding short 5' and 3' regions of EVM025 flanking an EGFP cassette under the control of a poxviral promoter (Fig.5.4*A*)(56). This EVM025 knockout vector, pJMT29, was transfected into EVMΔcrmA-infected cells, and recombinant viruses expressing EGFP were selected by fluorescence microscopy as described in Materials and Methods. EVMΔcrmA was used as the background strain to generate a virus that lacked both the caspase-8-inhibitor CrmA as well as EVM025, EVMΔcrmAΔ025. Purified virus lacking EVM025 was verified by PCR analysis and western blotting with anti-F1L. Viral DNA was purified from CV-1 cells infected with EVMΔcrmA or EVMΔcrmAΔ025. PCR from EVM chromosomal template DNA using primers specific for EVM025 generated a product of 1.4kb in size (Fig. 5.4*B*), corresponding to wild type EVM025. PCR analysis from EVMΔcrmAΔ025 DNA generated a product of 1.2kb in size (Fig. 5.4*B*). This

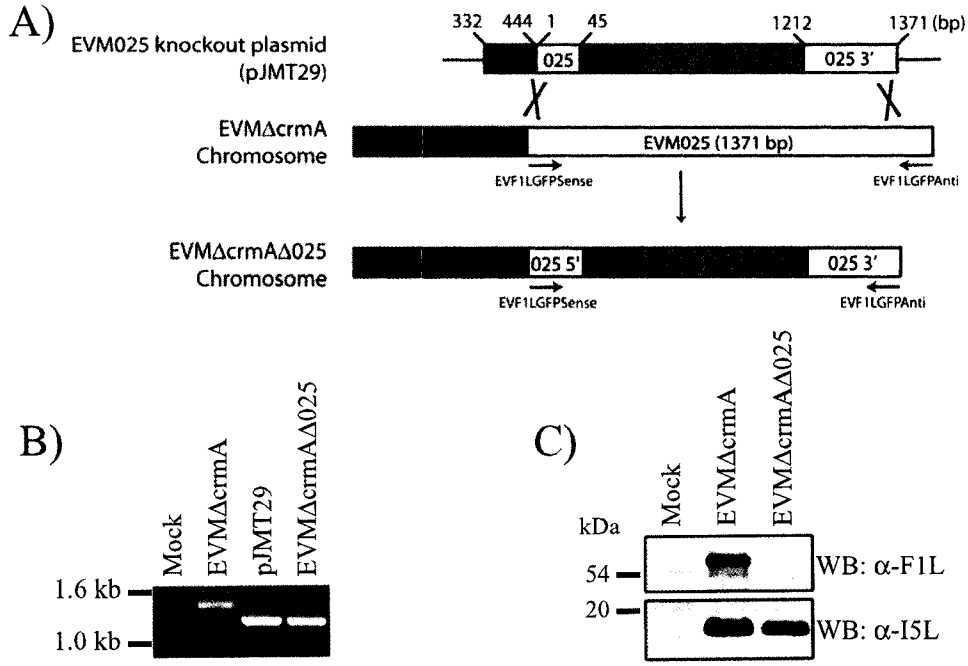

Figure 5.4. Generation of a Δ025 strain of ectromelia virus.
A, Strategy employed for the generation of a Δ025 strain of EVM. An EVM025 knockout vector, pJMT29, which encodes regions of EVM025 flanking an EGFP cassette under the control of a poxviral promoter (pE/L) was transfected into cells infected with EVMΔcrmA. Recombinant viruses were selected by EGFP expression. *B*, Agarose gel electrophoresis of PCR analysis using EVM025-specific primers EVF1LGFPSense and EVF1LGFPAnti. Template DNA was either EVM025ΔcrmA chromosome, EVMΔ025 chromosome, or the EVM025 knockout plasmid, pJMT29. *C*, Cells were infected with either EVMΔcrmA or EVMΔcrmAΔ025 for 16 hours at an MOI of 5, and were western blotted with anti-F1L. Samples were also immunoblotted for a viral late protein, I5L, as a control for virus infection.

corresponds to the expected size of EVM025 disrupted by the EGFP cassette, as PCR using the EVM025 knockout vector (pJMT29) as template also generated a 1.2kb PCR product (Fig. 5.4*B*). Alternatively, CV-1 cells were infected with either EVMΔcrmA or EVMΔcrmAΔ025 for 16 hours, and protein samples were western blotted with an anti-F1L antibody (329). Immunoblotting of EVMΔcrmA lysates revealed a 55kDa protein product which was no longer present in lysates infected with EVMΔcrmAΔ025 (Fig. 5.4*C*). Immunoblotting of either EVMΔcrmA or EVMΔcrmAΔ025-infected lysates with an antibody against the late viral protein I5L detected I5L in both wild type EVMΔcrmA and EVMΔcrmAΔ025-infected cells (Fig. 5.4*C*), as expected. Altogether, these results indicate that EVMΔcrmAΔ025 does not express EVM025, and that EVM025 is synthesized as a 55kDA protein.

5.2.4. EVM025 is required for the inhibition of apoptosis.

To determine whether EVM025 is essential for EVM-mediated inhibition of apoptosis, Jurkat cells were infected with EVMΔcrmA or EVMΔcrmAΔ025 for 12 hours, and treated with staurosporine to induce apoptosis through the mitochondria (27). Cells were harvested at 2, 4, or 6 hours post-treatment and analyzed by western blotting for cleavage of the apoptotic substrate PARP. As expected, uninfected Jurkat cells demonstrated PARP cleavage following staurosporine treatment (Fig. 5.5*A*) (173). Jurkat cells infected with EVMΔcrmA, however, were protected from staurosporine-induced PARP cleavage at all times post treatment (Fig. 5.5*A*). Cells infected with EVMΔcrmAΔ025 were not able to inhibit staurosporine-induced PARP cleavage (Fig. 5.5*A*), indicating that EVM025 is required for the inhibition of staurosporine-mediated apoptosis.

Staurosporine induces apoptosis at the mitochondria, so we assessed the ability of EVMΔcrmAΔ025 to inhibit cytochrome c release from mitochondria. Jurkat cells infected with EVMΔcrmA or EVMΔcrmAΔ025 were treated with staurosporine,

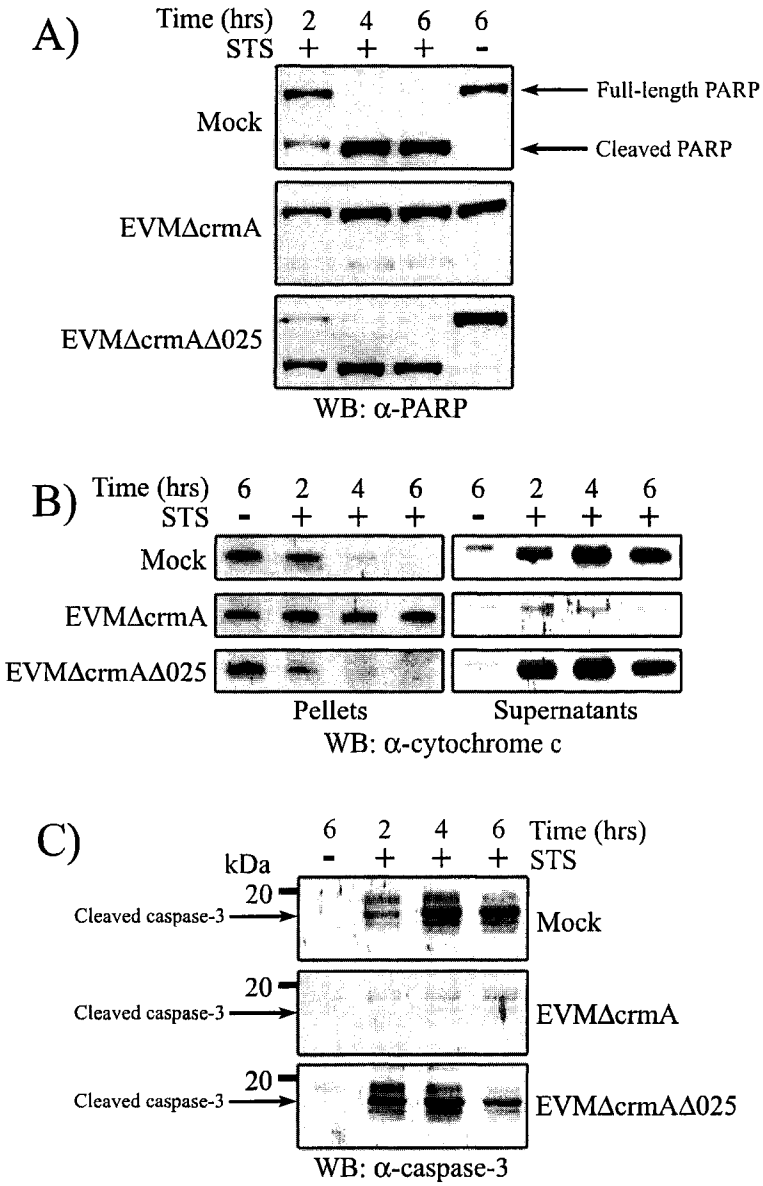

Figure 5.5. Expression of EVM025 is required to inhibit apoptosis.
A, Jurkat cells were infected with either EVMΔcrmA or EVMΔcrmAΔ025 at an MOI of 5 for 8 hours, treated with 1μM staurosporine (STS), and harvested at the indicated times post treatment. Samples were lysed in SDS-PAGE sample buffer containing 8M urea, and analyzed by western blotting with anti-PARP. *B*, Jurkat cells were infected and treated as in (A), and were fractionated at indicated times into pellet fractions (mitochondria), and supernatant fractions (cytosol) as described in the Materials and Methods. Samples were separated by SDS-PAGE and analyzed by western blotting with anti-cytochrome c. *C*, Supernatant fractions isolated in (B) were probed with anti-caspase-3 to detect cleaved active caspase-3 fragments.

fractionated into cytoplasmic or membrane mitochondrial fractions and western blotted with anti-cytochrome c. Uninfected Jurkat cells exhibited a gradual translocation of cytochrome c from the membrane pellet fraction to the supernatant fraction at 2, 4, and 6 hours post-treatment with staurosporine (Fig. 5.5*B*). Cells infected with EVMΔcrmA, however, completely retained cytochrome c in the pellet fraction, even at 6 hours post-treatment with staurosporine (Fig. 5.5*B*). Cells infected with EVMΔcrmAΔ025, however, were unable to inhibit the staurosporine-induced translocation of cytochrome c from the mitochondrial pellet into the supernatant (Fig. 5.5*B*). During apoptosis, procaspase-3 is cleaved into active caspase-3 fragments downstream of the mitochondria (111). Supernatants isolated from the aforementioned cytochrome c release assays were also probed with an anti-caspase-3 antibody (381). Mock-infected Jurkat cells exhibited cleaved active caspase-3 fragments at all time points post-staurosporine treatment (Fig. 5.5*C*). In contrast, cells infected with EVMΔcrmA displayed only minor amounts of cleaved caspase-3 (Fig. 5.5*C*), even at 6 hours post-treatment. Cells infected with EVMΔcrmAΔ025, however, were not able to inhibit staurosporine-induced caspase-3 cleavage (Fig. 5.5*C*), demonstrating that EVM025 is required for the inhibition of the intrinsic apoptotic pathway by ectromelia virus.

5.2.5. The transient expression of N-terminally truncated versions of EVM025 inhibits apoptosis

To assess the ability of EVM025 to inhibit apoptosis in the absence of virus infection, we attempted to clone and express the full-length form of EVM025 as an EGFP-fusion. All attempts to clone the full-length EVM025 open reading frame, however, were unsuccessful. Any plasmids obtained which appeared to contain EVM025 also displayed deletions or insertional elements which would have rendered EVM025 non-functional. As well, attempts to clone only the N-terminal repeat region were similarly unsuccessful, and the largest number of repeats that we have successfully

maintained in any vector in *E. coli.* is three. As a result, we generated EVM025 mutants lacking the N-terminal repeat region to investigate the ability of the C-terminal region of EVM025 to inhibit apoptosis. Although this C-terminus of EVM025 shows amino acid homology to F1L, there are a number of amino acid differences which may affect function. We generated one construct which lacked the entire repeat, EVM025(E255), and a second construct which contained two copies of the 'DNGIVQDI' repeat, EVM025(D237) (Fig. 5.6*A*). Both of these mutants were generated as N-terminal EGFP-fusions for transient expression.

To assess whether EVM025 lacking the N-terminal repeat can inhibit apoptosis in the absence of virus infection, HeLa cells were transfected to express either EGFP, EGFP-F1L, EGFP-EVM025(D237), EGFP-EVM025(E255), or EGFP-F1L(206-226) which localizes to the mitochondria but does not inhibit apoptosis (329). Cells were then treated with either TNFα or αFas for 6 hours, and stained with the mitochondrial-specific dye TMRE which labels healthy mitochondria with an intact membrane potential (228). Cells were analyzed by flow cytometry, and the percentage of EGFP-positive cells which displayed a loss of the mitochondrial membrane potential were calculated (Fig. 5.6*B* and *C*). Expression of EGFP or EGFP-F1L(206-226) did not inhibit TNFα or αFas-induced loss of the inner mitochondrial membrane potential (Fig. 5.6*B* and *C*). Expression of EGFP-F1L, on the other hand, inhibited mitochondrial membrane depolarization induced by both TNFα and αFas (Fig. 5.6*B* and *C*), as shown previously (329, 382). Expression of both EVM025(E255) and EVM025(D237) also inhibited TNFα- and αFas-induced apoptosis, similar to F1L (Fig. 5.6*B* and *C*). This demonstrated that EVM025 is a functional anti-apoptotic protein independent of other viral proteins, and that the N-terminal repeat region is not essential for anti-apoptotic activity *in vitro*.

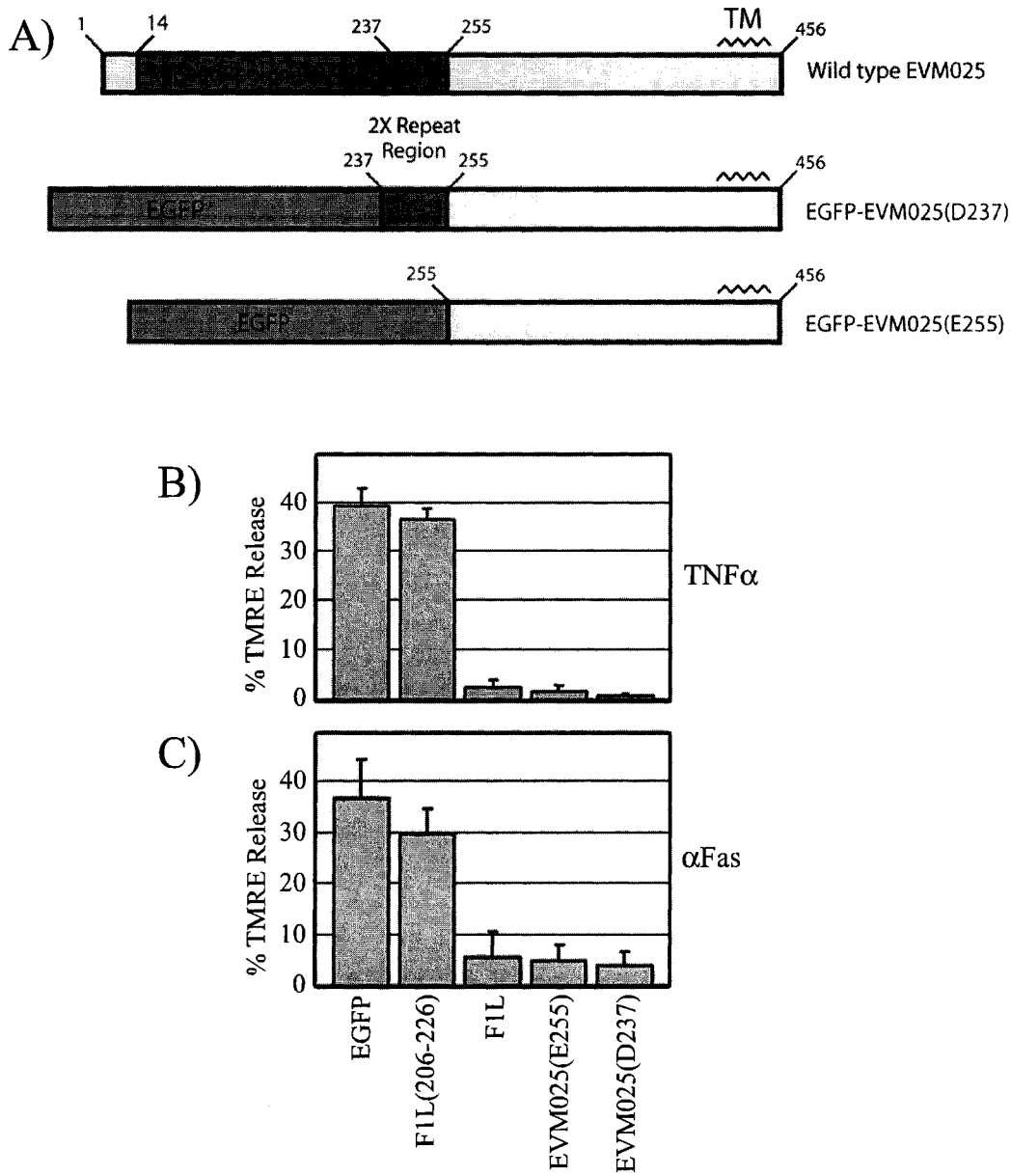

Figure 5.6. Transient expression of EVM025 truncation mutants inhibit apoptosis.
A, Schematic representation of EGFP-EVM025(E255) and EGFP-EVM025(D237). *B-C*, HeLa cells were transfected with 4μg of either pEGFP, pEGFP-F1L, pEGFP-F1L(206-226), pEGFP-EVM025(D237) (pJMT17) or pEGFP-EVM025(E255) (pJF2) for 16 hours. Cells were then treated with either TNFα (A) or αFas (B) in combination with cycloheximide for 6 hours, stained with TMRE, and analyzed by flow cytometry. TM, transmembrane domain.

5.2.6. Localization of EVM025

Staining of EVM-infected cells with anti-F1L revealed a mitochondrial staining pattern that co-localized with cytochrome c (Fig. 5.3*C*) (329), suggesting that endogenously expressed EVM025 localizes to the mitochondria (329). To verify whether EVM025(E255) and EVM025(D237) also localized to mitochondria, we expressed either EGFP, EGFP-F1L, EGFP-EVM025(E255), or EGFP-EVM025(D237) in HeLa cells, and co-stained with anti-cytochrome c to label mitochondria. As expected, EGFP displayed a diffuse cytoplasmic staining pattern that did not co-localize with cytochrome c (Fig. 5.7, panels a-c). EGFP-F1L demonstrated a punctate pattern which co-localized with cytochrome c (Fig. 5.7, panels d-f). Expression of both EGFP-EVM025(E255) and EGFP-EVM025(D237) also displayed a punctate staining pattern which overlapped with anti-cytochrome c (Fig. 5.7, panels g-l). Indeed, EVM025 is predicted to possess a C-terminal hydrophobic domain similar to the C-terminal hydrophobic domain from F1L (Fig. 5.1) (329). These results indicate that EVM025(E255) and EVM025(D237) also localize to the mitochondria, supporting the previous observation that full-length EVM025 localizes to the mitochondria (Fig. 5.3*C*) (329).

To examine the localization of the EVM025 truncation mutants lacking the N-terminal repeat region during virus infection, we generated two FLAG-tagged versions of EVM025, EVM025(E255) and EVM025(D231), which were placed under the control of a poxviral promoter (56). FLAG-EVM025(E255) does not contain any copies of the N-terminal repeat, while FLAG-EVM025(D231) was generated to contain three copies of the eight amino acid repeat. HeLa cells were infected with wild type ectromelia virus and transfected for 12 hours with either pSC66-FLAG-F1L, pJMT48 which encodes FLAG-EVM025(E255), or pJMT44 which encodes FLAG-EVM025(D231). Cells were fixed and sequentially stained with anti-cytochrome c, anti-mouse Alexa546, followed by anti-FLAG-FITC. Staining of untransfected cells displayed no FLAG staining, but did exhibit punctate mitochondrial cytochrome c staining (Fig. 5.8*A*, panels a-c). This indicated that

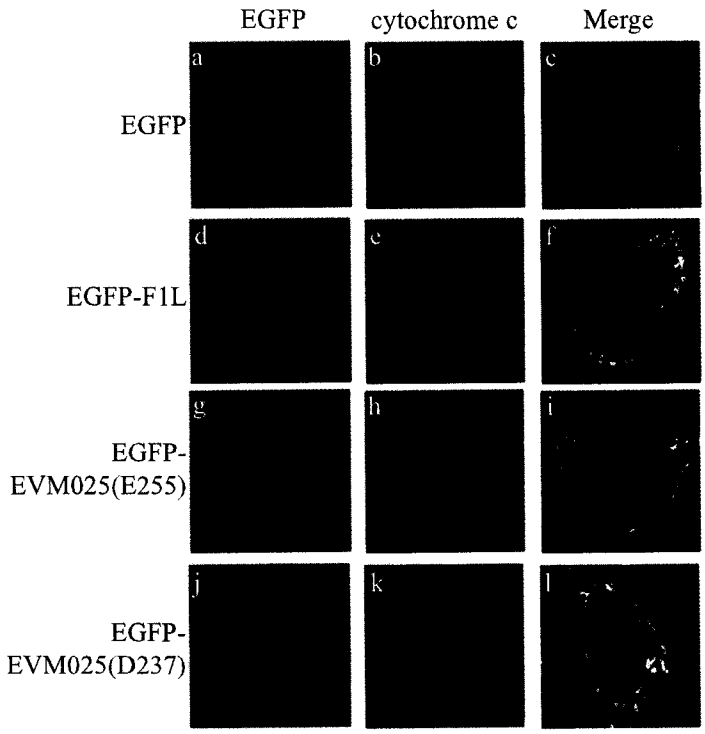

Figure 5.7. Localization of transiently expressed EVM025 truncation mutants.
A, HeLa cells were transfected with 2μg of either pEGFP, pEGFP-F1L, pJF2 to express EGFP-EVM025(E255),or pJMT17 to express EGFP-EVM025(D237), for 16 hours. Cells were fixed, stained with anti-cytochrome c followed by anti-mouse Alexa546 secondary antiobdy, and visualized using confocal microscopy.

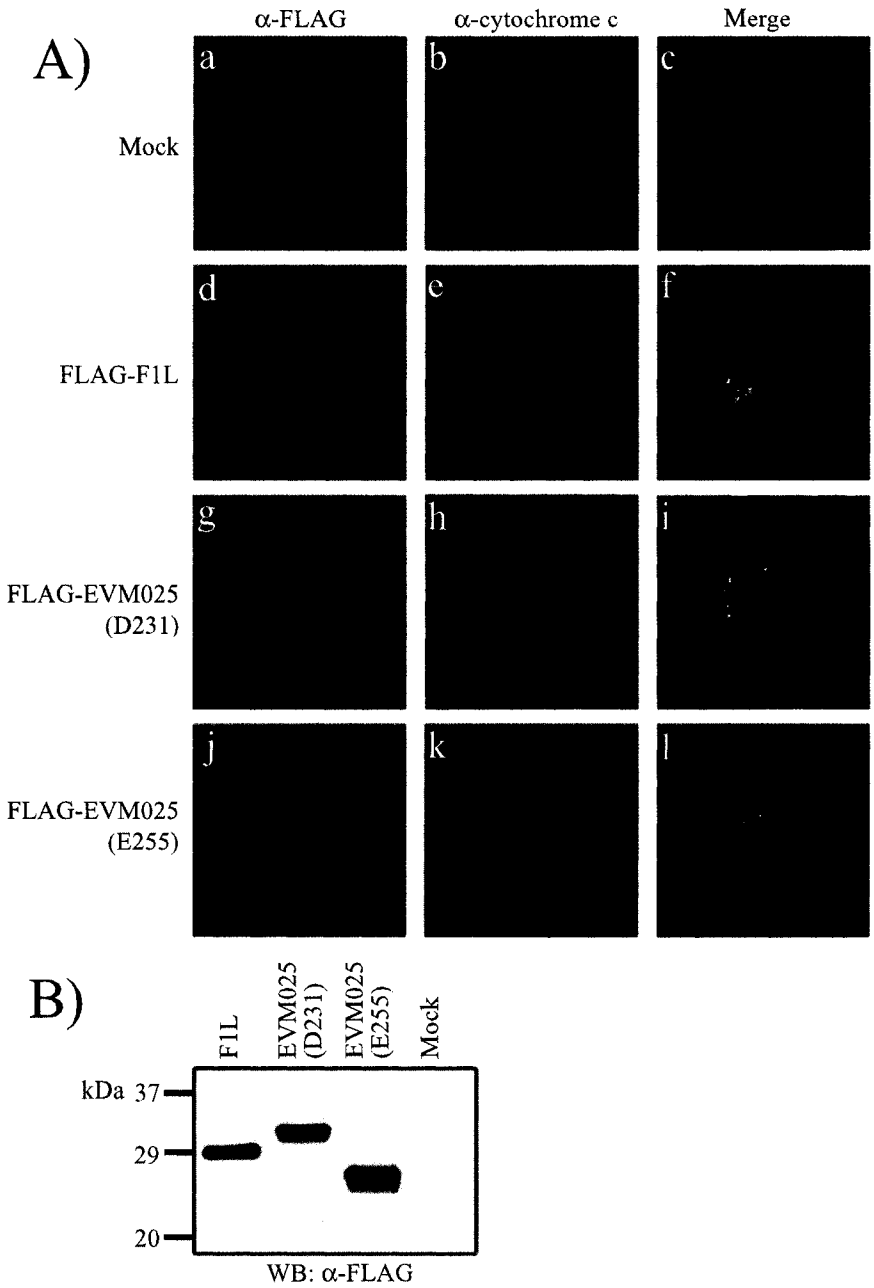

Figure 5.8. EVM025 localizes to the mitochondria during ectromelia infection.
A, HeLa cells were infected with EVM at an MOI of 1, and were transfected with either pSC66-FLAG-F1L, pJMT44 to express FLAG-EVM025(D231), or pJMT48 to express FLAG-EVM025(E255). At 16 hours post transfection, cells were fixed and stained with anti-cytchrome c, co-stained with anti-mouse-Alexa546, followed by staining with anti-FLAG-FITC, and were visualized using confocal microscopy. *B*, Cells were infected as in (A) and were harvested in SDS-PAGE sample buffer and immunoblotted with anti-FLAG(M2).

staining cells sequentially with anti-cytochrome c followed by anti-FLAG-FITC did not result in non-specific FLAG staining. Cells expressing FLAG-F1L showed a punctate anti-FLAG staining pattern for FLAG-F1L, which co-localized with mitochondrial cytochrome c (Fig. 5.8*A*, panels d-f). Expression of either FLAG-EVM025(D231) (Fig. 5.8*A*, panels g-i) or FLAG-EVM025(E255) (Fig. 5.8*A*, panels j-l), both demonstrated a punctate FLAG staining pattern which co-localized with cytochrome c (Fig. 5.8*A*). Alternatively, duplicate cell lysates of each infection/transfection were also harvested at 12 hours post-infection and western blotted with anti-FLAG. As shown in Fig. 5.8*B*, FLAG-F1L, FLAG-EVM025(E255) and FLAG-EVM025(D231) were all expressed at their predicted sizes (Fig. 5.8*B*). These results indicate that both EVM025(E255) and EVM025(D231) localize to the mitochondria during infection.

5.2.7. EVM025 inhibits Bax activation

We have previously demonstrated that vaccinia virus F1L inhibits the activation of the pro-apoptotic proteins Bak and Bax by two different mechanisms. F1L directly interacts with Bak to inhibit Bak activation and oligomerization (265, 379), while F1L inhibits Bax upstream of Bax activation in the absence of a direct interaction (350). Considering that EVM025 and F1L display a number of amino acid differences, we investigated whether EVM025 also modulates Bax and Bak. We first examined the ability of EVM025 to inhibit Bax activation by performing immunoprecipitations using anti-Bax(6A7) which specifically detects activated Bax (157, 158). HeLa cells were infected with either EVMΔcrmA or EVMΔcrmAΔ025 for 8 hours, treated with UV-light to induce apoptosis, and immunoprecipitated with anti-Bax (6A7). As expected, uninfected cells only exhibited Bax activation following treatment with UV-light (Fig. 5.9*A*). Cells infected with EVMΔcrmA were notably inhibited from UV-induced Bax-activation (Fig. 5.9*A*), while cells infected with EVMΔcrmAΔ025 were not (Fig. 5.9*A*). In fact, cells infected with EVMΔcrmAΔ025 in the absence of UV-light exhibited a small

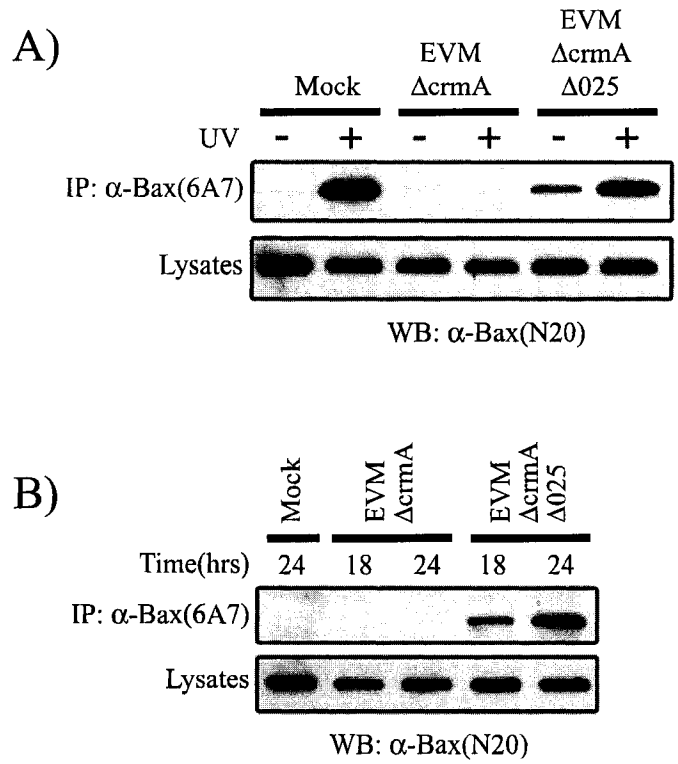

Figure 5.9. EVM025 is required for EVM-mediated inhibition of Bax N-terminal activation. *A*, HeLa cells were infected with either EVMΔcrmA or EVMΔcrmAΔ025 at an MOI of 5 for 12 hours, and treated with UV-light. Three hours after UV-stimulation, cells were lysed in 2% CHAPS lysis buffer and immunoprecipitated with anti-Bax (6A7). Immunoprecipitates and lysates were analyzed with anti-Bax(N20). B, HeLa cells were infected with EVMΔcrmA or EVMΔcrmAΔ025 for the indicated times, and immunoprecipitations were performed and analyzed as in (A).

amount of Bax activation suggesting that, similar to infection with VV(Cop)ΔF1L, infection with EVMΔcrmAΔ025 also induces apoptosis and Bax activation (Fig. 5.9*A*). To assess EVM-induced Bax activation, HeLa cells were infected with either EVMΔcrmA or EVMΔcrmAΔ025 for 18 or 24 hours, and 2% CHAPS lysates were immunoprecipitated with anti-Bax(6A7). Infection with EVMΔcrmAΔ025, but not with EVMΔcrmA, induced significant Bax activation at both 18 and 24 hours post-infection (Fig.5.9*B*), similar to our previous observations with VV(Cop)ΔF1L (350). These results suggest that EVM025 is capable of inhibiting Bax activation induced by both virus infection and intrinsic pro-apoptotic stimuli.

5.2.8. EVM025 Interacts with Bak, but not Bax

F1L has been shown to interact with Bak as a mechanism for the inhibition of Bak (265, 379). In contrast, F1L inhibits Bax activation without directly interacting with Bax (350). The predicted amino acid sequence of EVM025 displays a number of differences compared to F1L, so it is possible that EVM025 may use a different mechanism to inhibit apoptosis. Indeed, mutation of a single residue in F1L, methionine 67, was shown to abolish binding to Bak (265). To determine whether EVM025 can interact with Bak or Bax, we generated a recombinant vaccinia virus expressing FLAG-EVM025(E255). This recombinant virus was generated using VV(Cop)ΔF1L as the background virus, since this virus does not produce endogenous F1L (379). A plasmid expressing FLAG-EVM025(E255) from a poxviral promoter, pJMT48, was transfected into VV(Cop)ΔF1L-infected cells, and recombinant viruses were plaque purified based on expression of *lacZ* which serves as a selectable marker for recombination (56, 215). Purified VV(Cop)ΔF1L:FLAG-EVM025(E255) was isolated and used to determine if EVM025(E255) interacts with Bak or Bax during infection. HeLa cells were infected with either VV:FLAG-F1L or VV(Cop)ΔF1L:FLAG-EVM025(E255) for 12 hours, lysed in 2% CHAPS lysis buffer or 1% Triton-X-100, and immunoprecipitated with anti-

FLAG. Lysates and immunoprecipitates were probed with anti-FLAG(M2), anti-Bak(NT), or anti-Bax (N20). FLAG-F1L and FLAG-EVM025(E255) were immunoprecipitated with anti-FLAG (Fig. 5.10*A*), and substantial amounts of endogenous Bak were also co-precipitated in both FLAG-F1L and FLAG-EVM025(E255) samples (Fig. 5.10*A*) (350, 379). Immunoprecipitation of FLAG-EVM025(E255), however, did not co-precipitate any endogenous Bax (Fig. 5.10*A*), similar to observations with FLAG-F1L. The detergent CHAPS maintains the native conformation of the Bcl-2 family member Bax, while Triton-X-100 artificially induces a conformational change in Bax reminiscent of Bax activation (157, 158). Similar to previous results with F1L, lysis in Triton-X-100 induced an interaction between Bax and both FLAG-F1L and FLAG-EVM025(E255), suggesting that EVM025(E255) can also interact with artificially activated Bax. Despite the amino acid differences between F1L and EVM025(E255), these two proteins appear to interact constitutively with Bak, but only interact with activated Bax.

5.2.9. EVM025(E255) complements the anti-apoptotic deficiency in VV(Cop)ΔF1L

Infection with either VV(Cop)ΔF1L or EVMΔcrmAΔ025 results in virus-induced apoptosis (Fig 5.5, 5.9*B*) (379, 382). To assess whether EVM025(E255) could complement the anti-apoptotic defect present in VV(Cop)ΔF1L, cells were infected with VV(Cop), VV(Cop)ΔF1L, or the recombinant VV(Cop)ΔF1L:FLAG-EVM025(E255) for 18 or 24 hours. Cell lysates were then immunoprecipitated for active Bax and western blotted with anti-Bax(N20). As expected, VV(Cop)ΔF1L induced Bax activation at both time points, while VV(Cop) only induced a small amount of Bax activation (Fig. 5.10*B*). Infection with VV(Cop)ΔF1L:FLAG-EVM025(E255), however, did not induce Bax activation (Fig. 5.10*B*), indicating that expression of EVM025(E255) is capable of inhibiting apoptosis induced by infection with VV(Cop)ΔF1L. FLAG-EVM025(E255) is transcribed from a strong poxviral promoter, and EVM025(E255) protein is likely

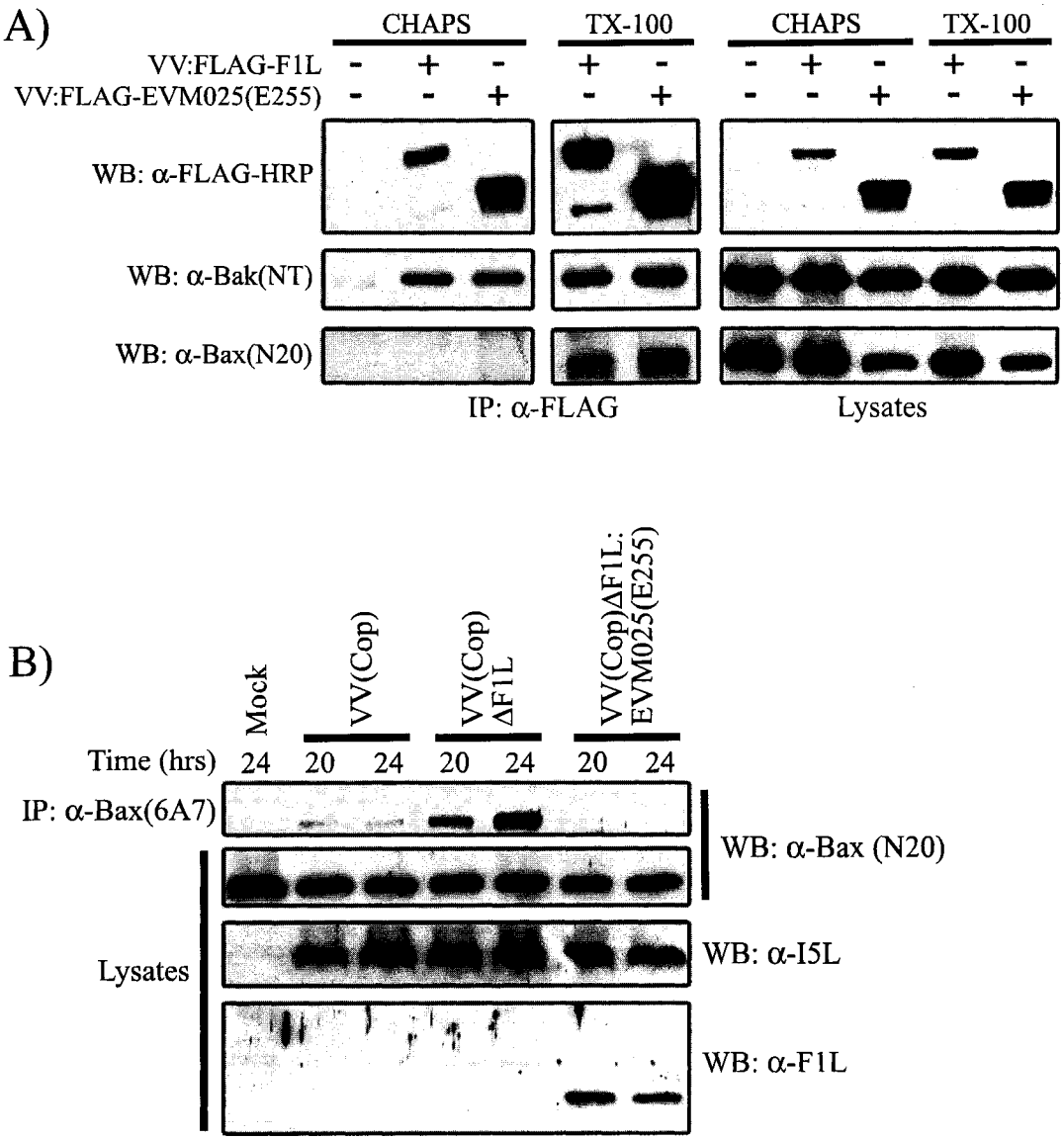

Figure 5.10. EVM025(E255) interacts with Bak. *A*, HeLa cells were infected with either VV:FLAG-F1L or VV(Cop)ΔF1L:FLAG-EVM025(E255) for 12 hours, lysed in either 2% CHAPS or 1% Triton-X-100 (TX-100) lysis buffer, and immunoprecipitated with anti-FLAG(M20. Immune complexes were precipitated with protein A beads and immunoblotted with anti-FLAG-HRP, anti-Bak(NT), or anti-Bax(N20). *B*, EVM025(E255) complements the anti-apoptotic deficiency of VV(Cop)ΔF1L. HeLa cells were infected with either VV(Cop), VV(Cop)ΔF1L, or VV(Cop)ΔF1L:FLAG-EVM025(E255) for 20 or 24 hours. Cells were lysed in 2% CHAPS lysis buffer and immunoprecipitated with anti-Bax(6A7). Immunoprecipitates were probed with anti-Bax(N20), and lysates were probed with anti-Bax(N20), anti-I5L, or anti-F1L.

synthesized at higher levels that endogenous F1L from VV(Cop). In support of this, lysates from VV(Cop)ΔF1L:FLAG-EVM025(E255)-infected cells, but not from VV(Cop)-infected cells, demonstrated the presence of a reactive protein when blotted with anti-F1L (Fig. 5.10*B*), corresponding to the expected size of FLAG-EVM025(E255). We routinely see a lack of endogenous F1L from VV(Cop)-infected lysates, and this may be due to the ubiquitination and degradation of F1L (Appendix B.2) (265). Western blotting with anti-I5L showed that all virus-infected lysates were infected and produced the late viral protein I5L (Fig. 5.10*B*). These results indicate that EVM025(E255) can complement the anti-apoptotic deficiency of VV(Cop)ΔF1L and that the N-terminal repeat region of EVM025 is unnecessary for the inhibition of VV-induced apoptosis.

5.3 Discussion

The vaccinia virus protein F1L is a mitochondrial-localized inhibitor of apoptosis that shares no homology with any other known regulators of apoptosis (379, 382). All of the orthopoxviral genomes sequenced to date, however, encode a predicted orthologue of F1L (www.poxvirus.org). As ectromelia virus is a natural pathogen of mice and causes a high rate of mortality in a variety of laboratory strains of mice, we hypothesized that the predicted orthologue of F1L from ectromelia, EVM025, would encode a functional anti-apoptotic protein. Here we show that ectromelia virus infection inhibits cytochrome c release and apoptosis (Fig. 5.2). Deletion of EVM025 from the genome of ectromelia severely compromised the ability of ectromelia virus infection to inhibit apoptosis induced by staurosporine (Fig. 5.5). Deletion of EVM025 also eliminated the ability of ectromelia virus to inhibit the activation of the pro-apoptotic protein Bax (Fig. 5.9), indicating that EVM025 is a potent anti-apoptotic protein produced during ectromelia virus infection.

The C-terminal half of EVM025 shares greater than 90% amino acid identity to F1L (Fig. 5.1). Near the C-terminus is the predicted transmembrane tail, which was

shown for F1L to be necessary and sufficient for mitochondrial localization (329). Mis-localization of F1L virtually eliminated the ability of F1L to inhibit apoptosis induced by TNFα or αFas (329), indicating the importance of mitochondrial localization. Expression of truncated versions of EVM025 lacking the N-terminal repeat exhibited mitochondrial localization in the presence and absence of virus infection (Fig. 5.7, 5.8), suggesting that the conserved C-terminal transmembrane tail present in EVM025 is functional.

Similar to F1L, EVM025(E255) has the capacity to interact with the pro-apoptotic protein Bak (Fig. 5.10). Although EVM025 also inhibits Bax activation (Fig. 5.9), we failed to see an interaction between EVM025(E255) and Bax in the presence of CHAPS (Fig 5.10). This parallels our previous observations with F1L (350), and suggests that EVM025 likely inhibits Bax activation upstream of Bax. While F1L does not interact with Bax under normal conditions, F1L does bind to Bax in the presence of the detergent Triton-X-100 (350), which reveals the BH3-domain of Bax. Similar to F1L, EVM025(E255) also interacts with Bax in the presence of Triton-X-100 (Fig. 5.10*A*), suggesting that EVM025 may also have the capacity to interact with BH3-domains. F1L interacts with the BH3-only protein BimL as a putative mechanism for inhibiting Bax activation (350). Our lab is currently investigating whether EVM025 also has the ability to interact with BimL and other BH3-only proteins.

Although EVM025 and F1L share a high degree of amino acid identity at the C-terminus, there are a number of amino acid changes between the two proteins (Fig. 5.1). At present, we have no information regarding the significance of any of these changes, although mutation of single amino acids in Bcl-2 family proteins can ablate anti- or pro-apoptotic function (302, 375, 376). Similarly, mutation of Met 67 to Pro of F1L eliminated the ability of F1L to interact with Bak and inhibit apoptosis (265). In addition, EVM025 is predicted to encode a large N-terminal repeat extension (Fig. 5.1), and EVM025 appears as a full length 55kDa protein by western blotting with an antibody

specific for F1L (Fig. 5.3, 5.4). Deletion of EVM025 from the genome eliminates the ability of EVM to inhibit apoptosis (Fig. 5.5), suggesting that full-length EVM025 protein is capable of inhibiting apoptosis. The function of the N-terminal repeat region is not known, although this repeat is not required for the inhibition of apoptosis *in vitro* (Fig. 5.6*B* and *C*). Removal of the entire repeat region had no significant effect on the anti-apoptotic activity of exogenously expressed EVM025 (Fig. 5.6*B* and *C*). As well, a version of EVM025 containing two copies of the 8 amino acid repeat, EVM025(D237), did not show any obvious enhanced anti-apoptotic ability over a truncation completely lacking the repeat region (Fig. 5.6). Whether the N-terminus of EVM025 has any added or specific function awaits further work in both murine cell lines as well as *in vivo* in a mouse infection model.

Ectromelia virus causes a lethal disease in many strains of mice, and as such makes an excellent model in which to study host:pathogen interactions. It will be of interest to determine whether our strain of EVM lacking EVM025 exhibits a decrease in pathogenesis *in vivo* in infected mice. Removal of other anti-apoptotic proteins from viral pathogens often results in a dramatic loss of viral pathogenicity, as myxoma virus lacking the anti-apoptotic M11L is completely attenuated in European rabbits (128, 254). It will also be of interest to examine whether the N-terminal repeat sequence has significance *in vivo* in a mouse model. F1L orthologues from multiple orthopoxviruses, such as cowpox, camelpox, and variola virus, are predicted to contain variable N-terminal extensions. It is interesting to speculate whether these extensions confer any secondary functions *in vivo*. We are currently generating ecombinant viruses which express truncated forms of EVM025 in place of full length EVM025 which will greatly aid in understanding the role of EVM025 and the N-terminus *in vivo*.

CHAPTER 6: Discussion

The inhibition of Bax activation by F1L

Apoptosis at the mitochondria is governed by two pro-apoptotic gatekeeper proteins, Bak and Bax (91, 385), as cells deficient in Bak and Bax are unable to release cytochrome c (91, 385). Our lab previously identified vaccinia virus F1L as a potent anti-apoptotic protein that localizes to the outer mitochondrial membrane to inhibit cytochrome c release (329, 379, 382). While F1L displays no obvious homology to cellular anti-apoptotic Bcl-2 family proteins, we later showed that F1L inhibits Bak activation and Bak oligomerization (265, 379). As a mechanism for the inhibition of Bak, F1L constitutively interacts with Bak in the absence of a pro-apoptotic stimulus (265, 379). We have shown that even following an apoptotic stimulus, F1L still interacts with Bak (Fig. 3.12), which appears to differ somewhat from cellular Bcl-2 family members. Bcl-2 has been shown to interact with the "open conformer" of Bak following induction with the BH3-only protein tBid (284), while Mcl-1 interacts with Bak prior to an apoptotic stimulus (81, 391). Following DNA-damage, Mcl-1 is displaced from Bak allowing Bak to undergo a conformational change resulting in cytochrome c release (81, 248). Our data suggests that F1L is able to interact with Bak prior to apoptosis, and does not appear to be displaced from this complex following an apoptotic stimulus (Fig. 3.12)(350). The exact mechanism of F1L interaction with Bak remains to be characterized, although a recent report suggests that F1L interacts with the BH3 domain of Bak (265). How F1L accomplishes this in the absence of a conformational change in Bak is currently unknown.

Both Bak and Bax are capable of inducing cytochrome c release, so it is not surprising that several viral proteins are able to inhibit both Bak and Bax (24, 39, 82, 148). While F1L can inhibit Bak activation, it remained unknown whether F1L could also inhibit Bax activation. Our data shows that F1L expression inhibits the N-terminal activation, oligomerization, and insertion of Bax into the outer mitochondrial membrane,

and that F1L can inhibit Bax activation independently of Bak (Chapter 3) (350). Although F1L interacts with Bak, we observed that F1L does not naturally interact with Bax, even following an apoptotic stimulus (Fig. 3.12) (350), suggesting that F1L interferes with Bax activity somewhere upstream. Intriguingly, we were able to artificially induce an interaction between Bax and F1L by using the detergent Triton-X-100 (Fig. 3.13). Triton-X-100 induces a conformational change in Bax that results in exposure of the BH3 domain and Bax oligomerization, similar to changes in Bax seen during apoptosis (12, 93, 126, 157, 158). Indeed, it has recently been shown that F1L can bind to BH3-peptides from Bak, Bax, and Bim (113), so we hypothesize that F1L may interact with the newly Triton-X-100-exposed BH3 domain of Bax. The affinity of F1L for the BH3 domain of Bax, however, is ten-fold lower than the affinity of F1L for the Bim BH3 domain (113), suggesting that F1L may show preferences for particular BH3 domains *in vivo*.

Although F1L interacts with the activated form Bax in Triton-X-100, we observed that F1L expression inhibited Bax activation during apoptosis in the absence of a direct interaction (Chapter 3) (350). It is therefore interesting to speculate whether F1L can directly inhibit Bax that is already present in an activated form. Although F1L appears to have the capacity to interact with activated Bax, this does not mean F1L can inhibit activated Bax. Future work would be required to investigate whether F1L could inhibit cytochrome c release or pore formation induced by the addition of recombinant oligomeric Bax or constitutively active Bax (*i.e.* BaxΔ184) (11, 244). If F1L inhibits activated Bax, this might function as a "back-up" mechanism to inhibit Bax activity and cytochrome c release. Alternatively, F1L may not be able to inhibit apoptosis induced by Bax, particularly if the primary function of F1L is to specifically inhibit the pro-apoptotic effects of BH3-only proteins.

Bax activation

Following an apoptotic stimulus, Bax undergoes at least one conformational change that reveals a C-terminal mitochondrial targeting domain, an N-terminal domain, the BH3 domain (126, 133, 156, 157). In addition, Bax targets to the mitochondria and inserts as a high molecular weight oligomer (11, 12, 126, 133, 347, 393). The mechanisms which control these events, however, are still controversial. One theory proposes that BH3-only proteins, specifically Bid, Bim, and PUMA, can directly interact with Bax to induce Bax activation (187, 194). This "direct activation" model has been supported by several biochemical studies (52, 65, 147, 187, 188, 194, 219, 353, 371). The "de-repressor" model, on the other hand, suggests that BH3-only proteins specifically repress Bcl-2-like anti-apoptotic proteins, thereby allowing Bak and Bax to become activated (54, 61, 88, 194, 392). Indeed, a recent report has indicated that no direct interaction was seen between Bax and any of the BH3-only proteins examined (392), although it remains possible that a "hit-and-run" event may govern BH3-mediated activation of Bak and Bax. If BH3-only proteins do not directly activate Bax, then one must question what exactly triggers Bax for activation? Considering that Bax is a naturally cytosolic protein that does not complex with anti-apoptotic Bcl-2 family members prior to apoptosis (157), the derepressor model does not completely explain the steps of Bax activation.

Multiple viral proteins inhibit Bax activation through different mechanisms (Fig. 6.1). Myxoma virus M11L is a mitochondrial-localized inhibitor of apoptosis that interacts with Bak (373), and has also been reported to recruit and interact with Bax at the mitochondria (332). The adenovirus protein E1B 19K interacts with the BH3-domain of the conformationally active form of Bax (143, 145, 257, 338) (Fig. 6.1), yet Bax oligomerization and insertion into the mitochondria are inhibited by E1B 19K expression (337). vMIA, encoded by human cytomegalovirus, inhibits cytochrome c release despite recruiting oligomerized Bax to the mitochondrial membrane (14, 124, 263). Unlike these

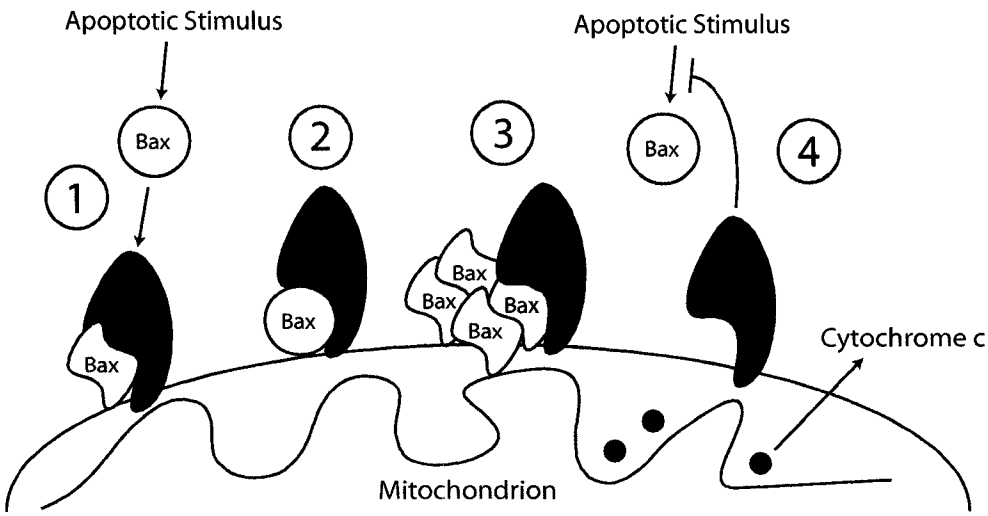

Figure 6.1. Mechanisms used by E1B 19K,M11L, vMIA, and F1L to inhibit Bax.
A, E1B 19K from Adenovirus interacts with the conformationally activated form of Bax following induction with an apoptotic stimulus (1). M11L interacts with Bax at the mitochondria following virus infection to prevent Bax activation (2). vMIA from human cytomegalovirus interacts with oligomerized Bax at the mitochondria (3). F1L from vaccinia virus inhibits Bax upstream of Bax activation (4).

other viral inhibitors, F1L, however, does not interact with Bax, suggesting F1L functions upstream of Bax activation (Fig 6.1) (350). By understanding the mechanisms that each of these viral proteins use to inhibit Bax, we may be able to better understand the actual signals that stimulate Bax activation. The steps regulating Bax activation are complex and controversial, so the use of viral proteins that appear to block Bax activation at various steps may aid in our understanding of the complex pathway leading to Bax activation and cytochrome c release.

In addition to viral proteins, a number of cellular proteins reportedly regulate and induce Bax activation, such as Map-1, Bif-1, and p53 (67, 68, 291, 344, 345, 359, 403). It has been reported that Map-1 overexpression, for instance, can induce cytochrome c release (344). Bif-1 (Bax-interacting factor-1) is believed to be an activator of Bak/Bax, as loss of Bif-1 interferes with Bak and Bax activation and apoptosis (343). Bif-1 was seen to interact with Bax at the mitochondria following an apoptotic stimulus but preceding Bax activation (343). p53 also activates Bax in the absence of any other Bcl-2 family proteins (67), and can displace BH3-only proteins from Bcl-x_L by interacting with Bcl-x_L (67). We do not know whether F1L can inhibit apoptosis mediated by any of these pro-apoptotic Bax regulators. It is also unknown how these proteins actually induce Bax activation. Examining whether viral proteins such as F1L can inhibit apoptosis mediated by these proteins may also aid in understanding how Bax activation is regulated.

F1L and BH3-only proteins

F1L binds constitutively to Bak, but only interacts with artificially activated Bax in Triton-X-100 (Fig. 3.13) (350). As F1L is able to potently inhibit Bax activation, we hypothesized that F1L functions upstream by inhibiting BH3-only protein activity (350). Indeed, a recent report indicated that F1L could interact with BH3 peptides from Bak, Bax, and the BH3-only protein BimL (113). We observed that F1L interacts with and inhibits apoptosis induced by the BH3-only protein BimL (Chapter 4) (350). Indeed,

ectopic BimL was seen to dramatically localize to the mitochondrial membrane in both the presence and absence of F1L (Fig. 4.7*A*). It is possible that F1L may act as a "sink" by sequestering available BH3-only proteins such as BimL at the mitochondria, thereby quenching the pro-apoptotic activity of BimL.

In addition to inhibiting apoptosis mediated by BimL, F1L expression inhibits mitochondrial permeability transition induced by the overexpression of the BH3-only proteins Bid and Bmf (Fig. 4.1), and recent work in our lab has shown that F1L expression also inhibits permeability transition induced by Bik and Puma (S. Campbell, K. Veugelers, M. Barry, unpublished results). We have also shown that the treatment of mitochondria with purified tBid induces Bax activation and cytochrome c release that is inhibited by F1L expression (Fig. 3.9)(350). Whether F1L has the capacity to interact with Bid or any other BH3-only proteins (*i.e.* Bmf, Bik, Puma) remains to be determined. It is of note that the BH3-domain from Bim is quite exposed and accessible compared to other BH3-only proteins (206).

We believe that the interaction between F1L and Bim is significant, as $Bim^{-/-}$ BMKs infected with VV(Cop)ΔF1L undergo apoptosis at a slower rate than wild type BMKs (Fig. 4.9) (350), thereby implicating Bim in the initiation of VV-induced apoptosis. In fact, infection with VV(Cop)ΔF1L induces apoptosis in both WT and $Bim^{-/-}$ BMKs, indicating that Bim is also not absolutely essential for VV-induced apoptosis (Fig. 4.9) (350). Infection with VV(Cop), however, was able to inhibit VV-induced apoptosis in both cell lines (Fig. 4.9) (350), demonstrating that F1L can inhibit VV-induced apoptosis in both the presence and absence Bim. As apoptotic activators other than Bim appear to be induced following VV-infection, F1L also appears capable of inhibiting these unknown pro-apoptotic signals. The identity of other BH3-only proteins activated during VV-infection is the subject of current research in our lab.

To date, neither vMIA nor M11L have been shown to interact with BH3-only proteins, and E1B 19K has only been shown to interact with Nbk/Bik (145). E1B 19K

does not interact with BimL, and intriguingly, E1B 19K expression does not inhibit BimL-induced apoptosis (250), despite interacting with and inhibiting both Bak and Bax. How Bim is able to circumvent the ability of E1B 19K to inhibit Bak and Bax activation is unknown. These results with E1B 19K differ from our observations with F1L, suggesting that these two viral proteins use different mechanisms to inhibit apoptosis. Adenovirus infection induces p53-dependent apoptosis and Bax activation which is blocked by E1B19K expression (90, 144, 286, 333). How vaccinia virus triggers apoptosis remains unknown, but it is possible that adenoviruses and poxviruses induce apoptosis via different BH3-only proteins. As a result, these viruses may have acquired mechanisms to block specific pro-apoptotic signals induced by virus infection or by the immune system.

Although we have shown that F1L and BimL co-precipitate (Fig. 4.7), it remains to be seen whether F1L interacts directly or indirectly with BimL. Mcl-1, an anti-apoptotic Bcl-2 family member that interacts with Bim, reportedly sequesters Bim in an inactive complex until apoptosis is initiated (140, 141). Following DNA damage, Mcl-1 levels decrease dramatically due to the loss of *de novo* synthesis of Mcl-1 and proteasomal degradation of Mcl-1, resulting the release of Bim and Bak, leading to apoptosis (81, 248). Mcl-1 does not appear to be reduced during infection with VV, suggesting that F1L may stabilize an Mcl-1:Bim complex at the mitochondria (S. Campbell and M. Barry, unpublished results). Alternatively, it is possible that F1L displaces Mcl-1 from Bim, essentially making Mcl-1 dispensable during virus infection. Whether F1L interacts with Mcl-1 remains to be seen, although initial work suggested that F1L and Mcl-1 do not co-elute from infected cells (379). It would be of interest to determine whether F1L directly interacts with BimL, or whether cellular intermediates such as Mcl-1 are required to facilitate the formation of a F1L:BimL complex.

Structure of viral inhibitors of apoptosis

F1L lacks obvious amino acid similarity to Bcl-2 family members, but F1L appears to be functionally similar to Bcl-2 (Chapter 3) (231, 240, 350, 379, 398). It is interesting to speculate that viral proteins such as F1L and M11L, despite sharing no significant amino acid similarity, may display structural similarities to Bcl-2 family proteins. The Bcl-2 family itself is largely related by the presence of a series of anti-parallel alpha-helices and conserved BH domains (Fig. 1.5). It has been suggested that both F1L and M11L possess one or more BH domains, although these regions contain low amino acid identity with BH domains from Bcl-2 family members (265, 373). In collaboration with Dr. B. Hazes, we have aligned F1L and M11L with Bcl-x_L (Fig. 6.2), and identified four putative BH domains (underlined residues). This alignment displays fairly low homology as expected, but gives us clues as to the alpha helical regions important in the protein (Fig 6.2, residues in bold). The asterisks located between the putative BH3 and BH1 domains indicate conserved hydrophobic residues which may form part of the hydrophobic groove (Fig. 6.2). This groove of Bcl-x_L is responsible for binding BH3 domains, so the corresponding residues in F1L are excellent targets for site-directed mutagenesis (239). Included in the alignment is an open reading frame from deerpox which exhibits predicted amino acid similarity to both F1L and M11L (2). Considering that F1L and M11L do not share significant sequence homology with each other, this deerpox virus gene may represent an evolutionary intermediate between M11L and F1L, and the comparison of multiple poxviral F1L or M11L orthologues may give clues as to which residues are critical for function.

Recently, M11L was crystallized by two groups and the three-dimensional structure revealed a fold similar to Bcl-2 family members (97, 189) (Fig. 6.3). M11L appears to interact with the BH3 peptide from Bak in the surface hydrophobic groove, and M11L can also bind to the BH3 domains from Bak, Bax, and Bim (97, 189). Whether the three dimensional structure of F1L also resembles Bcl-2 is unknown. Indeed, M11L

Figure 6.2. Alignment of poxviral mitochondrial inhibitors of apoptosis with Bcl-x_L.
Amino acid alignment of EVM025, VV(Cop) F1L, C7L from monkeypox virus (Mpx C7L), deerpox virus 022 (DPV 022), myxoma virus M11L (Myx M11L), and swinepox virus 012 (Swpx 012). Listed above is the sequence of Bcl-x_L with alpha helical regions in bold and numbered above (1-8). Also listed above are the locations of the four BH domains present in Bcl-x_L with BH domain residues underlined. Shaded residues indicate similar or identical residues. Residues shaded in yellow are amino acid changes in EVM025 not present in either of the other two orthopoxviral orthologues, VV(Cop) F1L or Mpx C7L (original alignment generated by Dr. B. Hazes, University of Alberta).

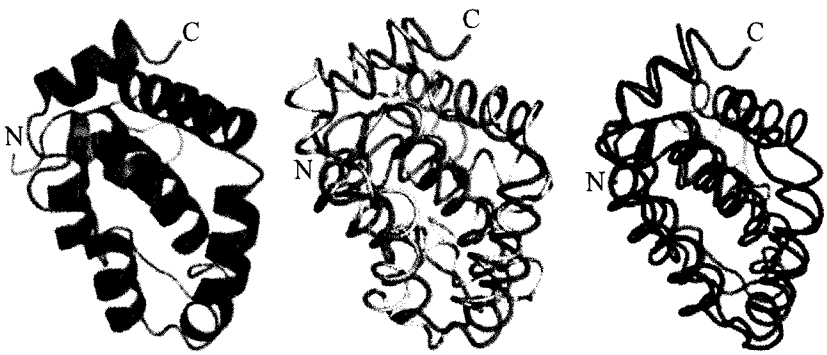

Figure 6.3. Structure of myxoma virus M11L and vaccinia virus N1L proteins. Diagrams detailing the alpha-helical nature of M11L from myxoma virus (in green) in comparison with mouse Bcl-x_L (middle panel, in yellow) and N1L from vaccinia virus (right panel, in blue). (Adapted from Kvansakul *et al.*, 2007. Mol. Cell. 25:933).

and F1L appear to have different effects on Bax, as M11L interacts with Bax at the mitochondria while F1L inhibits the steps leading to Bax activation in the absence of a direct interaction (332, 350). Differences between F1L and M11L may be the result of discrete differences in amino acid similarity and their overall structure. For instance, although Bcl-2 and Bcl-x_L are relatively similar in structure, the hydrophobic groove of Bcl-2 is longer than the groove of Bcl-x_L, and these two proteins consequently show different affinities for BH3 domains (187, 194, 259). Future work characterizing the structure of F1L would greatly improve our understanding of the mechanism of F1L, and would provide insight into the function of both F1L and cellular Bcl-2 family members.

It was suggested by Postigo and colleagues that, in addition to F1L, the vaccinia virus proteins A6L and N1L may also encode BH3-like domains (265). N1L was recently crystallized and consists of six alpha-helices which fold similar to Bcl-x_L and Mcl-1 (13) (Fig. 6.3). Although N1L has previously been shown to be a viral virulence factor that can inhibit TLR3-mediated NF-κB signaling (22, 28, 96, 181), N1L interacts with BH3-peptides from Bid, Bim and Bak, but not from Bad (13). The vaccinia virus protein A6L may also possess at least one BH-like domain (265). A6L has been reported to be a viral core protein required for proper virion formation (226). Whether A6L or N1L play any definitive role in the control of apoptosis remains to be determined. Infection with VV(Cop)ΔF1L does not inhibit apoptosis induced by multiple stimuli despite the fact that the genome of VV(Cop) contains both A6L and N1L open reading frames (123, 350, 379). Apoptosis induced by infection with VV(Cop)ΔF1L, however, is relatively slow, and growth curves of VV(Cop)ΔF1L on multiple MEF cell lines displayed no significant difference compared with wild type VV(Cop) (Fig. 3.11). It is possible that additional proteins such as N1L or A6L play specific roles in regulating apoptosis induced by particular pro-apoptotic stimuli such as VV-infection, although these hypothetical functions of N1L and A6L remain to be investigated.

Positional homology of F1L, M11L, FPV039

Vaccinia virus F1L, myxoma virus M11L, and another poxviral anti-apoptotic protein, fowlpox virus FPV039, are all mitochondrial-localized inhibitors of apoptosis and all interact with Bak (103, 382)(L. Banadyga and M. Barry, unpublished results). These proteins are functionally similar and share no significant amino acid similarity, although unlike F1L and M11L, FPV039 is an actual Bcl-2 homologue (5). What is particularly intriguing, however, is that these three viral open reading frames, as well as the F1L homologue from deerpox virus, all lie immediately adjacent to the open reading frame encoding the viral deoxyuridine triphosphatase (dUTPase) within their respective genomes (2, 5, 49, 123). It is possible that the conservation in genomic location, or "positional homology", of these poxviral anti-apoptotic open reading frames is indicative of a single gene acquisition event. Gradually through evolution, these proteins may have lost amino acid identity but maintained the necessary structural and functional aspects of anti-apoptotic Bcl-2 family members. FPV039, however, is more closely related to Bcl-2 and lies on the opposite side of the dUTPase, so it is possible that FPV039 was acquired separately and perhaps more recently in evolutionary history. Overall, the fact that M11L, F1L, and FPV039 all inhibit apoptosis and interact with Bak will allow us to investigate any putative conserved domains which facilitate the inhibition of apoptosis.

Activation of BH3-only proteins by Vaccinia virus

Apoptotic stimuli induce mitochondrial dysfunction through the activation/up-regulation of the BH3-only proteins (270, 330, 390), and infection with VVΔF1L induces apoptosis (379, 382). Interestingly, we show that infection of HeLa cells with either VV(Cop) or VV(Cop)ΔF1L induces the apparent phosphorylation of BimEL (Fig. 4.3). Inhibition of this phosphorylation, however, had no effect on the ability of VV(Cop)ΔF1L to induce apoptosis in HeLa cells, suggesting that the phosphorylation of BimEL is not solely responsible for VV-induced apoptosis (Fig. 4.5). $Bim^{-/-}$ BMKs were

partially resistant to VV-induced apoptosis (Fig. 4.9), suggesting that Bim is required to fully execute vaccinia virus-induced cell death. Western blotting of lysates from VV-infected BMK cells displayed the up-regulation of BimS and BimL, indicating that these proteins may be transcriptionally up-regulated following VV-infection (Fig. 4.9). Apoptosis, however, was not abolished in $Bim^{-/-}$ BMKs, suggesting that other BH3-only proteins are activated and involved in VV-induced apoptosis. The roles of BH3-only proteins are not yet fully defined, so characterizing BH3-only protein activation, up-regulation, and modification during VV-infection may reveal insight into how BH3-only proteins are activated. As well, BH3-only protein pathways are intimately linked to the innate cellular mechanisms which detect virus infection and induce apoptosis, so characterizing which proteins are activated following vaccinia virus infection may provide information regarding these innate cellular anti-viral pathways.

VV(Cop)ΔF1L is not the only strain of VV which induces apoptosis. VV lacking the gene E3L also induces apoptosis in infected cells, despite the fact that this virus expresses F1L (113, 192). E3L encodes a dsRNA binding protein which was originally identified as an interferon (IFN) resistance gene (58, 86). dsRNA is a by-product of viral replication and transcription, and has been shown to induce both interferon and apoptotic responses (57, 279, 280, 309). Expression of E3L protects cells from dsRNA-induced apoptosis but not apoptosis induced by other stimuli, suggesting that E3L specifically functions to protect cells from dsRNA-induced cytopathic effects (118, 176). Remarkably, treatment of VVΔE3L-infected cells with cytosine arabinoside, a nucleoside analogue which prevents virus DNA replication and the subsequent buildup of dsRNA, blocks VVΔE3L-induced apoptosis (176, 192).

dsRNA triggers the up-regulation of the BH3-only protein Noxa to induce apoptosis (336). Intriguingly, infection with VVΔE3L induces apoptosis in WT MEFs, but not in Noxa-deficient MEFs (113). As this virus expresses F1L, this suggests that F1L may not be able to counteract the pro-apoptotic effect of Noxa during virus-induced

apoptosis (113), despite the fact that F1L inhibits Bak and Bax activation induced by other stimuli (265, 350, 379). Other recent studies have shown that E3L is also a viral regulator of transcription and that the expression of viral proteins such as F1L may be decreased (211). It will therefore be interesting to examine whether the overexpression of F1L is capable of inhibiting VVΔE3L-induced, Noxa-induced, or dsRNA-induced apoptosis. If F1L is able to inhibit apoptosis mediated by only certain BH3-only proteins, this may reflect a specific evolutionary path. In the case of VV, the E3L protein may be completely effective at inhibiting the dsRNA-induced Noxa response, so it is possible that VV does not require F1L to inhibit dsRNA-mediated apoptosis. E1B 19K from adenovirus, for instance, does not inhibit BimL-mediated apoptosis (250), yet potently inhibits apoptosis induced by other intrinsic and extrinsic stimuli (90, 145, 257, 388). In evolutionary terms, it is possible that Bim is not activated during adenovirus infection, so E1B 19K does not need to inhibit Bim-mediated apoptosis.

F1L, mitochondrial membrane permeabilization, and mitochondrial morphology

We have shown that F1L expression inhibits the release of cytochrome c from mitochondria during apoptosis and that F1L can interact with Bak and BimL as potential mechanisms for inhibiting mitochondrial dysfunction during apoptosis (350, 382). Although Bcl-2 is believed to primarily function to control pro-apoptotic Bcl-2 family proteins, the expression of Bcl-2 can suppress mitochondrial membrane permeabilization *in vitro* in the absence of pro-apoptotic Bcl-2 family members (10, 42). Bcl-2 can inhibit pore formation by Bak, Bax, VDAC, and ANT *in vitro* (42, 313). As well, M11L from myxoma virus has been reported to interact with the PBR, a component of the PT pore (104). It remains to be determined whether F1L, like Bcl-2, can inhibit non-specific mitochondrial membrane permeabilization, although F1L can inhibit mitochondrial permeability transition induced by the addition of atractyloside, a chemical ligand of the PT pore (381). This suggests that F1L may have an additional mechanism to control the

mitochondria in addition to binding to Bak and BimL. It is not known whether F1L can maintain the integrity of the mitochondrial membrane in the absence of cellular Bcl-2 family proteins. Examining the biochemical attributes of F1L may help us characterize how F1L actually maintains the integrity of the mitochondrial membrane during cell death.

Bcl-2 undergoes a conformational change at the mitochondrial membrane during apoptosis (178), although the significance of this change is not understood. F1L is anchored into the mitochondrial membrane prior to an apoptotic stimulus, but whether F1L or other viral proteins undergo a similar conformational change following an apoptotic stimulus is unknown. It has been documented that Bax requires additional proteins as part of the so-called mitochondrial apoptosis channel (MAC) to facilitate cytochrome c release (92, 136, 282). This high-conductance channel is suppressed by Bcl-2 overexpression, and is detected in gel filtration fractions which also correspond to oligomeric Bax (92, 256). Expression of F1L inhibits Bax oligomerization and cytochrome c release, leading us to speculate that MAC formation may also be inhibited by F1L.

The mitochondrial inner membrane is comprised of a series of folds, or cristae, which create pockets known as intracristae spaces. These intracristae spaces contain more than 90% of the cytochrome c, so complete cytochrome c release during apoptosis requires cristae remodeling (299). Other pro-apoptotic factors such as SMAC/Diablo are not contained within the intracristae space and are released without cristae remodeling (255). The recent observation documenting the requirement of cristae remodeling during apoptosis points to the involvement of mitochondrial fission and fusion proteins in apoptosis (53, 223, 298, 401). During apoptosis, mitochondria typically become increasingly fragmented, and the inhibition of mitochondrial fragmentation appears to interfere with cytochrome c release (255). Similarly, the overexpression of proteins involved in mitochondrial fusion appears to inhibit Bak and Bax activation during

apoptosis (334). Intriguingly, Bak and Bax also play a regulatory role with respect to mitochondrial fission and fusion. Cells devoid of Bak and Bax exhibit short fragmented mitochondria, while re-expression of Bak or Bax results in mitochondrial elongation (171),.

Bak and Bax are not the only apoptotic regulator proteins which affect mitochondrial morphology. Expression of vMIA induces a cytopathic effect and mitochondria appear smaller and fragmented (171, 224, 264). Overexpression of Bax, but not BaxΔBH3, in these cells reverses vMIA-induced fragmentation (171). Drp1 (dynamin related protein 1) is required for cristae remodeling and cytochrome c release, and the BH3-only protein Bik induces cristae remodeling via Drp1 (122). Conversely, a protein involved in mediating mitochondrial fusion, Fzo1, has the ability to inhibit cytochrome c release and the activation of Bak and Bax (334). Aside from vMIA, no other viral anti-apoptotic proteins have been documented to alter mitochondrial morphology. Based on the observations that Bcl-2 family members are connected to mitochondrial fission and fusion, it would be interesting to investigate whether infection with VV or the expression of F1L has any effect on mitochondrial morphology. Any effect that F1L has on mitochondrial morphology may also help us to better understand how F1L inhibits cytochrome c release, and will also allow us to investigate the role that mitochondrial morphology plays in apoptosis and vaccinia virus infection.

Ectromelia virus EVM025: a functional anti-apoptotic protein

The ectromelia virus orthologue of F1L, EVM025, is predicted to be 55kDa in size, and contains a long N-terminal repeat, consisting of the eight amino acid motif 'DNGIVQDI' repeated 30 times (Fig. 5.1). F1L, on the other hand, contains this eight amino acid motif only once (Fig. 5.1). We have shown that EVM025 is produced as a 55kDa protein and inhibits apoptosis at the mitochondria, as a deletion virus EVMΔcrmAΔ025 does not inhibit cytochrome c release (Fig. 5.3, and 5.5). Interestingly,

the N-terminal extension is not required *in vitro*, as truncated versions of EVM025 lacking the N-terminal repeat region inhibited apoptosis induced by TNFα, αFas, and virus infection (Fig. 5.6 and 5.10). EVM025 is a functional anti-apoptotic protein, and like F1L, is able to interact with Bak (Fig 5.10). As well, EVM025 is also able to inhibit Bax activation (Fig. 5.9), although no interaction between a truncated version of EVM025, EVM025(E255), and Bax was observed (Fig. 5.10). These results suggest that EVM025, similar to F1L, may also function upstream of Bax activation. Whether EVM025 interacts with BH3-only proteins such as Bim remains to be determined. Our lab has shown that both F1L and versions of EVM025 lacking the N-terminal repeat region can inhibit mitochondrial dysfunction induced by the overexpression of the BH3-only proteins BimL, Bid, Bmf, Bik, and PUMA (Fig. 4.1) (S. Campbell, D. Quilty, K. Veugelers, and M. Barry, unpublished results), and we are currently investigating whether EVM025 interacts with any of these BH3-only proteins. Cellular anti-apoptotic proteins such as Bcl-x_L and Mcl-1 show different affinities for the various BH3-only proteins, suggesting that BH3-only proteins are not promiscuous with respect to binding all of the anti-apoptotic Bcl-2 family members, and vice versa. Whether the same is true for viral anti-apoptotic proteins such as EVM025 or F1L remains to be investigated.

We have shown that full length EVM025 is a functional anti-apoptotic protein, as a strain of EVM lacking EVM025 is unable to confer resistance to multiple apoptotic stimuli (Fig. 5.5 and 5.9). Future work will involve the use of this mutant strain of EVM in pathogenicity studies to examine the role of EVM025 in virus virulence. A natural pathogen of mice, EVM is an excellent model in which to study poxviral pathogenicity (102, 110). Deletion of open reading frames encoding apoptotic regulators from other viruses often results in dramatic attenuation, indicating the importance of the regulation of apoptosis during infection (128, 208, 254). Although endogenous full-length EVM025 is functional and inhibits apoptosis, we do not know the function, if any, of the N-terminal repeat region. The long N-terminal amino acid sequence does not exhibit any

obvious predicted secondary structure or share any homology with any known proteins, although EVM025 is seen as a full-length 55kDa protein in EVM-infected cells. As well, the sequence of the EVM025 orthologue from EV strain Naval is also predicted to contain 26 copies of the "DNGIVQDI" repeat. Our lab is currently investigating whether other strains of ectromelia virus also exhibit an elongated N-terminal repeat region. We attempted a number of methods to clone and examine full-length EVM025 from EVM. None of our attempts were successful, so we are unable to comment on the role of the complete N-terminal repeat region. We constructed two EVM025 truncations containing either zero or two copies of the eight amino acid motif that were similar in their ability to protect cells from apoptosis (Fig. 5.6), indicating that the repeat is non-essential *in vitro*, and that the presence of two copies of the repeat does not confer an obvious pro-survival advantage *in vitro*.

The presence of an N-terminal extension is not unique to the genome of ectromelia virus. F1L orthologues from cowpox, camelpox and variola virus all show the presence of a variable extension at the N-terminus. Certain strains of variola virus have multiple copies of an 'Asp-Asp-Ile' ('DDI') repeat, such as variola India 1953 (12 copies of "DDI"). Other strains of variola virus show no significant extension at the N-terminus, such as variola Afghanistan 1970 (2 copies of "DDI"). The function of these repeats is also unknown, and there is no obvious correlation between the length of the N-terminal extension and historical mortality rate data of these strains of variola. We can only speculate that these extensions may (1) confer an altered anti-apoptotic function *in vivo*; (2) possess a novel function; or (3) be dispensable altogether. Deletion of the repeat region from EVM025 does not abolish the ability of EVM025 to inhibit apoptosis *in vitro* (Fig. 5.6), suggesting that the basic anti-apoptotic function of EVM025 does not require the N-terminal repeat. This repeat region may confer anti-apoptotic properties specific to mouse cells, as the bulk of our work has been done in human tissue culture cells. EVM025 confers resistance to apoptosis in human cell lines, and F1L similarly confers

resistance to apoptosis in at least two mouse cell lines (Fig. 3.8-3.11)(379), suggesting that these viral inhibitors of apoptosis are functional *in vitro* in either murine or human cell lines. There may be discrete differences that can be ascribed to species specificity, such as the ability to interact with a particular BH3-only protein. Murine Noxa for instance has two BH3 domains, compared to the human Noxa which has one BH3 domain (251). Sequence alignment of human versus murine BimL, meanwhile, shows 85% amino acid identity, and a number of amino acid differences lie just outside the BH3 domain (250). The notion that EVM025 may confer properties specific for murine pro-apoptotic proteins is currently being investigated in our lab.

As our truncated version of EVM025 lacking the repeat region, EVM025(E255), inhibits apoptosis *in vitro*, it will be interesting to see whether truncated EVM025(E255) will still function in infected mice *in vivo*. Assuming that full-length EVM025 is required for *in vivo* pathogenicity, the generation of a strain of ectromelia which only encodes truncated EVM025(E255) would help to ascertain the *in vivo* function of the N-terminus, and any deficiency in pathogenicity would suggest that the repeat region is important for virus virulence. It is possible that the N-terminal repeat region of EVM025 plays a specific anti-apoptotic role in mice *in vivo* and contributes to the host range of ectromelia virus. Another possibility is that this domain has a function completely independent of apoptosis. Indeed, the mitochondrion is a dynamic organelle that takes part in a number of cellular pathways, and was even recently connected with the interferon pathway (308). It is possible that viral mitochondrial-localized proteins such as EVM025 and F1L may have other functions aside from the inhibition of apoptosis.

Expression of EVM025 and F1L

Intriguingly, western blotting of EVM-infected cell lysates with anti-F1L revealed substantial amounts of EVM025, while VV(Cop)-infected lysates exhibited no F1L whatsoever (Fig. 5.3). This antibody was generated against the first 120 amino acids of

F1L, and detects both FLAG-F1L as well as FLAG-EVM025(E255) lacking the N-terminal repeat region (Fig. 5.3, 5.10) (329). One hypothesis to explain why the F1L antibody does not detect F1L in VV(Cop)-infected lysates is that F1L messenger RNA (mRNA) may not be transcribed at high amounts. Indeed, there is a small 12 nucleotide insertion in the promoter region immediately upstream of F1L that is not present in front of EVM025. This small insertion may negatively affect the rate of transcription of F1L compared to EVM025, thereby accounting for the lack of a reactive F1L band with our anti-F1L antibody. Quantitative RT-PCR or northern blotting mRNA samples from EVM or VV-infected lysates would reveal whether EVM025 and F1L are transcribed at different rates. Although this is plausible, EGFP-fusions of F1L or EVM025(E255) behind the identical cytomegalovirus (CMV) promoter also do not express equally, as we consistently observe much higher expression of EGFP-EVM025(E255) compared to EGFP-F1L (S. Campbell, D. Quilty, and M. Barry, unpublished results). This suggests that another post-translational regulatory mechanism may control the expression of F1L and EVM025.

Another hypothesis to explain the lack of F1L detected by the F1L antibody is that F1L may be targeted for degradation. Degradation of proteins by the 26S proteasome is regulated by ubiquitination, whereby the 76 amino acid peptide ubiquitin is covalently attached to lysine residues from substrate proteins (168, 386). Ubiquitin molecules can then be ubiquitinated themselves, resulting in polyubiquitin chains which can target the ubiquitinated protein to the 26S proteasome for degradation. In support of this, preliminary polyubiquitination assays have demonstrated that F1L is ubiquitinated (Appendix B.2). As well, addition of the proteasome inhibitor MG132 dramatically increases expression of F1L (S. Campbell and M. Barry, unpublished results)(265). How F1L is ubiquitinated and the significance of this event remains to be investigated.

One class of E3 ubiquitin ligases, responsible for attaching ubiquitin to substrate proteins, possess a zinc-binding RING-domain. Intriguingly, a E3 ubiquitin ligase known

as MULE (Mcl-1 ubiquitin ligase E3) possesses a BH3 domain and localizes to the mitochondria (59). MULE interacts with and specifically polyubiquitinates the Bcl-2 family member Mcl-1, resulting in Mcl-1 degradation (378, 405). While Mcl-1 is the only known substrate for MULE, it is interesting to speculate that cellular proteins such as MULE may have anti-viral functions by targeting viral proteins such as F1L for degradation. As F1L interacts with BH3 domain-containing proteins (265, 350, 379), it is possible that F1L can also interact with the BH3 domain from MULE. The molecular events which regulate F1L and EVM025 ubiquitination remain to be determined. Pulse chase immunoprecipitations using ^{35}S-methionine would help establish the relative turn-over rates of F1L and EVM025, and would indicate whether F1L is degraded at a faster rate than EVM025. Considering that proteins are ubiquitinated on lysine residues, it should be noted that two lysine residues from F1L are changed to glutamate in EVM025(E255). As well, there are a number of other residues which differ between F1L and EVM025 that may also affect the rate of ubiquitination. Proteins are often modified by phosphorylation prior to their ubiquitination (197, 210). It is interesting to speculate that F1L orthologues may be differentially regulated by ubiquitin and that this may correlate with virus pathogenicity. It would be of interest to also investigate the ubiquitination of other orthopoxviral F1L orthologues in various hosts. Considering that vaccinia virus is not a natural human pathogen, it is tempting to speculate that mechanisms such as the ubiquitination of viral virulence determinants may play a role in determining overall virus pathogenicity.

Summary

At the initiation of these studies, little was known about the activation of Bax during vaccinia virus infection. We have shown here that vaccinia virus F1L can inhibit Bax activation in the absence of a direct interaction. F1L can, however, interact with the BH3-only protein BimL as a mechanism for inhibiting the steps leading to Bax

activation. Combined with other observations, we propose that F1L can interact with BH3-only proteins and BH3-domains from Bcl-2 family members as a mechanism for inhibiting apoptosis at the mitochondria. We have also shown that the F1L orthologue from ectromelia virus, EVM025, is a functional anti-apoptotic protein which interacts with Bak and inhibits Bax activation. Whether EVM025 is also capable of interacting with BH3 domains or BH3-only proteins remains to be determined, and future work will likely focus on how these poxviral inhibitors of apoptosis interact with Bcl-2 family members. Overall, this research has added valuable insight into understanding how these poxviral inhibitors of apoptosis function, and will hopefully lead to further discoveries detailing how viral and cellular proteins function to regulate the complex intrinsic apoptotic pathway.

References

1. **Adams, J. M., and S. Cory.** 1998. The Bcl-2 protein family: arbiters of cell survival. Science **281:**1322-6.

2. **Afonso, C. L., G. Delhon, E. R. Tulman, Z. Lu, A. Zsak, V. M. Becerra, L. Zsak, G. F. Kutish, and D. L. Rock.** 2005. Genome of deerpox virus. J Virol **79:**966-77.

3. **Afonso, C. L., J. G. Neilan, G. F. Kutish, and D. L. Rock.** 1996. An African swine fever virus Bcl-2 homolog, 5-HL, suppresses apoptotic cell death. J Virol **70:**4858-63.

4. **Afonso, C. L., E. R. Tulman, Z. Lu, E. Oma, G. F. Kutish, and D. L. Rock.** 1999. The genome of Melanoplus sanguinipes entomopoxvirus. J Virol **73:**533-52.

5. **Afonso, C. L., E. R. Tulman, Z. Lu, L. Zsak, G. F. Kutish, and D. L. Rock.** 2000. The genome of fowlpox virus. J Virol **74:**3815-31.

6. **Afonso, C. L., E. R. Tulman, Z. Lu, L. Zsak, N. T. Sandybaev, U. Z. Kerembekova, V. L. Zaitsev, G. F. Kutish, and D. L. Rock.** 2002. The genome of camelpox virus. Virology **295:**1-9.

7. **Alcami, A., and G. L. Smith.** 1995. Vaccinia, cowpox, and camelpox viruses encode soluble gamma interferon receptors with novel broad species specificity. J Virol **69:**4633-9.

8. **Andrade, A. A., P. N. Silva, A. C. Pereira, L. P. De Sousa, P. C. Ferreira, R. T. Gazzinelli, E. G. Kroon, C. Ropert, and C. A. Bonjardim.** 2004. The vaccinia virus-stimulated mitogen-activated protein kinase (MAPK) pathway is required for virus multiplication. Biochem J **381:**437-46.

9. **Annis, M. G., E. L. Soucie, P. J. Dlugosz, J. A. Cruz-Aguado, L. Z. Penn, B. Leber, and D. W. Andrews.** 2005. Bax forms multispanning monomers that oligomerize to permeabilize membranes during apoptosis. Embo J **24:**2096-103.

10. **Antonsson, B., F. Conti, A. Ciavatta, S. Montessuit, S. Lewis, I. Martinou, L. Bernasconi, A. Bernard, J. J. Mermod, G. Mazzei, K. Maundrell, F. Gambale, R. Sadoul, and J. C. Martinou.** 1997. Inhibition of Bax channel-forming activity by Bcl-2. Science **277:**370-2.

11. **Antonsson, B., S. Montessuit, S. Lauper, R. Eskes, and J. C. Martinou.** 2000. Bax oligomerization is required for channel-forming activity in liposomes and to trigger cytochrome c release from mitochondria. Biochem J **345 Pt 2:**271-8.

12. **Antonsson, B., S. Montessuit, B. Sanchez, and J. C. Martinou.** 2001. Bax is present as a high molecular weight oligomer/complex in the mitochondrial membrane of apoptotic cells. J Biol Chem **276:**11615-23.

13. **Aoyagi, M., D. Zhai, C. Jin, A. E. Aleshin, B. Stec, J. C. Reed, and R. C. Liddington.** 2007. Vaccinia virus N1L protein resembles a B cell lymphoma-2 (Bcl-2) family protein. Protein Sci **16:**118-24.

14. **Arnoult, D., L. M. Bartle, A. Skaletskaya, D. Poncet, N. Zamzami, P. U. Park, J. Sharpe, R. J. Youle, and V. S. Goldmacher.** 2004. Cytomegalovirus cell death suppressor vMIA blocks Bax- but not Bak-mediated apoptosis by binding and sequestering Bax at mitochondria. Proc Natl Acad Sci U S A **101:**7988-93.

15. **Ashkenazi, A.** 2002. Targeting death and decoy receptors of the tumour-necrosis factor superfamily. Nat Rev Cancer **2:**420-30.

16. **Ashkenazi, A., and V. M. Dixit.** 1999. Apoptosis control by death and decoy receptors. Curr Opin Cell Biol **11:**255-60.

17. **Baines, C. P., R. A. Kaiser, N. H. Purcell, N. S. Blair, H. Osinska, M. A. Hambleton, E. W. Brunskill, M. R. Sayen, R. A. Gottlieb, G. W. Dorn, J. Robbins, and J. D. Molkentin.** 2005. Loss of cyclophilin D reveals a critical role for mitochondrial permeability transition in cell death. Nature **434:**658-62.

18. **Barry, M., and R. C. Bleackley.** 2002. Cytotoxic T lymphocytes: all roads lead to death. Nat Rev Immunol **2:**401-9.

19. **Barry, M., J. A. Heibein, M. J. Pinkoski, S. F. Lee, R. W. Moyer, D. R. Green, and R. C. Bleackley.** 2000. Granzyme B short-circuits the need for caspase 8 activity during granule-mediated cytotoxic T-lymphocyte killing by directly cleaving Bid. Mol Cell Biol **20:**3781-94.

20. **Barry, M., S. Hnatiuk, K. Mossman, S. F. Lee, L. Boshkov, and G. McFadden.** 1997. The myxoma virus M-T4 gene encodes a novel RDEL-containing protein that is retained within the endoplasmic reticulum and is important for the productive infection of lymphocytes. Virology **239:**360-77.

21. **Barry, M., S. T. Wasilenko, T. L. Stewart, and J. M. Taylor.** 2004. Apoptosis regulator genes encoded by poxviruses. Prog Mol Subcell Biol **36:**19-37.

22. **Bartlett, N., J. A. Symons, D. C. Tscharke, and G. L. Smith.** 2002. The vaccinia virus N1L protein is an intracellular homodimer that promotes virulence. J Gen Virol **83:**1965-76.

23. **Bawden, A. L., K. J. Glassberg, J. Diggans, R. Shaw, W. Farmerie, and R. W. Moyer.** 2000. Complete genomic sequence of the Amsacta moorei entomopoxvirus: analysis and comparison with other poxviruses. Virology **274:**120-39.

24. **Benedict, C. A., P. S. Norris, and C. F. Ware.** 2002. To kill or be killed: viral evasion of apoptosis. Nat Immunol **3:**1013-8.

25. **Bernardi, P., and G. F. Azzone.** 1981. Cytochrome c as an electron shuttle between the outer and inner mitochondrial membranes. J Biol Chem **256:**7187-92.

26. **Bertin, J., R. C. Armstrong, S. Ottilie, D. A. Martin, Y. Wang, S. Banks, G. H. Wang, T. G. Senkevich, E. S. Alnemri, B. Moss, M. J. Lenardo, K. J. Tomaselli, and J. I. Cohen.** 1997. Death effector domain-containing herpesvirus and poxvirus proteins inhibit both Fas- and TNFR1-induced apoptosis. Proc Natl Acad Sci U S A **94:**1172-6.

27. **Bertrand, R., E. Solary, P. O'Connor, K. W. Kohn, and Y. Pommier.** 1994. Induction of a common pathway of apoptosis by staurosporine. Exp Cell Res **211:**314-21.

28. **Billings, B., S. A. Smith, Z. Zhang, D. K. Lahiri, and G. J. Kotwal.** 2004. Lack of N1L gene expression results in a significant decrease of vaccinia virus replication in mouse brain. Ann N Y Acad Sci **1030:**297-302.

29. **Birnbaum, M. J., R. J. Clem, and L. K. Miller.** 1994. An apoptosis-inhibiting gene from a nuclear polyhedrosis virus encoding a polypeptide with Cys/His sequence motifs. J Virol **68:**2521-8.

30. **Biswas, S. C., and L. A. Greene.** 2002. Nerve growth factor (NGF) down-regulates the Bcl-2 homology 3 (BH3) domain-only protein Bim and suppresses its proapoptotic activity by phosphorylation. J Biol Chem **277:**49511-6.

31. **Blomquist, M. C., L. T. Hunt, and W. C. Barker.** 1984. Vaccinia virus 19-kilodalton protein: relationship to several mammalian proteins, including two growth factors. Proc Natl Acad Sci U S A **81:**7363-7.

32. **Boise, L. H., M. Gonzalez-Garcia, C. E. Postema, L. Ding, T. Lindsten, L. A. Turka, X. Mao, G. Nunez, and C. B. Thompson.** 1993. bcl-x, a bcl-2-related gene that functions as a dominant regulator of apoptotic cell death. Cell **74:**597-608.

33. **Borzillo, G. V., K. Endo, and Y. Tsujimoto.** 1992. Bcl-2 confers growth and survival advantage to interleukin 7-dependent early pre-B cells which become factor independent by a multistep process in culture. Oncogene **7:**869-76.

34. **Bossy-Wetzel, E., D. D. Newmeyer, and D. R. Green.** 1998. Mitochondrial cytochrome c release in apoptosis occurs upstream of DEVD-specific caspase activation and independently of mitochondrial transmembrane depolarization. Embo J **17:**37-49.

35. **Bouillet, P., D. Metcalf, D. C. Huang, D. M. Tarlinton, T. W. Kay, F. Kontgen, J. M. Adams, and A. Strasser.** 1999. Proapoptotic Bcl-2 relative Bim required for certain apoptotic responses, leukocyte homeostasis, and to preclude autoimmunity. Science **286:**1735-8.

36. **Bouillet, P., J. F. Purton, D. I. Godfrey, L. C. Zhang, L. Coultas, H. Puthalakath, M. Pellegrini, S. Cory, J. M. Adams, and A. Strasser.** 2002. BH3-only Bcl-2 family member Bim is required for apoptosis of autoreactive thymocytes. Nature **415:**922-6.

37. **Boulton, S. J., and S. P. Jackson.** 1996. Saccharomyces cerevisiae Ku70 potentiates illegitimate DNA double-strand break repair and serves as a barrier to error-prone DNA repair pathways. Embo J **15:**5093-103.

38. **Bowie, A., E. Kiss-Toth, J. A. Symons, G. L. Smith, S. K. Dower, and L. A. O'Neill.** 2000. A46R and A52R from vaccinia virus are antagonists of host IL-1 and toll-like receptor signaling. Proc Natl Acad Sci U S A **97:**10162-7.

39. **Boya, P., A. L. Pauleau, D. Poncet, R. A. Gonzalez-Polo, N. Zamzami, and G. Kroemer.** 2004. Viral proteins targeting mitochondria: controlling cell death. Biochim Biophys Acta **1659:**178-89.

40. **Boya, P., B. Roques, and G. Kroemer.** 2001. New EMBO members' review: viral and bacterial proteins regulating apoptosis at the mitochondrial level. Embo J **20:**4325-31.

41. **Boyd, J. M., G. J. Gallo, B. Elangovan, A. B. Houghton, S. Malstrom, B. J. Avery, R. G. Ebb, T. Subramanian, T. Chittenden, R. J. Lutz, and et al.** 1995. Bik, a novel death-inducing protein shares a distinct sequence motif with Bcl-2 family proteins and interacts with viral and cellular survival-promoting proteins. Oncogene **11:**1921-8.

42. **Brenner, C., H. Cadiou, H. L. Vieira, N. Zamzami, I. Marzo, Z. Xie, B. Leber, D. Andrews, H. Duclohier, J. C. Reed, and G. Kroemer.** 2000. Bcl-2 and Bax regulate the channel activity of the mitochondrial adenine nucleotide translocator. Oncogene **19:**329-36.

43. **Brick, D. J., R. D. Burke, A. A. Minkley, and C. Upton.** 2000. Ectromelia virus virulence factor p28 acts upstream of caspase-3 in response to UV light-induced apoptosis. J Gen Virol **81:**1087-97.

44. **Brick, D. J., R. D. Burke, L. Schiff, and C. Upton.** 1998. Shope fibroma virus RING finger protein N1R binds DNA and inhibits apoptosis. Virology **249:**42-51.

45. **Brooks, M. A., A. N. Ali, P. C. Turner, and R. W. Moyer.** 1995. A rabbitpox virus serpin gene controls host range by inhibiting apoptosis in restrictive cells. J Virol **69:**7688-98.

46. **Brun, A., C. Rivas, M. Esteban, J. M. Escribano, and C. Alonso.** 1996. African swine fever virus gene A179L, a viral homologue of bcl-2, protects cells from programmed cell death. Virology **225:**227-30.

47. **Buller, R. M., and G. J. Palumbo.** 1991. Poxvirus pathogenesis. Microbiol Rev **55:**80-122.

48. **Burger, G., M. W. Gray, and B. F. Lang.** 2003. Mitochondrial genomes: anything goes. Trends Genet **19:**709-16.

49. **Cameron, C., S. Hota-Mitchell, L. Chen, J. Barrett, J. X. Cao, C. Macaulay, D. Willer, D. Evans, and G. McFadden.** 1999. The complete DNA sequence of myxoma virus. Virology **264:**298-318.

50. **Carroll, M. W., and B. Moss.** 1997. Poxviruses as expression vectors. Curr Opin Biotechnol **8:**573-7.

51. **Cartron, P. F., H. Arokium, L. Oliver, K. Meflah, S. Manon, and F. M. Vallette.** 2005. Distinct domains control the addressing and the insertion of Bax into mitochondria. J Biol Chem **280:**10587-98.

52. **Cartron, P. F., T. Gallenne, G. Bougras, F. Gautier, F. Manero, P. Vusio, K. Meflah, F. M. Vallette, and P. Juin.** 2004. The first alpha helix of Bax plays a necessary role in its ligand-induced activation by the BH3-only proteins Bid and PUMA. Mol Cell **16:**807-18.

53. **Cereghetti, G. M., and L. Scorrano.** 2006. The many shapes of mitochondrial death. Oncogene **25:**4717-24.

54. **Certo, M., V. Del Gaizo Moore, M. Nishino, G. Wei, S. Korsmeyer, S. A. Armstrong, and A. Letai.** 2006. Mitochondria primed by death signals determine cellular addiction to antiapoptotic BCL-2 family members. Cancer Cell **9:**351-65.

55. **Chai, J., C. Du, J. W. Wu, S. Kyin, X. Wang, and Y. Shi.** 2000. Structural and biochemical basis of apoptotic activation by Smac/DIABLO. Nature **406:**855-62.

56. **Chakrabarti, S., J. R. Sisler, and B. Moss.** 1997. Compact, synthetic, vaccinia virus early/late promoter for protein expression. Biotechniques **23:**1094-7.

57. **Chang, H. W., and B. L. Jacobs.** 1993. Identification of a conserved motif that is necessary for binding of the vaccinia virus E3L gene products to double-stranded RNA. Virology **194:**537-47.

58. **Chang, H. W., J. C. Watson, and B. L. Jacobs.** 1992. The E3L gene of vaccinia virus encodes an inhibitor of the interferon-induced, double-stranded RNA-dependent protein kinase. Proc Natl Acad Sci U S A **89:**4825-9.

59. **Chen, D., N. Kon, M. Li, W. Zhang, J. Qin, and W. Gu.** 2005. ARF-BP1/Mule is a critical mediator of the ARF tumor suppressor. Cell **121:**1071-83.

60. **Chen, G., P. E. Branton, E. Yang, S. J. Korsmeyer, and G. C. Shore.** 1996. Adenovirus E1B 19-kDa death suppressor protein interacts with Bax but not with Bad. J Biol Chem **271:**24221-5.

61. **Chen, L., S. N. Willis, A. Wei, B. J. Smith, J. I. Fletcher, M. G. Hinds, P. M. Colman, C. L. Day, J. M. Adams, and D. C. Huang.** 2005. Differential targeting of prosurvival Bcl-2 proteins by their BH3-only ligands allows complementary apoptotic function. Mol Cell **17:**393-403.

62. **Chen, N., M. I. Danila, Z. Feng, R. M. Buller, C. Wang, X. Han, E. J. Lefkowitz, and C. Upton.** 2003. The genomic sequence of ectromelia virus, the causative agent of mousepox. Virology **317:**165-86.

63. **Cheng, E. H., D. G. Kirsch, R. J. Clem, R. Ravi, M. B. Kastan, A. Bedi, K. Ueno, and J. M. Hardwick.** 1997. Conversion of Bcl-2 to a Bax-like death effector by caspases. Science **278:**1966-8.

64. **Cheng, E. H., T. V. Sheiko, J. K. Fisher, W. J. Craigen, and S. J. Korsmeyer.** 2003. VDAC2 inhibits BAK activation and mitochondrial apoptosis. Science **301:**513-7.

65. **Cheng, E. H., M. C. Wei, S. Weiler, R. A. Flavell, T. W. Mak, T. Lindsten, and S. J. Korsmeyer.** 2001. BCL-2, BCL-X(L) sequester BH3 domain-only molecules preventing BAX- and BAK-mediated mitochondrial apoptosis. Mol Cell **8:**705-11.

66. **Chipuk, J. E., L. Bouchier-Hayes, and D. R. Green.** 2006. Mitochondrial outer membrane permeabilization during apoptosis: the innocent bystander scenario. Cell Death Differ **13:**1396-402.

67. **Chipuk, J. E., T. Kuwana, L. Bouchier-Hayes, N. M. Droin, D. D. Newmeyer, M. Schuler, and D. R. Green.** 2004. Direct activation of Bax by p53 mediates mitochondrial membrane permeabilization and apoptosis. Science **303:**1010-4.

68. **Chipuk, J. E., U. Maurer, D. R. Green, and M. Schuler.** 2003. Pharmacologic activation of p53 elicits Bax-dependent apoptosis in the absence of transcription. Cancer Cell **4:**371-81.

69. **Chittenden, T., C. Flemington, A. B. Houghton, R. G. Ebb, G. J. Gallo, B. Elangovan, G. Chinnadurai, and R. J. Lutz.** 1995. A conserved domain in Bak, distinct from BH1 and BH2, mediates cell death and protein binding functions. Embo J **14:**5589-96.

70. **Chittenden, T., E. A. Harrington, R. O'Connor, C. Flemington, R. J. Lutz, G. I. Evan, and B. C. Guild.** 1995. Induction of apoptosis by the Bcl-2 homologue Bak. Nature **374:**733-6.

71. **Choe, S., M. J. Bennett, G. Fujii, P. M. Curmi, K. A. Kantardjieff, R. J. Collier, and D. Eisenberg.** 1992. The crystal structure of diphtheria toxin. Nature **357:**216-22.

72. **Chou, J. J., H. Li, G. S. Salvesen, J. Yuan, and G. Wagner.** 1999. Solution structure of BID, an intracellular amplifier of apoptotic signaling. Cell **96:**615-24.

73. **Cleary, M. L., S. D. Smith, and J. Sklar.** 1986. Cloning and structural analysis of cDNAs for bcl-2 and a hybrid bcl-2/immunoglobulin transcript resulting from the t(14;18) translocation. Cell **47:**19-28.

74. **Clem, R. J., and L. K. Miller.** 1994. Control of programmed cell death by the baculovirus genes p35 and iap. Mol Cell Biol **14:**5212-22.

75. **Cohen, J. J., R. C. Duke, V. A. Fadok, and K. S. Sellins.** 1992. Apoptosis and programmed cell death in immunity. Annu Rev Immunol **10:**267-93.

76. **Colombini, M.** 1979. A candidate for the permeability pathway of the outer mitochondrial membrane. Nature **279:**643-5.

77. **Cory, S., D. C. Huang, and J. M. Adams.** 2003. The Bcl-2 family: roles in cell survival and oncogenesis. Oncogene **22:**8590-607.

78. **Crompton, M.** 1999. The mitochondrial permeability transition pore and its role in cell death. Biochem J **341 (Pt 2):**233-49.

79. **Crook, N. E., R. J. Clem, and L. K. Miller.** 1993. An apoptosis-inhibiting baculovirus gene with a zinc finger-like motif. J Virol **67:**2168-74.

80. **Cuconati, A., K. Degenhardt, R. Sundararajan, A. Anschel, and E. White.** 2002. Bak and Bax function to limit adenovirus replication through apoptosis induction. J Virol **76:**4547-58.

81. **Cuconati, A., C. Mukherjee, D. Perez, and E. White.** 2003. DNA damage response and MCL-1 destruction initiate apoptosis in adenovirus-infected cells. Genes Dev **17:**2922-32.

82. **Cuconati, A., and E. White.** 2002. Viral homologs of BCL-2: role of apoptosis in the regulation of virus infection. Genes Dev **16:**2465-78.

83. **Cuddeback, S. M., H. Yamaguchi, K. Komatsu, T. Miyashita, M. Yamada, C. Wu, S. Singh, and H. G. Wang.** 2001. Molecular cloning and characterization of Bif-1. A novel Src homology 3 domain-containing protein that associates with Bax. J Biol Chem **276:**20559-65.

84. **Cunnion, K. M.** 1999. Tumor necrosis factor receptors encoded by poxviruses. Mol Genet Metab **67:**278-82.

85. **Datta, R., H. Kojima, D. Banach, N. J. Bump, R. V. Talanian, E. S. Alnemri, R. R. Weichselbaum, W. W. Wong, and D. W. Kufe.** 1997. Activation of a CrmA-insensitive, p35-sensitive pathway in ionizing radiation-induced apoptosis. J Biol Chem **272:**1965-9.

86. **Davies, M. V., H. W. Chang, B. L. Jacobs, and R. J. Kaufman.** 1993. The E3L and K3L vaccinia virus gene products stimulate translation through inhibition of the double-stranded RNA-dependent protein kinase by different mechanisms. J Virol **67:**1688-92.

87. **Davies, M. V., O. Elroy-Stein, R. Jagus, B. Moss, and R. J. Kaufman.** 1992. The vaccinia virus K3L gene product potentiates translation by inhibiting double-stranded-RNA-activated protein kinase and phosphorylation of the alpha subunit of eukaryotic initiation factor 2. J Virol **66:**1943-50.

88. **Day, C. L., L. Chen, S. J. Richardson, P. J. Harrison, D. C. Huang, and M. G. Hinds.** 2005. Solution structure of prosurvival Mcl-1 and characterization of its binding by proapoptotic BH3-only ligands. J Biol Chem **280:**4738-44.

89. **de Magalhaes, J. C., A. A. Andrade, P. N. Silva, L. P. Sousa, C. Ropert, P. C. Ferreira, E. G. Kroon, R. T. Gazzinelli, and C. A. Bonjardim.** 2001. A mitogenic signal triggered at an early stage of vaccinia virus infection: implication of MEK/ERK and protein kinase A in virus multiplication. J Biol Chem **276:**38353-60.

90. **Debbas, M., and E. White.** 1993. Wild-type p53 mediates apoptosis by E1A, which is inhibited by E1B. Genes Dev **7:**546-54.

91. **Degenhardt, K., R. Sundararajan, T. Lindsten, C. Thompson, and E. White.** 2002. Bax and Bak independently promote cytochrome C release from mitochondria. J Biol Chem **277:**14127-34.

92. **Dejean, L. M., S. Martinez-Caballero, L. Guo, C. Hughes, O. Teijido, T. Ducret, F. Ichas, S. J. Korsmeyer, B. Antonsson, E. A. Jonas, and K. W. Kinnally.** 2005. Oligomeric Bax is a component of the putative cytochrome c release channel MAC, mitochondrial apoptosis-induced channel. Mol Biol Cell **16:**2424-32.

93. **Desagher, S., A. Osen-Sand, A. Nichols, R. Eskes, S. Montessuit, S. Lauper, K. Maundrell, B. Antonsson, and J. C. Martinou.** 1999. Bid-induced conformational change of Bax is responsible for mitochondrial cytochrome c release during apoptosis. J Cell Biol **144:**891-901.

94. **Dijkers, P. F., K. U. Birkenkamp, E. W. Lam, N. S. Thomas, J. W. Lammers, L. Koenderman, and P. J. Coffer.** 2002. FKHR-L1 can act as a critical effector of cell death induced by cytokine withdrawal: protein kinase B-enhanced cell survival through maintenance of mitochondrial integrity. J Cell Biol **156:**531-42.

95. **Dijkers, P. F., R. H. Medema, J. W. Lammers, L. Koenderman, and P. J. Coffer.** 2000. Expression of the pro-apoptotic Bcl-2 family member Bim is regulated by the forkhead transcription factor FKHR-L1. Curr Biol **10:**1201-4.

96. **DiPerna, G., J. Stack, A. G. Bowie, A. Boyd, G. Kotwal, Z. Zhang, S. Arvikar, E. Latz, K. A. Fitzgerald, and W. L. Marshall.** 2004. Poxvirus protein N1L targets the I-kappaB kinase complex, inhibits signaling to NF-kappaB by the tumor necrosis factor superfamily of receptors, and inhibits NF-kappaB and IRF3 signaling by toll-like receptors. J Biol Chem **279:**36570-8.

97. **Douglas, A. E., K. D. Corbett, J. M. Berger, G. McFadden, and T. M. Handel.** 2007. Structure of M11L: A myxoma virus structural homolog of the apoptosis inhibitor, Bcl-2. Protein Sci **16:**695-703.

98. **Du, C., M. Fang, Y. Li, L. Li, and X. Wang.** 2000. Smac, a mitochondrial protein that promotes cytochrome c-dependent caspase activation by eliminating IAP inhibition. Cell **102:**33-42.

99. **Duckett, C. S., V. E. Nava, R. W. Gedrich, R. J. Clem, J. L. Van Dongen, M. C. Gilfillan, H. Shiels, J. M. Hardwick, and C. B. Thompson.** 1996. A conserved family of cellular genes related to the baculovirus iap gene and encoding apoptosis inhibitors. Embo J **15:**2685-94.

100. **Earl, P. L., and B. Moss.** 1991. Generation of recombinant vaccinia viruses, p. 16.17.1–16.17.16. *In* F. M. Ausubel, R. Brent, R. E. Kingston, D. D. Moore, J. G. Seidman, J. A. Smith, and K. Struhl (ed.), Current Protocols in Molecular Biology. Greene Publishing Associates & Wiley Interscience, New York.

101. **Eskes, R., S. Desagher, B. Antonsson, and J. C. Martinou.** 2000. Bid induces the oligomerization and insertion of Bax into the outer mitochondrial membrane. Mol Cell Biol **20:**929-35.

102. **Esteban, D. J., and R. M. Buller.** 2005. Ectromelia virus: the causative agent of mousepox. J Gen Virol **86:**2645-59.

103. **Everett, H., M. Barry, S. F. Lee, X. Sun, K. Graham, J. Stone, R. C. Bleackley, and G. McFadden.** 2000. M11L: a novel mitochondria-localized protein of myxoma virus that blocks apoptosis of infected leukocytes. J Exp Med **191:**1487-98.

104. **Everett, H., M. Barry, X. Sun, S. F. Lee, C. Frantz, L. G. Berthiaume, G. McFadden, and R. C. Bleackley.** 2002. The myxoma poxvirus protein, M11L, prevents

apoptosis by direct interaction with the mitochondrial permeability transition pore. J Exp Med **196:**1127-39.

105. **Everett, H., and G. McFadden.** 2002. Poxviruses and apoptosis: a time to die. Curr Opin Microbiol **5:**395-402.

106. **Faccio, L., C. Fusco, A. Chen, S. Martinotti, J. V. Bonventre, and A. S. Zervos.** 2000. Characterization of a novel human serine protease that has extensive homology to bacterial heat shock endoprotease HtrA and is regulated by kidney ischemia. J Biol Chem **275:**2581-8.

107. **Farrow, S. N., J. H. White, I. Martinou, T. Raven, K. T. Pun, C. J. Grinham, J. C. Martinou, and R. Brown.** 1995. Cloning of a bcl-2 homologue by interaction with adenovirus E1B 19K. Nature **374:**731-3.

108. **Favata, M. F., K. Y. Horiuchi, E. J. Manos, A. J. Daulerio, D. A. Stradley, W. S. Feeser, D. E. Van Dyk, W. J. Pitts, R. A. Earl, F. Hobbs, R. A. Copeland, R. L. Magolda, P. A. Scherle, and J. M. Trzaskos.** 1998. Identification of a novel inhibitor of mitogen-activated protein kinase kinase. J Biol Chem **273:**18623-32.

109. **Fenner, F.** 1996. Poxviruses. *In* B. N. Fields, D. M. Knipe, and P. M. Howley (ed.), Fields Virology. Lippencott-Raven Publishers, Philadelphia.

110. **Fenner, F., and M. Buller.** 1997. Mousepox. *In* N. Nathanson, et al. (ed.), Viral Pathogenesis. Lippencott-Raven Publishers, Philadelphia.

111. **Fernandes-Alnemri, T., G. Litwack, and E. S. Alnemri.** 1994. CPP32, a novel human apoptotic protein with homology to Caenorhabditis elegans cell death protein Ced-3 and mammalian interleukin-1 beta-converting enzyme. J Biol Chem **269:**30761-4.

112. **Fickenscher, H., S. Hor, H. Kupers, A. Knappe, S. Wittmann, and H. Sticht.** 2002. The interleukin-10 family of cytokines. Trends Immunol **23:**89-96.

113. **Fischer, S. F., H. Ludwig, J. Holzapfel, M. Kvansakul, L. Chen, D. C. Huang, G. Sutter, M. Knese, and G. Hacker.** 2006. Modified vaccinia virus Ankara protein F1L is a novel BH3-domain-binding protein and acts together with the early viral protein E3L to block virus-associated apoptosis. Cell Death Differ **13:**109-18.

114. **Fischer, U., R. U. Janicke, and K. Schulze-Osthoff.** 2003. Many cuts to ruin: a comprehensive update of caspase substrates. Cell Death Differ **10:**76-100.

115. **Fujiki, Y., A. L. Hubbard, S. Fowler, and P. B. Lazarow.** 1982. Isolation of intracellular membranes by means of sodium carbonate treatment: application to endoplasmic reticulum. J Cell Biol **93:**97-102.

116. **Gangappa, S., L. F. van Dyk, T. J. Jewett, S. H. Speck, and H. W. Virgin.** 2002. Identification of the in vivo role of a viral Bcl-2. J Exp Med **195:**931-40.

117. **Garcia, I., I. Martinou, Y. Tsujimoto, and J. C. Martinou.** 1992. Prevention of programmed cell death of sympathetic neurons by the bcl-2 proto-oncogene. Science **258:**302-4.

118. **Garcia, M. A., S. Guerra, J. Gil, V. Jimenez, and M. Esteban.** 2002. Anti-apoptotic and oncogenic properties of the dsRNA-binding protein of vaccinia virus, E3L. Oncogene **21:**8379-87.

119. **Garcia-Calvo, M., E. P. Peterson, B. Leiting, R. Ruel, D. W. Nicholson, and N. A. Thornberry.** 1998. Inhibition of human caspases by peptide-based and macromolecular inhibitors. J Biol Chem **273:**32608-13.

120. **Garcia-Saez, A. J., I. Mingarro, E. Perez-Paya, and J. Salgado.** 2004. Membrane-insertion fragments of Bcl-xL, Bax, and Bid. Biochemistry **43:**10930-43.

121. **Gedey, R., X. L. Jin, O. Hinthong, and J. L. Shisler.** 2006. Poxviral regulation of the host NF-kappaB response: the vaccinia virus M2L protein inhibits induction of NF-kappaB activation via an ERK2 pathway in virus-infected human embryonic kidney cells. J Virol **80:**8676-85.

122. **Germain, M., J. P. Mathai, H. M. McBride, and G. C. Shore.** 2005. Endoplasmic reticulum BIK initiates DRP1-regulated remodelling of mitochondrial cristae during apoptosis. Embo J **24:**1546-56.

123. **Goebel, S. J., G. P. Johnson, M. E. Perkus, S. W. Davis, J. P. Winslow, and E. Paoletti.** 1990. The complete DNA sequence of vaccinia virus. Virology **179:**247-66, 517-63.

124. **Goldmacher, V. S., L. M. Bartle, A. Skaletskaya, C. A. Dionne, N. L. Kedersha, C. A. Vater, J. W. Han, R. J. Lutz, S. Watanabe, E. D. Cahir McFarland, E. D. Kieff, E. S. Mocarski, and T. Chittenden.** 1999. A cytomegalovirus-encoded mitochondria-localized inhibitor of apoptosis structurally unrelated to Bcl-2. Proc Natl Acad Sci U S A **96:**12536-41.

125. **Goldstein, J. C., N. J. Waterhouse, P. Juin, G. I. Evan, and D. R. Green.** 2000. The coordinate release of cytochrome c during apoptosis is rapid, complete and kinetically invariant. Nat Cell Biol **2:**156-62.

126. **Goping, I. S., A. Gross, J. N. Lavoie, M. Nguyen, R. Jemmerson, K. Roth, S. J. Korsmeyer, and G. C. Shore.** 1998. Regulated targeting of BAX to mitochondria. J Cell Biol **143:**207-15.

127. **Graham, K. A., A. S. Lalani, J. L. Macen, T. L. Ness, M. Barry, L. Y. Liu, A. Lucas, I. Clark-Lewis, R. W. Moyer, and G. McFadden.** 1997. The T1/35kDa family of poxvirus-secreted proteins bind chemokines and modulate leukocyte influx into virus-infected tissues. Virology **229:**12-24.

128. **Graham, K. A., A. Opgenorth, C. Upton, and G. McFadden.** 1992. Myxoma virus M11L ORF encodes a protein for which cell surface localization is critical in manifestation of viral virulence. Virology **191:**112-24.

129. **Green, D. E., and A. Tzagoloff.** 1966. Role of lipids in the structure and function of biological membranes. J Lipid Res **7:**587-602.

130. **Green, D. R., and G. Kroemer.** 2004. The pathophysiology of mitochondrial cell death. Science **305:**626-9.

131. **Griffiths, G. J., B. M. Corfe, P. Savory, S. Leech, M. D. Esposti, J. A. Hickman, and C. Dive.** 2001. Cellular damage signals promote sequential changes at the N-terminus and BH-1 domain of the pro-apoptotic protein Bak. Oncogene **20:**7668-76.

132. **Griffiths, G. J., L. Dubrez, C. P. Morgan, N. A. Jones, J. Whitehouse, B. M. Corfe, C. Dive, and J. A. Hickman.** 1999. Cell damage-induced conformational changes of the pro-apoptotic protein Bak in vivo precede the onset of apoptosis. J Cell Biol **144:**903-14.

133. **Gross, A., J. Jockel, M. C. Wei, and S. J. Korsmeyer.** 1998. Enforced dimerization of BAX results in its translocation, mitochondrial dysfunction and apoptosis. Embo J **17:**3878-85.

134. **Gross, A., J. M. McDonnell, and S. J. Korsmeyer.** 1999. BCL-2 family members and the mitochondria in apoptosis. Genes Dev **13:**1899-911.

135. **Gubser, C., D. Bergamaschi, M. Hollinshead, X. Lu, F. J. van Kuppeveld, and G. L. Smith.** 2007. A new inhibitor of apoptosis from vaccinia virus and eukaryotes. PLoS Pathog **3:**e17.

136. **Guihard, G., G. Bellot, C. Moreau, G. Pradal, N. Ferry, R. Thomy, P. Fichet, K. Meflah, and F. M. Vallette.** 2004. The mitochondrial apoptosis-induced channel (MAC) corresponds to a late apoptotic event. J Biol Chem **279:**46542-50.

137. **Guo, B., D. Zhai, E. Cabezas, K. Welsh, S. Nouraini, A. C. Satterthwait, and J. C. Reed.** 2003. Humanin peptide suppresses apoptosis by interfering with Bax activation. Nature **423:**456-61.

138. **Halestrap, A.** 2005. Biochemistry: a pore way to die. Nature **434:**578-9.

139. **Halestrap, A. P., G. P. McStay, and S. J. Clarke.** 2002. The permeability transition pore complex: another view. Biochimie **84:**153-66.

140. **Han, J., L. A. Goldstein, B. R. Gastman, C. J. Froelich, X. M. Yin, and H. Rabinowich.** 2004. Degradation of Mcl-1 by granzyme B: implications for Bim-mediated mitochondrial apoptotic events. J Biol Chem **279:**22020-9.

141. **Han, J., L. A. Goldstein, B. R. Gastman, A. Rabinovitz, and H. Rabinowich.** 2005. Disruption of Mcl-1.Bim complex in granzyme B-mediated mitochondrial apoptosis. J Biol Chem **280:**16383-92.

142. **Han, J., L. A. Goldstein, B. R. Gastman, and H. Rabinowich.** 2006. Interrelated roles for Mcl-1 and BIM in regulation of TRAIL-mediated mitochondrial apoptosis. J Biol Chem **281:**10153-63.

143. **Han, J., D. Modha, and E. White.** 1998. Interaction of E1B 19K with Bax is required to block Bax-induced loss of mitochondrial membrane potential and apoptosis. Oncogene **17:**2993-3005.

144. **Han, J., P. Sabbatini, D. Perez, L. Rao, D. Modha, and E. White.** 1996. The E1B 19K protein blocks apoptosis by interacting with and inhibiting the p53-inducible and death-promoting Bax protein. Genes Dev **10:**461-77.

145. **Han, J., P. Sabbatini, and E. White.** 1996. Induction of apoptosis by human Nbk/Bik, a BH3-containing protein that interacts with E1B 19K. Mol Cell Biol **16:**5857-64.

146. **Hao, Z., G. S. Duncan, C. C. Chang, A. Elia, M. Fang, A. Wakeham, H. Okada, T. Calzascia, Y. Jang, A. You-Ten, W. C. Yeh, P. Ohashi, X. Wang, and T. W. Mak.** 2005. Specific ablation of the apoptotic functions of cytochrome C reveals a differential requirement for cytochrome C and Apaf-1 in apoptosis. Cell **121:**579-91.

147. **Harada, H., B. Quearry, A. Ruiz-Vela, and S. J. Korsmeyer.** 2004. Survival factor-induced extracellular signal-regulated kinase phosphorylates BIM, inhibiting its association with BAX and proapoptotic activity. Proc Natl Acad Sci U S A **101:**15313-7.

148. **Hardwick, J. M., and D. S. Bellows.** 2003. Viral versus cellular BCL-2 proteins. Cell Death Differ **10 Suppl 1:**S68-76.

149. **Hegde, R., S. M. Srinivasula, Z. Zhang, R. Wassell, R. Mukattash, L. Cilenti, G. DuBois, Y. Lazebnik, A. S. Zervos, T. Fernandes-Alnemri, and E. S. Alnemri.** 2002. Identification of Omi/HtrA2 as a mitochondrial apoptotic serine protease that disrupts inhibitor of apoptosis protein-caspase interaction. J Biol Chem **277:**432-8.

150. **Heimlich, G., A. D. McKinnon, K. Bernardo, D. Brdiczka, J. C. Reed, R. Kain, M. Kronke, and J. M. Jurgensmeier.** 2004. Bax-induced cytochrome c release from mitochondria depends on alpha-helices-5 and -6. Biochem J **378:**247-55.

151. **Hengartner, M. O.** 2000. The biochemistry of apoptosis. Nature **407:**770-6.

152. **Hicke, L.** 2001. Protein regulation by monoubiquitin. Nat Rev Mol Cell Biol **2:**195-201.

153. **Hnatiuk, S., M. Barry, W. Zeng, L. Liu, A. Lucas, D. Percy, and G. McFadden.** 1999. Role of the C-terminal RDEL motif of the myxoma virus M-T4 protein in terms of apoptosis regulation and viral pathogenesis. Virology **263:**290-306.

154. **Hockenbery, D., G. Nunez, C. Milliman, R. D. Schreiber, and S. J. Korsmeyer.** 1990. Bcl-2 is an inner mitochondrial membrane protein that blocks programmed cell death. Nature **348:**334-6.

155. **Hofmann, R. M., and C. M. Pickart.** 2001. In vitro assembly and recognition of Lys-63 polyubiquitin chains. J Biol Chem **276:**27936-43.

156. **Hsu, Y. T., K. G. Wolter, and R. J. Youle.** 1997. Cytosol-to-membrane redistribution of Bax and Bcl-X(L) during apoptosis. Proc Natl Acad Sci U S A **94:**3668-72.

157. **Hsu, Y. T., and R. J. Youle.** 1998. Bax in murine thymus is a soluble monomeric protein that displays differential detergent-induced conformations. J Biol Chem **273:**10777-83.

158. **Hsu, Y. T., and R. J. Youle.** 1997. Nonionic detergents induce dimerization among members of the Bcl-2 family. J Biol Chem **272:**13829-34.

159. **Hu, F. Q., C. A. Smith, and D. J. Pickup.** 1994. Cowpox virus contains two copies of an early gene encoding a soluble secreted form of the type II TNF receptor. Virology **204:**343-56.

160. **Hu, S., C. Vincenz, M. Buller, and V. M. Dixit.** 1997. A novel family of viral death effector domain-containing molecules that inhibit both CD-95- and tumor necrosis factor receptor-1-induced apoptosis. J Biol Chem **272:**9621-4.

161. **Huang, J., Q. Huang, X. Zhou, M. M. Shen, A. Yen, S. X. Yu, G. Dong, K. Qu, P. Huang, E. M. Anderson, S. Daniel-Issakani, R. M. Buller, D. G. Payan, and H. H. Lu.** 2004. The poxvirus p28 virulence factor is an E3 ubiquitin ligase. J Biol Chem **279:**54110-6.

162. **Huang, Q., A. M. Petros, H. W. Virgin, S. W. Fesik, and E. T. Olejniczak.** 2002. Solution structure of a Bcl-2 homolog from Kaposi sarcoma virus. Proc Natl Acad Sci U S A **99:**3428-33.

163. **Huang, Q., A. M. Petros, H. W. Virgin, S. W. Fesik, and E. T. Olejniczak.** 2003. Solution structure of the BHRF1 protein from Epstein-Barr virus, a homolog of human Bcl-2. J Mol Biol **332:**1123-30.

164. **Huttner, W. B., and A. Schmidt.** 2000. Lipids, lipid modification and lipid-protein interaction in membrane budding and fission--insights from the roles of endophilin A1 and synaptophysin in synaptic vesicle endocytosis. Curr Opin Neurobiol **10:**543-51.

165. **Imaizumi, K., M. Tsuda, Y. Imai, A. Wanaka, T. Takagi, and M. Tohyama.** 1997. Molecular cloning of a novel polypeptide, DP5, induced during programmed neuronal death. J Biol Chem **272:**18842-8.

166. **Inohara, N., L. Ding, S. Chen, and G. Nunez.** 1997. harakiri, a novel regulator of cell death, encodes a protein that activates apoptosis and interacts selectively with survival-promoting proteins Bcl-2 and Bcl-X(L). Embo J **16:**1686-94.

167. **Jenner, E.** 1966. An inquiry into the causes and effects of the variolae vaccinae, 1st Reprint ed. Dawsons, London.

168. **Joazeiro, C. A., and A. M. Weissman.** 2000. RING finger proteins: mediators of ubiquitin ligase activity. Cell **102:**549-52.

169. **Johnston, J. B., and G. McFadden.** 2003. Poxvirus immunomodulatory strategies: current perspectives. J Virol **77:**6093-100.

170. **Karbowski, M., S. Y. Jeong, and R. J. Youle.** 2004. Endophilin B1 is required for the maintenance of mitochondrial morphology. J Cell Biol **166:**1027-39.

171. **Karbowski, M., K. L. Norris, M. M. Cleland, S. Y. Jeong, and R. J. Youle.** 2006. Role of Bax and Bak in mitochondrial morphogenesis. Nature **443:**658-62.

172. **Kashkar, H., K. Wiegmann, B. Yazdanpanah, D. Haubert, and M. Kronke.** 2005. Acid sphingomyelinase is indispensable for UV light-induced Bax conformational change at the mitochondrial membrane. J Biol Chem **280:**20804-13.

173. **Kaufmann, S. H., S. Desnoyers, Y. Ottaviano, N. E. Davidson, and G. G. Poirier.** 1993. Specific proteolytic cleavage of poly(ADP-ribose) polymerase: an early marker of chemotherapy-induced apoptosis. Cancer Res **53**:3976-85.

174. **Kawanishi, M., S. Tada-Oikawa, and S. Kawanishi.** 2002. Epstein-Barr virus BHRF1 functions downstream of Bid cleavage and upstream of mitochondrial dysfunction to inhibit TRAIL-induced apoptosis in BJAB cells. Biochem Biophys Res Commun **297**:682-7.

175. **Kerr, J. F., A. H. Wyllie, and A. R. Currie.** 1972. Apoptosis: a basic biological phenomenon with wide-ranging implications in tissue kinetics. Br J Cancer **26**:239-57.

176. **Kibler, K. V., T. Shors, K. B. Perkins, C. C. Zeman, M. P. Banaszak, J. Biesterfeldt, J. O. Langland, and B. L. Jacobs.** 1997. Double-stranded RNA is a trigger for apoptosis in vaccinia virus-infected cells. J Virol **71**:1992-2003.

177. **Kiefer, M. C., M. J. Brauer, V. C. Powers, J. J. Wu, S. R. Umansky, L. D. Tomei, and P. J. Barr.** 1995. Modulation of apoptosis by the widely distributed Bcl-2 homologue Bak. Nature **374**:736-9.

178. **Kim, P. K., M. G. Annis, P. J. Dlugosz, B. Leber, and D. W. Andrews.** 2004. During apoptosis bcl-2 changes membrane topology at both the endoplasmic reticulum and mitochondria. Mol Cell **14**:523-9.

179. **Kluck, R. M., E. Bossy-Wetzel, D. R. Green, and D. D. Newmeyer.** 1997. The release of cytochrome c from mitochondria: a primary site for Bcl-2 regulation of apoptosis. Science **275**:1132-6.

180. **Komiyama, T., C. A. Ray, D. J. Pickup, A. D. Howard, N. A. Thornberry, E. P. Peterson, and G. Salvesen.** 1994. Inhibition of interleukin-1 beta converting enzyme by the cowpox virus serpin CrmA. An example of cross-class inhibition. J Biol Chem **269**:19331-7.

181. **Kotwal, G. J., A. W. Hugin, and B. Moss.** 1989. Mapping and insertional mutagenesis of a vaccinia virus gene encoding a 13,800-Da secreted protein. Virology **171**:579-87.

182. **Kotwal, G. J., and B. Moss.** 1988. Analysis of a large cluster of nonessential genes deleted from a vaccinia virus terminal transposition mutant. Virology **167**:524-37.

183. **Kozopas, K. M., T. Yang, H. L. Buchan, P. Zhou, and R. W. Craig.** 1993. MCL1, a gene expressed in programmed myeloid cell differentiation, has sequence similarity to BCL2. Proc Natl Acad Sci U S A **90**:3516-20.

184. **Krajewski, S., C. Blomqvist, K. Franssila, M. Krajewska, V. M. Wasenius, E. Niskanen, S. Nordling, and J. C. Reed.** 1995. Reduced expression of proapoptotic gene BAX is associated with poor response rates to combination chemotherapy and shorter survival in women with metastatic breast adenocarcinoma. Cancer Res **55**:4471-8.

185. **Kroemer, G., L. Galluzzi, and C. Brenner.** 2007. Mitochondrial membrane permeabilization in cell death. Physiol Rev **87**:99-163.

186. **Kroemer, G., and J. C. Reed.** 2000. Mitochondrial control of cell death. Nat Med **6:**513-9.

187. **Kuwana, T., L. Bouchier-Hayes, J. E. Chipuk, C. Bonzon, B. A. Sullivan, D. R. Green, and D. D. Newmeyer.** 2005. BH3 domains of BH3-only proteins differentially regulate Bax-mediated mitochondrial membrane permeabilization both directly and indirectly. Mol Cell **17:**525-35.

188. **Kuwana, T., M. R. Mackey, G. Perkins, M. H. Ellisman, M. Latterich, R. Schneiter, D. R. Green, and D. D. Newmeyer.** 2002. Bid, Bax, and lipids cooperate to form supramolecular openings in the outer mitochondrial membrane. Cell **111:**331-42.

189. **Kvansakul, M., M. F. van Delft, E. F. Lee, J. M. Gulbis, W. D. Fairlie, D. C. Huang, and P. M. Colman.** 2007. A structural viral mimic of prosurvival bcl-2: a pivotal role for sequestering proapoptotic bax and bak. Mol Cell **25:**933-42.

190. **Laemmli, U. K.** 1970. Cleavage of structural proteins during the assembly of the head of bacteriophage T4. Nature **227:**680-5.

191. **Law, K. M., and G. L. Smith.** 1992. A vaccinia serine protease inhibitor which prevents virus-induced cell fusion. J Gen Virol **73 (Pt 3):**549-57.

192. **Lee, S. B., and M. Esteban.** 1994. The interferon-induced double-stranded RNA-activated protein kinase induces apoptosis. Virology **199:**491-6.

193. **Lei, K., and R. J. Davis.** 2003. JNK phosphorylation of Bim-related members of the Bcl2 family induces Bax-dependent apoptosis. Proc Natl Acad Sci U S A **100:**2432-7.

194. **Letai, A., M. C. Bassik, L. D. Walensky, M. D. Sorcinelli, S. Weiler, and S. J. Korsmeyer.** 2002. Distinct BH3 domains either sensitize or activate mitochondrial apoptosis, serving as prototype cancer therapeutics. Cancer Cell **2:**183-92.

195. **Leu, J. I., P. Dumont, M. Hafey, M. E. Murphy, and D. L. George.** 2004. Mitochondrial p53 activates Bak and causes disruption of a Bak-Mcl1 complex. Nat Cell Biol **6:**443-50.

196. **Ley, R., K. E. Ewings, K. Hadfield, and S. J. Cook.** 2005. Regulatory phosphorylation of Bim: sorting out the ERK from the JNK. Cell Death Differ **12:**1008-14.

197. **Ley, R., K. E. Ewings, K. Hadfield, E. Howes, K. Balmanno, and S. J. Cook.** 2004. Extracellular signal-regulated kinases 1/2 are serum-stimulated "Bim(EL) kinases" that bind to the BH3-only protein Bim(EL) causing its phosphorylation and turnover. J Biol Chem **279:**8837-47.

198. **Ley, R., K. Hadfield, E. Howes, and S. J. Cook.** 2005. Identification of a DEF-type docking domain for extracellular signal-regulated kinases 1/2 that directs phosphorylation and turnover of the BH3-only protein BimEL. J Biol Chem **280:**17657-63.

199. **Li, H., H. Zhu, C. J. Xu, and J. Yuan.** 1998. Cleavage of BID by caspase 8 mediates the mitochondrial damage in the Fas pathway of apoptosis. Cell **94:**491-501.

200. **Li, L. Y., X. Luo, and X. Wang.** 2001. Endonuclease G is an apoptotic DNase when released from mitochondria. Nature **412**:95-9.

201. **Li, P., D. Nijhawan, I. Budihardjo, S. M. Srinivasula, M. Ahmad, E. S. Alnemri, and X. Wang.** 1997. Cytochrome c and dATP-dependent formation of Apaf-1/caspase-9 complex initiates an apoptotic protease cascade. Cell **91**:479-89.

202. **Li, Q., P. Liston, and R. W. Moyer.** 2005. Functional analysis of the inhibitor of apoptosis (iap) gene carried by the entomopoxvirus of Amsacta moorei. J Virol **79**:2335-45.

203. **Li, Q., P. Liston, N. Schokman, J. M. Ho, and R. W. Moyer.** 2005. Amsacta moorei Entomopoxvirus inhibitor of apoptosis suppresses cell death by binding Grim and Hid. J Virol **79**:3684-91.

204. **Lindsten, T., A. J. Ross, A. King, W. X. Zong, J. C. Rathmell, H. A. Shiels, E. Ulrich, K. G. Waymire, P. Mahar, K. Frauwirth, Y. Chen, M. Wei, V. M. Eng, D. M. Adelman, M. C. Simon, A. Ma, J. A. Golden, G. Evan, S. J. Korsmeyer, G. R. MacGregor, and C. B. Thompson.** 2000. The combined functions of proapoptotic Bcl-2 family members bak and bax are essential for normal development of multiple tissues. Mol Cell **6**:1389-99.

205. **Liu, Q. A., and M. O. Hengartner.** 1999. The molecular mechanism of programmed cell death in C. elegans. Ann N Y Acad Sci **887**:92-104.

206. **Liu, X., S. Dai, Y. Zhu, P. Marrack, and J. W. Kappler.** 2003. The structure of a Bcl-xL/Bim fragment complex: implications for Bim function. Immunity **19**:341-52.

207. **Liu, X., C. N. Kim, J. Yang, R. Jemmerson, and X. Wang.** 1996. Induction of apoptotic program in cell-free extracts: requirement for dATP and cytochrome c. Cell **86**:147-57.

208. **Loh, J., Q. Huang, A. M. Petros, D. Nettesheim, L. F. van Dyk, L. Labrada, S. H. Speck, B. Levine, E. T. Olejniczak, and H. W. Virgin.** 2005. A surface groove essential for viral Bcl-2 function during chronic infection in vivo. PLoS Pathog **1**:e10.

209. **Lomo, J., E. B. Smeland, S. Krajewski, J. C. Reed, and H. K. Blomhoff.** 1996. Expression of the Bcl-2 homologue Mcl-1 correlates with survival of peripheral blood B lymphocytes. Cancer Res **56**:40-3.

210. **Luciano, F., A. Jacquel, P. Colosetti, M. Herrant, S. Cagnol, G. Pages, and P. Auberger.** 2003. Phosphorylation of Bim-EL by Erk1/2 on serine 69 promotes its degradation via the proteasome pathway and regulates its proapoptotic function. Oncogene **22**:6785-93.

211. **Ludwig, H., Y. Suezer, Z. Waibler, U. Kalinke, B. S. Schnierle, and G. Sutter.** 2006. Double-stranded RNA-binding protein E3 controls translation of viral intermediate RNA, marking an essential step in the life cycle of modified vaccinia virus Ankara. J Gen Virol **87**:1145-55.

212. **Luo, X., I. Budihardjo, H. Zou, C. Slaughter, and X. Wang.** 1998. Bid, a Bcl2 interacting protein, mediates cytochrome c release from mitochondria in response to activation of cell surface death receptors. Cell **94:**481-90.

213. **Macen, J., A. Takahashi, K. B. Moon, R. Nathaniel, P. C. Turner, and R. W. Moyer.** 1998. Activation of caspases in pig kidney cells infected with wild-type and CrmA/SPI-2 mutants of cowpox and rabbitpox viruses. J Virol **72:**3524-33.

214. **Macen, J. L., K. A. Graham, S. F. Lee, M. Schreiber, L. K. Boshkov, and G. McFadden.** 1996. Expression of the myxoma virus tumor necrosis factor receptor homologue and M11L genes is required to prevent virus-induced apoptosis in infected rabbit T lymphocytes. Virology **218:**232-7.

215. **Mackett, M., G. L. Smith, and B. Moss.** 1984. General method for production and selection of infectious vaccinia virus recombinants expressing foreign genes. J Virol **49:**857-64.

216. **MacNeill, A. L., P. C. Turner, and R. W. Moyer.** 2006. Mutation of the Myxoma virus SERP2 P1-site to prevent proteinase inhibition causes apoptosis in cultured RK-13 cells and attenuates disease in rabbits, but mutation to alter specificity causes apoptosis without reducing virulence. Virology **356:**12-22.

217. **Malka, F., A. Lombes, and M. Rojo.** 2006. Organization, dynamics and transmission of mitochondrial DNA: focus on vertebrate nucleoids. Biochim Biophys Acta **1763:**463-72.

218. **Marani, M., D. Hancock, R. Lopes, T. Tenev, J. Downward, and N. R. Lemoine.** 2004. Role of Bim in the survival pathway induced by Raf in epithelial cells. Oncogene **23:**2431-41.

219. **Marani, M., T. Tenev, D. Hancock, J. Downward, and N. R. Lemoine.** 2002. Identification of novel isoforms of the BH3 domain protein Bim which directly activate Bax to trigger apoptosis. Mol Cell Biol **22:**3577-89.

220. **Marchal, J.** 1930. Infectious ectromelia. A hitherto undescribed virus disease of mice. J Pathol **33:**713-728.

221. **Marchetti, P., M. Castedo, S. A. Susin, N. Zamzami, T. Hirsch, A. Macho, A. Haeffner, F. Hirsch, M. Geuskens, and G. Kroemer.** 1996. Mitochondrial permeability transition is a central coordinating event of apoptosis. J Exp Med **184:**1155-60.

222. **Martins, L. M., I. Iaccarino, T. Tenev, S. Gschmeissner, N. F. Totty, N. R. Lemoine, J. Savopoulos, C. W. Gray, C. L. Creasy, C. Dingwall, and J. Downward.** 2002. The serine protease Omi/HtrA2 regulates apoptosis by binding XIAP through a reaper-like motif. J Biol Chem **277:**439-44.

223. **McBride, H. M., M. Neuspiel, and S. Wasiak.** 2006. Mitochondria: more than just a powerhouse. Curr Biol **16:**R551-60.

224. **McCormick, A. L., V. L. Smith, D. Chow, and E. S. Mocarski.** 2003. Disruption of mitochondrial networks by the human cytomegalovirus UL37 gene product viral mitochondrion-localized inhibitor of apoptosis. J Virol **77:**631-41.

225. **McDonnell, J. M., D. Fushman, C. L. Milliman, S. J. Korsmeyer, and D. Cowburn.** 1999. Solution structure of the proapoptotic molecule BID: a structural basis for apoptotic agonists and antagonists. Cell **96:**625-34.

226. **Meng, X., A. Embry, D. Sochia, and Y. Xiang.** 2007. Vaccinia virus A6L encodes a virion core protein required for formation of mature virion. J Virol **81:**1433-43.

227. **Messud-Petit, F., J. Gelfi, M. Delverdier, M. F. Amardeilh, R. Py, G. Sutter, and S. Bertagnoli.** 1998. Serp2, an inhibitor of the interleukin-1beta-converting enzyme, is critical in the pathobiology of myxoma virus. J Virol **72:**7830-9.

228. **Metivier, D., B. Dallaporta, N. Zamzami, N. Larochette, S. A. Susin, I. Marzo, and G. Kroemer.** 1998. Cytofluorometric detection of mitochondrial alterations in early CD95/Fas/APO-1-triggered apoptosis of Jurkat T lymphoma cells. Comparison of seven mitochondrion-specific fluorochromes. Immunol Lett **61:**157-63.

229. **Mihara, K.** 2000. Targeting and insertion of nuclear-encoded preproteins into the mitochondrial outer membrane. Bioessays **22:**364-71.

230. **Mikhailov, V., M. Mikhailova, K. Degenhardt, M. A. Venkatachalam, E. White, and P. Saikumar.** 2003. Association of Bax and Bak homo-oligomers in mitochondria. Bax requirement for Bak reorganization and cytochrome c release. J Biol Chem **278:**5367-76.

231. **Mikhailov, V., M. Mikhailova, D. J. Pulkrabek, Z. Dong, M. A. Venkatachalam, and P. Saikumar.** 2001. Bcl-2 prevents Bax oligomerization in the mitochondrial outer membrane. J Biol Chem **276:**18361-74.

232. **Minn, A. J., P. Velez, S. L. Schendel, H. Liang, S. W. Muchmore, S. W. Fesik, M. Fill, and C. B. Thompson.** 1997. Bcl-x(L) forms an ion channel in synthetic lipid membranes. Nature **385:**353-7.

233. **Mitchell, P., and J. Moyle.** 1965. Evidence discriminating between the chemical and the chemiosmotic mechanisms of electron transport phosphorylation. Nature **208:**1205-6.

234. **Mitchell, P., and J. Moyle.** 1965. Stoichiometry of proton translocation through the respiratory chain and adenosine triphosphatase systems of rat liver mitochondria. Nature **208:**147-51.

235. **Moldoveanu, T., Q. Liu, A. Tocilj, M. Watson, G. Shore, and K. Gehring.** 2006. The X-ray structure of a BAK homodimer reveals an inhibitory zinc binding site. Mol Cell **24:**677-88.

236. **Moreau, C., P. F. Cartron, A. Hunt, K. Meflah, D. R. Green, G. Evan, F. M. Vallette, and P. Juin.** 2003. Minimal BH3 peptides promote cell death by antagonizing anti-apoptotic proteins. J Biol Chem **278:**19426-35.

237. **Moss, B.** 1996. Poxviridae: The Viruses and Their Replication. *In* B. N. Fields, D. M. Knipe, and P. M. Howley (ed.), Fields Virology, 3rd ed. Lippincott-Raven Publishers, Philadelphia.

238. **Mossman, K., S. F. Lee, M. Barry, L. Boshkov, and G. McFadden.** 1996. Disruption of M-T5, a novel myxoma virus gene member of poxvirus host range superfamily, results in dramatic attenuation of myxomatosis in infected European rabbits. J Virol **70:**4394-410.

239. **Muchmore, S. W., M. Sattler, H. Liang, R. P. Meadows, J. E. Harlan, H. S. Yoon, D. Nettesheim, B. S. Chang, C. B. Thompson, S. L. Wong, S. L. Ng, and S. W. Fesik.** 1996. X-ray and NMR structure of human Bcl-xL, an inhibitor of programmed cell death. Nature **381:**335-41.

240. **Murphy, K. M., U. N. Streips, and R. B. Lock.** 2000. Bcl-2 inhibits a Fas-induced conformational change in the Bax N terminus and Bax mitochondrial translocation. J Biol Chem **275:**17225-8.

241. **Muzio, M., A. M. Chinnaiyan, F. C. Kischkel, K. O'Rourke, A. Shevchenko, J. Ni, C. Scaffidi, J. D. Bretz, M. Zhang, R. Gentz, M. Mann, P. H. Krammer, M. E. Peter, and V. M. Dixit.** 1996. FLICE, a novel FADD-homologous ICE/CED-3-like protease, is recruited to the CD95 (Fas/APO-1) death--inducing signaling complex. Cell **85:**817-27.

242. **Nakagawa, T., S. Shimizu, T. Watanabe, O. Yamaguchi, K. Otsu, H. Yamagata, H. Inohara, T. Kubo, and Y. Tsujimoto.** 2005. Cyclophilin D-dependent mitochondrial permeability transition regulates some necrotic but not apoptotic cell death. Nature **434:**652-8.

243. **Nakano, K., and K. H. Vousden.** 2001. PUMA, a novel proapoptotic gene, is induced by p53. Mol Cell **7:**683-94.

244. **Nechushtan, A., C. L. Smith, Y. T. Hsu, and R. J. Youle.** 1999. Conformation of the Bax C-terminus regulates subcellular location and cell death. Embo J **18:**2330-41.

245. **Nechushtan, A., C. L. Smith, I. Lamensdorf, S. H. Yoon, and R. J. Youle.** 2001. Bax and Bak coalesce into novel mitochondria-associated clusters during apoptosis. J Cell Biol **153:**1265-76.

246. **Nerenberg, B. T., J. Taylor, E. Bartee, K. Gouveia, M. Barry, and K. Fruh.** 2005. The poxviral RING protein p28 is a ubiquitin ligase that targets ubiquitin to viral replication factories. J Virol **79:**597-601.

247. **Nguyen, M., D. G. Millar, V. W. Yong, S. J. Korsmeyer, and G. C. Shore.** 1993. Targeting of Bcl-2 to the mitochondrial outer membrane by a COOH-terminal signal anchor sequence. J Biol Chem **268:**25265-8.

248. **Nijhawan, D., M. Fang, E. Traer, Q. Zhong, W. Gao, F. Du, and X. Wang.** 2003. Elimination of Mcl-1 is required for the initiation of apoptosis following ultraviolet irradiation. Genes Dev **17:**1475-86.

249. **Nunez, G., L. London, D. Hockenbery, M. Alexander, J. P. McKearn, and S. J. Korsmeyer.** 1990. Deregulated Bcl-2 gene expression selectively prolongs survival of growth factor-deprived hemopoietic cell lines. J Immunol **144:**3602-10.

250. **O'Connor, L., A. Strasser, L. A. O'Reilly, G. Hausmann, J. M. Adams, S. Cory, and D. C. Huang.** 1998. Bim: a novel member of the Bcl-2 family that promotes apoptosis. Embo J **17:**384-95.

251. **Oda, E., R. Ohki, H. Murasawa, J. Nemoto, T. Shibue, T. Yamashita, T. Tokino, T. Taniguchi, and N. Tanaka.** 2000. Noxa, a BH3-only member of the Bcl-2 family and candidate mediator of p53-induced apoptosis. Science **288:**1053-8.

252. **Oda, K. I., and W. K. Joklik.** 1967. Hybridization and sedimentation studies on "early" and "late" vaccinia messenger RNA. J Mol Biol **27:**395-419.

253. **Oltvai, Z. N., C. L. Milliman, and S. J. Korsmeyer.** 1993. Bcl-2 heterodimerizes in vivo with a conserved homolog, Bax, that accelerates programmed cell death. Cell **74:**609-19.

254. **Opgenorth, A., K. Graham, N. Nation, D. Strayer, and G. McFadden.** 1992. Deletion analysis of two tandemly arranged virulence genes in myxoma virus, M11L and myxoma growth factor. J Virol **66:**4720-31.

255. **Parone, P. A., D. I. James, S. Da Cruz, Y. Mattenberger, O. Donze, F. Barja, and J. C. Martinou.** 2006. Inhibiting the mitochondrial fission machinery does not prevent Bax/Bak-dependent apoptosis. Mol Cell Biol **26:**7397-408.

256. **Pavlov, E. V., M. Priault, D. Pietkiewicz, E. H. Cheng, B. Antonsson, S. Manon, S. J. Korsmeyer, C. A. Mannella, and K. W. Kinnally.** 2001. A novel, high conductance channel of mitochondria linked to apoptosis in mammalian cells and Bax expression in yeast. J Cell Biol **155:**725-31.

257. **Perez, D., and E. White.** 2000. TNF-alpha signals apoptosis through a bid-dependent conformational change in Bax that is inhibited by E1B 19K. Mol Cell **6:**53-63.

258. **Perkus, M. E., S. J. Goebel, S. W. Davis, G. P. Johnson, E. K. Norton, and E. Paoletti.** 1991. Deletion of 55 open reading frames from the termini of vaccinia virus. Virology **180:**406-10.

259. **Petros, A. M., A. Medek, D. G. Nettesheim, D. H. Kim, H. S. Yoon, K. Swift, E. D. Matayoshi, T. Oltersdorf, and S. W. Fesik.** 2001. Solution structure of the antiapoptotic protein bcl-2. Proc Natl Acad Sci U S A **98:**3012-7.

260. **Petros, A. M., D. G. Nettesheim, Y. Wang, E. T. Olejniczak, R. P. Meadows, J. Mack, K. Swift, E. D. Matayoshi, H. Zhang, C. B. Thompson, and S. W. Fesik.** 2000. Rationale for Bcl-xL/Bad peptide complex formation from structure, mutagenesis, and biophysical studies. Protein Sci **9:**2528-34.

261. **Pickup, D. J., B. S. Ink, W. Hu, C. A. Ray, and W. K. Joklik.** 1986. Hemorrhage in lesions caused by cowpox virus is induced by a viral protein that is related to plasma protein inhibitors of serine proteases. Proc Natl Acad Sci U S A **83:**7698-702.

262. **Polster, B. M., J. Pevsner, and J. M. Hardwick.** 2004. Viral Bcl-2 homologs and their role in virus replication and associated diseases. Biochim Biophys Acta **1644:**211-27.

263. **Poncet, D., N. Larochette, A. L. Pauleau, P. Boya, A. A. Jalil, P. F. Cartron, F. Vallette, C. Schnebelen, L. M. Bartle, A. Skaletskaya, D. Boutolleau, J. C. Martinou, V. S. Goldmacher, G. Kroemer, and N. Zamzami.** 2004. An anti-apoptotic viral protein that recruits Bax to mitochondria. J Biol Chem **279:**22605-14.

264. **Poncet, D., A. L. Pauleau, G. Szabadkai, A. Vozza, S. R. Scholz, M. Le Bras, J. J. Briere, A. Jalil, R. Le Moigne, C. Brenner, G. Hahn, I. Wittig, H. Schagger, C. Lemaire, K. Bianchi, S. Souquere, G. Pierron, P. Rustin, V. S. Goldmacher, R. Rizzuto, F. Palmieri, and G. Kroemer.** 2006. Cytopathic effects of the cytomegalovirus-encoded apoptosis inhibitory protein vMIA. J Cell Biol **174:**985-96.

265. **Postigo, A., J. R. Cross, J. Downward, and M. Way.** 2006. Interaction of F1L with the BH3 domain of Bak is responsible for inhibiting vaccinia-induced apoptosis. Cell Death Differ **13:**1651-62.

266. **Priault, M., B. Chaudhuri, A. Clow, N. Camougrand, and S. Manon.** 1999. Investigation of bax-induced release of cytochrome c from yeast mitochondria permeability of mitochondrial membranes, role of VDAC and ATP requirement. Eur J Biochem **260:**684-91.

267. **Putcha, G. V., S. Le, S. Frank, C. G. Besirli, K. Clark, B. Chu, S. Alix, R. J. Youle, A. LaMarche, A. C. Maroney, and E. M. Johnson, Jr.** 2003. JNK-mediated BIM phosphorylation potentiates BAX-dependent apoptosis. Neuron **38:**899-914.

268. **Putcha, G. V., K. L. Moulder, J. P. Golden, P. Bouillet, J. A. Adams, A. Strasser, and E. M. Johnson.** 2001. Induction of BIM, a proapoptotic BH3-only BCL-2 family member, is critical for neuronal apoptosis. Neuron **29:**615-28.

269. **Puthalakath, H., D. C. Huang, L. A. O'Reilly, S. M. King, and A. Strasser.** 1999. The proapoptotic activity of the Bcl-2 family member Bim is regulated by interaction with the dynein motor complex. Mol Cell **3:**287-96.

270. **Puthalakath, H., and A. Strasser.** 2002. Keeping killers on a tight leash: transcriptional and post-translational control of the pro-apoptotic activity of BH3-only proteins. Cell Death Differ **9:**505-12.

271. **Puthalakath, H., A. Villunger, L. A. O'Reilly, J. G. Beaumont, L. Coultas, R. E. Cheney, D. C. Huang, and A. Strasser.** 2001. Bmf: a proapoptotic BH3-only protein regulated by interaction with the myosin V actin motor complex, activated by anoikis. Science **293:**1829-32.

272. **Quan, L. T., A. Caputo, R. C. Bleackley, D. J. Pickup, and G. S. Salvesen.** 1995. Granzyme B is inhibited by the cowpox virus serpin cytokine response modifier A. J Biol Chem **270:**10377-9.

273. **Rathmell, J. C., and C. B. Thompson.** 1999. The central effectors of cell death in the immune system. Annu Rev Immunol **17:**781-828.

274. **Ray, C. A., R. A. Black, S. R. Kronheim, T. A. Greenstreet, P. R. Sleath, G. S. Salvesen, and D. J. Pickup.** 1992. Viral inhibition of inflammation: cowpox virus encodes an inhibitor of the interleukin-1 beta converting enzyme. Cell **69:**597-604.

275. **Ray, C. A., and D. J. Pickup.** 1996. The mode of death of pig kidney cells infected with cowpox virus is governed by the expression of the crmA gene. Virology **217:**384-91.

276. **Rehling, P., N. Pfanner, and C. Meisinger.** 2003. Insertion of hydrophobic membrane proteins into the inner mitochondrial membrane--a guided tour. J Mol Biol **326:**639-57.

277. **Reisner, A. H.** 1985. Similarity between the vaccinia virus 19K early protein and epidermal growth factor. Nature **313:**801-3.

278. **Revilla, Y., A. Cebrian, E. Baixeras, C. Martinez, E. Vinuela, and M. L. Salas.** 1997. Inhibition of apoptosis by the African swine fever virus Bcl-2 homologue: role of the BH1 domain. Virology **228:**400-4.

279. **Rivas, C., J. Gil, Z. Melkova, M. Esteban, and M. Diaz-Guerra.** 1998. Vaccinia virus E3L protein is an inhibitor of the interferon (i.f.n.)-induced 2-5A synthetase enzyme. Virology **243:**406-14.

280. **Romano, P. R., F. Zhang, S. L. Tan, M. T. Garcia-Barrio, M. G. Katze, T. E. Dever, and A. G. Hinnebusch.** 1998. Inhibition of double-stranded RNA-dependent protein kinase PKR by vaccinia virus E3: role of complex formation and the E3 N-terminal domain. Mol Cell Biol **18:**7304-16.

281. **Rostovtseva, T. K., B. Antonsson, M. Suzuki, R. J. Youle, M. Colombini, and S. M. Bezrukov.** 2004. Bid, but not Bax, regulates VDAC channels. J Biol Chem **279:**13575-83.

282. **Roucou, X., S. Montessuit, B. Antonsson, and J. C. Martinou.** 2002. Bax oligomerization in mitochondrial membranes requires tBid (caspase-8-cleaved Bid) and a mitochondrial protein. Biochem J **368:**915-21.

283. **Roulston, A., R. C. Marcellus, and P. E. Branton.** 1999. Viruses and apoptosis. Annu Rev Microbiol **53:**577-628.

284. **Ruffolo, S. C., and G. C. Shore.** 2003. BCL-2 selectively interacts with the BID-induced open conformer of BAK, inhibiting BAK auto-oligomerization. J Biol Chem **278:**25039-45.

285. **Russell, J. H., and T. J. Ley.** 2002. Lymphocyte-mediated cytotoxicity. Annu Rev Immunol **20:**323-70.

286. **Sabbatini, P., S. K. Chiou, L. Rao, and E. White.** 1995. Modulation of p53-mediated transcriptional repression and apoptosis by the adenovirus E1B 19K protein. Mol Cell Biol **15:**1060-70.

287. **Saelens, X., N. Festjens, L. Vande Walle, M. van Gurp, G. van Loo, and P. Vandenabeele.** 2004. Toxic proteins released from mitochondria in cell death. Oncogene **23:**2861-74.

288. **Salvesen, G. S., and C. S. Duckett.** 2002. IAP proteins: blocking the road to death's door. Nat Rev Mol Cell Biol **3:**401-10.

289. **Sambrook, J., and D. Russel.** 2001. Molecular Cloning: A Laboratory Manual, 3rd ed. Cold Spring Harbor Laboratory Press, Cold Spring Harbor, NY.

290. **Sattler, M., H. Liang, D. Nettesheim, R. P. Meadows, J. E. Harlan, M. Eberstadt, H. S. Yoon, S. B. Shuker, B. S. Chang, A. J. Minn, C. B. Thompson, and S. W. Fesik.** 1997. Structure of Bcl-xL-Bak peptide complex: recognition between regulators of apoptosis. Science **275:**983-6.

291. **Sawada, M., W. Sun, P. Hayes, K. Leskov, D. A. Boothman, and S. Matsuyama.** 2003. Ku70 suppresses the apoptotic translocation of Bax to mitochondria. Nat Cell Biol **5:**320-9.

292. **Scaffidi, C., S. Fulda, A. Srinivasan, C. Friesen, F. Li, K. J. Tomaselli, K. M. Debatin, P. H. Krammer, and M. E. Peter.** 1998. Two CD95 (APO-1/Fas) signaling pathways. Embo J **17:**1675-87.

293. **Scaffidi, C., I. Schmitz, J. Zha, S. J. Korsmeyer, P. H. Krammer, and M. E. Peter.** 1999. Differential modulation of apoptosis sensitivity in CD95 type I and type II cells. J Biol Chem **274:**22532-8.

294. **Schendel, S. L., M. Montal, and J. C. Reed.** 1998. Bcl-2 family proteins as ion-channels. Cell Death Differ **5:**372-80.

295. **Schinzel, A., T. Kaufmann, M. Schuler, J. Martinalbo, D. Grubb, and C. Borner.** 2004. Conformational control of Bax localization and apoptotic activity by Pro168. J Cell Biol **164:**1021-32.

296. **Schreiber, M., and G. McFadden.** 1994. The myxoma virus TNF-receptor homologue (T2) inhibits tumor necrosis factor-alpha in a species-specific fashion. Virology **204:**692-705.

297. **Schreiber, M., K. Rajarathnam, and G. McFadden.** 1996. Myxoma virus T2 protein, a tumor necrosis factor (TNF) receptor homolog, is secreted as a monomer and dimer that each bind rabbit TNFalpha, but the dimer is a more potent TNF inhibitor. J Biol Chem **271:**13333-41.

298. **Scorrano, L.** 2005. Proteins that fuse and fragment mitochondria in apoptosis: con-fissing a deadly con-fusion? J Bioenerg Biomembr **37:**165-70.

299. **Scorrano, L., M. Ashiya, K. Buttle, S. Weiler, S. A. Oakes, C. A. Mannella, and S. J. Korsmeyer.** 2002. A distinct pathway remodels mitochondrial cristae and mobilizes cytochrome c during apoptosis. Dev Cell **2:**55-67.

300. **Scorrano, L., and S. J. Korsmeyer.** 2003. Mechanisms of cytochrome c release by proapoptotic BCL-2 family members. Biochem Biophys Res Commun **304:**437-44.

301. **Sedger, L. M., S. R. Osvath, X. M. Xu, G. Li, F. K. Chan, J. W. Barrett, and G. McFadden.** 2006. Poxvirus tumor necrosis factor receptor (TNFR)-like T2 proteins contain a conserved preligand assembly domain that inhibits cellular TNFR1-induced cell death. J Virol **80:**9300-9.

302. **Sedlak, T. W., Z. N. Oltvai, E. Yang, K. Wang, L. H. Boise, C. B. Thompson, and S. J. Korsmeyer.** 1995. Multiple Bcl-2 family members demonstrate selective dimerizations with Bax. Proc Natl Acad Sci U S A **92:**7834-8.

303. **Seet, B. T., J. B. Johnston, C. R. Brunetti, J. W. Barrett, H. Everett, C. Cameron, J. Sypula, S. H. Nazarian, A. Lucas, and G. McFadden.** 2003. Poxviruses and immune evasion. Annu Rev Immunol **21:**377-423.

304. **Seet, B. T., and G. McFadden.** 2002. Viral chemokine-binding proteins. J Leukoc Biol **72:**24-34.

305. **Sen, G. C.** 2001. Viruses and interferons. Annu Rev Microbiol **55:**255-81.

306. **Senkevich, T. G., E. V. Koonin, and R. M. Buller.** 1994. A poxvirus protein with a RING zinc finger motif is of crucial importance for virulence. Virology **198:**118-28.

307. **Senkevich, T. G., E. J. Wolffe, and R. M. Buller.** 1995. Ectromelia virus RING finger protein is localized in virus factories and is required for virus replication in macrophages. J Virol **69:**4103-11.

308. **Seth, R. B., L. Sun, C. K. Ea, and Z. J. Chen.** 2005. Identification and characterization of MAVS, a mitochondrial antiviral signaling protein that activates NF-kappaB and IRF 3. Cell **122:**669-82.

309. **Sharp, T. V., F. Moonan, A. Romashko, B. Joshi, G. N. Barber, and R. Jagus.** 1998. The vaccinia virus E3L gene product interacts with both the regulatory and the substrate binding regions of PKR: implications for PKR autoregulation. Virology **250:**302-15.

310. **Sharpe, J. C., D. Arnoult, and R. J. Youle.** 2004. Control of mitochondrial permeability by Bcl-2 family members. Biochim Biophys Acta **1644:**107-13.

311. **Shi, Y.** 2002. Mechanisms of caspase activation and inhibition during apoptosis. Mol Cell **9:**459-70.

312. **Shimizu, S., A. Konishi, T. Kodama, and Y. Tsujimoto.** 2000. BH4 domain of antiapoptotic Bcl-2 family members closes voltage-dependent anion channel and inhibits apoptotic mitochondrial changes and cell death. Proc Natl Acad Sci U S A **97:**3100-5.

313. **Shimizu, S., M. Narita, and Y. Tsujimoto.** 1999. Bcl-2 family proteins regulate the release of apoptogenic cytochrome c by the mitochondrial channel VDAC. Nature **399:**483-7.

314. **Shimizu, S., Y. Shinohara, and Y. Tsujimoto.** 2000. Bax and Bcl-xL independently regulate apoptotic changes of yeast mitochondria that require VDAC but not adenine nucleotide translocator. Oncogene **19:**4309-18.

315. **Shisler, J. L., and X. L. Jin.** 2004. The vaccinia virus K1L gene product inhibits host NF-kappaB activation by preventing IkappaBalpha degradation. J Virol **78:**3553-60.

316. **Shisler, J. L., and B. Moss.** 2001. Molluscum contagiosum virus inhibitors of apoptosis: The MC159 v-FLIP protein blocks Fas-induced activation of procaspases and degradation of the related MC160 protein. Virology **282:**14-25.

317. **Shisler, J. L., T. G. Senkevich, M. J. Berry, and B. Moss.** 1998. Ultraviolet-induced cell death blocked by a selenoprotein from a human dermatotropic poxvirus. Science **279:**102-5.

318. **Silverman, G. A., P. I. Bird, R. W. Carrell, F. C. Church, P. B. Coughlin, P. G. Gettins, J. A. Irving, D. A. Lomas, C. J. Luke, R. W. Moyer, P. A. Pemberton, E. Remold-O'Donnell, G. S. Salvesen, J. Travis, and J. C. Whisstock.** 2001. The serpins are an expanding superfamily of structurally similar but functionally diverse proteins. Evolution, mechanism of inhibition, novel functions, and a revised nomenclature. J Biol Chem **276:**33293-6.

319. **Smith, C. A., T. Davis, D. Anderson, L. Solam, M. P. Beckmann, R. Jerzy, S. K. Dower, D. Cosman, and R. G. Goodwin.** 1990. A receptor for tumor necrosis factor defines an unusual family of cellular and viral proteins. Science **248:**1019-23.

320. **Smith, C. A., T. Davis, J. M. Wignall, W. S. Din, T. Farrah, C. Upton, G. McFadden, and R. G. Goodwin.** 1991. T2 open reading frame from the Shope fibroma virus encodes a soluble form of the TNF receptor. Biochem Biophys Res Commun **176:**335-42.

321. **Smith, C. A., F. Q. Hu, T. D. Smith, C. L. Richards, P. Smolak, R. G. Goodwin, and D. J. Pickup.** 1996. Cowpox virus genome encodes a second soluble homologue of cellular TNF receptors, distinct from CrmB, that binds TNF but not LT alpha. Virology **223:**132-47.

322. **Smith, C. A., T. D. Smith, P. J. Smolak, D. Friend, H. Hagen, M. Gerhart, L. Park, D. J. Pickup, D. Torrance, K. Mohler, K. Schooley, and R. G. Goodwin.** 1997. Poxvirus genomes encode a secreted, soluble protein that preferentially inhibits beta chemokine activity yet lacks sequence homology to known chemokine receptors. Virology **236:**316-27.

323. **Smith, G. L., and G. McFadden.** 2002. Smallpox: anything to declare? Nat Rev Immunol **2:**521-7.

324. **Smith, G. L., J. A. Symons, and A. Alcami.** 1999. Immune modulation by proteins secreted from cells infected by vaccinia virus. Arch Virol Suppl **15:**111-29.

325. **Smith, G. L., A. Vanderplasschen, and M. Law.** 2002. The formation and function of extracellular enveloped vaccinia virus. J Gen Virol **83:**2915-31.

326. **Soucie, E. L., M. G. Annis, J. Sedivy, J. Filmus, B. Leber, D. W. Andrews, and L. Z. Penn.** 2001. Myc potentiates apoptosis by stimulating Bax activity at the mitochondria. Mol Cell Biol **21:**4725-36.

327. **Spriggs, M. K., D. E. Hruby, C. R. Maliszewski, D. J. Pickup, J. E. Sims, R. M. Buller, and J. VanSlyke.** 1992. Vaccinia and cowpox viruses encode a novel secreted interleukin-1-binding protein. Cell **71:**145-52.

328. **Stennicke, H. R., C. A. Ryan, and G. S. Salvesen.** 2002. Reprieval from execution: the molecular basis of caspase inhibition. Trends Biochem Sci **27:**94-101.

329. **Stewart, T. L., S. T. Wasilenko, and M. Barry.** 2005. Vaccinia virus F1L protein is a tail-anchored protein that functions at the mitochondria to inhibit apoptosis. J Virol **79:**1084-98.

330. **Strasser, A.** 2005. The role of BH3-only proteins in the immune system. Nat Rev Immunol **5:**189-200.

331. **Stuart, D., K. Graham, M. Schreiber, C. Macaulay, and G. McFadden.** 1991. The target DNA sequence for resolution of poxvirus replicative intermediates is an active late promoter. J Virol **65:**61-70.

332. **Su, J., G. Wang, J. W. Barrett, T. S. Irvine, X. Gao, and G. McFadden.** 2006. Myxoma virus M11L blocks apoptosis through inhibition of conformational activation of Bax at the mitochondria. J Virol **80:**1140-51.

333. **Subramanian, T., B. Tarodi, and G. Chinnadurai.** 1995. p53-independent apoptotic and necrotic cell deaths induced by adenovirus infection: suppression by E1B 19K and Bcl-2 proteins. Cell Growth Differ **6:**131-7.

334. **Sugioka, R., S. Shimizu, and Y. Tsujimoto.** 2004. Fzo1, a protein involved in mitochondrial fusion, inhibits apoptosis. J Biol Chem **279:**52726-34.

335. **Sugiyama, T., S. Shimizu, Y. Matsuoka, Y. Yoneda, and Y. Tsujimoto.** 2002. Activation of mitochondrial voltage-dependent anion channel by a pro-apoptotic BH3-only protein Bim. Oncogene **21:**4944-56.

336. **Sun, Y., and D. W. Leaman.** 2005. Involvement of Noxa in cellular apoptotic responses to interferon, double-stranded RNA, and virus infection. J Biol Chem **280:**15561-8.

337. **Sundararajan, R., A. Cuconati, D. Nelson, and E. White.** 2001. Tumor necrosis factor-alpha induces Bax-Bak interaction and apoptosis, which is inhibited by adenovirus E1B 19K. J Biol Chem **276:**45120-7.

338. **Sundararajan, R., and E. White.** 2001. E1B 19K blocks Bax oligomerization and tumor necrosis factor alpha-mediated apoptosis. J Virol **75:**7506-16.

339. **Susin, S. A., N. Zamzami, M. Castedo, T. Hirsch, P. Marchetti, A. Macho, E. Daugas, M. Geuskens, and G. Kroemer.** 1996. Bcl-2 inhibits the mitochondrial release of an apoptogenic protease. J Exp Med **184:**1331-41.

340. **Suzuki, M., R. J. Youle, and N. Tjandra.** 2000. Structure of Bax: coregulation of dimer formation and intracellular localization. Cell **103:**645-54.

341. **Suzuki, Y., Y. Imai, H. Nakayama, K. Takahashi, K. Takio, and R. Takahashi.** 2001. A serine protease, HtrA2, is released from the mitochondria and interacts with XIAP, inducing cell death. Mol Cell **8:**613-21.

342. **Symons, J. A., A. Alcami, and G. L. Smith.** 1995. Vaccinia virus encodes a soluble type I interferon receptor of novel structure and broad species specificity. Cell **81:**551-60.

343. **Takahashi, Y., M. Karbowski, H. Yamaguchi, A. Kazi, J. Wu, S. M. Sebti, R. J. Youle, and H. G. Wang.** 2005. Loss of bif-1 suppresses bax/bak conformational change and mitochondrial apoptosis. Mol Cell Biol **25:**9369-82.

344. **Tan, K. O., N. Y. Fu, S. K. Sukumaran, S. L. Chan, J. H. Kang, K. L. Poon, B. S. Chen, and V. C. Yu.** 2005. MAP-1 is a mitochondrial effector of Bax. Proc Natl Acad Sci U S A **102:**14623-8.

345. **Tan, K. O., K. M. Tan, S. L. Chan, K. S. Yee, M. Bevort, K. C. Ang, and V. C. Yu.** 2001. MAP-1, a novel proapoptotic protein containing a BH3-like motif that associates with Bax through its Bcl-2 homology domains. J Biol Chem **276:**2802-7.

346. **Tan, T. T., K. Degenhardt, D. A. Nelson, B. Beaudoin, W. Nieves-Neira, P. Bouillet, A. Villunger, J. M. Adams, and E. White.** 2005. Key roles of BIM-driven apoptosis in epithelial tumors and rational chemotherapy. Cancer Cell **7:**227-38.

347. **Tan, Y. J., W. Beerheide, and A. E. Ting.** 1999. Biophysical characterization of the oligomeric state of Bax and its complex formation with Bcl-XL. Biochem Biophys Res Commun **255:**334-9.

348. **Tarodi, B., T. Subramanian, and G. Chinnadurai.** 1994. Epstein-Barr virus BHRF1 protein protects against cell death induced by DNA-damaging agents and heterologous viral infection. Virology **201:**404-7.

349. **Taylor, J. M., and M. Barry.** 2006. Near death experiences: poxvirus regulation of apoptotic death. Virology **344:**139-50.

350. **Taylor, J. M., D. Quilty, L. Banadyga, and M. Barry.** 2006. The vaccinia virus protein F1L interacts with Bim and inhibits activation of the pro-apoptotic protein Bax. J Biol Chem **281:**39728-39.

351. **Teoh, M. L., P. V. Turner, and D. H. Evans.** 2005. Tumorigenic poxviruses up-regulate intracellular superoxide to inhibit apoptosis and promote cell proliferation. J Virol **79:**5799-811.

352. **Terradillos, O., S. Montessuit, D. C. Huang, and J. C. Martinou.** 2002. Direct addition of BimL to mitochondria does not lead to cytochrome c release. FEBS Lett **522:**29-34.

353. **Terrones, O., B. Antonsson, H. Yamaguchi, H. G. Wang, J. Liu, R. M. Lee, A. Herrmann, and G. Basanez.** 2004. Lipidic pore formation by the concerted action of proapoptotic BAX and tBID. J Biol Chem **279:**30081-91.

354. **Tewari, M., and V. M. Dixit.** 1995. Fas- and tumor necrosis factor-induced apoptosis is inhibited by the poxvirus crmA gene product. J Biol Chem **270:**3255-60.

355. **Thome, M., P. Schneider, K. Hofmann, H. Fickenscher, E. Meinl, F. Neipel, C. Mattmann, K. Burns, J. L. Bodmer, M. Schroter, C. Scaffidi, P. H. Krammer, M. E.**

Peter, and J. Tschopp. 1997. Viral FLICE-inhibitory proteins (FLIPs) prevent apoptosis induced by death receptors. Nature **386:**517-21.

356. **Thornberry, N. A., and Y. Lazebnik.** 1998. Caspases: enemies within. Science **281:**1312-6.

357. **Tosi, M. F.** 2005. Innate immune responses to infection. J Allergy Clin Immunol **116:**241-9.

358. **Tsujimoto, Y., and C. M. Croce.** 1986. Analysis of the structure, transcripts, and protein products of bcl-2, the gene involved in human follicular lymphoma. Proc Natl Acad Sci U S A **83:**5214-8.

359. **Tsuruta, F., J. Sunayama, Y. Mori, S. Hattori, S. Shimizu, Y. Tsujimoto, K. Yoshioka, N. Masuyama, and Y. Gotoh.** 2004. JNK promotes Bax translocation to mitochondria through phosphorylation of 14-3-3 proteins. Embo J **23:**1889-99.

360. **Tulman, E. R., C. L. Afonso, Z. Lu, L. Zsak, G. F. Kutish, and D. L. Rock.** 2004. The genome of canarypox virus. J Virol **78:**353-66.

361. **Turner, P. C., M. C. Sancho, S. R. Thoennes, A. Caputo, R. C. Bleackley, and R. W. Moyer.** 1999. Myxoma virus Serp2 is a weak inhibitor of granzyme B and interleukin-1beta-converting enzyme in vitro and unlike CrmA cannot block apoptosis in cowpox virus-infected cells. J Virol **73:**6394-404.

362. **Upton, C., L. Schiff, S. A. Rice, T. Dowdeswell, X. Yang, and G. McFadden.** 1994. A poxvirus protein with a RING finger motif binds zinc and localizes in virus factories. J Virol **68:**4186-95.

363. **Upton, J. P., A. J. Valentijn, L. Zhang, and A. P. Gilmore.** 2007. The N-terminal conformation of Bax regulates cell commitment to apoptosis. Cell Death Differ **14:**932-942.

364. **van Delft, M. F., and D. C. Huang.** 2006. How the Bcl-2 family of proteins interact to regulate apoptosis. Cell Res **16:**203-13.

365. **Vander Heiden, M. G., N. S. Chandel, E. K. Williamson, P. T. Schumacker, and C. B. Thompson.** 1997. Bcl-xL regulates the membrane potential and volume homeostasis of mitochondria. Cell **91:**627-37.

366. **Vaux, D. L., S. Cory, and J. M. Adams.** 1988. Bcl-2 gene promotes haemopoietic cell survival and cooperates with c-myc to immortalize pre-B cells. Nature **335:**440-2.

367. **Vaux, D. L., and J. Silke.** 2005. IAPs, RINGs and ubiquitylation. Nat Rev Mol Cell Biol **6:**287-97.

368. **Verhagen, A. M., J. Silke, P. G. Ekert, M. Pakusch, H. Kaufmann, L. M. Connolly, C. L. Day, A. Tikoo, R. Burke, C. Wrobel, R. L. Moritz, R. J. Simpson, and D. L. Vaux.** 2002. HtrA2 promotes cell death through its serine protease activity and its ability to antagonize inhibitor of apoptosis proteins. J Biol Chem **277:**445-54.

369. **Virgin, H. W. t., P. Latreille, P. Wamsley, K. Hallsworth, K. E. Weck, A. J. Dal Canto, and S. H. Speck.** 1997. Complete sequence and genomic analysis of murine gammaherpesvirus 68. J Virol **71:**5894-904.

370. **Vos, J. C., and H. G. Stunnenberg.** 1988. Derepression of a novel class of vaccinia virus genes upon DNA replication. Embo J **7:**3487-92.

371. **Walensky, L. D., K. Pitter, J. Morash, K. J. Oh, S. Barbuto, J. Fisher, E. Smith, G. L. Verdine, and S. J. Korsmeyer.** 2006. A stapled BID BH3 helix directly binds and activates BAX. Mol Cell **24:**199-210.

372. **Walker, J. R., R. A. Corpina, and J. Goldberg.** 2001. Structure of the Ku heterodimer bound to DNA and its implications for double-strand break repair. Nature **412:**607-14.

373. **Wang, G., J. W. Barrett, S. H. Nazarian, H. Everett, X. Gao, C. Bleackley, K. Colwill, M. F. Moran, and G. McFadden.** 2004. Myxoma virus M11L prevents apoptosis through constitutive interaction with Bak. J Virol **78:**7097-111.

374. **Wang, G. Q., E. Wieckowski, L. A. Goldstein, B. R. Gastman, A. Rabinovitz, A. Gambotto, S. Li, B. Fang, X. M. Yin, and H. Rabinowich.** 2001. Resistance to granzyme B-mediated cytochrome c release in Bak-deficient cells. J Exp Med **194:**1325-37.

375. **Wang, K., A. Gross, G. Waksman, and S. J. Korsmeyer.** 1998. Mutagenesis of the BH3 domain of BAX identifies residues critical for dimerization and killing. Mol Cell Biol **18:**6083-9.

376. **Wang, K., X. M. Yin, D. T. Chao, C. L. Milliman, and S. J. Korsmeyer.** 1996. BID: a novel BH3 domain-only death agonist. Genes Dev **10:**2859-69.

377. **Wang, X.** 2001. The expanding role of mitochondria in apoptosis. Genes Dev **15:**2922-33.

378. **Warr, M. R., S. Acoca, Z. Liu, M. Germain, M. Watson, M. Blanchette, S. S. Wing, and G. C. Shore.** 2005. BH3-ligand regulates access of MCL-1 to its E3 ligase. FEBS Lett **579:**5603-8.

379. **Wasilenko, S. T., L. Banadyga, D. Bond, and M. Barry.** 2005. The vaccinia virus F1L protein interacts with the proapoptotic protein Bak and inhibits Bak activation. J Virol **79:**14031-43.

380. **Wasilenko, S. T., and M. Barry.** Unpublshed Results.

381. **Wasilenko, S. T., A. F. Meyers, K. Vander Helm, and M. Barry.** 2001. Vaccinia virus infection disarms the mitochondrion-mediated pathway of the apoptotic cascade by modulating the permeability transition pore. J Virol **75:**11437-48.

382. **Wasilenko, S. T., T. L. Stewart, A. F. Meyers, and M. Barry.** 2003. Vaccinia virus encodes a previously uncharacterized mitochondrial-associated inhibitor of apoptosis. Proc Natl Acad Sci U S A **100:**14345-50.

383. **Wehrle, P. F.** 1980. A reality in our time--certification of the global eradication of smallpox. J Infect Dis **142:**636-8.

384. **Wei, M. C., T. Lindsten, V. K. Mootha, S. Weiler, A. Gross, M. Ashiya, C. B. Thompson, and S. J. Korsmeyer.** 2000. tBID, a membrane-targeted death ligand, oligomerizes BAK to release cytochrome c. Genes Dev **14:**2060-71.

385. **Wei, M. C., W. X. Zong, E. H. Cheng, T. Lindsten, V. Panoutsakopoulou, A. J. Ross, K. A. Roth, G. R. MacGregor, C. B. Thompson, and S. J. Korsmeyer.** 2001. Proapoptotic BAX and BAK: a requisite gateway to mitochondrial dysfunction and death. Science **292:**727-30.

386. **Weissman, A. M.** 2001. Themes and variations on ubiquitylation. Nat Rev Mol Cell Biol **2:**169-78.

387. **Weston, C. R., K. Balmanno, C. Chalmers, K. Hadfield, S. A. Molton, R. Ley, E. F. Wagner, and S. J. Cook.** 2003. Activation of ERK1/2 by deltaRaf-1:ER* represses Bim expression independently of the JNK or PI3K pathways. Oncogene **22:**1281-93.

388. **White, E., P. Sabbatini, M. Debbas, W. S. Wold, D. I. Kusher, and L. R. Gooding.** 1992. The 19-kilodalton adenovirus E1B transforming protein inhibits programmed cell death and prevents cytolysis by tumor necrosis factor alpha. Mol Cell Biol **12:**2570-80.

389. **Whitfield, J., S. J. Neame, L. Paquet, O. Bernard, and J. Ham.** 2001. Dominant-negative c-Jun promotes neuronal survival by reducing BIM expression and inhibiting mitochondrial cytochrome c release. Neuron **29:**629-43.

390. **Willis, S. N., and J. M. Adams.** 2005. Life in the balance: how BH3-only proteins induce apoptosis. Curr Opin Cell Biol **17:**617-25.

391. **Willis, S. N., L. Chen, G. Dewson, A. Wei, E. Naik, J. I. Fletcher, J. M. Adams, and D. C. Huang.** 2005. Proapoptotic Bak is sequestered by Mcl-1 and Bcl-xL, but not Bcl-2, until displaced by BH3-only proteins. Genes Dev **19:**1294-305.

392. **Willis, S. N., J. I. Fletcher, T. Kaufmann, M. F. van Delft, L. Chen, P. E. Czabotar, H. Ierino, E. F. Lee, W. D. Fairlie, P. Bouillet, A. Strasser, R. M. Kluck, J. M. Adams, and D. C. Huang.** 2007. Apoptosis initiated when BH3 ligands engage multiple Bcl-2 homologs, not Bax or Bak. Science **315:**856-9.

393. **Wolter, K. G., Y. T. Hsu, C. L. Smith, A. Nechushtan, X. G. Xi, and R. J. Youle.** 1997. Movement of Bax from the cytosol to mitochondria during apoptosis. J Cell Biol **139:**1281-92.

394. **Yan, N., L. Gu, D. Kokel, J. Chai, W. Li, A. Han, L. Chen, D. Xue, and Y. Shi.** 2004. Structural, biochemical, and functional analyses of CED-9 recognition by the proapoptotic proteins EGL-1 and CED-4. Mol Cell **15:**999-1006.

395. **Yanez, R. J., J. M. Rodriguez, M. L. Nogal, L. Yuste, C. Enriquez, J. F. Rodriguez, and E. Vinuela.** 1995. Analysis of the complete nucleotide sequence of African swine fever virus. Virology **208:**249-78.

396. **Yang, E., J. Zha, J. Jockel, L. H. Boise, C. B. Thompson, and S. J. Korsmeyer.** 1995. Bad, a heterodimeric partner for Bcl-XL and Bcl-2, displaces Bax and promotes cell death. Cell **80:**285-91.

397. **Yethon, J. A., R. F. Epand, B. Leber, R. M. Epand, and D. W. Andrews.** 2003. Interaction with a membrane surface triggers a reversible conformational change in Bax normally associated with induction of apoptosis. J Biol Chem **278:**48935-41.

398. **Yi, X., X. M. Yin, and Z. Dong.** 2003. Inhibition of Bid-induced apoptosis by Bcl-2. tBid insertion, Bax translocation, and Bax/Bak oligomerization suppressed. J Biol Chem **278:**16992-9.

399. **Yin, X. M., Z. N. Oltvai, and S. J. Korsmeyer.** 1994. BH1 and BH2 domains of Bcl-2 are required for inhibition of apoptosis and heterodimerization with Bax. Nature **369:**321-3.

400. **Yoshida, H., Y. Y. Kong, R. Yoshida, A. J. Elia, A. Hakem, R. Hakem, J. M. Penninger, and T. W. Mak.** 1998. Apaf1 is required for mitochondrial pathways of apoptosis and brain development. Cell **94:**739-50.

401. **Youle, R. J., and M. Karbowski.** 2005. Mitochondrial fission in apoptosis. Nat Rev Mol Cell Biol **6:**657-63.

402. **Zha, J., H. Harada, E. Yang, J. Jockel, and S. J. Korsmeyer.** 1996. Serine phosphorylation of death agonist BAD in response to survival factor results in binding to 14-3-3 not BCL-X(L). Cell **87:**619-28.

403. **Zhai, D., F. Luciano, X. Zhu, B. Guo, A. C. Satterthwait, and J. C. Reed.** 2005. Humanin binds and nullifies Bid activity by blocking its activation of Bax and Bak. J Biol Chem **280:**15815-24.

404. **Zhang, L., S. Shimizu, K. Sakamaki, S. Yonehara, and Y. Tsujimoto.** 2004. A caspase-8-independent signaling pathway activated by Fas ligation leads to exposure of the Bak N terminus. J Biol Chem **279:**33865-74.

405. **Zhong, Q., W. Gao, F. Du, and X. Wang.** 2005. Mule/ARF-BP1, a BH3-only E3 ubiquitin ligase, catalyzes the polyubiquitination of Mcl-1 and regulates apoptosis. Cell **121:**1085-95.

406. **Zhou, J., X. Y. Sun, G. J. Fernando, and I. H. Frazer.** 1992. The vaccinia virus K2L gene encodes a serine protease inhibitor which inhibits cell-cell fusion. Virology **189:**678-86.

407. **Zhou, Q., S. Snipas, K. Orth, M. Muzio, V. M. Dixit, and G. S. Salvesen.** 1997. Target protease specificity of the viral serpin CrmA. Analysis of five caspases. J Biol Chem **272:**7797-800.

408. **Zong, W. X., C. Li, G. Hatzivassiliou, T. Lindsten, Q. C. Yu, J. Yuan, and C. B. Thompson.** 2003. Bax and Bak can localize to the endoplasmic reticulum to initiate apoptosis. J Cell Biol **162:**59-69.

Appendix A.

The poxvial RING protein p28 is a ubiquitin ligase

The results contained in figures A.1-A.3 have been published:
Nerenberg, B.T.H.*, **J. Taylor***, E. Bartee, K. Gouveia, M. Barry. and K. Fruh. 2005. The poxviral RING-finger protein p28 is a ubiquitin ligase that targets ubiquitin to viral replication factories. Journal of Virology. 79:597-601.
(* denotes authors contributed equally)

All of the recombinant vaccinia viruses were constructed by J. Taylor, and the results presented in Fig. A.3 *A-G* were contributed by J. Taylor. The first draft of this manuscript was written by B. Nerenberg and J. Taylor. Major editorial contributions were made by M. Barry and K. Fruh.

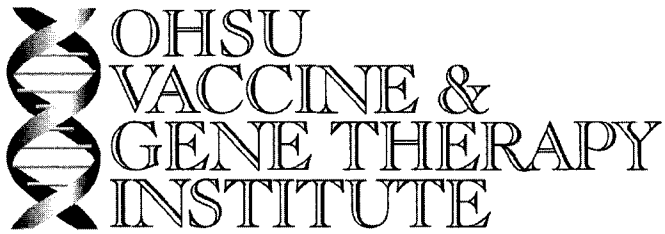

Klaus Früh, Ph.D.
Professor, Molecular Microbiology & Immunology
Director, Gene Microarray Shared Resource

Oregon Health & Science University
West Campus
505 NW 185th Ave.
Beaverton, OR 97006

Tel.: 503 418-2735
Fax.: 503 418-2701
fruehk@ohsu.edu
Sunday, June 24, 2007

To John Taylor
(Fax: 780-492-9828
Ph: 780-492-7437)

Dear John,
This letter is to confirm my permission to include data from the following collaborative study in your thesis: Nerenberg, B. T., J. Taylor, E. Bartee, K. Gouveia, M. Barry, and K. Früh. 2005. The poxviral RING protein p28 is a ubiquitin ligase that targets ubiquitin to viral replication factories. J Virol 79:597-601. I enjoyed collaborating with you and I wish you good luck for your thesis defense.

Yours sincerely,

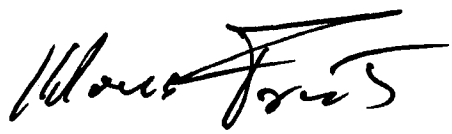

John Taylor
621 Heritage Medical Research Centre
Dept. of Medical Microbiology and Immunology
University of Alberta
Edmonton, Alberta
T5R 1E6
Canada
Ph. 913-588-7050
Fx. 913-588-7295

Journals Department
American Society for Microbiology
1752 N Street, N.W.
Washington, DC
20036-2904
USA
Fax: 202-942-9355

June 4, 2006

To Whom It May Concern:

I am currently preparing to defend my Ph.D. dissertation from the lab of Dr. Michele Barry at the University of Alberta, Edmonton, Alberta Canada, entitled "*The inhibition of apoptosis and Bax activation by mitochondrial anti-apoptotic proteins encoded by vaccinia virus and ectromelia virus*", and I would like to request official permission to use portions of our manuscript: Nerenberg, B.T.H.*, **J. Taylor***, E. Bartee, K. Gouveia, M. Barry. and K. Fruh. 2005. The poxviral RING-finger protein p28 is a ubiquitin ligase that targets ubiquitin to viral replication factories. Journal of Virology. 79:597-601.

Sincerely,

John Taylor
Ph.D. Candidate
University of Alberta

PERMISSION GRANTED
CONTINGENT ON AUTHOR PERMISSION (which you must obtain)
AND APPROPRIATE CREDIT
American Society for Microbiology
Journals Department
Date 6-5-07

Abstract

The poxviral RING protein p28 is a virulence factor whose molecular function is unknown. Many cellular RING-containing proteins act as ubiquitin ligases (RING-E3s) connecting selected substrate proteins to the ubiquitination machinery. Here we demonstrate that vaccinia virus p28 and its homologue in myxoma virus, M143R, can mediate the formation of polyubiquitin conjugates, while RING mutants of both p28 and M143R cannot. Furthermore, p28 is ubiquitinated in vivo and ubiquitin colocalizes with p28 to virus factories independently of an intact RING domain. These results implicate the ubiquitin system in poxviral virulence.

Results and Discussion

Poxviruses are large, complex viruses that replicate in the cytoplasm of infected cells (10). The poxviral RING (really interesting new gene) domain protein, p28, localizes to viral factories and is encoded by members of the leporipoxviruses and orthopoxviruses (11, 12, 14). Notable exceptions include vaccinia virus (VV) strain WR, which contains a truncated copy of p28, and VV strain Copenhagen, which lacks p28 entirely (11, 12, 14). Although the precise molecular function of p28 is presently unknown, p28 expression has been linked to apoptosis inhibition and a p28 knockout in ectromelia virus was strongly attenuated, resulting in reduced growth in macrophages and the complete clearance of virus from infected mice (2, 3, 11, 12).

Recently, a number of RING-containing proteins have been shown to act as ubiquitin ligases (RING-E3s) which simultaneously interact with a specific substrate and a ubiquitin-conjugating enzyme (ubc), or E2, to mediate substrate-specific ubiquitination (7). In vitro, RING-E3s catalyze the formation of polyubiquitin in the presence of ubiquitin, ubiquitin-activating enzyme (E1), E2, and ATP (8). Given the highly conserved RING domain in p28, we examined whether VV p28 and the myxoma virus (MV) homologue, M143R, display ubiquitin ligase activity in vitro. VV p28, derived from strain IHD-W (14), and M143R, from MV strain Lausanne, were fused to glutathione *S*-transferase (GST) and purified from *Escherichia coli* as described previously (9). Mutations in the RING domains of M143R and p28 were constructed by replacing two conserved cysteines, C173 and C176, with serine, which disrupts the ability of RING

domains to complex with zinc and abolishes E3 ligase activity (9). Furthermore, the RING domain of p28 was deleted by truncation at residue 184, resulting in a construct consistent with the p28 truncation in VV strain WR. At a concentration of 3 μM, each GST fusion was combined in vitro with 50 nM rabbit E1 (Boston Biochem), 0.5 μM human E2 UbcH5a (gift of R. Everett and purified as described previously (1)), 10 mM ATP, and 28 μM ubiquitin. Negative and positive controls consisted of GST and the RING domain of herpes simplex virus type 1 ICP0 (1), respectively. The in vitro ubiquitination reaction was performed in a solution of 20 μl of 50 mM Tris-HCl (pH 7.5), 200 mM NaCl, 1 mM dithiothreitol for 90 min at 30°C, and high-molecular-weight (HMW) ubiquitin conjugate formation was determined by immunoblotting with ubiquitin-specific antibody P4D1 (Santa Cruz Biotechnology). As expected, the RING domain of ICP0 catalyzed the formation of multiubiquitin adducts in the presence of UbcH5a, whereas GST was inactive (Fig. A.1). HMW-ubiquitinated products were also observed in the presence of p28 and M143R, but not when the RING domain was truncated or lacked crucial cysteines (Fig. A.1). These HMW bands likely consist of multiple ubiquitin adducts or ubiquitinated E1 or E2, because reprobing the blot with anti-GST did not reveal additional ubiquitinated bands of wild-type p28 compared to those of RING mutant p28 (data not shown). Thus, we conclude that p28 and M143R can function as RING-E3 ubiquitin ligases in vitro.

To determine whether p28 affects ubiquitination in vivo, we examined the distribution of ubiquitin in VV-infected cells in the presence of wild-type or truncated p28 by using an infection/transfection strategy described previously (14). Under the control of the synthetic early-late poxviral promoter in pSC66 (4, 6), four versions of p28 with an N-terminal FLAG tag (DYKDDDDK) were expressed: wild-type p28, p28C173S/C176S, p28(1-204), and p28(1-184). Comparable expression levels and correct sizes of these constructs were verified by immunoblot (data not shown). To facilitate the detection of ubiquitination events occurring during poxviral infection, we inserted a hemagglutinin (HA) epitope-tagged form of ubiquitin (13) into pSC66 (4). HeLa cells were infected with VV-WR at an MOI of 5 and were cotransfected with HA-ubiquitin and either p28 or enhanced green fluorescent protein (EGFP) in pSC66 as a control (15). The distribution of both p28 and HA-ubiquitin was determined by confocal microscopy at

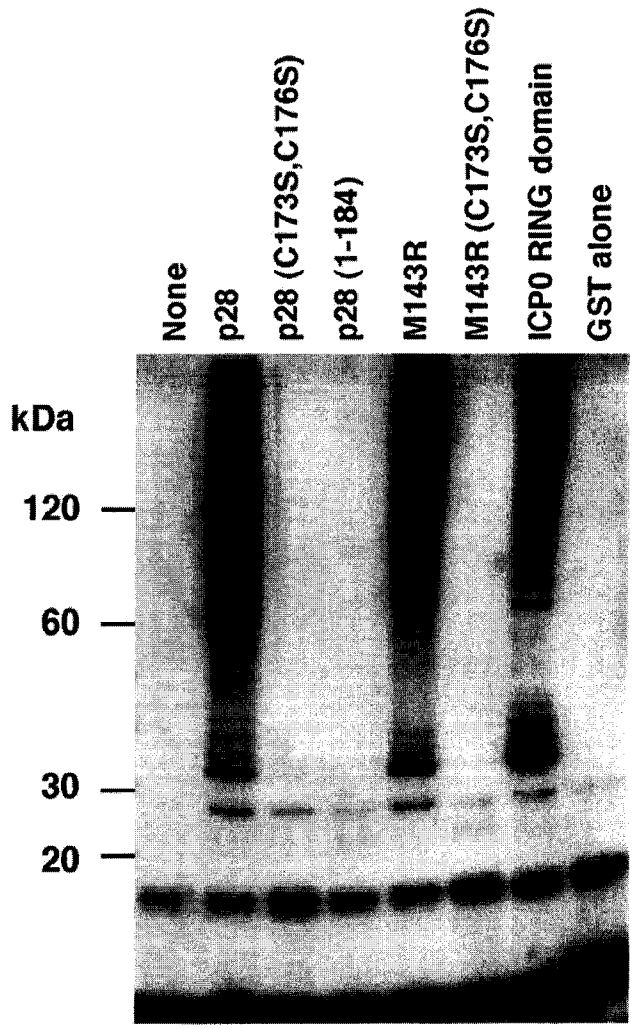

Figure A.1. p28 has ubiquitin ligase activity *in vitro.*
Purified GST fusion proteins were combined in an in vitro ubiquitination reaction with E1, UbcH5a (E2), ATP, and ubiquitin. Reactions were separated by sodium dodecyl sulfate-polyacrylamide gel electrophoresis and were probed with anti-ubiquitin (P4D1; Santa Cruz Biotechnology). Western blotting with anti-ubiquitin shows the appearance of high-molecular-mass ubiquitin adducts in reactions containing either GST-p28, GST-M143R, or GST-ICP0 compared to reactions with no GST-fusion, GST alone, the C173S/C176S double mutants of both p28 and M143R, or p28(1-184).

16 h post-infection. Cells were fixed with paraformaldehyde, permeabilized, and blocked with bovine serum albumin and fish gelatin as described previously (9). p28 was detected using fluorescein isothiocyanate (FITC)-conjugated anti-FLAG antibody (M2; Sigma), rabbit anti-I3L was used to detect virus factories (16), and mouse monoclonal anti-HA (HA-7; Sigma) was used to visualize ubiquitin. Primary antibodies were detected with goat anti-rabbit Alexa Fluor 350 (Molecular Probes) and goat anti-mouse Rhodamine B (Biosource, Camarillo, Calif.), respectively. Mouse Fc fragment (Cortex Biochem, San Leandro, Calif.) was used to block potential binding of the anti-FLAG to the anti-mouse secondary antibody. Absence of cross-reactivity was verified in control experiments (data not shown). Images for each fluorescence channel were obtained sequentially by confocal microscopy (Fig. A.2).

As expected from previous studies, both full-length p28, p28(C173S/C176S), and p28(1-204) localized exclusively to virus factories and displayed similar staining patterns (Fig. A.2), while p28(1-184) showed both cytoplasmic and viral factory staining (12, 14). In the presence of cotransfected EGFP, we observed a diffuse cytoplasmic distribution of HA-ubiquitin that was excluded from viral factories (Fig. A.2). Similarly, HA-ubiquitin was excluded from viral factories when cotransfected with p28(1-184), despite a partial localization of p28(1-184) to viral factories. In stark contrast, cotransfection of both full-length p28 and p28(1-204) resulted in a strong enrichment of ubiquitin at viral factories. The same staining pattern was also seen using His-tagged ubiquitin (His_6) (data not shown) (13), suggesting that ubiquitin is enriched in virus factories upon expression of p28. To determine if such ubiquitin enrichment could also be observed with endogenous ubiquitin, we used antibody FK-2 (Affiniti), which specifically detects conjugated ubiquitin. Cells infected with a recombinant VV-WR expressing FLAG-p28 showed colocalization of conjugated ubiquitin as determined by colocalization with the virus factory marker I3L (Fig. A.2*B*). No colocalization was observed in VV-WR-infected cells (Fig. A.2*B*). Colocalization was not observed in all cells but was most obvious in cells that displayed well-developed and large virus factories.

The colocalization of ubiquitin with p28 in virus factories could be the consequence of p28-mediated ubiquitination of poxviral or host proteins in this compartment; however, colocalization occurred independent of a functional RING

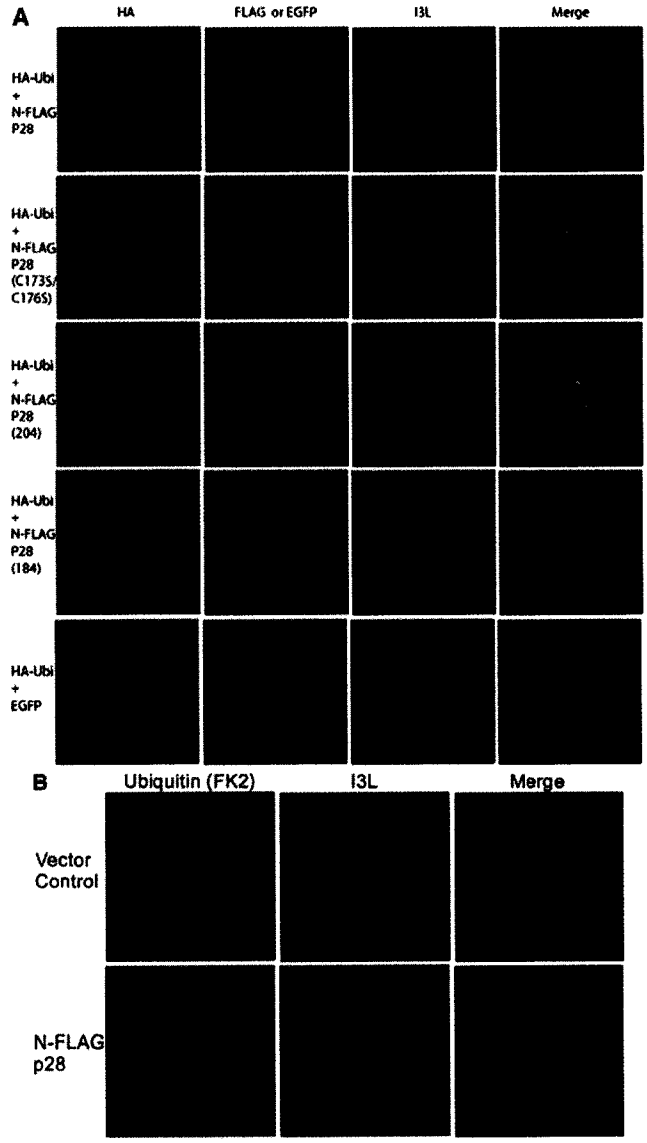

Figure A.2. p28-dependent accumulation of ubiquitin in viral replication factories. *A*, Colocalization with HA-ubiquitin. HeLa cells were infected with VV-WR, transfected with HA-ubiquitin, and cotransfected with either FLAG-p28, FLAG-p28(C173S/C176S), FLAG-p28(1-204), FLAG-p28(1-184), or EGFP. Cells were fixed and stained as described in the text to visualize HA-ubiquitin, FLAG constructs, EGFP, and I3L. All p28 constructs tested localized to virus factories, although FLAG-p28(1-184) was also cytoplasmic. HA-ubiquitin was excluded from viral factories in the absence of p28, while in the presence of FLAG-p28, FLAG-p28(C173S/C176S), or FLAG-p28(1-204), HA-ubiquitin was enriched in virus factories. In contrast, HA-ubiquitin was excluded from viral factories upon transfection with FLAG-p28(1-184). (B) Colocalization with endogenous ubiquitin. HeLa cells were infected with VV-WR FLAG-p28 or VV-WR for 16 h and stained with anti-ubiquitin antibody FK2 and anti-I3L. Ubi, ubiquitin.

domain, suggesting that colocalization could also be the result of ubiquitination of p28. To examine if p28 was ubiquitinated, we generated recombinant VV-WR expressing FLAG-p28, FLAG-M143R, HA-ubiquitin, or His-ubiquitin according to standard procedures (4). CV-1 cells were infected with VV-FLAG-p28 or VV-FLAG-M143R for 16 h at an MOI of 5 in the presence or absence of VV-HA-ubiquitin, and FLAG-tagged p28 or M143R was immunoprecipitated using immunoprecipitation (RIPA) buffer and anti-FLAG antibody (M2; Sigma). Immunoblotting the precipitates with anti-FLAG antibody revealed, as expected, a predominant band in the 28-kDa range in cells infected with VV-FLAG-p28 and VV-FLAG-M143R but not in VV-HA-ubiquitin (Fig. A.3*A* and *D*). In addition, several HMW species were also observed which could represent ubiquitinated p28 or M143R. Co-infection with HA-ubiquitin slightly increased the size of HMW FLAG-tagged M143R (Fig. A.3*D*), while generally lower amounts of all FLAG-tagged bands were observed as a result of coinfection. Immunoblotting the anti-FLAG precipitates with anti-HA revealed low background levels in VV-HA-ubiquitin-infected cells (Fig. A.3*B* and *E*). However, coinfection of VV-HA-ubiquitin with either p28 or M143R, followed by immunoprecipitation with anti-FLAG and immunoblotting with anti-HA, resulted in the presence of HMW HA-tagged bands, including those that correspond to HMW FLAG-tagged forms of p28 or M143R (Fig. A.3*B* and *E*). Importantly, only the HMW species were recognized with anti-HA, whereas the predominant 28-kDa protein detected by anti-Flag was not reactive with anti-HA. Similar observations were made using an antibody against endogenous ubiquitin (Fig. A.3*C* and *F*), indicating that p28 and M143R are ubiquitinated during viral infection, which has been observed for other RING-E3 ligases (5). To determine if the ubiquitination of p28 was the result of autoubiquitination, we coinfected cells with VV expressing either FLAG-tagged wild-type or RING mutant p28 together with VV-His-ubiquitin. Ubiquitinated proteins were isolated by using nickel-chelate affinity chromatography and were probed for the presence of p28 by using anti-FLAG. HMW bands occurred in both wild-type and mutant p28-expressing cells that also expressed His-ubiquitin, but they did not occur in cells that were only infected with p28-expressing VV (Fig. A.3*G*). Therefore, we conclude that autoubiquitination of p28 is unlikely to be the reason for ubiquitination

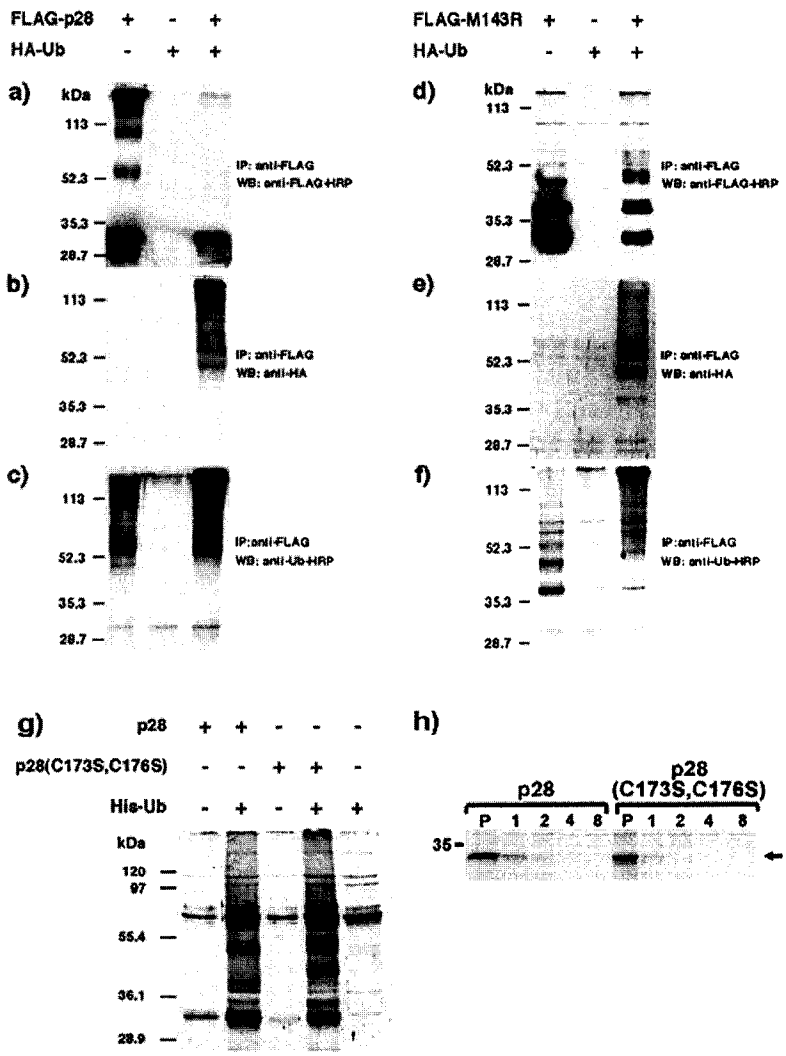

Figure A.3. Ubiquitination of p28 and M143R. CV-1 cells were infected with the indicated recombinant viruses at an MOI of 5. Sixteen hours postinfection, cells were treated with 25 μM MG132 for 4 h, lysed in RIPA buffer, and immunoprecipitated with anti-FLAG antibody (M2; Sigma). Immunoprecipitates were separated by SDS-PAGE and were blotted with either anti-FLAG-HRP (a and d), anti-HA (b and e), or anti-ubiquitin-HRP (c and f). (g) CV-1 cells were infected with the indicated viruses at an MOI of 2 for 16 h, treated with 25 μM MG132 for 4 h, and lysed in 1% NP-40. Cleared lysates were incubated with Ni2+ resin for 2 h at 4°C, and bound proteins were eluted using 1 M imidazole in 500 mM NaCl and 20 mM Tris (pH 7.9) and concentrated by acetone precipitation. Samples were separated by SDS-PAGE and probed with anti-FLAG-HRP (M2). (h) HeLa cells were infected with the indicated viruses at an MOI of 5 for 16 h and were metabolically labeled with [35S]methionine (0.1 mCi/ml) for 30 min, and the label was chased for the indicated hours. Cells were lysed, and p28 was immunoprecipitated using anti-FLAG. WB, Western blot; IP, immunoprecipitation; Ub, ubiquitin.

of p28. Probably as a result of this ubiquitination, both wild-type and mutant p28 are short lived (Fig. A.3*H*).

p28 is the first ubiquitin ligase identified in members of the orthopoxviruses. At present, the substrates of p28 and its myxoma virus homologue, M143R, are unknown, but they themselves seem to be targets for ubiquitination, which may contribute to the observed accumulation of ubiquitin in the replication factories. It remains to be demonstrated how the ubiquitin ligase function of p28 relates to its role as a virulence factor and its previously observed requirement for infection of macrophages and inhibition of apoptosis (2, 3, 12). This is the first evidence that p28 functions as a ubiquitin ligase. Recently, however, it was shown that myxoma virus encodes another ubiquitin ligase, M153R, which targets immune receptors for degradation (9). Our observations that p28/M143R and M153R function as ubiquitin ligases clearly suggest that regulation of ubiquitination during poxvirus infection is an important and recurring theme.

References

1. **Boutell, C., S. Sadis, and R. D. Everett.** 2002. Herpes simplex virus type 1 immediate-early protein ICP0 and is isolated RING finger domain act as ubiquitin E3 ligases in vitro. J Virol **76:**841-50.
2. **Brick, D. J., R. D. Burke, A. A. Minkley, and C. Upton.** 2000. Ectromelia virus virulence factor p28 acts upstream of caspase-3 in response to UV light-induced apoptosis. J Gen Virol **81:**1087-97.
3. **Brick, D. J., R. D. Burke, L. Schiff, and C. Upton.** 1998. Shope fibroma virus RING finger protein N1R binds DNA and inhibits apoptosis. Virology **249:**42-51.
4. **Chakrabarti, S., J. R. Sisler, and B. Moss.** 1997. Compact, synthetic, vaccinia virus early/late promoter for protein expression. Biotechniques **23:**1094-7.
5. **Chen, A., F. E. Kleiman, J. L. Manley, T. Ouchi, and Z. Q. Pan.** 2002. Autoubiquitination of the BRCA1*BARD1 RING ubiquitin ligase. J Biol Chem **277:**22085-92.
6. **Davison, A. J., and B. Moss.** 1990. New vaccinia virus recombination plasmids incorporating a synthetic late promoter for high level expression of foreign proteins. Nucleic Acids Res **18:**4285-6.
7. **Joazeiro, C. A., and A. M. Weissman.** 2000. RING finger proteins: mediators of ubiquitin ligase activity. Cell **102:**549-52.
8. **Joazeiro, C. A., S. S. Wing, H. Huang, J. D. Leverson, T. Hunter, and Y. C. Liu.** 1999. The tyrosine kinase negative regulator c-Cbl as a RING-type, E2-dependent ubiquitin-protein ligase. Science **286:**309-12.

9. **Mansouri, M., E. Bartee, K. Gouveia, B. T. Hovey Nerenberg, J. Barrett, L. Thomas, G. Thomas, G. McFadden, and K. Fruh.** 2003. The PHD/LAP-domain protein M153R of myxomavirus is a ubiquitin ligase that induces the rapid internalization and lysosomal destruction of CD4. J Virol **77:**1427-40.
10. **Moss, B.** 1996. Poxviridae: The Viruses and Their Replication. *In* B. N. Fields, D. M. Knipe, and P. M. Howley (ed.), Fields Virology, 3rd ed. Lippincott-Raven Publishers, Philadelphia.
11. **Senkevich, T. G., E. V. Koonin, and R. M. Buller.** 1994. A poxvirus protein with a RING zinc finger motif is of crucial importance for virulence. Virology **198:**118-28.
12. **Senkevich, T. G., E. J. Wolffe, and R. M. Buller.** 1995. Ectromelia virus RING finger protein is localized in virus factories and is required for virus replication in macrophages. J Virol **69:**4103-11.
13. **Treier, M., L. M. Staszewski, and D. Bohmann.** 1994. Ubiquitin-dependent c-Jun degradation in vivo is mediated by the delta domain. Cell **78:**787-98.
14. **Upton, C., L. Schiff, S. A. Rice, T. Dowdeswell, X. Yang, and G. McFadden.** 1994. A poxvirus protein with a RING finger motif binds zinc and localizes in virus factories. J Virol **68:**4186-95.
15. **Wasilenko, S. T., T. L. Stewart, A. F. Meyers, and M. Barry.** 2003. Vaccinia virus encodes a previously uncharacterized mitochondrial-associated inhibitor of apoptosis. Proc Natl Acad Sci U S A **100:**14345-50.
16. **Welsch, S., L. Doglio, S. Schleich, and J. Krijnse Locker.** 2003. The vaccinia virus I3L gene product is localized to a complex endoplasmic reticulum-associated structure that contains the viral parental DNA. J Virol **77:**6014-28.

Appendix B: Supplemental Results

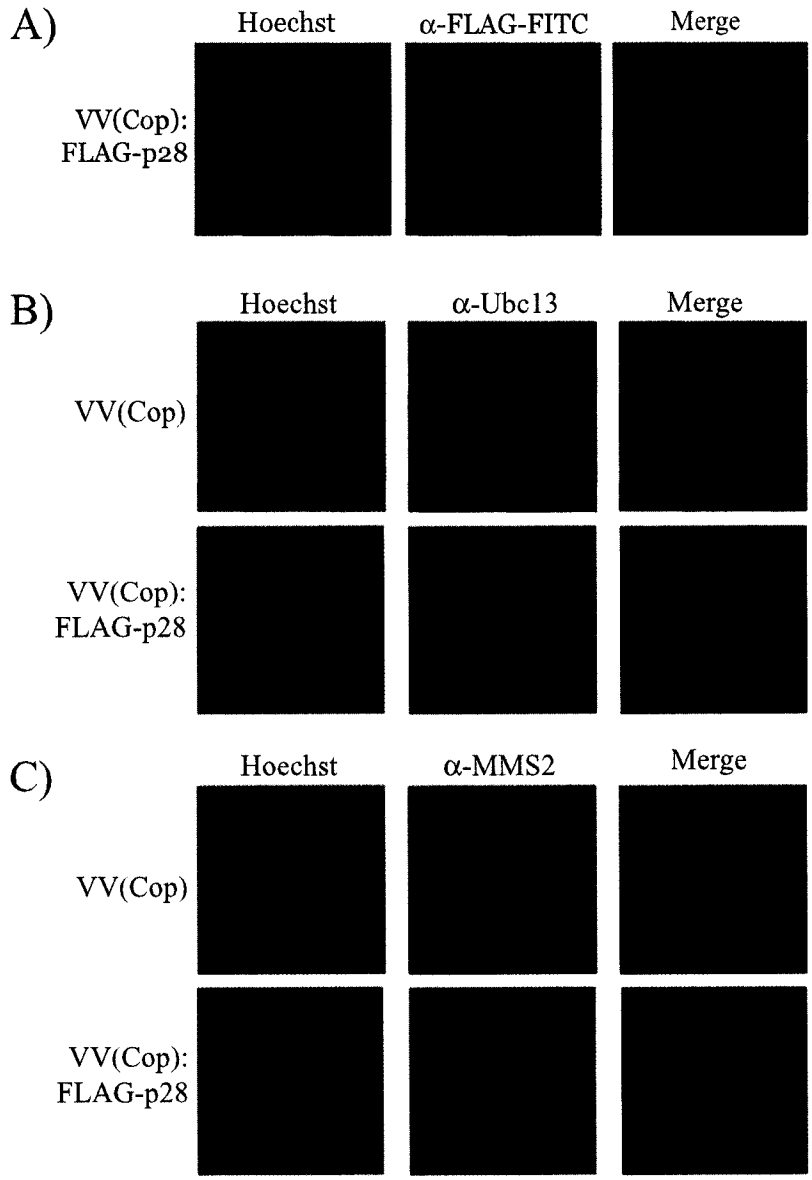

Figure B.1. Ubc13 and MMS2 appear to be enriched at virus factories in the presence of p28. HeLa cells were infected at an MOI of 5 for 16 hours with either VV(Cop) or VV(Cop):BN65 which expressed FLAG-p28. Cells were fixed in 4% paraformaldehyde and stained with either anti-FLAG-FITC (A), anti-Ubc13 (B) or anti-MMS2 (C) at 1:200, and costained with anti-mouse-Alexa546 (B and C). Cells were co-stained with Hoechst 33342 and visualized with confocal microscopy.

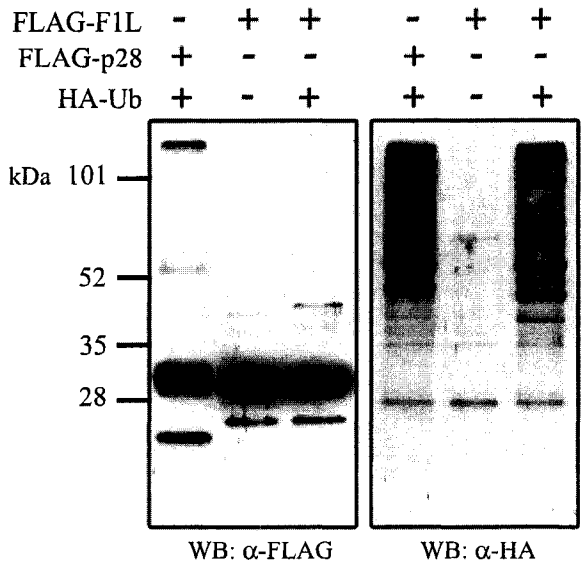

Figure B.2. F1L is ubiquitinated.
HeLa cells were infected with VV:FLAG-F1L alone, or VVWR:HA-ubiquitin along with either VV:FLAG-F1L or VVWR:FLAG-p28 at an MOI of 5 for 16 hours. Four hours prior to lysis, cells were treated wtih 25uM MG132. Cells were lysed in RIPA buffer and immunoprecipitated with anti-FLAG(M2).Immunoprecipitates were western blotted with either anti-FLAG-HRP or anti-HA.

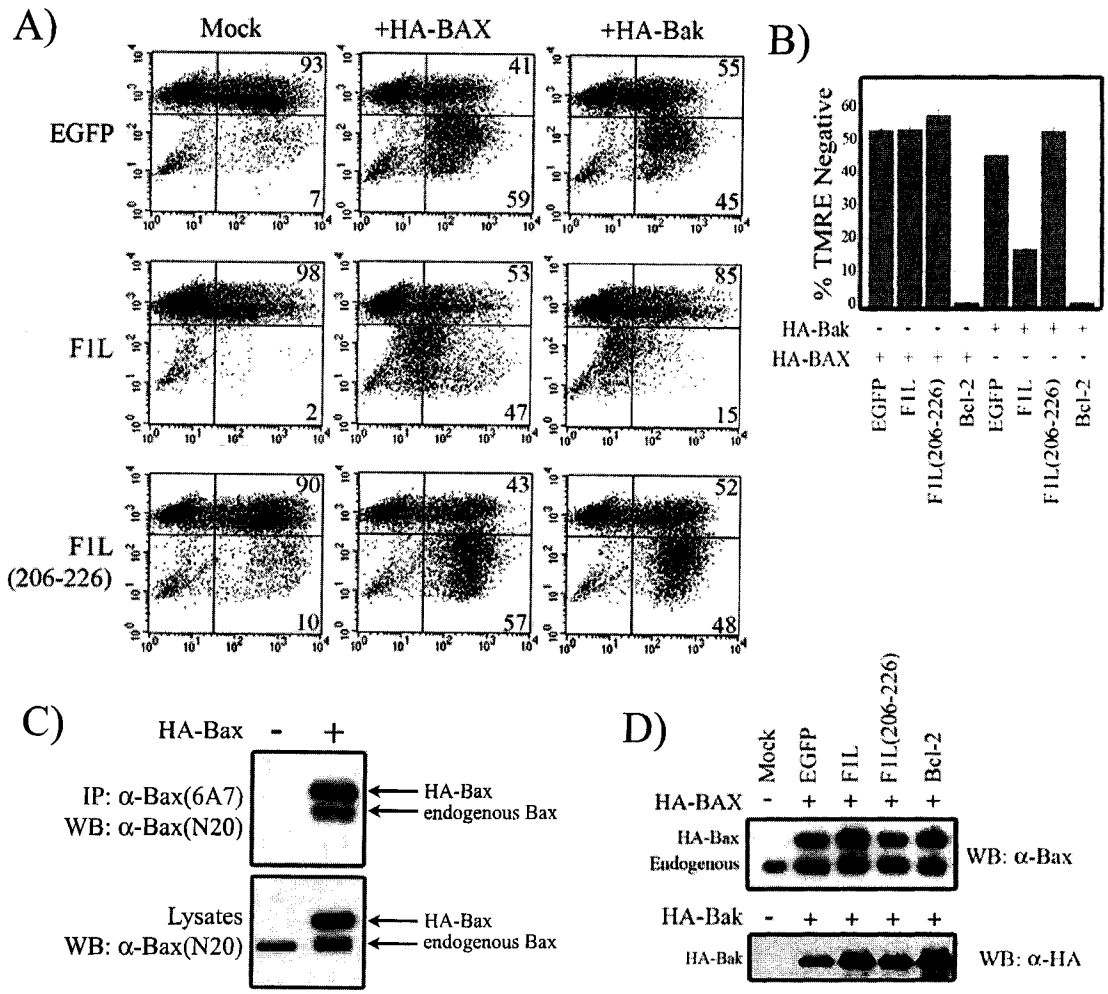

Figure B.3. F1L inhibits apoptosis induced by Bak overexpression, but not Bax-overexpression. *A*, Hela cells were co-transfected with one of pEGFP, pEGFP-F1L or pEGFP-F1L(206-226) along with either pcDNA3-HA-Bak or pcDNA3-HA-Bax for 16 hours. Cells were stained with TMRE to label healthy mitochondria and analyzed by flow cytometry. One representative data plot from each sample is shown, and the percentages in the upper right hand quadrant indicate healthy cells, while percentages in the lower right quadrant indicate apoptotic cells. *B*, Graphical representation of results obtained from (A), with averages and standard deviations obtained from experiments done in triplicate. *C*, Expression of HA-Bax induces Bax activation. HeLa cells were transfected with pcDNA3-HA-Bax for 16 hours, and immunoprecipitated with anti-Bax(6A7). Immunoprecipitates and lysates were probed with anti-Bax(N20). *D*, Samples from (A) were analyzed by western blotting with either anti-Bax or anti-HA to detect levels of transfected Bax or Bak respectively.

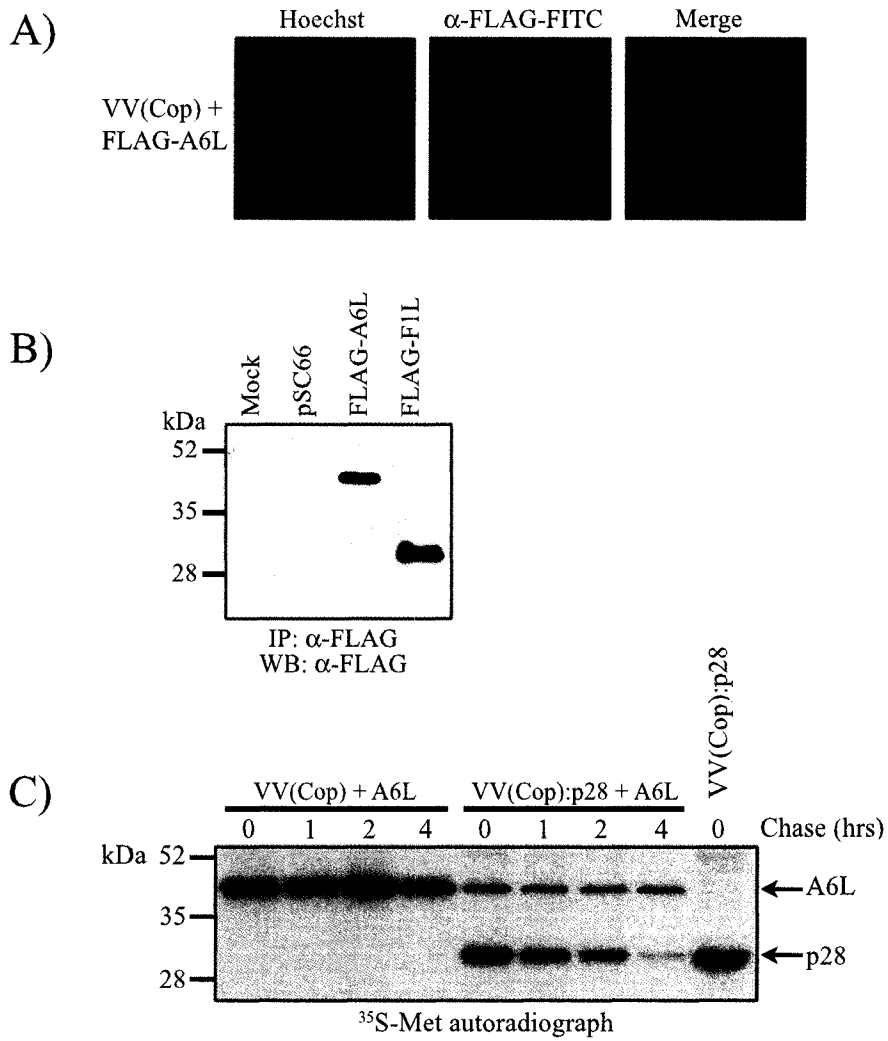

Figure B.4. Vaccinia virus A6L protein is cytoplasmic and is stable in the presence of p28.
A, HeLa cells were infected with VV(Cop) at an MOI of 3 and transfected with pJMT34 to express FLAG-tagged A6L under the early/late poxviral promoter from pSC66. At 12 hours post-transfection, cells were fixed and staing with anti-FLAG-FITC (1:200), and co-stained with Hoechst 33342 to label DNA. Cells were mounted and visualized using confocal microscopy.
B, HeLa cells were infected with VV(Cop) and transfected with either empty vetor (pSC66), FLAG-A6L (pJMT34), or FLAG-F1L (pJMT36) for 16 hours. Cells were lysed in 1% NP-40 and immunoprecipitated withanti-FLAG. IPs were western blotted with anti-FLAG-HRP. *B*, HeLa cells were infected with either VV(Cop) or VV(Cop):FLAG-p28, and transfected with pJMT34 (FLAG-A6L behind poxviral promoter). At 4 hours post-infection/transfection, cells were pulsed with ^{35}S-Methionine for 30 minutes,and chased with cold media for the indicated times, Samples were harvestedat 0,1,2, and 4 hours post-chase, lysed in 1% NP-40, and immunoprecipitatedwith anti-FLAG. Immunoprecipitates were separated by SDS-PAGE and exposed to autoradiography. FLAG-p28 is noticeably lost over time, whereas A6L levels appear to be stable for 4 hours in the presence or absence of p28.

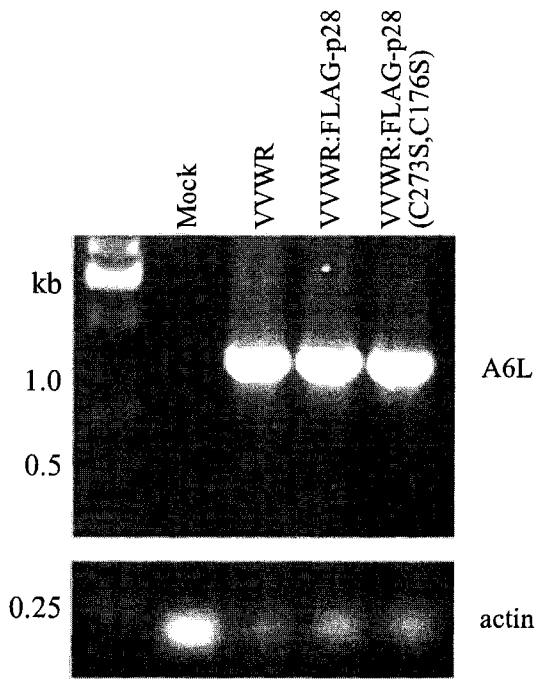

Figure B.5. A6L mRNA is expressed from recombinant VVWR expressing p28. HeLa cells were infected at an MOI of 5 with either VVWR, VVWR:FLAG-p28, or VVWR:FLAG-p28(C173S,C176S) for 16 hours. Total RNA was isolated and used in an RT-PCR reaction with A6L-specific primers, or β-actin primers as a control. Products were separated on a 0.8% agarose gel.